MECHANISMS OF TRANSCRIPTIONAL REGULATION BY PROTEINS IN THE NAD+ METABOLIC PATHWAY

A Dissertation

Presented to the Faculty of the Graduate School

of Cornell University

in Partial Fulfillment of the Requirements for the Degree of

Doctor in Philosophy

by

Kristine Marie Frizzell

January 2011

MECHANISMS OF TRANSCRIPTIONAL REGULATION BY PROTEINS IN THE NAD+ METABOLIC PATHWAY

Kristine Marie Frizzell, Ph.D.

Cornell University 2011

Poly(ADP-ribosyl)ation (PARylation) is an enzymatic reaction whereby ADP-ribose units from donor NAD^+ molecules are covalently attached onto target proteins. The regulation of this reaction is overseen by two nuclear enzymes, Poly(ADP-ribose) polymerase-1 (PARP-1) and poly(ADP-ribose) glycohydrolase (PARG), that modify target proteins in the nucleus by the addition and removal, respectively, of ADP-ribose polymers. While PARP-1 has generally been studied with respect to its role in DNA damage repair and cell death pathways, recent studies have revealed a role for PARP-1 in transcriptional regulation. The role of PARG in transcriptional regulation, however, is less characterized. In this study, I have investigated the coordinate patterns of gene regulation by PARP-1 and PARG *in vivo* using genomic and gene-specific analyses.

Specifically, I show that PARP-1 and PARG coordinately regulate global patterns of gene expression by affecting genes in the same direction and with similar magnitudes. Further analysis revealed that PARP-1 and PARG localized to the promoters of both positively and negatively regulated target genes in parallel binding patterns. I also show that PARP-1 and PARG enzymatic activities are required for some, but not all, target genes. My results indicate that PARP-1 and PARG, two nuclear enzymes with opposing enzymatic activities, localize to target promoters and act in a similar, rather than antagonistic, manner to regulate gene expression.

In a follow-up study, I have used a novel method known as Global Run-on Sequencing (GRO-seq) to define the role of PARP-1 on the estrogen-regulated transcriptome at the level of the nascent transcript, rather than steady-state mRNA

levels. I have produced libraries from MCF-7 cells treated with vehicle or 17β-estradiol (E2) under three conditions: (i) a control knockdown; (ii) a control knockdown plus a PARP inhibitor, PJ34; and (iii) a PARP-1 knockdown. I have determined that the estrogen response is highly maintained under PARP-1 knockdown or inhibition. Accordingly, upon estrogen treatment, PARP-1 localization patterns are largely unaffected. However, deeper analyses reveal a small number of genes where PARP-1 knockdown or inhibition reduces the estrogen response at the transcription level (GRO-seq) and at the steady state mRNA level (RT-qPCR).

The NAD^+ metabolite generated from the PARP-1/PARG reaction, ADP-ribose (ADPR), is a small molecule ligand that is used by macro domain-containing proteins. The histone variant macroH2A1 is one such protein that has generally been studied with respect to its role in transcriptional repression on the inactive *X* chromosome. However, recent studies have begun to explore a role for macroH2A1 in autosomal gene regulation, as a transcriptional repressor and a transcriptional activator. Recent results from the Kraus lab have shown that the transcriptional coactivator Proline-, glutamic acid-, and leucine-rich protein 1 (PELP1) interacts with the macro domain of macroH2A1 in a ligand-independent manner and shows a similar genomic localization pattern. I have followed up these observations by investigating the mechanisms of gene regulation by macroH2A1 and its interacting proteins using gene-specific analyses. Specifically, I have shown that macroH2A1 recruits PELP1 to macroH2A1 target gene promoters, but PELP1 is dispensable for the nucleosomal deposition of macroH2A1 at these loci. Together, macroH2A1 and PELP1 cooperatively regulate the expression of a subset of macroH2A1 target genes.

Collectively, my studies expand our understanding of the cooperative actions of proteins in the NAD^+ metabolic pathway in regulating transcription.

BIOGRAPHICAL SKETCH

Kristine Marie Frizzell was born and raised in Plymouth, Massachusetts. In 1999, she graduated from Plymouth North High School and began her undergraduate studies at Merrimack College in North Andover, Massachusetts. There, she gained a strong background in biology, biochemistry, and mathematics, including topics in genetics, molecular biology, and forensic science technologies. It was during this time that she met the love of her life, James Patrick Hussey, Jr. Kristine completed her course work in 2003, graduating Magna Cum Laude with honors and received a Bachelor of Science degree in Biochemistry. She received a MERCK/AAAS Undergraduate Research Grant and participated in an intern research program at MERCK & Co., Inc. in West Point, PA during the summer of 2003. In the same year, she began her graduate career at Cornell University in the field of Biochemistry, Molecular, and Cell Biology (BMCB). In 2004, she joined the lab of Dr. W. Lee Kraus to study the molecular mechanisms of transcriptional regulation by Poly(ADP-ribose) Polymerase-1. She received multiple awards, including the American Heart Association Pre-doctoral Fellowship in 2007. Kristine and Jay married in October of 2008 beginning their family and life's journey together. In 2010, she successfully defended her Ph.D. thesis and completed what she deems the hardest challenge she had ever been faced with. She looks forward to the next one – motherhood.

To my parents,

for your support and encouragement,

friendship, and never-ending love.

And to my husband,

for pushing me further than I thought possible,

for your tremendous patience,

for making me laugh <u>every day</u>,

and for your willingness to cook.

ACKNOWLEDGMENTS

I would like to thank my advisor, Dr. W. Lee Kraus, for his accepting me as his student and for his continual guidance. His teachings and efforts have helped me develop from a naïve undergraduate to a knowledgeable and successful scientific researcher. Lee, for all you have done toward my scientific development, I am exceedingly grateful. I wish you luck on your next adventure in Dallas.

I would also like to thank my committee members, Dr. John T. Lis and Dr. Ruth Collins, for their advice and support over the years. Especially to Ruth, who took the time to talk when I needed it and encouraged me to keep going. To Diane Colf, the first person I met here at Cornell and the last person I say goodbye to, it has been quite a journey and you have been there every step of the way. Thank you for helping me through year after year; I appreciate everything you have done.

I am extremely grateful to those that made my day-to-day life one that I'll never forget. To work with such wonderful people from different backgrounds and cultures has been quite the experience. I have enjoyed great conversations and scientific interactions with each member of the Kraus lab and their teachings both in science and in life have proved invaluable to me. First, to my bay-mate, Dr. Matthew J. Gamble, thank you for pushing me to always strive for the next level. You have taught me a great deal about success and the ways of the scientific world. Your lessons will always stick with me. You are a great friend and lab life is simply not the same without you. To Dr. Donald D. Ruhl, you have taught me "simple-science". You are a great teacher and your love for the "cool-ness" in science is something I try hard to find. Thank you for putting up with my millions of questions, for your scientific guidance, and just listening to me when I needed it.

I would like to thank Dr. Gary D. Isaacs and Dr. Miltiadis Kininis for setting the path for me to follow in the lab. Your ability to build your projects around new ideas and methodologies is a skill I hope to master one day. I have tremendous appreciation for the constant support of the fellow PARPers in the lab, Dr. Raga Krishnakumar, Dr. Tong Zhang, Xin Luo, Jhoanna (Berrocal) Noonan, Bryan Gibson, and Dr. David A. Wacker, who know and understand the struggles endured in PARP-related projects. I have learned so much from each of you and I thank you for your contributions toward my projects. Your suggestions and critiques have helped me become a better researcher. Dr. Nasun Hah, Miao Sun, and Xin, who made extensive contributions to my project over the last year, stepped up to help me when I needed it most. Thank you for your time and effort, and your willingness to provide relief services. I extend a deep gratitude toward Elizabeth Fogarty, who kept our lab running. Without you, Liz, I would not have been able to succeed, so thank you.

I have had the pleasure of working with some of the most talented and knowledgeable postdocs in our lab. And, although my interactions were limited, they were still rewarding. I want to thank Dr. Nina Heldring for being such a wonderful and joyful person. Nina, you made me smile every day and that made a big difference. Dr. Charles Danko is extremely skilled in the art of answering scientific questions with a computer program. His work is beyond my understanding most of the time, but he has the ability to explain it in a way that seems so simple; a skill I try to model. Charles, you are a wonderful comic relief (in a quirky sort of way); thank you for making me see things from your angle. To our newest postdoc, Dr. Shrikanth Gadad, you have made a big impact in such a short time. Your knowledge extends beyond the edges of the universe and I will forever try to catch up.

To our newest lab members, Fang Ye and Ziying Liu, I wish you the best of luck in your Kraus lab adventure. I also enjoyed many interactions with Molly Shook,

Kristine Hope, and Kevin Conley, who were only a part of the lab for a short time, but certainly left their marks. And, to my lab-mates in the beginning, Dr. Mi Young Kim, Dr. Edwin Cheung, Dr. Nicolas Gévry, and Dr. Mari Acevedo, I am thankful for your advice as I began my graduate career. Thank you to my undergraduate researchers, Christine Yang and Emily Reasor, for making me a better teacher; it was a pleasure working with you and I wish you the best of luck as you move on from Cornell. In addition, a big thanks to all of our rotation students, undergraduate researchers, and undergraduate workers, who made a big difference along the way.

I have made many dear friends since I have been here; some have moved on to bigger and better things. They have all have taught me so much about what truly matters. I am forever indebted to each of them for walking beside me with nothing but support and encouragement as I faced challenge after challenge. Words cannot convey my love and appreciation toward each of them. I would especially like to thank Dr. Ann (Bernard) Demogines and Mrs. Jhoanna (Berrocal) Noonan, who are truly the best friends anyone could ever have. You stood by me on the happiest day of my life and supported me in the utmost fashion; it is something I will never forget. I know we have lots of reunions to look forward to! To the "Three Amigos" (Don, Matt, and Gary), it's been interesting and beyond comical to say the least. You are wonderful friends and I wish you all the success in your new endeavors; you deserve it! Your families are lucky to have such great men in their lives.

Liz, it's been so much fun getting to know you and sharing life's journey with you. You have done great things thus far, especially being a mom, and I know you'll do great things in the future. To Jenny (Gehman) Weber, thank you for your friendship from the very beginning, there's no one else I would have wanted by my side. And, to Katherine Keickhafer, thank you for listening when I needed it. I will definitely miss our breakfast dates! I wish you and Will the best of luck with your

next adventure in life, and have FUN! And, finally, to Raga, Xin, Don and Matt, who have been my crutch over the last year, your kind words have made a great impact on me as a person and have forever changed my outlook on life…thank you.

I would like to particularly thank my NY family for their love and support. Joe and Marianne Bortle, you have made a home away from home for us and I thank you dearly for taking us in as part of your family. My appreciation to you for everything you have done for us in immeasurable. Mike, Keith, Erica, Nadine, and Justin, we will forever be your brother and sister, accent and all. Little Jay, our fellow Sox fanatic, you have been such a great friend to us. You'll always have a place to stay in Boston! And to all the family/crew in Syracuse and Rochester, thank you for including us and making us feel like we have a place in your lives. You all have a place in ours. We will definitely return for wine-tours, the Bortle Bash, and the Glen! We thank you from the bottom of our hearts and we love you all!

I want to thank my new family, Jim, Donna, and Erin Hussey, who have taken me in with love and affection. Jim and Donna, I am so grateful for your encouragement and support. You have made me feel like your own daughter. You are an inspiration to Jay and I, a model of how we want to be when we grow up. You have raised a wonderful son, who has made my life complete. You should be extremely proud of the man he has become. Thank you for all you have done for us. Erin, I am so glad you are my sister. Thank you for standing by me and giving me the confidence to push further. I am so proud of your accomplishments and I know you will be even more successful in the future than you already are! And to Uncle Bob and Aunt Jean, the "NY Hussey's", even though we are going back to MA, you can think of us as the Hussey's that finally made it out your way! I truly enjoyed our get-togethers and I look forward to many more to come when we come back to visit!

To Auntie Connie, you are a model of independence and strength. You have given me and taught me more than you know. You are very dear to my heart and I thank you for all you have done for me. I love you very much! To Nana and Pa DeMasi and Nana and Papa Frizzell, I know you have been watching over me from heaven and I hope I have made you proud. I miss you and love you all so much. And, to the rest of my colossal-size family, thank you for cheering me on!

Bobby, you are my number one brother and, despite our differences, I love you very much. My wish for you is to find your passion and to make it your life's accomplishment. Know that Jay and I will support you no matter what. Thank you for supporting me through the years; it means more than you know.

During the last few years, I have lost two of the greatest friends anyone could ask for. They gave me unconditional love, always wanted to have fun, and simply made me smile and laugh every time I saw them. Jake and Barron, you will always be my puppies, and I know you are playing together once again. Be good to one another and share your toys.

I am unable to adequately express my love and appreciation toward my parents, Bob and Paula Frizzell, for absolutely everything they have done for me. Mom and Dad, thank you for showing me endless support for my life decisions. You have taught me to succeed in love, cherish friendships, and support family no matter what the cost. You are models of strength, determination, and encouragement and you have shown me the importance of laughter to get through life. My accomplishments are a direct reflection of your hard work and parental guidance and I can only hope that I have made you half as proud as I am to be your daughter. I strive to be just like you one day (although Jay says "too late") and pass on your life lessons to my children. Mom and Dad, thank you for everything and I love you!

Most of all, I want to thank my husband, Jay Hussey, who has exemplified the true meaning of marriage. Jay, you are my best friend and you have pushed me to become more than I ever thought I could be. You have encouraged me to be a better person and never let me give up. And, although not a patient person by nature, you have displayed the utmost patience with me as I have gone through this endeavor. Just by being there and making me laugh every day got me through this. I could not have completed this without you. I am so lucky to be able to share my life with you and I look forward to the next chapter. Thank you and I love you!

After completing this journey, I have come to realize two things. First, I now have the confidence to say, "I am good enough and I will be successful." And, second, I have the best husband in the world…I think I'll keep him around for a while. ♣♥

TABLE OF CONTENTS

LIST OF FIGURES

LIST OF TABLES

LIST OF ABBREVIATIONS

α^{32}P-CTP	CTP labeled with ^{32}P in the alpha position
ADPR	ADP-ribose
AMD	Auto-modification domain
ANOVA	Analysis of variance
BER	Base excision repair
BranchMut	Excessive PAR Branching mutant
Br-UTP	Bromo-UTP, an NTP analog
BRCA1	Breast Cancer 1
BRCT	BRCA1 C-terminus motif
ΔBRCT	BRCA1 C-terminus motif domain deleted mutant
CATD	Catalytic domain
ΔCAT	Catalytic domain deleted mutant
CatMut	Catalytically inactive mutant
CDCS	Charcoal/dextran-treated bovine calf serum
cDNA	Complementary DNA
ChIP	Chromatin immunoprecipitation
ChIP-qPCR	Chromatin immunoprecipitation coupled to qPCR
ChIP-Western	Chromatin immunoprecipitation coupled to Western blot
DAVID	Database for Annotation, Visualization, and Integrated Discovery
DBD	DNA-binding domain
DBDMut	DNA-binding inactive mutant
ΔDBD	DNA-binding domain deleted mutant
DBD-NBD	DNA-binding domain and NAD^+-binding domain fusion

DNA	Deoxyribonucleic acid
dox	Doxycycline
E2	17β-estradiol, estrogen
ENCODE	Encyclopedia of DNA Elements
ERα	Estrogen receptor alpha
ESC	Embryonic stem cells
FACS	Fluorescence-activated cell sorting
FDR	False discovery rate
Fwd	Forward
GCOS	GeneChip operating software
GO	Gene ontology
GRO-seq	Global run-on sequencing
GT	Gallotannin, or tannic acid, i.e. PARG inhibitor
H3K27me3	Histone 3 lysine 27 trimethylation
H3K9me2	Histone 3 lysine 9 dimethylation
H3K9me3	Histone 3 lysine 9 trimethylation
HPLC	High pressure liquid chromatography
KD	Knockdown
Luc	Luciferase
macroH2A1, mH2A1	Histone variant macroH2A1
MCF-7	Michigan Cancer Foundation-7
MEM	Minimal essential medium
mRNA	Messenger RNA
NAD^+	Nicotinamide adenine dinucleotide (oxidized form)
NADS	NAD^+ Synthetase
NAMPT	Nicotinamide phosphoribosyltransferase

NBD	NAD^+-binding domain
ΔNBD	NAD^+-binding domain deleted mutant
NES	Nuclear export signal
NLS	Nuclear localization signal
NMNAT-1, -2, or -3	Nicotinamide mononucleotide adenylyltransferase
NPT	Nicotinate phosphoribosyl transferase
NRK1, or 2	Nicotinic acid riboside kinase
NRO	Nuclear run-on
PAR	Poly(ADP-ribose)
PARG	Poly(ADP-ribose) Glycohydrolase
PARP-1	Poly(ADP-ribose) Polymerase-1
PARPs	Poly(ADP-ribose) Polymerases
PARylation	Poly(ADP-ribosyl)ation
pCMV5	Mammalian expression vector
PCR	Polymerase chain reaction
PELP1	Proline, glutamate, and leucine rich protein 1
pET19b	Bacterial expression vector
PhosMut	Phosphorylation mimic mutant
PI	Pausing index
PJ34	PJ34, i.e. PARP inhibitor
pSUPER	Retroviral shRNA expression vector
pSUPER-TO	Retroviral shRNA expression vector (Tet-inducible)
pQCXIH	Retroviral mammalian expression vector
qPCR	Quantitative PCR
RNA	Ribonucleic acid
RNA Pol II	RNA polymerase II

RT-qPCR	Reverse transcription coupled with qPCR
Rvs	Reverse
SEM	Standard error of the mean
shRNA	Short hairpin RNA
SIRT1	Sirtuin 1
TetR	Tet repressor
TO	Tet operon
TPA	12-O-Tetradecanoylphorbol-13-acetate
TSS	Transcription start site
UTR	Untranslated region (5’ or 3’)
Wt	Wild-type

CHAPTER 1

PAR-Regulating Enzymes: Biological Functions And Therapeutic Potential*

* This chapter contains sections from two published reviews, namely, (i) Wacker DA, Frizzell KM, Zhang T, and Kraus WL. Regulation of Chromatin Structure and Chromatin-dependent Transcription by Poly(ADP-ribose) Polymerase-1: Possible Targets for Drug-based Therapies. *Subcellular Biochemistry*. 2007; 41:45-69. © The JJIAM Publishing Committee and Springer; and (ii) Frizzell KM and Kraus WL. PARP Inhibitors and the Treatment of Breast Cancer: Beyond BRCA1/2? *Breast Cancer Research*. 2009; 11:111. © BioMed Central The Open Access Publisher. Minor modifications have been made.

1.1. Summary

Poly(ADP-ribosyl)ation (PARylation) is an enzymatic reaction identified nearly 50 years ago whereby ADP-ribose units from donor nicotinamide adenine dinucleotide (NAD^+) molecules are covalently attached in succession onto target proteins (Chambon et al., 1963). This post-translational modification occurs via glycosidic ribose-ribose linkages to form linear or branched structures and is collectively known as poly(ADP-ribose) (PAR) (D'Amours et al., 1999). The regulation of PAR is overseen by a multitude of enzymes; in particular, those that polymerize and those that hydrolyze PAR chains (D'Amours et al., 1999; Kim et al., 2005). Herein, I discuss the molecular functions and interplay of these enzymes in various cellular activities. Of particular focus, I highlight the findings from knockout animal models and discuss the contributions to physiological and disease states. Finally, I discuss the development of PARP-1 and PARG chemical inhibitors, their therapeutic applications, and their future potential for disease treatments.

1.2. Synthesis of PAR by PARPs

PAR Polymerases (PARPs) have been identified from bacteria to humans, although absent from yeast (Hassa et al., 2006; Otto et al., 2005). In mammalian cells, PAR is mainly produced by PARP-1 (Hassa and Hottiger, 2008), the founding member of the PARP family (Ame et al., 2004), which is comprised of 17 additional members, identified as such through catalytic domain conservation (Ame et al., 2004; Hakme et al., 2008; Hassa and Hottiger, 2008; Schreiber et al., 2006). Some members possess only the ability to transfer a single ADP ribose molecule onto target proteins.

Recently, a more accurate nomenclature has been proposed in order to distinguish mono(ADP-ribosyl) transferases (mARTs) from PARPs (Hottiger et al., 2010).

PARP family members are located in nearly all cellular compartments, including the nucleus, cytoplasm, and mitochondria. PARPs 1-5 [PARP-1, PARP-2, PARP-3, PARP-4 (a.k.a. v-PARP), and PARP-5a and PARP-5b (a.k.a. tankyrase-1 and -2)] are genuine PARPs, containing a conserved glutamate (Glu 988 in PARP-1) that confers PARP catalytic activity (Krishnakumar and Kraus, 2010). They are all exclusively localized in the nucleus, with the exception of PARP-4, which also localizes to vault particles (Ame et al., 2004; Hakme et al., 2008; Hassa and Hottiger, 2008; Schreiber et al., 2006). PARPs 6-8, 10-12, and 14-16 are identified or putative mARTs, some of which can be found in the nucleus, although not exclusively. Some PARPs, such as PARP-9 and -13 (also partially nuclear), lack specific NAD^+ binding or conserved catalytic residues and are likely inactive (Kleine et al., 2008). Many of the PARP family members function in a wide variety of cellular processes, including DNA repair, transcription, genomic maintenance, apoptosis, cell signaling, and cell-cycle regulation. However, the functions of some members are less defined or have yet to be identified (Ame et al., 2004; Hakme et al., 2008; Hassa and Hottiger, 2008; Schreiber et al., 2006). Both subcellular localization and function are likely to be defined by the particular structural and functional domains they each contain. Understanding the domain structures for each PARP family member will provide useful information toward understanding their individual functions.

PARP-1 is a highly conserved ~116 kDa nuclear protein (D'Amours et al., 1999) consisting of three major domains: (i) an amino-terminal DNA binding domain (DBD), (ii) a central auto-modification domain (AMD), and (iii) a carboxy-terminal catalytic domain (CATD) (Figure 1.1A; (Krishnakumar and Kraus, 2010)). The DBD contains two zinc finger motifs (Cys-Cys-His-Cys; FI/Zn1 and FII/Zn2), which confer

PARP-1 binding to damaged DNA, specific sequences, structures, or nucleosomes (Kraus, 2008; Kraus and Lis, 2003). Recently, a third zinc-binding domain, termed Zn3, was identified to bind zinc, but not to DNA and specific residues within this domain have been shown to mediate the DNA-dependent activation of PARP-1 enzymatic function (Langelier et al., 2010; Langelier et al., 2008; Tao et al., 2008). In addition, the DBD contains a nuclear localization signal (NLS) and a caspase-3 cleavage site (Hakme et al., 2008; Schreiber et al., 2006). The AMD contains a BRCA1 C-terminus-like motif (BRCT), which plays important roles in mediating protein-protein interactions that can also allosterically stimulate PARP-1 catalytic activity (D'Amours et al., 1999; Kim et al., 2005; Kraus and Lis, 2003). The CATD contains a 50 amino acid active site termed the "PARP signature motif", which confers NAD^+ binding and ADP-ribosyl transferase activity (Figure 1.1B; (D'Amours et al., 1999; Rolli et al., 2000)). The CATD, and more specifically the PARP signature motif, are highly conserved through evolution, as well as among PARP family members. Not only is the primary amino acid sequence conserved, crystal structures of many of the PARP family member catalytic domains have displayed highly analogous folds and structures to one another (Krishnakumar and Kraus, 2010).

1.3. Functional Consequences of PAR Modification

PARP-1 catalytic activity is regulated through a variety of allosteric mechanisms, including physical interactions that can stimulate its catalytic function. Although PARP-1 enzymatic activity is targeted to many nuclear proteins including transcription factors, histones, and DNA repair factors, the main target is PARP-1 itself (Kim et al., 2005). Whether this auto-PARylation reaction occurs in *cis* or *trans* has been debated, but is primarily thought to be intermolecular (Altmeyer and

Hottiger, 2009; Alvarez-Gonzalez and Mendoza-Alvarez, 1995; Langelier et al., 2010; Mendoza-Alvarez and Alvarez-Gonzalez, 1993; Mendoza-Alvarez and Alvarez-Gonzalez, 1999). The actual residues of modification on target proteins are lysine, glutamate, and aspartate residues. Some studies have begun to identify modification sites of target proteins, but the list is not extensive (Altmeyer and Hottiger, 2009).

The PAR modification itself can contain as many as 200 ADP-ribose (ADPR) units and can vary in length and complexity. Based on its chemical similarity to DNA and RNA, PAR has been referred to as the "third type of nucleic acid" (D'Amours et al., 1999), which is highly negative in charge. The structure and complexity of PAR itself (linear or branched) may also vary depending on the specific PARP enzyme that synthesizes it and the cellular condition under which it is synthesized (Figure 1.1B). In addition, since many of the PARPs perform the same enzymatic reaction using the same NAD^+ substrate, determining which PARP is responsible for modifying a protein has been more than challenging *in vivo*. However, a recent study utilized a clickable NAD^+ analog to label PARP-1 or tankyrase-1 target proteins in cells and subsequently affinity purified and identified the PARylated proteins by mass spectrometry (Jiang et al., 2010). Although this study brings the field one step closer, more work needs to be done to truly identify targets of specific PARP proteins.

What are the functional consequences of such a massive post-translational modification? PAR modification on target proteins can impact their function and important molecular interactions. PAR may alter the activity of PARylated proteins by functioning as a site-specific covalent modification or a steric hindrance (Kim et al., 2005; Krishnakumar and Kraus, 2010). For example, inhibition of PARP-1's DNA binding activity by autoPARylation may be the result of charge repulsion between PAR and DNA, or steric effects of PAR that mask PARP-1's DBD (D'Amours et al., 1999). PARylation of some transcription factors (*i.e.,* p53, CREB) affects their DNA-

Figure 1.1. PARP-1 and PARG are regulators of protein PARylation. *A,* Schematic diagram of the human PARP-1 and PARG structural and functional domains. For PARP-1 (*top*), the DNA binding domain, zinc fingers (FI and FII), nuclear localization signal (NLS), third zinc binding domain (Zn3), automodification domain, BRCA1 c-terminal-like motif (BRCT) are shown. The PARP "signature" motif is also shown within the catalytic domain and NAD^+-binding region. The star indicates the region of modification of PARP-1 itself. For PARG (*bottom*), the nuclear localization signal (NLS) and nuclear export signal (NES) are shown within the regulatory domain, and the active site is shown within the catalytic domain. *B*, PARP-1 and PARG chemical reaction. PARP-1 utilizes NAD^+ to PARylate target proteins in the nucleus. The by-produce of this reaction is nicotinamide, a natural PARP inhibitor. PARG hydrolyzes PAR chains through endo- and exo-glycosidic activities to release ADPR monomers and short polymers.

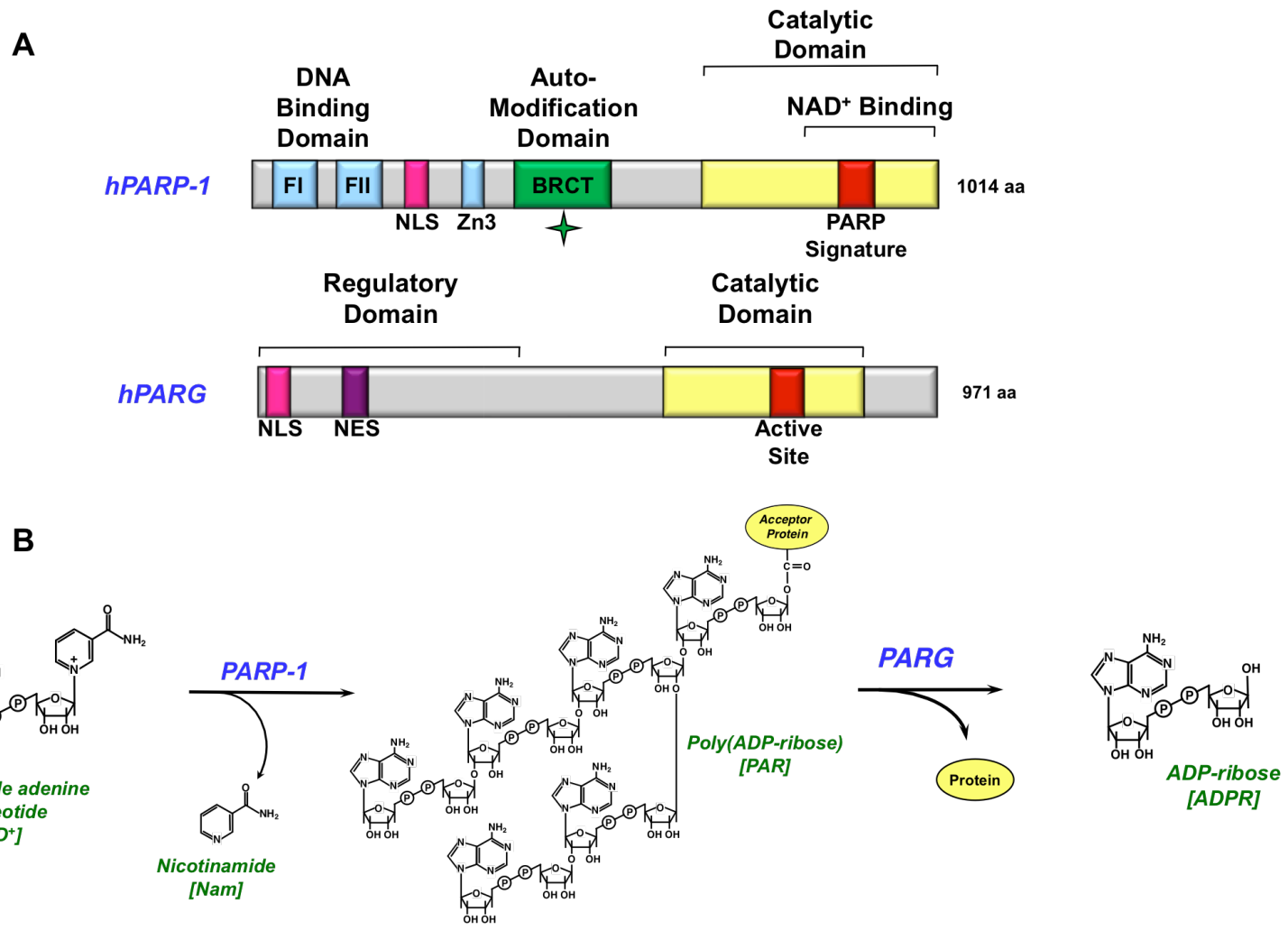
A
Catalytic Domain
DNA Binding Domain
Auto-Modification Domain
NAD+ Binding
hPARP-1
FI
FII
BRCT
1014 aa
NLS
Zn3
PARP Signature
Regulatory Domain
Catalytic Domain
hPARG
971 aa
NLS
NES
Active Site
B
Acceptor Protein
PARP-1
PARG
Nicotinamide adenine dinucleotide [NAD+]
Nicotinamide [Nam]
Poly(ADP-ribose) [PAR]
Protein
ADP-ribose [ADPR]

binding activities, leading to alterations of transcriptional outcomes (Kim et al., 2005). PARylation can also inhibit the formation of transcription complexes by preventing or promoting certain protein-protein interactions at gene promoters (Ju et al., 2004; Pavri et al., 2005). In addition, PARylation of histones, for example, may alter the chromatin conformation by preventing or promoting the association of chromatin binding proteins or other chromatin components (Krishnakumar et al., 2008).

Furthermore, PAR may act as a protein-binding matrix for a variety of nuclear proteins. To date, at least three types of PAR-binding motifs or domains have been identified, namely (i) an eight-amino acid PAR-binding motif, (ii) a PAR-binding zinc-finger motif, and (iii) macrodomains. Proteins that contain these motifs or domains interact with PAR, which leads to the targeting of those proteins to sites of PAR synthesis or to the regulation of the protein activity upon PAR binding. For example, the histone variant macroH2A1.1 is recruited to sites of DNA damage-induced PARP-1 activation and PAR synthesis in the nucleus, the result of which leads to chromatin compaction, altering DNA repair responses (Timinszky et al., 2009). In fact, the interaction of macroH2A1.1 with PARP-1 is dependent on the ability of macroH2A1.1 to bind PAR (Timinszky et al., 2009). Interestingly, macrodomains can also bind other NAD^+ metabolites, such as O-acetyl-ADP-ribose, the byproduct of sirtuin-mediated deacetylase reactions, and ADPR, the resulting product of PAR hydrolysis reactions (Karras et al., 2005). These metabolites have the ability to compete with PAR-binding, ultimately disrupting macroH2A1.1-protein interactions. DEK, an oncoprotein involved in DNA repair and chromatin organization, is PARylated by PARP-1 leading to its release from the chromatin (Gamble and Fisher, 2007; Kappes et al., 2008). Recently, DEK was shown to bind PAR via three functional PAR-binding sites in a manner dependent on PAR length and can interfere with the multimerization activities of DEK (Fahrer et al., 2010).

This demonstrates that the modification of proteins by PARP-1 and the interaction with the PAR modification can play separate roles, but may not be mutually exclusive.

1.4. Catabolism of PAR by PARG

The major enzyme responsible for the degradation of PAR is Poly(ADP-ribose) Glycohydrolase (PARG) (Amé et al., 2000; Davidovic et al., 2001), which catalyzes the hydrolysis of PAR to produce ADP-ribose monomers and short polymers (Figure 1.1B; (Davidovic et al., 2001)) via endo- and exoglycosidic enzymatic activities. While PARG is the major contributor to PAR degradation, other enzymatic activities exist than can also remove PAR or ADPR monomers from target proteins (*i.e.,* poly- and mono(ADP-ribosyl) protein hydrolase and mono(ADP-ribosyl) protein lysase (Hassa and Hottiger, 2008; Kim et al., 2005)). In addition, a recent study has identified a "PARG-like" protein, namely ADP-ribose-protein-hydrolase-3 (ARH3), shown to possess intrinsic PARG activity, but has yet to be fully characterized (Oka et al., 2006). This finding suggests that the mammalian genome may actually encode other proteins with PAR hydrolysis functions. Perhaps their roles in PAR removal may be distinctly defined based on the structure of individual PAR molecules.

PARG is a highly active enzyme but has been relatively hard to study due to its low cellular abundance (Davidovic et al., 2001; Meyer-Ficca et al., 2005a). Although PARP-1 may be present at a 5- to 20-fold molar excess over PARG in some cell types, PARG has a higher specific activity than PARP-1 and its enzymatic activity increases with increased PAR length (D'Amours et al., 1999). Specifically, highly branched or short polymers are degraded slowly and long linear polymers are degraded quickly (Hassa and Hottiger, 2008). This rapid hydrolysis results in a bulk PAR half-life of as

little as one minute (under certain conditions), while the short ADPR polymers can have a half-life of up to ten minutes (Bonicalzi et al., 2005).

There is only one gene encoding PARG in humans, but multiple splice variants and cleavage products have been reported, all of which have catalytic activity (D'Amours et al., 1999; Lin et al., 1997; Meyer-Ficca et al., 2004). The longer sets of isoforms (~100 – ~110 kDa) are likely shuttled between the nucleus and cytoplasm, while the shorter isoform (~65 kDa) resides solely in the cytoplasm (Bonicalzi et al., 2005; Meyer-Ficca et al., 2004; Meyer-Ficca et al., 2005a; Min and Wang, 2009). The larger PARG isoforms consists of two major domains: (i) an amino-terminal regulatory domain, and (ii) a carboxy-terminal catalytic domain (Figure 1.1A; (Bonicalzi et al., 2005; Min and Wang, 2009)). The regulatory domain contains both a nuclear localization signal and a nuclear export signal, which mediate shuttling between the nuclear and cytoplasmic compartments. The catalytic domain contains the PARG active site, which confers both endoglycosidic and exoglycosidic activity to rapidly hydrolyze PAR (Kim et al., 2005; Kraus, 2008; Min and Wang, 2009). While PARP-1 and PARG enzymatic actions are intimately linked, the details of their functional interplay have not been explored in detail.

1.5. Regulation of PARP-1 and PARG Enzymatic Activities

PARP-1 and PARG enzymatic activities regulate the dynamics of PAR, as described above. However, the activation or inactivation of the enzymes themselves is also subject to regulatory mechanisms. Although the regulators of PARP-1 enzymatic activity have been studied in some depth, recent studies have uncovered new modes of PARP-1 enzymatic regulation. Only a few methods of regulating PARG enzymatic activity have been determined, but it is feasible to think that many of the same

regulatory mechanisms for PARP-1 can be applicable to PARG and vice versa (Figure 1.2). However, much work needs to be done in order to fully understand the regulatory mechanisms of both of these enzymes.

1.5.1. Interactions with DNA and Proteins

As mentioned above, PARP-1 enzymatic function can be allosterically modulated by a variety of mechanisms. In particular, PARP-1 activity is stimulated upon binding to DNA sequences, structures (*i.e.,* double strand or single strand breaks, crossovers, or hairpins), and nucleosomes via interactions involving the DBD (Kim et al., 2005; Kraus, 2008). A similar mechanism for PARG activation has yet to be identified, likely due to the lack of a DBD. However, a recent study determined that PARG localizes to gene promoters in a pattern similar to that of PARP-1, even without possessing a classic DNA binding domain (Frizzell et al., 2009). In support of this, PARP-1 and PARG have been shown to interact under certain conditions and in certain cell-types (Keil et al., 2006). It has been suggested that PARG interaction with PARP-1 can regulate PARP-1 activity (Cortes et al., 2004), but whether or not PARP-1 can modulate PARG activity remains unanswered.

In addition, PARP-1 binding within various protein complexes may also contribute to the regulation of PARP-1 activity. In this regard, PARP-1 is a known component of complexes involved in DNA repair, transcription, insulators, and DNA methylation. The interactions with specific proteins (*i.e.,* XRCC1, Mediator, CTCF, and Dnmt-1; (Caiafa et al., 2009; Caiafa and Zlatanova, 2009; El-Khamisy et al., 2003; Farrar et al., 2010; Guastafierro et al., 2008; Hassa et al., 2005; Heale et al., 2006; Ju et al., 2004; Malanga and Althaus, 2005; Pavri et al., 2005; Pleschke et al., 2000; Zampieri et al., 2009)) can stimulate PARP-1 activity, and in some cases, are targets of PARylation by PARP-1 (Kim et al., 2005; Kraus, 2008; Kraus and Lis,

2003). It is logical to suppose that PARG interactions with similar proteins may also regulate PARG activity, even if the interaction is less stable than that of PARP-1.

1.5.2. Post-translational Modifications

Like many other nuclear proteins, PARP-1 (and other PARPs) and PARG are subject to a host of covalent post-translational modifications that can alter their enzymatic functions. Studies focused on PARP-1 have begun to shed light on the functional consequences of some modifications while others are less well understood. These include PARylation, phosphorylation, acetylation, SUMOylation, and ubiquitylation (Krishnakumar and Kraus, 2010). For example, PARylation of PARP-1 can inhibit its DNA binding and catalytic activities (D'Amours et al., 1999), as well as cause the release of PARP-1 from chromatin (Kim et al., 2004; Tulin and Spradling, 2003; Wacker et al., 2007), while phosphorylation and acetylation of PARP-1 can stimulate its enzymatic activity under certain conditions (Hassa et al., 2005; Kauppinen et al., 2006; Rajamohan et al., 2009; Zhang et al., 2007). SUMOylation and ubiquitylation of PARP-1 are fairly recent discoveries that seem to modulate the role of PARP-1 as a regulator of chromatin structure and transcription (Krishnakumar and Kraus, 2010; Martin et al., 2009; Messner et al., 2009). How these modifications specifically regulate PARP-1 DNA binding or enzymatic activities have not been defined. But, the role of PARP-1 in regulating chromatin structure and transcription can depend on its enzymatic activity in some cases (Petesch and Lis, 2008).

On the other hand, a recent proteomic analysis has identified phosphorylation sites for PARG (as well as PARP-1 and PARP-2) caused by various kinases (Gagne et al., 2008), the consequence of which has yet to be elucidated. It is likely that these other modifications exist for PARG but have not been identified to date. It will be interesting to determine which modifications occur for both PARP-1 and PARG and if

Figure 1.2. Regulating the enzymatic state of PARP-1 and PARG in vivo. As described in the text, there are multiple factors that determine whether or not PARP-1 and PARG are enzymatically inactive or active. These factors include physical interactions, modifications, and substrate availability. They can have both positive and negative contributions toward either state and are likely not mutually exclusive. Together, they contribute to the regulation of PARP-1 and PARG enzymatic activities.

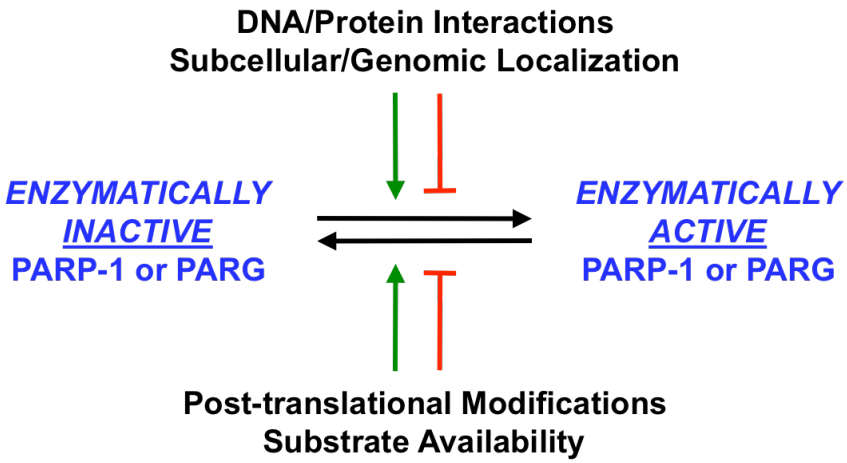
DNA/Protein Interactions
Subcellular/Genomic Localization
ENZYMATICALLY
INACTIVE
PARP-1 or PARG
ENZYMATICALLY
ACTIVE
PARP-1 or PARG
Post-translational Modifications
Substrate Availability

similar enzymes are responsible for those modifications. This information may be helpful in understanding the interplay of PARP-1 and PARG molecular actions.

1.5.3. Substrate Availability

One of the most important factors in the regulation of PARP-1 and PARG enzymatic activities is the availability of their respective substrates. Therefore, local concentrations of NAD^+ and PAR are important, and can be modulated. NAD^+ is synthesized in the nucleus (and other cellular compartments) through a de novo pathway and a salvage pathway [(Berger et al., 2004; Rongvaux et al., 2003), reviewed in (Kim et al., 2005)]. The salvage pathway leads from nicotinamide and is catalyzed by the enzymes nicotinamide phosphoribosyltransferase (NAMPT) and nicotinamide mononucleotide adenylyltransferase (NMNAT-1, the nuclear form). Nicotinamide, the byproduct of the PARP-1 (and SIRT1) reaction, is a natural inhibitor of PARP-1 (and SIRT1). The production of NAD^+ and subsequent depletion of nicotinamide can positively contribute to PARP-1 action by supplying a local pool of NAD^+ (Pillai et al., 2005). Accordingly, NMNAT-1 has been shown to physically interact with PARP-1, stimulating its activity (Berger et al., 2004). A recent study has demonstrated that SIRT1 can recruit NMNAT-1 to target gene promoters, most likely to supply NAD^+ for SIRT1-dependent deacetylase reactions (Zhang et al., 2009). Although not yet shown, a similar mechanism likely exists for PARP-1-dependent PARylation reactions. In addition, PARP-1, SIRT1, and other NAD^+-utilizing enzymes (*i.e.,* other PARPs, etc.) may compete for the nuclear or local NAD^+ supply, which may also contribute to the regulation of PARP-1 activity.

All of these modes of PARP-1 regulation can ultimately lead to changes in how much PAR is synthesized and how complex its overall structure is. As noted above, the length and branching complexity of PAR, can determine how active PARG

is in degrading the PAR modification. Specifically, short polymers in low abundance or highly branched polymers are not catabolized as fast as long linear polymers (Bonicalzi et al., 2005). This in turn, can modulate the half-life of PAR as well as the production of ADPR, the end result of the PARG hydrolysis reaction.

1.5.4. Subcellular and Genomic Localization

The localization of PARP-1 and PARG among subcellular compartments is likely to contribute to their overall function, including their enzymatic activities. This is more clearly demonstrated in the case of PARG, where more than one isoform exists and their subcellular localizations are different. For example, the longer isoforms of PARG can shuttle between the nucleus and cytoplasm, while the shorter isoform is found in the mitochondria (Bonicalzi et al., 2005; Meyer-Ficca et al., 2004; Meyer-Ficca et al., 2005a; Min and Wang, 2009). While the full-length isoform is highly active, the cytoplasmic isoforms are in higher abundance and also exhibit high activity (Bonicalzi et al., 2005). It is feasible that the actual localization of the individual molecules determines their function, and subsequently, the importance of their activities. Interestingly, the PARG-like protein ARH3 also localizes to the mitochondria (Oka et al., 2006), and may contribute to PAR regulation in that context. Although PARP-1 is mainly nuclear, a recent study has determined that there exists a small pool of PARP-1 that localizes to the mitochondria in a manner dependent on mitofilin interaction (Rossi et al., 2009). It is becoming increasingly clear why various PARPs and PARG (or PARG-like proteins) localize to the same subcellular compartments, namely for localized PAR regulation. However, more work is necessary to determine what the concerted actions of these enzymes are and how their enzymatic (and potentially other) functions are regulated within those compartments.

Recently, it was determined that PARP-1 localizes to the promoters of expressed genes (Krishnakumar et al., 2008). Likewise, a gene-specific analysis of PARG localization patterns on chromatin in the same cell line revealed that PARG also binds gene promoters in a similar pattern as PARP-1 (Frizzell et al., 2009). In fact, PARP-1 and PARG promoter localization is, in some cases, dependent on one another (Frizzell et al., 2009). It has also been reported that PARP-1 can bind to intergenic regions, although the consequence of this binding pattern was not investigated (Krishnakumar et al., 2008). The promoter and intergenic binding of these factor(s) suggests that they may play different roles depending on where the factor(s) are localized, which may also depend on the chromatin structure, composition, and histone modifications (Krishnakumar et al., 2008). It will be interesting to understand the role of PARP-1 binding to intergenic regions and in what cellular functions does it participate from these locations.

1.6. Molecular Actions of PAR-regulating Enzymes

PARP-1, and likely PARG, molecular actions contribute to a variety of cellular processes, including DNA damage detection and repair, cell death pathways, insulator function, regulation of DNA methylation patterns, and regulation of chromatin structure and transcription. For the latter, PARP-1 has also been linked to a variety of signal-mediated transcriptional pathways. The regulation of many of these processes contributes to the broad roles of PARP-1 and PARG in maintaining genomic integrity. Since these molecular actions have been reviewed extensively elsewhere, we provide a brief description for each and highlight the major findings to date. In addition, we speculate as to the contributions of PARG in each process (Table 1.1).

1.6.1. DNA Damage Detection and Repair

PARylation of proteins upon DNA damage induced by oxidation, alkylation, and ionizing radiation is a rapid and dramatic response. PARP-1 binding to sites of DNA damage, including single- and double-strand breaks, potently activates its enzymatic activity (Kim et al., 2005). PARP-1 has been shown to play a role in at least three DNA repair pathways: single-strand break (SSB) repair, double-strand break (DSB) repair, and, base excision repair (BER) (Bouchard et al., 2003; Woodhouse and Dianov, 2008). In addition, PARP-1 may also play a role in the repair of oxidative base damage or UV-induced pyrimidine dimers in a pathway dependent on Cockayne syndrome B protein (Flohr et al., 2003). Notably, PARP-2 has also been implicated in BER (Schreiber et al., 2002; Yelamos et al., 2006), which confirms the notion that PARP-1 and PARP-2 have redundant functions. In support of this, PARP-1 and PARP-2 double knockout mice show considerable genomic instability prior to embryonic lethality (Menissier de Murcia et al., 2003). Under low levels of DNA damage, PARP-1 acts as a survival factor by detecting and binding DNA damage sites. However, when DNA damage levels are extremely high, PARP-1 promotes cell death through at least two modes, (i) energy failure-induced necrosis by massively depleting NAD^+ levels (and ultimately ATP), and (ii) apoptosis-inducing factor-dependent apoptosis (Kim et al., 2005; Krishnakumar and Kraus, 2010).

The role of PARP-1 in DNA repair and the outcomes listed above are likely to be determined by which repair proteins are physically associating or recruited to sites of DNA damage and PARylation. For example, PARP-1 can interact with, and in some cases PARylate, DNA damage detection and response proteins (*i.e.,* ATM, p53; (Bouchard et al., 2003)), DNA repair proteins (*i.e.,* XRCC1, DNA ligase III; (El-Khamisy et al., 2003; Pleschke et al., 2000)), and chromatin components (*i.e.,* H1, H2B) that regulate the opening of chromatin structure. Interestingly, PARG has been

Table 1.1. Potential roles for PARG in cellular processes involving PARP-1. While PARP-1 is known to function in various cellular processes, a role of PARG in these processes is just beginning to emerge. This table summarizes known or speculated connections for PARG to many of the cellular processes of which PARP-1 is known to be involved. This suggests a potential role for PARG in these cellular functions, and warrants further investigation.

Speculated Roles for PARG in Various Cellular Processes

(a) DNA Repair (SSBR, DSBR, BER)
- PARG interacts with DNA repair proteins (*i.e.,* XRCC1; (Keil et al., 2006))
- PARG contributes to local ATP production via PAR hydrolysis?
- PARG regulates PARP-1 PARylation activity?

(b) Cell Death Pathways (Apoptosis, necrosis)
- PARG contributes to local ATP production via PAR hydrolysis?
- Mitochondrial PARG involved in AIF release?
- PARG regulates PAR after caspase-dependent cleavage?

(c) Insulator Function
- PARG dynamically regulates PAR at insulators?

(d) Regulation of DNA Methylation
- PARG regulates Dnmt1 expression? (Zampieri et al., 2009)
- PARG regulates DNMT1 activity via DNMT1-PAR binding?

(e) Modulation of Chromatin Structure
- PARG promoter binding is similar to PARP-1 (Frizzell et al., 2009)
- PARG dynamically regulates PARylation of histones/chromatin-binding factors?

(f) Transcriptional Regulation (Basal, signal-mediated)
- PARG functions as a transcriptional coregulator (Hanai et al., 2004)
- PARG dictates the localization of transcriptional coregulators (Tulin et al., 2005)
- PARG directly regulates PARP-1 function?
- PARG dynamically regulates PAR and/or ADPR at promoters?

shown to interact with some of the same proteins (*i.e.,* XRCC1; (Keil et al., 2006)), which may be dependent on a physical interaction with PARP-1 itself. Although the role of PARG in DNA damage repair is not completely understood, some studies suggest that PARG contributes in at least two ways. First, by creating free ADPR via PAR hydrolysis, PARG (and ADP-ribose pyrophosphorylase) participates in the local production of ATP molecules. In this regard, ATP is absolutely required for the DNA replication and ligase activities that occur in order to sufficiently repair damaged DNA sites (Oei and Ziegler, 2000). Second, PARG may regulate the activity of PARP-1 in the PARylation of target proteins. This action of PARG has yet to be shown, but the idea makes sense considering the deletion of the full-length PARG isoform in mice down-regulates PARP-1 auto-modification. Overall, the actions of PARP-1 and PARG in DNA damage repair and detection are considerable, but more studies are needed to discern the exact mechanisms of action within each repair pathway.

1.6.2. Cell Death Pathways

Under conditions of extensive DNA damage, PARP-1 acts to promote cell death, as noted above. To do so, PARP-1 acts in at least two ways, (i) energy failure-induced necrosis, and (ii) apoptosis-inducing factor (AIF)-dependent apoptosis (Kim et al., 2005). With respect to the former, PARP-1 over-activation leads to massive depletion of NAD^+ and ATP pools, and subsequently, complete cellular energy failure. In this regard, actively dividing cells that are dependent on ATP are more sensitive to this catastrophic energy depletion, resulting in necrotic cell death (Zong et al., 2004). With respect to the latter, in a more ordered response, PARP-1 activation induces the translocation of AIF from the mitochondria to the nucleus (Yu et al., 2002). There, AIF induces chromatin condensation and subsequent DNA fragmentation (Susin et al., 1999). The mechanism of how PARP-1 triggers the release of AIF from mitochondria

is not clear, but may involve the small fraction of PARP-1 that localizes to the mitochondria. PARG may be involved in this process by preventing massive cell death through replenishing ATP pools, therefore guiding the cell toward apoptosis as opposed to necrosis (Table 1.1; (Desnoyers et al., 1995)). It is also possible that the mitochondrial PARG is involved in AIF release. The decision to enter a necrotic versus apoptotic pathway is likely to be regulated by a number of factors (*i.e.,* type, strength, and duration of the DNA damage stimulus) and much work is needed to understand the triggering mechanisms of one pathway versus the other.

Once a cell is committed to the apoptotic pathway, caspase-dependent cleavage of both PARP-1 and PARG occurs (Affar et al., 2001; Boulares et al., 1999). For PARP-1, this cleavage results in a short N-terminal fragment and a longer C-terminal fragment that retains basal activity, but lacks the ability to be induced by DNA damage (Kaufmann et al., 1993). This can protect the cell from ATP depletion and from entering the necrotic pathway. Likewise, PARG cleavage results in the generation of a C-terminal fragment that retains full PAR hydrolysis activity (Affar et al., 2001). Although not completely understood, the caspase-dependent cleavage of PARP-1 and PARG suggest a higher level of regulation for these two enzymes as they modulate PAR metabolism during apoptosis.

1.6.3. Insulator Function

Some time ago, PARP-1 was implicated in regulating the DNA-binding factor CTCF, at transcriptional insulators (Yu et al., 2004). Specifically, the ability of CTCF to limit the extent of expression of a specific locus (*i.e., Igf2-H19*), through changes in chromatin structure, was dependent on PARylation. More generally, this group showed that many sites of PARylation were also sites of CTCF occupancy on the genome, although the functional significance of this observation was not clear. Also,

CTCF was immunoprecipitated from cells and it was determined that it was, indeed, PARylated. More recently, the PARylation sites of the CTCF protein were determined (Farrar et al., 2010). And, upon mutating these sites, CTCF function in transcriptional activation, insulator function, and the inhibition of cell proliferation were disrupted, demonstrating a functional significance of PARylation of CTCF. Interestingly, PARP-1 and CTCF were recruited to the same genomic loci, and presumably interact, in a manner independent of CTCF PARylation. Although PARG has not been studied for a role in insulator function, it is feasible to imagine that PARG contributes to the dynamic regulation of PAR at insulators.

1.6.4. Regulation of DNA Methylation Patterns

One of the newest roles for PARP-1 in the cell is regulating DNA methylation patterns, which is generally associated with gene repression. PARP-1 can regulate the expression and activity of the DNA methyltransferase Dnmt1 (Caiafa et al., 2009; Caiafa and Zlatanova, 2009; Guastafierro et al., 2008), the enzyme that creates this stable, epigenetic mark on DNA. Specifically, PARP-1 binds to the promoter of the Dnmt1 gene and protects it from silencing by DNA methylation in a PAR-dependent manner. Interestingly, over-expression of PARG leads to atypical DNA methylation at the Dnmt1 promoter, leading to Dnmt1 silencing (Zampieri et al., 2009). Although a role for PARP-1 in regulating DNA methylation has been emerging, this study is the first to demonstrate a role and a mechanism for PARG in this process. Interestingly, Dnmt1 can bind PAR, which inhibits its methyltransferase activity (Reale et al., 2005). Furthermore, PARyation of CTCF may contribute to this process by providing a PAR source for the inactivation of Dnmt1 (Guastafierro et al., 2008). Further studies are needed to fully elucidate the mechanisms of PARP-1 and PARG function in this area.

1.6.5. Regulation of Chromatin Structure

Several studies demonstrating the regulation of chromatin structure by PARP-1 and PARG have emerged over the last decade. Modulation of chromatin structure can affect the transcriptional outcomes of underlying genes as well as the ability of DNA repair and replication enzymes to access the DNA during DNA repair and cell death pathways. As shown in the earlier studies, PARP-1 could disrupt chromatin structure by PARylating histones, which resulted in the destabilization of nucleosomes (Huletsky et al., 1989; Mathis and Althaus, 1987; Poirier et al., 1982). Other studies have shown that PARP-1 can PARylate chromatin-associated (non-histone) proteins or complexes, also resulting in changes in chromatin structure. For example, the nucleosome remodeling ATPase, ISWI, is inactivated upon PARylation in *Drosophila* (Sala et al., 2008). In addition, proteins containing PAR-binding motifs or domains can be recruited to sites of PARylation in the genome (Timinszky et al., 2009). If such proteins are chromatin-associated components, such as the histone variant macroH2A1, chromatin structure could also be affected. Furthermore, biochemical assays show that PARP-1 can bind to nucleosomes and compact the chromatin by bringing neighboring nucleosomes together (Kim et al., 2005; Wacker et al., 2007). In the presence of NAD^+, PARP-1 undergoes auto-PARylation and releases from the nucleosomes, resulting in the decondensation of chromatin (Kim et al., 2005; Wacker et al., 2007). This action can be reversed with the addition of PARG, resulting in the reduction of PAR and the allowing of PARP-1 to re-engage interactions with nucleosomes, as expected (Kim et al., 2005). Many studies in *Drosophila* have shown that PARP inhibition or disruption of the dPARP gene blocks PAR accumulation, chromatin decondensation, and transcription at inducible genes (*i.e.,* the heat shock gene, *Hsp70*) (Petesch and Lis, 2008; Tulin et al., 2003; Tulin and Spradling, 2003; Tulin et al., 2002). Interestingly, one study suggests that dPARP is required for the

wholesale opening of the chromatin at the *Hsp70* locus upon heat shock in a transcription-independent manner, further emphasizing a role for PARP-1 in the regulation of chromatin structure (Petesch and Lis, 2008).

Although the biochemical results suggest a simple model of chromatin compaction and decondensation *in vitro*, the mechanisms of chromatin structure regulation in mammalian systems are somewhat less clear. A recent genomic localization study demonstrated that PARP-1 localizes to the promoters of almost all actively transcribed genes (Krishnakumar et al., 2008), suggesting a role for PARP-1 in promoting chromatin formation that is permissive to transcription. Likewise, a recent study showed that PARG localizes to promoters of a subset of genes in a pattern similar to that of PARP-1 (Frizzell et al., 2009), although the genomic localization pattern is still unknown. PARP-1 has been shown to be able to modulate the association of chromatin-binding factors, such as the linker histone H1 and DEK, both of which function in transcriptional repression (Gamble and Fisher, 2007; Kappes et al., 2008). Additionally, PARylation of the insulator protein CTCF can lead to the compaction of chromatin to higher order structures (Guastafierro et al., 2008). In almost all of these examples, the enzymatic functions of PARP-1 and PARG are required to regulate chromatin structure through PARylation of histones or associated factors. However, the functional consequences of specific chromatin structure formation at specific genomic regions remain to be determined.

The regulation of chromatin structure in mammalian systems seems to be more complicated than that in *Drosophila*, for example, where more than one mechanism of regulation may apply. Also, there have been no reports of wholesale opening or closing of chromatin structure at specific gene loci in mammalian cells; however, localized changes in chromatin structure or composition have been described (Ju et al., 2006; Kim et al., 2004; Krishnakumar et al., 2008). This suggests that PARP-1

function in the regulation of chromatin structure in higher order eukaryotes may have evolved beyond the simpler models described in *Drosophila*.

1.6.6. Transcriptional Regulation

Many studies have demonstrated a clear role for PARP-1 in transcriptional regulation, but only a handful of studies have demonstrated a role for PARG in gene expression. Furthermore, while PARP-1, and likely PARG, localizes to a large percentage of expressed genes (Krishnakumar et al., 2008), only a small percentage of those genes are actually regulated by PARP-1 (Frizzell et al., 2009). This suggests that transcriptional regulation is likely to involve multiple mechanisms. Although the data for PARG is still emerging, many of the same mechanisms of transcriptional regulation are likely to apply. Specifically, PARP-1 has been shown to regulate gene expression through (i) regulation of chromatin structure (discussed above), (ii) coregulator action, and (iii) insulator function (discussed below).

In the case of coregulator function, PARP-1 may be recruited to target promoters as a functional endpoint of signaling pathways. PARP-1 interactions with transcription factors (*i.e.,* NFκB, E2F-1; (Hassa et al., 2001; Hassa et al., 2005; Simbulan-Rosenthal et al., 2003)) or transcription complexes (*i.e.,* Mediator; (Ju et al., 2004; Pavri et al., 2005)) at promoters can mediate gene expression outcomes. For example, PARP-1 has been shown to mediate the exchange of (i) an inactive cdk8-positive Mediator subunit for an active cdk8-negative Mediator subunit during retinoic acid signaling (Pavri et al., 2005), and (ii) a TLE1 corepressor complex for a HAT-containing coactivator complex during signal-dependent gene regulation in neuronal cells (Ju et al., 2004). Interestingly, in addition to factor exchange, PARP-1 has been shown to recruit topoisomerase IIβ (TopoIIβ), which can cleave the promoter during hormone-induced transcriptional activation (Ju et al., 2006; Ju et al., 2004). This

result suggests a new potential mechanism of general transcriptional activation (*i.e.,* promoter cleavage), and it demonstrates a multi-pronged approach for gene regulation by PARP-1. Also, PARP-1 enzymatic activity is required for some of these functions and is likely to be cell type-, gene-, and signal-specific. For example, HES1-mediated transcription requires PARP-1 enzymatic activity, but not for NFκB- or RAR-mediated transcription (Hassa and Hottiger, 2002; Kraus and Lis, 2003).

Very few studies have focused on regulation of gene expression by PARG. Use of a PARG inhibitor activated pro-inflammatory genes in macrophages in a PAR-dependent manner (Rapizzi et al., 2004), suggesting a role for PARG in gene expression, although the mechanism of action is unknown. One can speculate that perhaps PARG acts to regulate PARP-1 activity at target genes. Or, perhaps PARG can regulate gene expression as a coactivator-like protein. It was demonstrated in *Drosophila* that the absence of PARG activity could disrupt chromatin remodeling and transcription during development (Hanai et al., 2004). One additional study suggests that PARG may take on an even more prominent role in regulating transcription by dictating the location of transcriptional coregulators (Tulin et al., 2005).

Interestingly, a recently published global analysis of transcriptional regulation showed that both PARP-1 and PARG regulate a similar set of target genes, and that they do so in a similar manner (Frizzell et al., 2009). That is, they regulate the same genes in similar directions (both positive and negative) and with similar magnitudes. This result coupled with the promoter localization patterns of PARP-1 and PARG, suggests a concerted action of PARP-1 and PARG. Furthermore, this study demonstrated a gene-specific requirement for both PARP-1 and PARG enzymatic activities with respect to gene regulatory outcomes (Frizzell et al., 2009).

1.6.7. Signal-mediated Transcriptional Regulation

A growing body of evidence suggests that PARP-1 functions in signal-mediated transcriptional responses in the absence of DNA damage. A few signaling pathways have received considerable attention over the past few years and have yielded interesting mechanisms of regulation by PARP-1. They include, NFκB-dependent proinflammatory responses, heat shock, hormone signaling, and kinase-dependent signaling. For example, in response to inflammatory stimuli, PARP-1 is acetylated by p300/CBP and subsequently interacts with NFκB subunits and components of the Mediator complex to stimulate pro-inflammatory target genes as a classic coactivator (Hassa et al., 2003; Hassa et al., 2005). Recent studies also link PARP-1 to the activation of players of the pro-inflammatory pathway upstream of NFκB (*i.e.,* IκB kinase) through PARylation activity (Stilmann et al., 2009). In this regard, PARG may be able to add an additional level of regulation of NFκB-dependent transcription by modulating the activation of IκB. However, since the coactivator function of PARP-1 in this system seemingly does not require PARylation activity, it will be interesting to determine if and how PARG functions at those gene targets. Notably, PARG inhibition alters the expression of proinflammatory response genes (Erdelyi et al., 2005; Rapizzi et al., 2004), although the mechanism is unclear.

The studies focused on the heat shock response have elucidated many facets of transcriptional regulation by PARP-1 through its role in modulating chromatin structure. The results may be specific to *Drosophila*, as they have yet to be demonstrated parallel in mammalian systems, however the concepts may still apply. As noted above, upon heat shock, dPARP is activated and participates in the chromatin decondensation (a.k.a. "puffing") at heat shock loci (Petesch and Lis, 2008; Tulin et al., 2003; Tulin and Spradling, 2003). It was recently shown that this involves nucleosome loss across the heat shock loci in a transcription-independent

manner (Petesch and Lis, 2008). What controls this mechanism of action is not currently known, but may involve interactions with other factors involved in the heat shock response at heat shock loci. PARG-dependent hydrolysis of PAR may contribute to this process, but has yet to be shown.

Through regulation of chromatin structure and coregulator complex components, PARP-1 has been shown to play a role in classic signaling pathways involving hormone signaling (*i.e.,* estrogen, retinoic acid; (Ju et al., 2004; Pavri et al., 2005)) and kinase cascades (*i.e.,* Erk1/2, JNK1, CaMKIIδ; (Cohen-Armon et al., 2007; Ju et al., 2004; Kauppinen et al., 2006; Mathieu et al., 2008)). In some cases, these types of signaling pathways may overlap. In addition, some signaling pathways have been shown to result in phosphorylation of PARP-1, which can alter its activity (Kauppinen et al., 2006). Similarly, PARG has been shown to be a target of phosphorylation, however, it is not known what the functional significance of this is. Since PARP-1, and likely PARG, is modified by various post-translational modifications, it is feasible to think that the signaling cascades that govern those other types of enzymes may also regulate PARP-1 (and PARG) actions.

In all of these examples, the factors involved in determining the overall function in one signaling pathway over another, coactivator action versus chromatin modulator action, and resulting direction of gene regulation has yet to be identified. It is likely that a host of determinants function to distinguish the various roles of PARP-1, including the signal- and cell-type, the duration of the signal, and specific genes, as well as some factors previously mentioned above (*i.e.,* post-translational modifications of PARP-1, subcellular or genomic localization, and substrate availability).

1.7. Global Gene Expression Studies

Genomic expression studies have been used to identify PARP-1-regulated genes in various cell types, some of which are derived from knockout animal models. This type of analysis has yielded various ontological categories of genes whose expression depends on PARP-1 or PARG actions, which provide insights into the molecular and biological functions of PAR-regulating enzymes.

Comparisons of wild type- and PARP-$1^{-/-}$-derived cell lines (*i.e.,* MEFs, heart endothelial cells, liver-derived, and embryonic stem cells) using mouse expression microarrays (Carrillo et al., 2004; Ogino et al., 2007; Saenz et al., 2008; Simbulan-Rosenthal et al., 2000; Zingarelli et al., 2003) resulted in genes enchriched in apoptosis, metabolism, cell cycle control, DNA synthesis/repair, stress or immune response, signal transduction, transcription, chromosomal integrity, and protein processing. In MCF-7 cells, similar ontological categories were enriched by PARP-1- and PARG-regulated genes; namely, metabolism, stress response, cell structure, and GTPase regulation (Frizzell et al., 2009). These data sets corroborate many studies showing PARP-1 and PARG function in molecular actions such as DNA repair, stress response, cell cycle control, signal transduction, and transcription. In addition, these data suggest more broad functions for PARP-1 and PARG in cancer, inflammation, differentiation, and development. The cellular actions of these PAR-regulating enzymes contribute directly to physiological and pathophysiological conditions.

1.8. Physiological and Pathophysiological Actions of PAR-regulating Enzymes

Parp-1 and *Parg* knockout animal models have been generated and fairly well characterized in *M. musculus* and *D. melanogaster*. However, only a handful of studies have described PARP-1 or PARG homologs in *C. elegans* and *A. thaliana*.

This section focuses on the contributions of PARP-1 and PARG in various physiological and pathophysiological conditions, including aging, inflammation, differentiation, and carcinogenesis, as determined by knockout animal models (Table 1.2). The data described herein is primarily from mouse and fly models, however, findings from other animal and plant models are mentioned where appropriate.

1.8.1. Viability and Genomic Integrity

Due to their roles in maintaining genomic integrity and DNA damage repair, it was quite surprising that the first developed *Parp-1*$^{-/-}$, *Parp-2*$^{-/-}$, and *Parg*$^{\Delta 2\text{-}3/\Delta 2\text{-}3}$ mice are viable and exhibit minimal phenotypes (Cortes et al., 2004; Masutani et al., 1999a; Masutani et al., 1999b; Menissier de Murcia et al., 2003; Wang et al., 1995; Wang et al., 1997). For *Parp-1*$^{-/-}$ mice and *Parp-1*$^{-/-}$-derived embryonic fibroblasts, initial observations reported an increased genomic instability associated with a higher frequency of sister chromatid exchange, homologous recombination, and micronuclei formation (de Murcia et al., 1997; Kim et al., 2005; Wang et al., 1997). Under certain conditions, genetic backgrounds, or in response to chemical agents, additional phenotypes were revealed. Upon exposure to ionizing radiation or alkylating agents, an the frequencies of DNA deletions/insertions, chromosome rearrangements, and chromatid breaks increased, and the ability to repair the DNA was disrupted (Halappanavar et al., 1999; Masutani et al., 1999a; Masutani et al., 1999b; Menissier de Murcia et al., 2003; Shibata et al., 2005; Simbulan-Rosenthal et al., 1999; Trucco et al., 1998; Wang et al., 1995; Wang et al., 1997; Yu et al., 2002). This type of hypersensitivity to DNA damaging agents was also evident in *Parp-2*$^{-/-}$ mice (Menissier de Murcia et al., 2003). These results further corroborate the notion that PARP-1 and PARP-2 have overlapping and redundant functions. In fact, *Parp-1*$^{-/-}$/*Parp-2*$^{-/-}$ double knockout mice display embryonic lethality prior to E8.0 (Menissier

de Murcia et al., 2003). Interestingly, *Parp-1*$^{+/-}$/*Parp-2*$^{-/-}$ mice show female-specific embryonic lethality by E9.5, which was linked to *X* chromosome instability in those females (Menissier de Murcia et al., 2003). *Parg*$^{\Delta 2\text{-}3/\Delta 2\text{-}3}$ mice (deletion of exons 2 and 3, resulting in targeted depletion of the 110-kDa isoform) were shown to also be highly sensitive to genotoxic stresses, exhibiting increased lethality (Cortes et al., 2004). Interestingly, a *Parg*$^{\Delta 4/\Delta 4}$ embyos (deletion of exon 4, resulting in complete depletion of all isoforms) displayed embryonic lethality at E3.5, which was attributed to increased apoptosis in embryonic tissues (Koh et al., 2004).

The mild or context-dependent phenotypes of the *Parp-1*$^{-/-}$ and *Parg*$^{-/-}$ mice are likely due to functional redundancy with other PARP family members or PARG isoforms, respectively. However, in *Drosophila*, the story is quite different, as flies only have a single PARP-1-like gene, and a single PARG gene that seemingly encodes a single protein isoform. The phenotype for *Parp*$^{-/-}$ (null) or *Parp*$^{CH1/CH1}$ (reduction in expression) in *Drosophila* is quite dramatic, resulting in larval lethality, likely due to increased bacterial infection, changes in chromatin structure, and defective gene expression (Miwa et al., 1999; Tulin and Spradling, 2003; Tulin et al., 2002). Interestingly, the phenotype for *Parg*$^{27.1}$/*Y* and *Parg*$^{27.1/27.1}$ (deletion of the catalytic domain) mutants display PAR accumulation and temperature-dependent lethality (Hanai et al., 2004). For example, the mutant exhibited larval lethality at the normal development temperature (25°C), but at 29°C, ¼ of the larvae developed to the adult stage and exhibited neurodegenerative phenotypes and a reduced lifespan.

The phenotype of increased sensitivity to genotoxic stresses is corroborated by studies in worm and plant models. Just a few years ago, the PARP-1- and PARG-like genes in *C. elegans* were identified. Although genetic manipulations (*i.e.,* knockouts) have yet to be made, one study characterized the knockdown of the *Parg* homologues, *pme-3* and *pme-4*, also exhibit sensitivity to ionizing radiation (St-Laurent et al.,

2007). Likewise, in *A. thaliana*, the PARP-1-like genes have been identified, but no genetic manipulations exist. However, mutant *Parg1* seedlings exhibit growth inhibition and are hypersensitive to DNA damaging agents (Adams-Phillips et al., 2010). Taken together, these results demonstrate the importance of regulating PAR in animals and plants for the maintenance of genomic integrity, gene expression, and development, among other biological processes. Still, more work is needed to fully characterize these models in order to gain a complete understanding of the physiological contributions of PARP-1 and PARG.

1.8.2. Inflammation and Stress Responses

PARP-1 has been implicated in inflammation and stress responses in a wide range of studies from animals to plants. From simplistic models (*i.e.,* bacterial infection) to more complex models (*i.e.,* streptozotocin-induced diabetes or ischemia/reperfusion), PARP-1 is a key component of immunity and inflammatory responses in various tissues, including the brain and heart. In many cases, PARP-1 activity is highly increased upon cellular stress (Nossa et al., 2009; Tulin and Spradling, 2003) and $Parp^{-/-}$ confers a protective effect against infections, toxins, and injury (Ha, 2004; Mabley et al., 2001; Oliver et al., 1999). Conversely, $Parg^{\Delta 2\text{-}3/\Delta 2\text{-}3}$ (110 kDa targeted deletion) increases the sensitivity in response to various stresses (Cortes et al., 2004), a result suggesting that PARG plays a protective role against such system shocks. From what is known about PARP-1 and PARG molecular functions, it is safe to say that their roles in modulating inflammatory responses involve multiple actions. For example, PARP-1 could increase cell death and mediate pro-inflammatory gene transcription (through NF-κB pathway) in response to a single agent (Kim et al., 2005). In this regard, $Parp^{-/-}$ mice display a down-regulation of pro-inflammatory genes (Hassa and Hottiger, 2002; Shall and de Murcia, 2000; Zingarelli et al., 1998),

while *Parg*$^{\Delta 2\text{-}3/\Delta 2\text{-}3}$ mice show an increase of cytokines in the blood serum (Cortes et al., 2004), This result is likely due to an increase in pro-inflammatory gene expression, a result also seen with PARG inhibitor treatment (Rapizzi et al., 2004).

In a model of neuronal injury, the generation of reactive oxygen species and nitric oxide cause an increase in DNA damage and PARP-1 activation, leading to necrotic cell death (Cole and Perez-Polo, 2004). In *Parp*$^{-/-}$ mice, this neurotoxic effect is blocked (Cole and Perez-Polo, 2004; Ha and Snyder, 2000; Mandir et al., 2000; Zhang et al., 1994). Interestingly, *Parg*$^{27.1/27.1}$ (deletion of the catalytic domain) in *Drosophila* exhibit progressive neurodegeneration in adult flies that survive the embryonic lethal phenotype (Hanai et al., 2004). Together these results suggest that the regulation of PAR is important in mediating normal neuronal functions in response to injury. Likewise, in a model of cerebral ischemia/reperfusion, PARP-1 activity is also increased and *Parp*$^{-/-}$ or chemical inhibition exerts a beneficial effect (Eliasson et al., 1997; Virag and Szabo, 2002). However, in this model, treatment with a PARG inhibitor can also have a protective effect (Lu et al., 2003). This protective effects was also shown in a kidney ischemia/reperfusion model where *Parg*$^{\Delta 2\text{-}3/\Delta 2\text{-}3}$ attenuated the injury and inflammation phenotype (Patel et al., 2005). The differences noted here might be due to the type or severity of injury, tissue-type, or genetic manipulation. In any case, the result stands that PARP-1 and PARG regulation of PAR is strikingly important in modulating responses to stress, inflammation, and injury.

PARP-1 and PARG homologues in the *Arabidopsis* model have recently been studied in regard to abiotic and biotic stress responses, respectively, in knockdown, mutant, or knockout studies (Adams-Phillips et al., 2010; De Block et al., 2005; Vanderauwera et al., 2007). Interestingly, it was shown that the *tej* mutation in the PARG gene disrupted circadian clock-regulated transcription (Panda et al., 2002), which may have also an effect on stress responses. Collectively, PARP-1 disruption

Table 1.2. Summary of combination knockout animals and their phenotypes. Parp-1$^{-/-}$ mice have been combined with several knockout mice to determine the consequences of a double knockout animal in overall viability, genomic integrity, developmental processes, and carcinogenesis. Although studied under specific contexts with regard to specific questions, their reported phenotypes are interesting, nonetheless, and justify further investigation in each field.

Combination Knockout	Phenotypes *(ref)*
(a) Parp-1$^{-/-}$/Parp-2$^{-/-}$	- Embryonic lethality at E8.0 *(Menissier de Murcia et al., 2003)*
(b) Parp-1$^{-/-}$/Parg(110)$^{-/-}$	- Spermiogenesis defects (reduced nuclear elongation and chromatin condensation) *(Meyer-Ficca et al., 2009)*
(c) Parp-1$^{-/-}$/p53$^{-/-}$ (exon 2)	- Enhanced tumorigenesis in mammary, lung, prostate, skin, and brain tissue - Severe chromosome abberations - Disruption of transcriptional responses *(Tong et al., 2001; Tong et al., 2003)*
Parp-1$^{-/-}$/p53$^{-/-}$ (exon 4)	- High genomic instability - Decreased tumor formation in T-cell lymphomas - Disruption of transcriptional responses *(Conde et al., 2001)*
(d) Parp-1$^{-/-}$/SCID (DNA-PK mut)	- Severely high frequency of T-cell lymphoma *(Morrison et al., 1997)*
(e) Parp-1$^{-/-}$/Atm$^{-/-}$	- Embryonic lethality at E8.0 - Increased apoptosis *(Menisser-de Murcia et al., 2001)*
(f) Parp-1$^{-/-}$/H2AX$^{-/-}$	- Embryonic lethality *(Orsburn et al., 2010)*
(g) Parp-1$^{-/-}$/53BP1$^{-/-}$	- Modestly enhances growth retardation, genomic instability, and radiosensitivity phenotypes of *Parp-1$^{-/-}$* *(Orsburn et al., 2010)*
(h) Parp-1$^{-/-}$/Polβ$^{-/-}$	- Reverses the MMS-dependent sensitivity of *Polβ$^{-/-}$* *(Jelezcova et al., 2010)*
(i) Parp-1$^{-/-}$/Ku80$^{-/-}$	- Embryonic lethality - Increased apoptosis *(Henrie et al., 2003)*
(j) Parp-1$^{-/-}$/Sirt1$^{-/-}$	- Increased telomere abnormalities - Decreased cell growth - Increased pot-natal lethality - Reverses genomic abnormalities, nucleolar disorganization, and mitotic defects of *Sirt1$^{-/-}$* *(El Ramy et al., 2009)*

results in resistance, while PARG disruption results in sensitivity to various stresses in plants, much like the results from mouse and fly models.

1.8.3. Juvenile-onset Diabetes

Type-1 diabetes results in the destruction of insulin-producing β-cells of the pancreas. During this process, cytokines, reactive oxygen species, and nitric oxide are released, contributing to β-cell death (Bluestone et al., 2010). Many groups have shown that PARP-1 null mice display resistance to the induction of type-1 diabetes by streptozotocin treatment (Gonzalez et al., 2002; Mabley et al., 2001; Oliver et al., 1999; Pieper et al., 1999). In this regard, *Parp-1*$^{-/-}$ mice show reduced hyperglycemia, normal blood glucose, normal pancreatic islet structure, and a lower incidence of diabetes as compared to wild type counterparts upon streptozotocin treatment (Mabley et al., 2001; Pieper et al., 1999). A similar finding was shown upon treatment with a PARP inhibitor (Mabley et al., 2001). *Parp-1*$^{+/-}$ mice also provide protection, though not as dramatic as the null animal (Pieper et al., 1999). Interestingly, *Parg(110)*$^{-/-}$ mice (targeted depletion of the 110 kDa isoform) displayed an increased susceptibility to streptozotocin-induced diabetes (Cortes et al., 2004). PARP-1 has also been shown to bind and regulate the *Reg* gene, which is known to mediate islet-cell regeneration, in a PAR-dependent manner (Akiyama et al., 2001). Given the role of PARP-1 in gene regulation through chromatin modulation and coregulator action, it is feasible to think that gene regulatory aspects may also contribute to this process. This is supported by the idea that PARP-1 is linked to endothelial dysfunction, an underlying condition to many diabetes-related symptoms, through NF-κB activation (Garcia Soriano et al., 2001). These data suggest that PAR-regulation is important in pancreatic β-cell pathology and the onset of type-1 diabetes.

1.8.4. Differentiation and Development

PARP-1, PARP-2, and PARG knockout mice develop normally (Cortes et al., 2004; Koh et al., 2004; Masutani et al., 1999a; Masutani et al., 1999b; Menissier de Murcia et al., 2003; Wang et al., 1995; Wang et al., 1997), however, the combination of PARP-1/PARP-2 double knockout is embryonic lethal (Menissier de Murcia et al., 2003). Interestingly, the complete knockout of PARG in mice, rather than just the 110 kDa isoform, results in embryonic lethality (Koh et al., 2004). In *Drosophila*, the knockout animals have a more dramatic phenotype, that is, dPARP and dPARG knockouts are lethal at the larval stage (Cortes et al., 2004; Koh et al., 2004). Collectively, these results suggest that PARPs and PARG are critical for embryonic development (Menissier de Murcia et al., 2003). This requirement is likely due to a variety of factors, including maintenance of genomic integrity and transcriptional responses. New studies are beginning to shed light on the actions of PARPs and PARG in differentiation and development, however, there is still much to be learned.

Germline – Recent studies have suggested a role for PARP-1 and PARP-2 in germline development. *Parp-1*$^{-/-}$ and *Parp-2*$^{-/-}$ mice are fertile (de Murcia et al., 1997; Masutani et al., 1999a; Menissier de Murcia et al., 2003; Wang et al., 1995), but display some defects in oogenesis and spermiogenesis. For example, *Parp-1*$^{-/-}$ female mice show meiotic defects, including persistent H2AX phosphorylation, increased double strand DNA breaks, deficient sister chromatid cohesion, suggesting a role for PARP-1 in maintaining chromatin states during oogenesis (Yang et al., 2009). On the other hand, *Parp-2*$^{-/-}$ male mice have lower fertility attributed to defects in meiotic sex chromosome inactivation (Dantzer et al., 2006). During spermiogenesis, massive reorganization of the nucleus occurs; cells elongate, chromatin condenses, transcription stops, and histones are replaced by basic proteins (Quenet et al., 2009a). Interestingly, PAR levels are at their highest in spermatids where the higher rates of

chromatin nucleoprotein exchanges take place (Meyer-Ficca et al., 2005b). In absence of PARP-2, nuclear elongation is delayed and *X*- and *Y*-linked expression persists (Dantzer et al., 2006; Quenet et al., 2009b). In addition, *Parp-1*$^{-/-}$, *Parg(110)*$^{-/-}$, and *Parp-1*$^{-/-}$*Parg(110)*$^{-/-}$ double knockout mice exhibit reduced nuclear elongation and chromatin condensation (Meyer-Ficca et al., 2009). Notably, macroH2A1 and PARP-1 physically and functionally interact to regulate *X* chromosome inactivation (Nusinow et al., 2007), so a functional connection between the PAR-regulating enzymes and macroH2A1 may be causal for such germline phenotypes.

Stem Cells – Recently, studies have revealed a role for PARP-1 in stem cell differentiation and reprogramming. As noted above, gene expression experiments using embryonic stem cells (ESCs) derived from PARP-1 null mice show altered expression patterns compared to their wild type counterparts (Ogino et al., 2007). A recent study has identified PARP-1 as a cofactor of Oct4 and Sox2 inhibitory transcription factors that function in maintaining the pluripotent state of ESCs (Gao et al., 2009). Upon induction of differentiation, PARP-1 physically interacts with and PARylates Sox2, leading to the dissociation of Sox2 from the FGF4 enhancer and its subsequent degradation. This action causes an increase in FGF4 expression and promotes differentiation. Interestingly, another study suggests that PARP-1 can inhibit ESC differentiation (Hemberger et al., 2003). Specifically, the study shows that ESCs derived from *Parp-1*$^{-/-}$ mice promotes the development of teratocarcinoma-like tumors when injected subcutaneously into nude mice. These results suggest that PARP-1 may primarily regulate the pluripotency of ESCs, rather than differentiation.

Other Cell Differentiation Models – PARP-1 and PARP-2 have also been shown to be involved in the differentiation of other cell types, including neuronal, immune, endodermal, and fat cells (Ambrose et al., 2009; Bai et al., 2007; Ju et al., 2004; Morrison et al., 1997; Quenet et al., 2008). Although not explicitly shown with

regard to neuronal differentiation morphology, PARP-1 was shown to regulate neuronal gene expression by regulating factor exchange at the promoters of genes required for differentiation (Ju et al., 2004). In immune-related cells, PARP-1 is required for T cell-dependent antibody responses (Ambrose et al., 2009) and PARP-2 is required for T cell survival during thymopoiesis (Yelamos et al., 2006). Interestingly, another study shows that PARP-1 knockout in mice actually promotes the formation of a specific type of functional T cell ($CD4^+/CD25^+/Foxp3^+$) (Nasta et al., 2010). The endodermal differentiation models yielded slightly different results in that PARP-1 and PARP-2 function in sequence to promote the full differentiation of embryonic carcinoma F9 cells into primitive endoderm-like cells and finally into parietal endoderm-like cells (Quenet et al., 2008). Interestingly, even though PARP-1 and PARP-2 act independently of one another, they both act through physical and functional interactions with the heterochromatin-associated proteins HP1 and TIF1β. PARP-2 has been implicated in adipogenesis, whereby it functions as a coregulator of the PPARγ adipogenic transcription factor (Bai et al., 2007). And, recently, PARP-1 was shown to antagonize adipogenesis progression (Devalaraja-Narashimha and Padanilam, 2010), although the molecular mechanisms of this action have not been determined. Importantly, this model of adipogenesis can be linked to the onset and development of type-2 diabetes and obesity.

Collectively, the studies of stem cell and other models of cellular differentiation have revealed somewhat controversial roles for PARP-1 in the differentiation process. While some studies have determined that PARP-1 promotes differentiation, others have suggested PARP-1 inhibits differentiation. There does not seem to be a unified function for PARP-1 in these processes. This indicates that there are other determinants that may regulate PARP-1 action, such as cell type and microenvironment. In addition, there seems to be a controversy as to whether PARP-1

and PARP-2 cooperate or antagonize one another in these systems, suggesting they may have multiple independent functions. There is still much to learn about the molecular mechanisms as to how these PAR-regulating enzymes act to regulate the differentiation process. As the field progresses, it will be interesting to see how PARPs and PARG regulate these differentiation systems.

1.8.5. Carcinogenesis

Carcinogenesis is the process by which normal cells transform into cancer cells. This progression is likely mediated by a host of cellular processes, including genome and cell cycle maintenance, proliferation, differentiation, and cell death pathways. PARPs and PARG have been implicated in all of these aspects in the cell, as discussed above. Therefore, it is certainly likely that disruptions in their functions can contribute to cancer development. *Parp-1*$^{-/-}$, *Parp-2*$^{-/-}$, and *Parg*$^{-/-}$ mice have not been reported to develop spontaneous tumors, most likely due to functional redundancy by other PARPs or PARG-like proteins, leading to a viable mouse. However, in the context of chemically induced or transgenic mouse models of cancer, *Parp-1*$^{-/-}$ can cause increased tumor formation (Kim et al., 2005; Masutani et al., 2005). For example, in *Parp-1*$^{-/-}$ mice, models of cancer induced by the chemical agents N-nitrosobis(2-hydroxypropyl)amine and azoxymethane displayed a higher incidence of liver and colon tumors compared to their *Parp-1*$^{+/+}$ counterparts (Nozaki et al., 2003; Tsutsumi et al., 2001). Notably, combinations of these types of cancer models and *Parp-2*$^{-/-}$ or *Parg*$^{-/-}$ deletions have yet to be investigated.

The combination of *Parp-1*$^{-/-}$ mice with other knockout animals known to play roles in DNA damage repair or cancer development have suggested important functional interactions between PARP-1 and other factors. Many of these factors have already been identified as PARP-1-interacting proteins or PARP-1 targets of

PARylation. For example, the simultaneous depletion of PARP-1 and p53, a tumor suppressor gene required for cell cycle checkpoints and apoptosis following DNA damage (Hofseth et al., 2004), displays enhanced tumorigenesis in mammary, lung, prostate, skin, and brain tissues (Tong et al., 2001; Tong et al., 2003). The increase in tumor formation is attributed to severe chromosome aberrations (*i.e.,* aneuploidy, fragmentations, long and heterogeneous telomeres) and disrupted transcriptional responses (*i.e.,* Math1-dependent transcription in the brain). Interestingly, another group investigated the same double-knockout mouse, however the targeted exon for genetic manipulation was different (Conde et al., 2001). This mouse also displayed a higher genomic instability, but tumor formation was somewhat reduced. These contradictory results suggest that perhaps the genetic backgrounds of the mice or the differing targeted exons contribute to the diparities in these studies.

The increase in tumorigenesis in the p53 model was not the only study to report this type of phenotype. Interestingly, the corroborating reports also involve proteins of the DNA damage response and cell death pathways. Severe combined immunodeficiency (SCID) mice contain a mutation in the gene encoding the DNA-PK catalytic subunit (Prkdc), leading to lyphocyte developmental arrest (Schuler et al., 1986). *Parp-1*$^{-/-}$ in the background of the SCID model displays a severely high frequency of T-cell lymphoma (Morrison et al., 1997), indicating that PARP-1 and DNA-PK cooperate to minimize genomic damage. Similarly, in *Parp-1*$^{-/-}$ in combination with *Atm*$^{-/-}$, the gene encoding a double-strand break repair and cell cycle checkpoint protein, show embryonic lethality by E8.0 caused by increased apoptosis (Menisser-de Murcia et al., 2001). In a further analysis of ATM-regulated factors, it was shown that H2AX is essential for viability in a PARP-1-deficient background, while 53BP1 enhances PARP-1-deficient phenotypes to be slightly more dramatic (*i.e.,* growth retardation, genomic instability) (Orsburn et al., 2010). Together, these

results suggest a functional interplay between PARP-1 and p53, DNA-PK, ATM and ATM-regulating factors, all components of DNA damage response and cell cycle control pathways, in the control of aberrant cell growth and carcinogenesis.

Although not investigated with respect to tumor formation, the combination of *Parp-1*$^{-/-}$ with the knockout of other DNA repair factors, like those involved in base-excision repair (BER), exhibit similar phenotypes as those described above. For example, the double knockout mouse for PARP-1 and DNA Polβ, shown to interact and function in BER, synergistically enhanced the defects in both short and long patch BER of 8-oxoG lesions (Dantzer et al., 2000; Le Page et al., 2003). Interestingly, a recent study describes the relationship of PARP-1 and DNA Polβ in double knockout-derived MEFs. In this case, *Polβ*$^{-/-}$ alone is sensitive to the DNA damaging agent, MMS, while the *Parp-1*$^{-/-}$ and *Polβ*$^{-/-}$ together reverses this effect (Jelezcova et al., 2010). PARP-1 may therefore function as a tumor suppressor by initiating cell death. Finally, PARP-1 interacts with Ku80, a protein in the non-homologous end joining (NHEJ) pathway. The double knockout *Parp-1*$^{-/-}$ and *Ku80*$^{-/-}$ mouse resulted in embryonic lethality and increased level of apoptosis (Henrie et al., 2003), much like that seen in the *Parp-1*$^{-/-}$*/Atm*$^{-/-}$ mouse. Therefore, it is likely that these phenotypes are a pre-cursor to an increase in genetic aberrations and subsequent tumor development.

1.8.6. Aging

The accumulation of DNA damage over time underlies the aging process. Since PARP-1 (and other PARPs) play prominent roles in maintaining genomic integrity, they have been implicated in aging and longevity (Beneke et al., 2004; Burkle et al., 2005a; Burkle et al., 2005b; Burkle et al., 1992). Initially, this connection became apparent with the conclusion that PARP activity correlated with species life span (Grube and Burkle, 1992). In this regard, the regulation of PAR by

PARG may be important in the aging process that has yet to be addressed. Although this field has not been studied extensively, studies are beginning to unveil the potential role of PARP-1 in the aging process. For example, PARP-1 interacts with WRN, a helicase involved in DNA replication and repair processes (Lebel et al., 2003). Interestingly, WRN mutations are prevelant in a genetic disorder leading to premature aging in humans (Lee et al., 2005). In addition, PARP-1 and other PARPs function in maintaining telomere length (Chiang et al., 2006; Dantzer et al., 2004; Smith et al., 1998), which is important in replicating cells to prevent senescence.

Importantly, PARP-1 has been shown to have a functional interplay with SIRT1, a NAD^+-dependent deacetylase and major contributor of the aging process and aging-related diseases (Donmez and Guarente, 2010; Zhang and Kraus, 2010). PARP-1 and SIRT1 can compete with one another for nuclear NAD^+, as well as the by-product of their enzymatic reactions, nicotinamide, a natural inhibitor of both enzymes (Donmez and Guarente, 2010; Kim et al., 2005; Zhang and Kraus, 2010). This supports the previously suggested notion that PARP-1 and SIRT1 function antagonistically (Kolthur-Seetharam et al., 2006). In fact, PARP-1 activation by PCAF-dependent acetylation leads to cell-death, while deacetylation of PARP-1 by SIRT1 promotes cell survival (Rajamohan et al., 2009). Interestingly, *Parp-1*$^{-/-}$*Sirt1*$^{-/-}$ double knockout mice display increased telomeric abnormalities, decreased cell growth, and increased post-natal lethality (El Ramy et al., 2009). However, *Parp-1*$^{-/-}$ deletion in the *Sirt1*$^{-/-}$ background can reverse *Sirt1*$^{-/-}$-specific phenotypes, such as abnormal pericentric heterochromatin, nucleolar disorganization, and mitotic defects (El Ramy et al., 2009). In *Drosophila*, dPARP and dPARG may contribute to the regulation of dSir2 (the *Drosophila* homolog of the mammalian SIRT1) by modulating its chromatin localization (Tulin et al., 2005). Collectively, these results

provide evidence for PARP-1 and PARG in the aging process through genomic maintenance and functional interactions with various proteins.

1.9. Therapeutic Applications of PARP-1 and PARG Inhibitors

Chemical inhibition of PARP-1 activity has potential therapeutic applications in both acute and chronic diseases. For example, PARP-1 inhibitors can potentially enhance the cytotoxicity of DNA-damaging anticancer drugs, reduce parenchymal cell necrosis in conditions such as stroke or myocardial infarction, and inhibit inflammation and tissue injury pathways in conditions such as circulatory shock diabetes mellitus (Jagtap and Szabo, 2005). As noted above, PARP-1 deficiency or inhibition in mouse and cell models exerts protective effects against pathological cell death and inflammatory responses. Thus, PARP-1 has been an attractive therapeutic target for chemical inhibition. One concern, however, is that chronic use of PARP-1 inhibitors could pose a long-term risk for genomic instability and secondary cancers (Jagtap and Szabo, 2005). Clinical trials currently underway will help to resolve if this concern is justified. Studies examining the interplay between PARP-1 and SIRT1 (see above) suggest that chemical modulators of SIRT1 activity may also be useful as therapeutic agents for treating PARP-1-dependent diseases.

1.9.1. Chemistry and Development of PARP-1 Inhibitors

Nicotinamide (NAm), a product of PARP-1 enzymatic action on NAD^+ and a weak inhibitor of PARP-1 activity (Curtin, 2006), was used as a model for the first PARP-1 inhibitors, including benzamide and 3-aminobenzamide (3AB, Figure 1.3A; (Shall, 1975)). Benzamide and 3AB inhibit PARP-1 activity in the mM range and may also inhibit other PARP family members (*e.g.*, PARP-2 and tankyrase; (Ame et

al., 1999; Smith et al., 1998), thus lacking the potency and specificity required for therapeutic purposes. Banasik *et al.* developed 1,5-dihydroisoquinoline and a variety of other inhibitors (Banasik et al., 1992), which were used in turn to develop even more inhibitors with greater specificity, potency, and solubility, including PD128763 (Arundel-Suto et al., 1991; Suto et al., 1991), NU1025 (Griffin et al., 1995), and NU1085 (Bryant and Helleday, 2004; Curtin, 2006). These inhibitors are 50- to 100-fold more potent than benzamides, inhibiting PARP-1 activity in the μM to nM concentration range. Although the improvements are striking, PD128763, NU1025, and NU1085 may still not be potent enough for clinical use.

The "benzamide" style of PARP-1 inhibitor has recently been improved based on X-ray crystal structure data. The incorporation of bi-, tri-, and tetra-cyclic frameworks, and cyclic lactam rings, which interact more strongly with the catalytic residue Glu988 (*e.g.*, AG14361), has generated even more potent and specific PARP-1 inhibitors (Curtin, 2006; Jagtap and Szabo, 2005; Tao et al., 2006; Wells et al., 2006). X-ray crystal structures have revealed that most PARP-1 inhibitors bind to the active site and mimic the nicotinamide moiety of NAD^+ (Jagtap and Szabo, 2005; Oliver et al., 2004; Ruf et al., 1998; Ruf et al., 1996). The key structural features for high potency inhibition include an electron-rich aromatic ring system, a non-cleavable bond at the 3-position of the benzamide moiety, and a carboxamide group placed in a favorable position so as to restrict free rotation of the molecule (Curtin, 2006).

Although these new generation inhibitors have been improved considerably since the development of the benzamide and 3AB prototypes, the development of inhibitors that are specific for a single PARP have proved considerably more difficult. This is mainly due to the extremely high level of PARP catalytic domain conservation (Hakme et al., 2008; Schreiber et al., 2006), which can lead to off-target effects, as was shown to occur in a mouse model of diabetes (Mabley et al., 2001). However,

two classes of inhibitors, namely quinazolinone and quinoxaline have displayed higher selectivity toward PARP-1 and PARP-2, respectively (Hassa and Hottiger, 2008; Ishida et al., 2005; Ishida et al., 2006; Iwashita et al., 2004). In addition, one compound has been reported to inhibit tankyrases 1 and 2 (PARP-5a and -5b), but has not been tested against other PARPs (Huang et al., 2009). Overall, the progression and development of PARP inhibitors has improved specificity, potency, solubility, and pharmokinetics, which are beginning to prove favorable for therapeutic applications.

1.9.2. Chemistry and Development of PARG Inhibitors

The development of PARG inhibitors is considerably less well developed than PARP inhibitors. The early inhibitor classes, tannins (water-soluble polyphenols), were extracted from green tea leaves and include gallotannins, ellagitannins, and condensed tannins (Figure 1.3B; (Tanuma et al., 1989a; Tanuma et al., 1989b; Tsai et al., 1991)). Condensed tannins are polymers of flavan-3-ols (Barbehenn et al., 2006) and did not appreciably inhibit PARG activity *in vitro* (Tsai et al., 1991). However, both gallotannins (partial noncompetitive) and ellagitannins (competitive) showed inhibitory activity *in vitro* (Tsai et al., 1991). Penta-galloyl glucose is the precursor for both gallotannins and ellagitannins. While extra galloyl groups are added to penta-galloyl glucose to make gallotannins, ellagitannins contain two or more neighboring galloyl groups that are oxidatively coupled to form rigid groups, such as hexahydroxydiphenoyl (HHDP) units (Barbehenn et al., 2006; Okuda et al., 2000). Gallotannins are the most widely used inhibitor and inhibits PARG in the mid-μM concentration range (Bonicalzi et al., 2005). Ellagitannins, including nobotannin B (dimer), E (trimer), and K (tetramer), while identified some years ago (Tsai et al., 1992), are just now being investigated in more detail. These compounds inhibit PARG in the low-μM concentration range (Tsai et al., 1992). Although their actual

IC_{50} decreases with increasingly complex structure (*i.e.,* tetramer), only nobotannin B was found to be a competitive inhibitor (Tsai et al., 1992).

More recently developed PARG inhibitors include adenosine diphosphate-(hydroxymethyl)-pyrrolidinediol (ADP-HPD) (Slama et al., 1995a) and mono-galloyl glucose derivatives (Formentini et al., 2008). ADP-HPD is also a partial noncompetitive inhibitor, but has an IC_{50} in the mid-nM range, which significantly improved the potency of PARG inhibitors (Slama et al., 1995a). This is likely due to the direct interactions between the adenine ring and a conserved residue in the PARG active site (tyrosine 795, Y795) (Koh et al., 2003). This inhibitor, while potent *in vitro*, is not cell permeable and is suspect to phosphodiesterase cleavage, rendering the inhibitor useless (Slama et al., 1995b). A cell permeable derivative has been developed, 8-octylamino ADP-HPD, but has yet to be full characterized *in vivo* (Coyle et al., 2003). Also, mono-galloyl glucose compounds were found to be just as potent as ADP-HPD (Formentini et al., 2008). In this class, perhaps the less complex the structure, the more potent and specific the inhibitor will be. The use of the current inhibitors for molecular and animal studies has yielded useful information toward understanding PARG functions and potential therapeutic applications. However, the conclusions from these studies could be vastly improved with the use of more specific and potent PARG inhibitors. For example, a recent study developed a PAR derivative, poly(epsilonADP-ribose), which cannot be cleaved by PARG, but can inhibit its PAR hydrolase activity, presumably by competing with ADP-ribose (Shirato et al., 2007).

Recent studies have revealed some controversy with regard to the efficacy and overall experimental use of the current PARG inhibitors. One group suggests that neither gallotannins nor the currently available synthetic inhibitors (*i.e.,* GPI 16552) had a detectable effect on PARG function in intact cells due to lack of cell permeability and potential anti-oxidant properties (Falsig et al., 2004). Another study

Figure 1.3. PARP-1 and PARG chemical inhibitors. *A*, Chemical structures of PARP-1 inhibitors discussed in the text. Nicotinamide, a byproduct of the PARP-1 enzymatic reaction (shown in Figure 1.1) and a natural inhibitor of PARP-1 activity, served as a model for the first synthetic PARP-1 inhibitors, including 3-aminobenzamide. Inhibitor development progressed with greater specificity, potency, and solubility, evolving into such inhibitors as PJ-34, ABT-888, and Olaparib. These enhanced features allowed for their use in cell and animal models, as well as in human clinical trials for cancer treatments. *B*, Chemical structures of PARG inhibitors discussed in the text. Early classes of PARG inhibitors include tannins, which were extracted from green tea leaves. While gallotannins (*i.e.,* tannic acid) are the most commonly used inhibitors, ellagitannins (*i.e.,* nobotannin B) are being more recently investigated as they have a higher potency than gallotannins. A synthetic PARG inhibitor, ADP-HPD, greatly improved potency of inhibition, but is limited in use due to its lack of cell permeability.

A

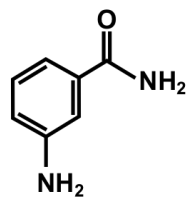

3-aminobenzamide

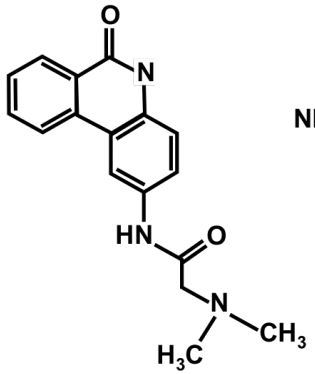

PJ-34

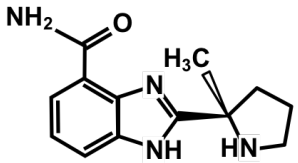

ABT-888

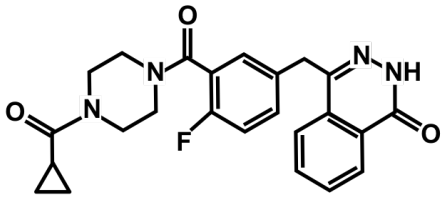

Olaparib

B

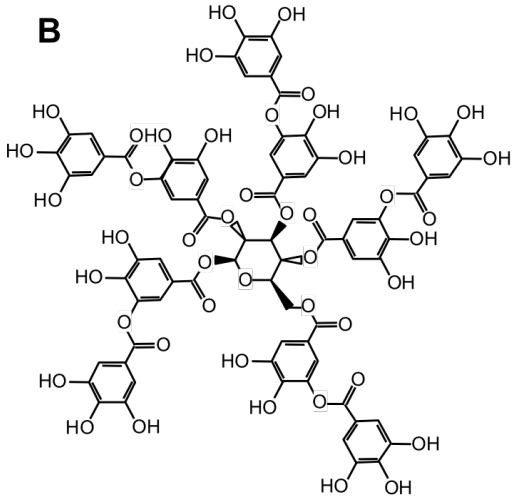

Tannic Acid

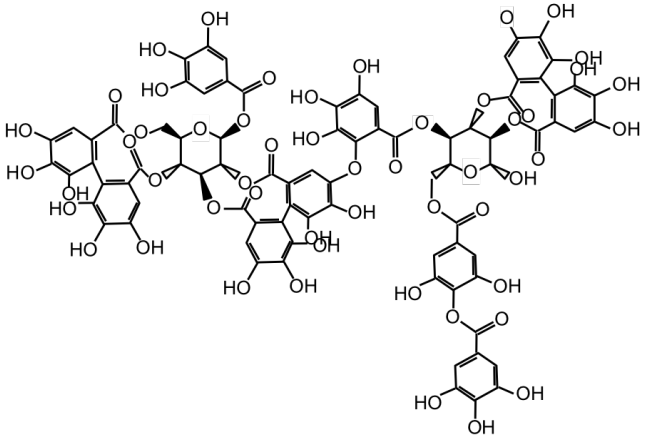

Nobotannin B

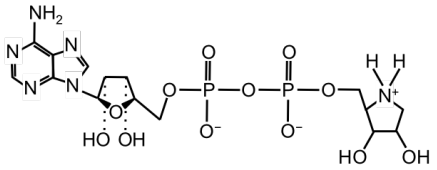

ADP-HPD

compared expression effects in A549 cells upon treatment with PJ34 (a PARP inhibitor) and gallotannin. The authors concluded that the effects of gallotannin on gene expression could not be attributed to PARG inhibition, based on the idea that PARP inhibition did not affect the same genes. This interpretation should be taken with caution, since it is possible that these enzymes can take on roles independent of one another and their enzymatic activities, leading to transcriptional regulation (Frizzell et al., 2009; Krishnakumar and Kraus, 2010). In fact, re-expressing wild type and catalytically inactive mutants in the context of a PARG knockdown corroborated the transcriptional effects of gallotannin at target genes, demonstrating that the effects of gallotannin are through PARG inhibition (Frizzell et al., 2009).

1.9.3. Potential Therapeutic Applications (Experimental Models)

PARP-1 and PARG inhibitors may ultimately have utility as therapeutic agents for the treatment of cancers, cardiovascular diseases, diabetes mellitus and other diseases. The examples presented here are only a few of the potential therapeutic applications of PARP-1 and PARG inhibitors for the treatment of diseases. Current clinical trials will provide an indication of whether PARP-1 inhibitors will ultimately become widely used therapeutic agents. And, although the current data for PARG inhibitors is in the beginning stages, the future applications are promising.

Cancer – PARP-1 inhibitors promote cell death in chemically-treated or radiation therapy-treated cancers by impairing DNA damage response and repair pathways, and ultimately promoting apoptosis (Bryant and Helleday, 2004; Curtin et al., 2004; Delaney et al., 2000; Inbar-Rozensal et al., 2009; Tentori et al., 2002b). The efficacy of some anti-cancer chemotherapies or radiotherapies is improved when they are administered with PARP-1 inhibitors. For example, in mouse models and human cancer cell lines, the efficacy of temozolomide, an anti-cancer alkylating agent that

damages DNA and inhibits DNA replication, is improved when co-administered with the PARP-1 inhibitor NU1025, which blocks PARP-1's DNA repair activities (Delaney et al., 2000; Tentori et al., 2002a; Tentori et al., 2002b). Some PARP-1 inhibitors, such as AG14361, are being tested in clinical trials as therapeutic agents for cancers ((Curtin et al., 2004); described below). In many cases, the cancers in question already have a genetic aberration causing a defect in a DNA repair process. The goal for PARP-1 inhibitors is to target these particular cells and impair the "back-up" repair pathway, ultimately leading to cell death, an effect that has been shown by many groups to occur in cell models (Inbar-Rozensal et al., 2009). In a model of acute promyelocytic leukemia, NB4 cells undergo granulocytic differentiation in response to all-*trans* retinoic acid. Interestingly, co-treamtment with a PARP inhibitor triggered apoptosis, rather than differentiation (Berry et al., 2000), demonstrating another method in which PARP-1 inhibitors could be useful for treating cancer.

Although their non-specific proteins interaction and high molecular weights have been limiting their use for therapeutic applications (Lipinski et al., 2001), similar types of results have been demonstrated using PARG inhibitors. For example, treatment with gallotannin and nobotannin reduced astrocyte cell death upon hydrogen peroxide treatment (Ying et al., 2001; Ying and Swanson, 2000). In a model of melanoma, GPI 16552 showed a synergistic inhibition of melanoma growth and metastasis in combination with temozolomide (Tentori et al., 2005). In addition, gallotannin was found to suppress tumor growth factors in a CT26 colon carcinoma cell lines (Lin et al., 2009). The results from these studies suggest the potential for PARG inhibitors in the treatment of cancer, although much work is needed in experimental trials before moving on to clinical trials.

Inflammation and Stress Response – PARP-1 inhibitors can provide protection from cardiovascular diseases. Acute and chronic cardiovascular disease can lead to

the release of oxidants and free radicals that promote DNA damage within cells, as well as the release of toxic mediators to nearby tissues. Inhibition of PARP-1 can attenuate these effects, promoting cell survival and improved cellular function within the affected area. Some PARP-1 inhibitors, such as PJ34, may also have utility as therapeutic agents in diabetes mellitus, acting to protect against islet necrosis by reducing the levels of nitric oxide and reactive oxygen species through reduced cytokine production (Beneke et al., 2004; Tentori et al., 2002a). Additionally, PJ34 can reduce hyperactivation of PARP-1 in response to massive DNA damage, thereby blocking the PARP-1-dependent necrotic cell death pathway. The ability of PARP-1 inhibitors to block pathological inflammatory responses may have therapeutic utility. However, treating patients chronically with PARP-1 inhibitors increases the potential for long-term consequences of accumulating DNA breaks in normal tissues, which is a major concern for this type of application (Ferraris, 2010). This concern is corroborated by a severe diabetes model, where the continued use of PARP-1 inhibitors lead to the development of β-cell tumors due to the survival of damaged cells and the increase in genomic instability (Yamagami et al., 1985).

The use of PARG inhibitors in such models of inflammation are far more limited, but are beginning to display potential and warrant further investigation. For example, treatment with the PARG inhibitors GPI 18214 and GPI 16552 reduced zymosan-induced peritonitis and mortality in mice (Genovese et al., 2004). These particular inhibitors have also been shown to protect mice from dinitrobezene sulfonic acid-induced colitis by blocking pro-inflammatory cytokine production and cell death (Cuzzocrea et al., 2007). A similar protective effect of GPI 16552 was also found in a model of spinal cord inflammation (Cuzzocrea et al., 2006), a mouse model of stroke (Lu et al., 2003), and a neuronal cell model of hydrogen peroxide-induced cell death

(Ying et al., 2001). Collectively, these results display the potential of using both PARP-1 and PARG inhibitors in the treatment of diseases.

1.9.4. Clinical Trials

Currently, over 50 clinical trials involving PARP inhibitors are active, actively recruiting participants or just completed, according to the registry of federally and privately supported clinical trials conducted in the United States and around the world (Table 1.3; www.clinicaltrials.gov). Collectively, there are eight PARP inhibitors represented spanning all phases of the clinical trial process; notably, there are no trials involving PARG inhibitors. Although pharmaceutical companies are supporting the majority of trials, there are a few being conducted by various research and academic institutions in collaboration with the company responsible for the development of the inhibitor. And, while the overwhelming majority of trials are focused on cancer, two trials are investigating INO-1001 (Phase II) with respect to heart disease.

The ongoing clinical trials demonstrate the wide-range of applications and great potential for PARP inhibitors in cancer treatment. There are at least 15 different types of cancer being investigated, ranging from those of the reproductive tissues (*i.e.,* breast, uterus, ovary, fallopian tube, prostate), immune system (*i.e.,* lymphoma, leukemia), and central nervous system (*i.e.,* glioma, glioblastoma), among others. There is also a broad range of tumor stages and aggressive behaviors represented (*i.e.,* solid tumors, metastatic, advanced, recurrent/relapsed). The inhibitors are being investigated for anti-tumor activity in both genetically "normal" and "altered" cancer types (*i.e.,* mutations in *p53* or *BRCA1/2*). In addition, they are being tested as single agents and in combinations with standard radiotherapies and chemotherapies. All of these conditions are detailed in recent reviews (Fauzee et al., 2010; Ferraris, 2010; Rouleau et al., 2010; Underhill et al., 2010)).

Of particular interest are those focusing cancers of the breast and ovary, where PARP inhibitors have shown the most promise. There has been increasing evidence linking PARP-1 to breast cancer. For example, PARP-1-deficient mice exhibit increased spontaneous mammary carcinoma formation, the latency of which is increased by mutations in *p53* (Tong et al., 2007). In addition, PARP activity in human peripheral blood lymphocytes has been linked with breast cancer (Pero et al., 1990) and low levels of PARP-1 gene expression are associated with increased genetic instability in breast cancers (Bieche et al., 1996). Furthermore, certain polymorphisms in PARP-1 may contribute to the development of breast cancers and influence the effectiveness of hormone therapies (Cao et al., 2007). Interestingly, PARP inhibition (1) sensitizes p53-deficient breast cancer cells to doxorubicin-induced apoptosis (Munoz-Gamez et al., 2005) and (2) selectively kills breast cancer cells with hereditary inactivating mutations in *BRCA1* and *BRCA2*, which encode proteins critical for DNA repair by homologous recombination (Drew and Calvert, 2008). Finally, the PARP inhibitor, olaparib, has anti-tumor activity in breast or ovarian cancers containing *BRCA1* and *BRCA2* mutations at safely administrable doses with minimal side effects (Audeh et al., 2010; Fong et al., 2009; Tutt et al., 2010).

Interestingly, a recent study provides evidence that certain PARP inhibitors might also inhibit the growth and promote the death of non-hereditary breast cancer cells lacking mutations in *BRCA1* or *BRCA2* (Inbar-Rozensal et al., 2009). In addition, breast cancers harboring the "triple-negative" characteristic (*i.e.,* those that do not express estrogen receptor (ER), progesterone receptor (PR), and the human epidermal growth factor receptor HER2) also exhibit an increase in PARP-1 expression (Tuma, 2009). HER2 is a cell membrane receptor tyrosine kinase involved in signaling pathways leading to cell proliferation (Lohrisch and Piccart, 2001). Functional connections between HER2, ERKs, and PARP-1 might play a role in

Table 1.3. Summary of clinical trials for PARP inhibitors. Based on the government website (www.clinicaltrials.gov), there exist over 50 clinical trials involving PARP inhibitors. This table summarizes the ongoing or recently completed clinical trials for eight independent PARP inhibitors. Overall, these trials cover multiple cancer types stemming from a variety of tissues, as well as stages of growth, metastasis, and aggressive behaviors. In addition, many trials are focused on cancers with genetic abnormalities. And, finally, about 70% of these trials are conducting combination therapies with commonly used radio- or chemo-therapy agents. Notably, there are no trials involving PARG inhibitors.

Compound	Sponsor	Phase	Condition
MK4827	Merck	I	Advanced solid tumors, ovarian neoplasms, prostate cancer
E7016	Eisai	I	Advanced solid tumors; in combination with temozolomide
CEP-9722	Cephalon	I	Advanced solid tumors; in combination with temozolomide
INO-1001	Inotek	II	Heart disease; patients having heart surgery involving heart-lung bypass
	Inotek	II	Acute myocardial infarction; acute heart attack patients undergoing primary percutaneous coronary intervention
AG-014699	Pfizer	I	Advanced solid tumors; in combination with carboplatin, paclitaxel, cisplatin, epirubicin, pemetrexed, or cyclophosphamide
	Cancer Research UK	II	Advanced, metastatic or BRCA1/2 mutatant breast or ovarian cancer
	Hoosier Oncology Group	II	Triple negative and BRCA1/2 mutant breast cancer; in combination with cisplatin
BSI-201 (iniparib)	BiPar	I & II	Malignant gliomas; in combination with temozolomide
	BiPar	II	Platinum-sensitive recurrent ovarian cancer
	BiPar	II	Triple-negative breast cancer; in combination with gemcitabine or carboplatin
	BiPar	II	Triple-negative breast cancer brain metastasis; in compination with irinotecan

Table 1.3 (continued)

	Sanofi-Aventis	II	Non-small cell lung carcinoma; in combination with gemcitabine or cisplatin
	Sanofi-Aventis	II	Metastatic triple-negative breast cancer; in combination with gemcitabine or carboplatin
	Sanofi-Aventis	II	Triple-negative breast cancer; in combination with paclitaxel
	BiPar	II	BRCA1/2 mutant-associated advanced epithelial ovarian, fallopian tube, or primary peritoneal cancer
	BiPar	II	Breast cancer; in combination with gemcitabine or carboplatin
	BiPar	III	Advanced squamous cell lung cancer; in combination with gemcitabine or carboplatin
ABT-888 (veliparib)	Abbott	I	Metstatic prostate cancer; in combination with temozolomide
	Abbott	I	Colorectal cancer; solid tumors
	Pediatric Brain Tumor Consortium	I	Recurrent or refractory central nervous system tumors in young patients; in combination with temozolomide
	Univ. of Maryland Greenbaum Cancer Center	I	Acute Leukemia; in combination with temozolomide
	Gynecologic Oncology Group	I	Newly diagnosed stage II, III, or IV ovarian epithelial, fallopian tube, primary peritoneal cancer; in combination with carboplatin, paclitaxel, or bevacizumab

Table 1.3 (continued)

Abbott	I	Brain or nervous system neoplasms, neoplasm metastasis, brain or nervous system diseases; in combination with whole brain radiation therapy
Abbott	I	Advanced solid tumors; in combination with carboplatin or gemcitabine
National Cancer Institute	I	Solid tumors, lymphomas, or leukemia; in combination with cyclophosphamide
National Cancer Institute	I	Advanced or refractory solid tumors, lymphomas, or leukemia; in combination with topotecan
Fred Hutchinson Cancer Research Center	I	Recurrent or metastatic, triple negative, BRCA1/2 mutant, male, or late stage breast cancer; in combination with cisplatin, or vinorelbine ditartrate
Abbott	I	Non-hematologic malignancies, metastatic melanoma, breast, ovarianc, primary peritoneal, fallopian tube, or liver cancer; in combination with temozolomide
National Cancer Institute	I	Leukemia, lymphoma, or regratory solid tumors
Georgetown Univ.	II	Colorectal cancer; in combination with temozolomide
Massachusetts General Hospital	II	Metastatis or BRCA1/2 mutant breast caner; in combination with temozolomide
Georgetown Univ.	II	Liver cancer; in combination with temozolomide

Table 1.3(continued)

AZD-2281 (olaparib)	AstraZeneca	I	Triple-negative breast or advanced ovarian cancer; in combination with carboplatin or paclitaxel
	National Cancer Institute	I	BRCA1/2 mutant, hereditary, triple negative, unresectable breast or ovarian cancer; in combinatin with carboplatin
	AstraZeneca	I	Pancreatic cancer; in combination with gemcitabine
	AstraZeneca	I	Ovarian neoplasms or BRCA1/2 mutant cancer
	National Cancer Institute	I	Unresectable or metastatic solid tumors; in combination with cisplatin or gemcitabine
	AstraZeneca	I	Malignant solid tumors; in combination with tepotecan
	AstraZeneca	I	Melanoma neoplasms; in combination with dacarbazine
	AstraZeneca	I	Neoplasm metasasis or solid metastatic tumors
	AstraZeneca	I	Advanced solid tumors; in combination with bevacizumab
	AstraZeneca	II	Gastric cancer; in combination with paclitaxel
	AstraZeneca	II	colorectal cancer with microsatellite instability phenotype
	AstraZeneca	II	BRCA1/2 mutant ovarian or breast, prostate, pancreatic, or advanced solid tumors
	AstraZeneca	II	Ovarian neoplasms; in combination with liposomal doxorubicin

Table 1.3 (continued)

AstraZeneca	II	Advanced ovarian cancer; in combination with paclitaxel or carboplatin
AstraZeneca	II	Ovarian carcinoma, BRCA1/2 mutant or triple-negative breast cancer
AstraZeneca	II	Platinum-sensitive serous ovarian cancer
AstraZeneca	II	BRCA-positive breast neoplasms
AstraZeneca	II	BRCA-positive ovarian neoplasms

determining the sensitivity of breast cancers to PARP inhibitors. This sub-type of breast cancer is now a major target for PARP inhibitor anti-tumor activity, and the results thus far are promising (Hashimoto and Tamura, 2010). These intriguing results might lead the way to new approaches for treating a broad spectrum of breast cancers.

It will be important to understand the mechanism of action for any of the inhibitors that have an effect on tumor growth and progression. For example, based on the previous results with the BRCA1/2-deficent cells, the assumption is that the ultimate target of the PARP inhibition is a DNA repair pathway. Although some tumors are apparently wild type for BRCA1/2, they may harbor mutations in genes encoding other DNA repair and checkpoint proteins (*e.g.*, Rad51, Chk1/2) that could render them sensitive to PARP inhibitors. Importantly, nuclear PARPs, such as PARP-1 and PARP-2, also play key roles in gene regulation (Kim et al., 2005; Kraus, 2008); so transcriptional effects cannot be ruled out as the cause of PARP inhibitor sensitivity. Experiments with depletion of specific PARPs will help to determine the relevant targets. In addition, there may be cell cycle effects caused by the PARP inhibitors through signal transduction pathways involving cell cycle proteins (*e.g.*, p21, cyclins, cdc2,) and ERK-dependent kinase cascades. This is a reasonable hypothesis given the involvement of these pathways in cell cycle progression and proliferation in a variety of cancers as well as the connection between ERK2 and PARP-1 activation (Cohen-Armon et al., 2007). Information of this kind will be extremely useful for the design of next-generation inhibitors for specific cancers.

1.10. Perspectives

Two enzymes in the nucleus, PARP-1 and PARG, oversee the majority of PARylation activity in the cell. Based on the summary presented here, it is clear that

these enzymes are involved in numerous molecular activities, from DNA damage repair and cell death to transcriptional regulation. It is also clear that their molecular functions dictate their physiological functions. However, in order to achieve a complete understanding of both aspects, further investigation is required. For example, we are just beginning to understand the functional consequences of the PAR modification and ADPR as a signaling molecule and/or protein-binding platform. Understanding how these contribute to overall PARP-1/PARG molecular functions is necessary. In addition, we are lacking considerable information about how these enzymes cooperate or oppose one another. Just because they have enzymatic activities that polymerize or hydrolyze the PAR modification, does not mean they always counter each other's actions. In this regard, having side-by-side comparisons of cell or animal models would be informative. In addition, having tissue-specific knockout animal models will also aid in our understanding of PARP-1/PARG function and increase the knowledge base for improving inhibitor development.

It is absolutely imperative that the development of next generation PARP-1 and PARG inhibitors is significantly enhanced. Even though PARP inhibitors have advanced over the last few years, we are still lacking inhibitors specific to single PARP family members. Disrupting PARP-1 functions outside of NAD^+ binding might be useful in this regard, for example interrupting complex formation. In addition, understanding the size and branching properties of PAR itself can also yield information useful for generating inhibitors that mimic PAR. For PARG, the overall chemical structure needs to be revamped, allowing for higher specificity, potency, and cell permeability. It is expected that the use of PARP-1 and PARG inhibitors in clinical trials will be far more extensive in the coming years, as they are proving useful for a multitude of diseases. It will be exciting to see the potential for more therapeutic applications as the field progresses.

REFERENCES

Adams-Phillips, L., Briggs, A. G., and Bent, A. F. (2010). Disruption of poly(ADP-ribosyl)ation mechanisms alters responses of Arabidopsis to biotic stress. Plant Physiol *152*, 267-280.

Affar, E. B., Germain, M., Winstall, E., Vodenicharov, M., Shah, R. G., Salvesen, G. S., and Poirier, G. G. (2001). Caspase-3-mediated processing of poly(ADP-ribose) glycohydrolase during apoptosis. J Biol Chem *276*, 2935-2942.

Akiyama, T., Takasawa, S., Nata, K., Kobayashi, S., Abe, M., Shervani, N. J., Ikeda, T., Nakagawa, K., Unno, M., Matsuno, S., and Okamoto, H. (2001). Activation of Reg gene, a gene for insulin-producing beta -cell regeneration: poly(ADP-ribose) polymerase binds Reg promoter and regulates the transcription by autopoly(ADP-ribosyl)ation. Proc Natl Acad Sci U S A *98*, 48-53.

Altmeyer, M., and Hottiger, M. O. (2009). Poly(ADP-ribose) polymerase 1 at the crossroad of metabolic stress and inflammation in aging. Aging (Albany NY) *1*, 458-469.

Alvarez-Gonzalez, R., and Mendoza-Alvarez, H. (1995). Dissection of ADP-ribose polymer synthesis into individual steps of initiation, elongation, and branching. Biochimie *77*, 403-407.

Ambrose, H. E., Willimott, S., Beswick, R. W., Dantzer, F., de Murcia, J. M., Yelamos, J., and Wagner, S. D. (2009). Poly(ADP-ribose) polymerase-1 (Parp-1)-deficient mice demonstrate abnormal antibody responses. Immunology *127*, 178-186.

Amé, J.-C., Jacobson, E. L., and Jacobson, M. K. (2000). ADP-ribose polymer metabolism. In From DNA Damage and Stress Signalling to Cell Death: Poly ADP-Ribosylation Reactions, G. de Murcia, and S. Shall, eds. (New York, Oxford University Press), pp. 1-34.

Ame, J. C., Rolli, V., Schreiber, V., Niedergang, C., Apiou, F., Decker, P., Muller, S., Hoger, T., Menissier-de Murcia, J., and de Murcia, G. (1999). PARP-2, A novel mammalian DNA damage-dependent poly(ADP-ribose) polymerase. J Biol Chem *274*, 17860-17868.

Ame, J. C., Spenlehauer, C., and de Murcia, G. (2004). The PARP superfamily. Bioessays *26*, 882-893.

Arundel-Suto, C. M., Scavone, S. V., Turner, W. R., Suto, M. J., and Sebolt-Leopold, J. S. (1991). Effect of PD 128763, a new potent inhibitor of poly(ADP-ribose) polymerase, on X-ray-induced cellular recovery processes in Chinese hamster V79 cells. Radiat Res *126*, 367-371.

Audeh, M. W., Carmichael, J., Penson, R. T., Friedlander, M., Powell, B., Bell-McGuinn, K. M., Scott, C., Weitzel, J. N., Oaknin, A., Loman, N.*, et al.* (2010). Oral poly(ADP-ribose) polymerase inhibitor olaparib in patients with BRCA1 or BRCA2 mutations and recurrent ovarian cancer: a proof-of-concept trial. Lancet *376*, 245-251.

Bai, P., Houten, S. M., Huber, A., Schreiber, V., Watanabe, M., Kiss, B., de Murcia, G., Auwerx, J., and Menissier-de Murcia, J. (2007). Poly(ADP-ribose) polymerase-2 [corrected] controls adipocyte differentiation and adipose tissue function through the regulation of the activity of the retinoid X receptor/peroxisome proliferator-activated receptor-gamma [corrected] heterodimer. J Biol Chem *282*, 37738-37746.

Banasik, M., Komura, H., Shimoyama, M., and Ueda, K. (1992). Specific inhibitors of poly(ADP-ribose) synthetase and mono(ADP-ribosyl)transferase. J Biol Chem *267*, 1569-1575.

Barbehenn, R. V., Jones, C. P., Hagerman, A. E., Karonen, M., and Salminen, J. P. (2006). Ellagitannins have greater oxidative activities than condensed tannins and galloyl glucoses at high pH: potential impact on caterpillars. J Chem Ecol *32*, 2253-2267.

Beneke, S., Diefenbach, J., and Burkle, A. (2004). Poly(ADP-ribosyl)ation inhibitors: promising drug candidates for a wide variety of pathophysiologic conditions. Int J Cancer *111*, 813-818.

Berger, F., Ramirez-Hernandez, M. H., and Ziegler, M. (2004). The new life of a centenarian: signalling functions of NAD(P). Trends Biochem Sci *29*, 111-118.

Berry, D. M., Williams, K., and Meckling-Gill, K. A. (2000). All trans retinoic acid induces apoptosis in acute promyelocytic NB4 cells when combined with isoquinolinediol, a poly(ADP-ribose) polymerase inhibitor. Leuk Res *24*, 307-316.

Bieche, I., de Murcia, G., and Lidereau, R. (1996). Poly(ADP-ribose) polymerase gene expression status and genomic instability in human breast cancer. Clin Cancer Res *2*, 1163-1167.

Bluestone, J. A., Herold, K., and Eisenbarth, G. (2010). Genetics, pathogenesis and clinical interventions in type 1 diabetes. Nature *464*, 1293-1300.

Bonicalzi, M. E., Haince, J. F., Droit, A., and Poirier, G. G. (2005). Regulation of poly(ADP-ribose) metabolism by poly(ADP-ribose) glycohydrolase: where and when? Cell Mol Life Sci *62*, 739-750.

Bouchard, V. J., Rouleau, M., and Poirier, G. G. (2003). PARP-1, a determinant of cell survival in response to DNA damage. Exp Hematol *31*, 446-454.

Boulares, A. H., Yakovlev, A. G., Ivanova, V., Stoica, B. A., Wang, G., Iyer, S., and Smulson, M. (1999). Role of poly(ADP-ribose) polymerase (PARP) cleavage in apoptosis. Caspase 3-resistant PARP mutant increases rates of apoptosis in transfected cells. J Biol Chem *274*, 22932-22940.

Bryant, H. E., and Helleday, T. (2004). Poly(ADP-ribose) polymerase inhibitors as potential chemotherapeutic agents. Biochem Soc Trans *32*, 959-961.

Burkle, A., Brabeck, C., Diefenbach, J., and Beneke, S. (2005a). The emerging role of poly(ADP-ribose) polymerase-1 in longevity. Int J Biochem Cell Biol *37*, 1043-1053.

Burkle, A., Diefenbach, J., Brabeck, C., and Beneke, S. (2005b). Ageing and PARP. Pharmacol Res *52*, 93-99.

Burkle, A., Grube, K., and Kupper, J. H. (1992). Poly(ADP-ribosyl)ation: its role in inducible DNA amplification, and its correlation with the longevity of mammalian species. Exp Clin Immunogenet *9*, 230-240.

Caiafa, P., Guastafierro, T., and Zampieri, M. (2009). Epigenetics: poly(ADP-ribosyl)ation of PARP-1 regulates genomic methylation patterns. FASEB J *23*, 672-678.

Caiafa, P., and Zlatanova, J. (2009). CCCTC-binding factor meets poly(ADP-ribose) polymerase-1. J Cell Physiol *219*, 265-270.

Cao, W. H., Wang, X., Frappart, L., Rigal, D., Wang, Z. Q., Shen, Y., and Tong, W. M. (2007). Analysis of genetic variants of the poly(ADP-ribose) polymerase-1 gene in breast cancer in French patients. Mutat Res *632*, 20-28.

Carrillo, A., Monreal, Y., Ramirez, P., Marin, L., Parrilla, P., Oliver, F. J., and Yelamos, J. (2004). Transcription regulation of TNF-alpha-early response genes by poly(ADP-ribose) polymerase-1 in murine heart endothelial cells. Nucleic Acids Res *32*, 757-766.

Chambon, P., Weill, J. D., and Mandel, P. (1963). Nicotinamide mononucleotide activation of new DNA-dependent polyadenylic acid synthesizing nuclear enzyme. Biochem Biophys Res Commun *11*, 39-43.

Chiang, Y. J., Nguyen, M. L., Gurunathan, S., Kaminker, P., Tessarollo, L., Campisi, J., and Hodes, R. J. (2006). Generation and characterization of telomere length maintenance in tankyrase 2-deficient mice. Mol Cell Biol *26*, 2037-2043.

Cohen-Armon, M., Visochek, L., Rozensal, D., Kalal, A., Geistrikh, I., Klein, R., Bendetz-Nezer, S., Yao, Z., and Seger, R. (2007). DNA-independent PARP-1 activation by phosphorylated ERK2 increases Elk1 activity: a link to histone acetylation. Mol Cell *25*, 297-308.

Cole, K., and Perez-Polo, J. R. (2004). Neuronal trauma model: in search of Thanatos. Int J Dev Neurosci *22*, 485-496.

Conde, C., Mark, M., Oliver, F. J., Huber, A., de Murcia, G., and Menissier-de Murcia, J. (2001). Loss of poly(ADP-ribose) polymerase-1 causes increased tumour latency in p53-deficient mice. Embo J *20*, 3535-3543.

Cortes, U., Tong, W. M., Coyle, D. L., Meyer-Ficca, M. L., Meyer, R. G., Petrilli, V., Herceg, Z., Jacobson, E. L., Jacobson, M. K., and Wang, Z. Q. (2004). Depletion of the 110-kilodalton isoform of poly(ADP-ribose) glycohydrolase increases sensitivity to genotoxic and endotoxic stress in mice. Mol Cell Biol *24*, 7163-7178.

Coyle, D. L., Kim, H., Jacobson, E., and Jacobson, M. (2003). Synthesis and characterization of potent and selective cell permeable iinhibitors of poly(ADP-ribose) glycohydrolase. Med Sci Mon. *9*, 15.

Curtin, N. J. (2006). PARP inhibitors and cancer therapy. In Poly(ADP-Ribosyl)ation, A. Bürkle, ed. (Georgetown, Landes Bioscience), pp. 218-233.

Curtin, N. J., Wang, L. Z., Yiakouvaki, A., Kyle, S., Arris, C. A., Canan-Koch, S., Webber, S. E., Durkacz, B. W., Calvert, H. A., Hostomsky, Z., and Newell, D. R. (2004). Novel poly(ADP-ribose) polymerase-1 inhibitor, AG14361, restores sensitivity to temozolomide in mismatch repair-deficient cells. Clin Cancer Res *10*, 881-889.

Cuzzocrea, S., Genovese, T., Mazzon, E., Crisafulli, C., Min, W., Di Paola, R., Muia, C., Li, J. H., Esposito, E., Bramanti, P.*, et al.* (2006). Poly(ADP-ribose) glycohydrolase activity mediates post-traumatic inflammatory reaction after experimental spinal cord trauma. J Pharmacol Exp Ther *319*, 127-138.

Cuzzocrea, S., Mazzon, E., Genovese, T., Crisafulli, C., Min, W. K., Di Paola, R., Muia, C., Li, J. H., Malleo, G., Xu, W.*, et al.* (2007). Role of poly(ADP-ribose) glycohydrolase in the development of inflammatory bowel disease in mice. Free Radic Biol Med *42*, 90-105.

D'Amours, D., Desnoyers, S., D'Silva, I., and Poirier, G. (1999). Poly(ADP-ribosyl)ation reactions in the regulation of nuclear functions. Biochem J *342*, 249-268.

Dantzer, F., de La Rubia, G., Menissier-De Murcia, J., Hostomsky, Z., de Murcia, G., and Schreiber, V. (2000). Base excision repair is impaired in mammalian cells lacking Poly(ADP-ribose) polymerase-1. Biochemistry *39*, 7559-7569.

Dantzer, F., Giraud-Panis, M. J., Jaco, I., Ame, J. C., Schultz, I., Blasco, M., Koering, C. E., Gilson, E., Menissier-de Murcia, J., de Murcia, G., and Schreiber, V. (2004). Functional interaction between poly(ADP-Ribose) polymerase 2 (PARP-2) and TRF2: PARP activity negatively regulates TRF2. Mol Cell Biol *24*, 1595-1607.

Dantzer, F., Mark, M., Quenet, D., Scherthan, H., Huber, A., Liebe, B., Monaco, L., Chicheportiche, A., Sassone-Corsi, P., de Murcia, G., and Menissier-de Murcia, J. (2006). Poly(ADP-ribose) polymerase-2 contributes to the fidelity of male meiosis I and spermiogenesis. Proc Natl Acad Sci U S A *103*, 14854-14859.

Davidovic, L., Vodenicharov, M., Affar, E. B., and Poirier, G. G. (2001). Importance of poly(ADP-ribose) glycohydrolase in the control of poly(ADP-ribose) metabolism. Exp Cell Res *268*, 7-13.

De Block, M., Verduyn, C., De Brouwer, D., and Cornelissen, M. (2005). Poly(ADP-ribose) polymerase in plants affects energy homeostasis, cell death and stress tolerance. Plant J *41*, 95-106.

de Murcia, J. M., Niedergang, C., Trucco, C., Ricoul, M., Dutrillaux, B., Mark, M., Oliver, F. J., Masson, M., Dierich, A., LeMeur, M.*, et al.* (1997). Requirement of poly(ADP-ribose) polymerase in recovery from DNA damage in mice and in cells. Proc Natl Acad Sci U S A *94*, 7303-7307.

Delaney, C. A., Wang, L. Z., Kyle, S., White, A. W., Calvert, A. H., Curtin, N. J., Durkacz, B. W., Hostomsky, Z., and Newell, D. R. (2000). Potentiation of temozolomide and topotecan growth inhibition and cytotoxicity by novel poly(adenosine diphosphoribose) polymerase inhibitors in a panel of human tumor cell lines. Clin Cancer Res *6*, 2860-2867.

Desnoyers, S., Shah, G. M., Brochu, G., Hoflack, J. C., Verreault, A., and Poirier, G. G. (1995). Biochemical properties and function of poly(ADP-ribose) glycohydrolase. Biochimie *77*, 433-438.

Devalaraja-Narashimha, K., and Padanilam, B. J. (2010). PARP1 deficiency exacerbates diet-induced obesity in mice. J Endocrinol *205*, 243-252.

Donmez, G., and Guarente, L. (2010). Aging and disease: connections to sirtuins. Aging Cell *9*, 285-290.

Drew, Y., and Calvert, H. (2008). The potential of PARP inhibitors in genetic breast and ovarian cancers. Ann N Y Acad Sci *1138*, 136-145.

El Ramy, R., Magroun, N., Messadecq, N., Gauthier, L. R., Boussin, F. D., Kolthur-Seetharam, U., Schreiber, V., McBurney, M. W., Sassone-Corsi, P., and Dantzer, F. (2009). Functional interplay between Parp-1 and SirT1 in genome integrity and chromatin-based processes. Cell Mol Life Sci *66*, 3219-3234.

El-Khamisy, S. F., Masutani, M., Suzuki, H., and Caldecott, K. W. (2003). A requirement for PARP-1 for the assembly or stability of XRCC1 nuclear foci at sites of oxidative DNA damage. Nucleic Acids Res *31*, 5526-5533.

Eliasson, M. J., Sampei, K., Mandir, A. S., Hurn, P. D., Traystman, R. J., Bao, J., Pieper, A., Wang, Z. Q., Dawson, T. M., Snyder, S. H., and Dawson, V. L. (1997). Poly(ADP-ribose) polymerase gene disruption renders mice resistant to cerebral ischemia. Nat Med *3*, 1089-1095.

Erdelyi, K., Kiss, A., Bakondi, E., Bai, P., Szabo, C., Gergely, P., Erdodi, F., and Virag, L. (2005). Gallotannin inhibits the expression of chemokines and inflammatory cytokines in A549 cells. Mol Pharmacol *68*, 895-904.

Fahrer, J., Popp, O., Malanga, M., Beneke, S., Markovitz, D. M., Ferrando-May, E., Burkle, A., and Kappes, F. (2010). High-Affinity Interaction of Poly(ADP-ribose) and the Human DEK Oncoprotein Depends upon Chain Length. Biochemistry.

Falsig, J., Christiansen, S. H., Feuerhahn, S., Burkle, A., Oei, S. L., Keil, C., and Leist, M. (2004). Poly(ADP-ribose) glycohydrolase as a target for neuroprotective intervention: assessment of currently available pharmacological tools. Eur J Pharmacol *497*, 7-16.

Farrar, D., Rai, S., Chernukhin, I., Jagodic, M., Ito, Y., Yammine, S., Ohlsson, R., Murrell, A., and Klenova, E. (2010). Mutational analysis of the poly(ADP-ribosyl)ation sites of the transcription factor CTCF provides an insight into the mechanism of its regulation by poly(ADP-ribosyl)ation. Mol Cell Biol *30*, 1199-1216.

Fauzee, N. J., Pan, J., and Wang, Y. L. (2010). PARP and PARG Inhibitors-New Therapeutic Targets in Cancer Treatment. Pathol Oncol Res.

Ferraris, D. V. (2010). Evolution of poly(ADP-ribose) polymerase-1 (PARP-1) inhibitors. From concept to clinic. J Med Chem *53*, 4561-4584.

Flohr, C., Burkle, A., Radicella, J. P., and Epe, B. (2003). Poly(ADP-ribosyl)ation accelerates DNA repair in a pathway dependent on Cockayne syndrome B protein. Nucleic Acids Res *31*, 5332-5337.

Fong, P. C., Boss, D. S., Yap, T. A., Tutt, A., Wu, P., Mergui-Roelvink, M., Mortimer, P., Swaisland, H., Lau, A., O'Connor, M. J.*, et al.* (2009). Inhibition of

poly(ADP-ribose) polymerase in tumors from BRCA mutation carriers. N Engl J Med *361*, 123-134.

Formentini, L., Arapistas, P., Pittelli, M., Jacomelli, M., Pitozzi, V., Menichetti, S., Romani, A., Giovannelli, L., Moroni, F., and Chiarugi, A. (2008). Mono-galloyl glucose derivatives are potent poly(ADP-ribose) glycohydrolase (PARG) inhibitors and partially reduce PARP-1-dependent cell death. Br J Pharmacol *155*, 1235-1249.

Frizzell, K. M., Gamble, M. J., Berrocal, J. G., Zhang, T., Krishnakumar, R., Cen, Y., Sauve, A. A., and Kraus, W. L. (2009). Global analysis of transcriptional regulation by poly(ADP-ribose) polymerase-1 and poly(ADP-ribose) glycohydrolase in MCF-7 human breast cancer cells. J Biol Chem *284*, 33926-33938.

Gagne, J. P., Moreel, X., Gagne, P., Labelle, Y., Droit, A., Chevalier-Pare, M., Bourassa, S., McDonald, D., Hendzel, M. J., Prigent, C., and Poirier, G. G. (2008). Proteomic Investigation of Phosphorylation Sites in Poly(ADP-ribose) Polymerase-1 and Poly(ADP-ribose) Glycohydrolase. J Proteome Res.

Gamble, M. J., and Fisher, R. P. (2007). SET and PARP1 remove DEK from chromatin to permit access by the transcription machinery. Nat Struct Mol Biol *14*, 548-555.

Gao, F., Kwon, S. W., Zhao, Y., and Jin, Y. (2009). PARP1 poly(ADP-ribosyl)ates Sox2 to control Sox2 protein levels and FGF4 expression during embryonic stem cell differentiation. J Biol Chem *284*, 22263-22273.

Garcia Soriano, F., Virag, L., Jagtap, P., Szabo, E., Mabley, J. G., Liaudet, L., Marton, A., Hoyt, D. G., Murthy, K. G., Salzman, A. L.*, et al.* (2001). Diabetic endothelial dysfunction: the role of poly(ADP-ribose) polymerase activation. Nat Med *7*, 108-113.

Genovese, T., Di Paola, R., Catalano, P., Li, J. H., Xu, W., Massuda, E., Caputi, A. P., Zhang, J., and Cuzzocrea, S. (2004). Treatment with a novel poly(ADP-ribose) glycohydrolase inhibitor reduces development of septic shock-like syndrome induced by zymosan in mice. Crit Care Med *32*, 1365-1374.

Gonzalez, C., Menissier De Murcia, J., Janiak, P., Bidouard, J. P., Beauvais, C., Karray, S., Garchon, H. J., and Levi-Strauss, M. (2002). Unexpected sensitivity of nonobese diabetic mice with a disrupted poly(ADP-Ribose) polymerase-1 gene to streptozotocin-induced and spontaneous diabetes. Diabetes *51*, 1470-1476.

Griffin, R. J., Pemberton, L. C., Rhodes, D., Bleasdale, C., Bowman, K., Calvert, A. H., Curtin, N. J., Durkacz, B. W., Newell, D. R., Porteous, J. K., and et al. (1995). Novel potent inhibitors of the DNA repair enzyme poly(ADP-ribose)polymerase (PARP). Anticancer Drug Des *10*, 507-514.

Grube, K., and Burkle, A. (1992). Poly(ADP-ribose) polymerase activity in mononuclear leukocytes of 13 mammalian species correlates with species-specific life span. Proc Natl Acad Sci U S A *89*, 11759-11763.

Guastafierro, T., Cecchinelli, B., Zampieri, M., Reale, A., Riggio, G., Sthandier, O., Zupi, G., Calabrese, L., and Caiafa, P. (2008). CCCTC-binding factor activates PARP-1 affecting DNA methylation machinery. J Biol Chem *283*, 21873-21880.

Ha, H. C. (2004). Defective transcription factor activation for proinflammatory gene expression in poly(ADP-ribose) polymerase 1-deficient glia. Proc Natl Acad Sci U S A *101*, 5087-5092.

Ha, H. C., and Snyder, S. H. (2000). Poly(ADP-ribose) polymerase-1 in the nervous system. Neurobiol Dis *7*, 225-239.

Hakme, A., Wong, H. K., Dantzer, F., and Schreiber, V. (2008). The expanding field of poly(ADP-ribosyl)ation reactions. 'Protein Modifications: Beyond the Usual Suspects' Review Series. EMBO Rep *9*, 1094-1100.

Halappanavar, S. S., Rhun, Y. L., Mounir, S., Martins, L. M., Huot, J., Earnshaw, W. C., and Shah, G. M. (1999). Survival and proliferation of cells expressing caspase-uncleavable Poly(ADP-ribose) polymerase in response to death-inducing DNA damage by an alkylating agent. J Biol Chem *274*, 37097-37104.

Hanai, S., Kanai, M., Ohashi, S., Okamoto, K., Yamada, M., Takahashi, H., and Miwa, M. (2004). Loss of poly(ADP-ribose) glycohydrolase causes progressive neurodegeneration in Drosophila melanogaster. Proc Natl Acad Sci U S A *101*, 82-86.

Hashimoto, K., and Tamura, K. (2010). [Breakthrough breast cancer treatment--PARP inhibitor, BRCA, and triple negative breast cancer]. Gan To Kagaku Ryoho *37*, 1187-1191.

Hassa, P. O., Buerki, C., Lombardi, C., Imhof, R., and Hottiger, M. O. (2003). Transcriptional coactivation of nuclear factor-kappaB-dependent gene expression by p300 is regulated by poly(ADP)-ribose polymerase-1. J Biol Chem *278*, 45145-45153.

Hassa, P. O., Covic, M., Hasan, S., Imhof, R., and Hottiger, M. O. (2001). The enzymatic and DNA binding activity of PARP-1 are not required for NF-kappa B coactivator function. J Biol Chem *276*, 45588-45597.

Hassa, P. O., Haenni, S. S., Buerki, C., Meier, N. I., Lane, W. S., Owen, H., Gersbach, M., Imhof, R., and Hottiger, M. O. (2005). Acetylation of PARP-1 by p300/CBP regulates coactivation of NF-kappa B-dependent transcription. J Biol Chem.

Hassa, P. O., Haenni, S. S., Elser, M., and Hottiger, M. O. (2006). Nuclear ADP-ribosylation reactions in mammalian cells: where are we today and where are we going? Microbiol Mol Biol Rev *70*, 789-829.

Hassa, P. O., and Hottiger, M. O. (2002). The functional role of poly(ADP-ribose)polymerase 1 as novel coactivator of NF-kappaB in inflammatory disorders. Cell Mol Life Sci *59*, 1534-1553.

Hassa, P. O., and Hottiger, M. O. (2008). The diverse biological roles of mammalian PARPS, a small but powerful family of poly-ADP-ribose polymerases. Front Biosci *13*, 3046-3082.

Heale, J. T., Ball, A. R., Jr., Schmiesing, J. A., Kim, J. S., Kong, X., Zhou, S., Hudson, D. F., Earnshaw, W. C., and Yokomori, K. (2006). Condensin I interacts with the PARP-1-XRCC1 complex and functions in DNA single-strand break repair. Mol Cell *21*, 837-848.

Hemberger, M., Nozaki, T., Winterhager, E., Yamamoto, H., Nakagama, H., Kamada, N., Suzuki, H., Ohta, T., Ohki, M., Masutani, M., and Cross, J. C. (2003). Parp1-deficiency induces differentiation of ES cells into trophoblast derivatives. Dev Biol *257*, 371-381.

Henrie, M. S., Kurimasa, A., Burma, S., Menissier-de Murcia, J., de Murcia, G., Li, G. C., and Chen, D. J. (2003). Lethality in PARP-1/Ku80 double mutant mice reveals physiological synergy during early embryogenesis. DNA Repair (Amst) *2*, 151-158.

Hofseth, L. J., Hussain, S. P., and Harris, C. C. (2004). p53: 25 years after its discovery. Trends Pharmacol Sci *25*, 177-181.

Hottiger, M. O., Hassa, P. O., Luscher, B., Schuler, H., and Koch-Nolte, F. (2010). Toward a unified nomenclature for mammalian ADP-ribosyltransferases. Trends Biochem Sci *35*, 208-219.

Huang, S. M., Mishina, Y. M., Liu, S., Cheung, A., Stegmeier, F., Michaud, G. A., Charlat, O., Wiellette, E., Zhang, Y., Wiessner, S*., et al.* (2009). Tankyrase inhibition stabilizes axin and antagonizes Wnt signalling. Nature *461*, 614-620.

Huletsky, A., de Murcia, G., Muller, S., Hengartner, M., Menard, L., Lamarre, D., and Poirier, G. G. (1989). The effect of poly(ADP-ribosyl)ation on native and H1-depleted chromatin. A role of poly(ADP-ribosyl)ation on core nucleosome structure. J Biol Chem *264*, 8878-8886.

Inbar-Rozensal, D., Castiel, A., Visochek, L., Castel, D., Dantzer, F., Izraeli, S., and Cohen-Armon, M. (2009). A selective eradication of human non-hereditary breast cancer cells by phenanthridine derived poly(ADP-ribose) polymerase inhibitors. Breast Cancer Research.

Ishida, J., Hattori, K., Yamamoto, H., Iwashita, A., Mihara, K., and Matsuoka, N. (2005). 4-Phenyl-1,2,3,6-tetrahydropyridine, an excellent fragment to improve the potency of PARP-1 inhibitors. Bioorg Med Chem Lett *15*, 4221-4225.

Ishida, J., Yamamoto, H., Kido, Y., Kamijo, K., Murano, K., Miyake, H., Ohkubo, M., Kinoshita, T., Warizaya, M., Iwashita, A*., et al.* (2006). Discovery of potent and selective PARP-1 and PARP-2 inhibitors: SBDD analysis via a combination of X-ray structural study and homology modeling. Bioorg Med Chem *14*, 1378-1390.

Iwashita, A., Tojo, N., Matsuura, S., Yamazaki, S., Kamijo, K., Ishida, J., Yamamoto, H., Hattori, K., Matsuoka, N., and Mutoh, S. (2004). A novel and potent poly(ADP-ribose) polymerase-1 inhibitor, FR247304 (5-chloro-2-[3-(4-phenyl-3,6-dihydro-1(2H)-pyridinyl)propyl]-4(3H)-quinazo linone), attenuates neuronal damage in in vitro and in vivo models of cerebral ischemia. J Pharmacol Exp Ther *310*, 425-436.

Jagtap, P., and Szabo, C. (2005). Poly(ADP-ribose) polymerase and the therapeutic effects of its inhibitors. Nat Rev Drug Discov *4*, 421-440.

Jelezcova, E., Trivedi, R. N., Wang, X. H., Tang, J. B., Brown, A. R., Goellner, E. M., Schamus, S., Fornsaglio, J. L., and Sobol, R. W. (2010). Parp1 activation in mouse embryonic fibroblasts promotes Pol beta-dependent cellular hypersensitivity to alkylation damage. Mutat Res *686*, 57-67.

Jiang, H., Kim, J. H., Frizzell, K. M., Kraus, W. L., and Lin, H. (2010). Clickable NAD analogues for labeling substrate proteins of poly(ADP-ribose) polymerases. J Am Chem Soc *132*, 9363-9372.

Ju, B. G., Lunyak, V. V., Perissi, V., Garcia-Bassets, I., Rose, D. W., Glass, C. K., and Rosenfeld, M. G. (2006). A topoisomerase IIbeta-mediated dsDNA break required for regulated transcription. Science *312*, 1798-1802.

Ju, B. G., Solum, D., Song, E. J., Lee, K. J., Rose, D. W., Glass, C. K., and Rosenfeld, M. G. (2004). Activating the PARP-1 sensor component of the groucho/ TLE1 corepressor complex mediates a CaMKinase IIdelta-dependent neurogenic gene activation pathway. Cell *119*, 815-829.

Kappes, F., Fahrer, J., Khodadoust, M. S., Tabbert, A., Strasser, C., Mor-Vaknin, N., Moreno-Villanueva, M., Burkle, A., Markovitz, D. M., and Ferrando-May, E. (2008). DEK is a poly(ADP-ribose) acceptor in apoptosis and mediates resistance to genotoxic stress. Mol Cell Biol *28*, 3245-3257.

Karras, G. I., Kustatscher, G., Buhecha, H. R., Allen, M. D., Pugieux, C., Sait, F., Bycroft, M., and Ladurner, A. G. (2005). The macro domain is an ADP-ribose binding module. Embo J *24*, 1911-1920.

Kaufmann, S. H., Desnoyers, S., Ottaviano, Y., Davidson, N. E., and Poirier, G. G. (1993). Specific proteolytic cleavage of poly(ADP-ribose) polymerase: an early marker of chemotherapy-induced apoptosis. Cancer Res *53*, 3976-3985.

Kauppinen, T. M., Chan, W. Y., Suh, S. W., Wiggins, A. K., Huang, E. J., and Swanson, R. A. (2006). Direct phosphorylation and regulation of poly(ADP-ribose) polymerase-1 by extracellular signal-regulated kinases 1/2. Proc Natl Acad Sci U S A *103*, 7136-7141.

Keil, C., Grobe, T., and Oei, S. L. (2006). MNNG-induced cell death is controlled by interactions between PARP-1, poly(ADP-ribose) glycohydrolase, and XRCC1. J Biol Chem *281*, 34394-34405.

Kim, M. Y., Mauro, S., Gevry, N., Lis, J. T., and Kraus, W. L. (2004). NAD+-dependent modulation of chromatin structure and transcription by nucleosome binding properties of PARP-1. Cell *119*, 803-814.

Kim, M. Y., Zhang, T., and Kraus, W. L. (2005). Poly(ADP-ribosyl)ation by PARP-1: 'PAR-laying' NAD+ into a nuclear signal. Genes Dev *19*, 1951-1967.

Kleine, H., Poreba, E., Lesniewicz, K., Hassa, P. O., Hottiger, M. O., Litchfield, D. W., Shilton, B. H., and Luscher, B. (2008). Substrate-assisted catalysis by PARP10 limits its activity to mono-ADP-ribosylation. Mol Cell *32*, 57-69.

Koh, D. W., Lawler, A. M., Poitras, M. F., Sasaki, M., Wattler, S., Nehls, M. C., Stoger, T., Poirier, G. G., Dawson, V. L., and Dawson, T. M. (2004). Failure to degrade poly(ADP-ribose) causes increased sensitivity to cytotoxicity and early embryonic lethality. Proc Natl Acad Sci U S A *101*, 17699-17704.

Koh, D. W., Patel, C. N., Ramsinghani, S., Slama, J. T., Oliveira, M. A., and Jacobson, M. K. (2003). Identification of an inhibitor binding site of poly(ADP-ribose) glycohydrolase. Biochemistry *42*, 4855-4863.

Kolthur-Seetharam, U., Dantzer, F., McBurney, M. W., de Murcia, G., and Sassone-Corsi, P. (2006). Control of AIF-mediated Cell Death by the Functional Interplay of SIRT1 and PARP-1 in Response to DNA Damage. Cell Cycle *5*.

Kraus, W. L. (2008). Transcriptional control by PARP-1: chromatin modulation, enhancer-binding, coregulation, and insulation. Curr Opin Cell Biol *20*, 294-302.

Kraus, W. L., and Lis, J. (2003). PARP goes transcription. Cell *113*, 677-683.

Krishnakumar, R., Gamble, M. J., Frizzell, K. M., Berrocal, J. G., Kininis, M., and Kraus, W. L. (2008). Reciprocal binding of PARP-1 and histone H1 at promoters specifies transcriptional outcomes. Science *319*, 819-821.

Krishnakumar, R., and Kraus, W. L. (2010). The PARP side of the nucleus: molecular actions, physiological outcomes, and clinical targets. Mol Cell *39*, 8-24.

Langelier, M. F., Ruhl, D. D., Planck, J. L., Kraus, W. L., and Pascal, J. M. (2010). The Zn3 domain of human poly(ADP-ribose) polymerase-1 (PARP-1) functions in both DNA-dependent poly(ADP-ribose) synthesis activity and chromatin compaction. J Biol Chem *285*, 18877-18887.

Langelier, M. F., Servent, K. M., Rogers, E. E., and Pascal, J. M. (2008). A third zinc-binding domain of human poly(ADP-ribose) polymerase-1 coordinates DNA-dependent enzyme activation. J Biol Chem *283*, 4105-4114.

Le Page, F., Schreiber, V., Dherin, C., De Murcia, G., and Boiteux, S. (2003). Poly(ADP-ribose) polymerase-1 (PARP-1) is required in murine cell lines for base excision repair of oxidative DNA damage in the absence of DNA polymerase beta. J Biol Chem *278*, 18471-18477.

Lebel, M., Lavoie, J., Gaudreault, I., Bronsard, M., and Drouin, R. (2003). Genetic cooperation between the Werner syndrome protein and poly(ADP-ribose) polymerase-1 in preventing chromatid breaks, complex chromosomal rearrangements, and cancer in mice. Am J Pathol *162*, 1559-1569.

Lee, J. W., Harrigan, J., Opresko, P. L., and Bohr, V. A. (2005). Pathways and functions of the Werner syndrome protein. Mech Ageing Dev *126*, 79-86.

Lin, L., Li, J., Wang, Y. L., and Lin, X. (2009). Relationship of PARG with PARP, VEGF, and b-FGF in Colorectal Carcinoma. Chinese Journal of Cancer Research *21*, 135-141.

Lin, W., Ame, J. C., Aboul-Ela, N., Jacobson, E. L., and Jacobson, M. K. (1997). Isolation and characterization of the cDNA encoding bovine poly(ADP-ribose) glycohydrolase. J Biol Chem *272*, 11895-11901.

Lipinski, C. A., Lombardo, F., Dominy, B. W., and Feeney, P. J. (2001). Experimental and computational approaches to estimate solubility and permeability in drug discovery and development settings. Adv Drug Deliv Rev *46*, 3-26.

Lohrisch, C., and Piccart, M. (2001). HER2/neu as a predictive factor in breast cancer. Clin Breast Cancer *2*, 129-135.

Lu, X. C., Massuda, E., Lin, Q., Li, W., Li, J. H., and Zhang, J. (2003). Post-treatment with a novel PARG inhibitor reduces infarct in cerebral ischemia in the rat. Brain Res *978*, 99-103.

Mabley, J. G., Suarez-Pinzon, W. L., Hasko, G., Salzman, A. L., Rabinovitch, A., Kun, E., and Szabo, C. (2001). Inhibition of poly (ADP-ribose) synthetase by gene disruption or inhibition with 5-iodo-6-amino-1,2-benzopyrone protects mice from multiple-low-dose-streptozotocin-induced diabetes. Br J Pharmacol *133*, 909-919.

Malanga, M., and Althaus, F. R. (2005). The role of poly(ADP-ribose) in the DNA damage signaling network. Biochem Cell Biol *83*, 354-364.

Mandir, A. S., Poitras, M. F., Berliner, A. R., Herring, W. J., Guastella, D. B., Feldman, A., Poirier, G. G., Wang, Z. Q., Dawson, T. M., and Dawson, V. L. (2000). NMDA but not non-NMDA excitotoxicity is mediated by Poly(ADP-ribose) polymerase. J Neurosci *20*, 8005-8011.

Martin, N., Schwamborn, K., Schreiber, V., Werner, A., Guillier, C., Zhang, X. D., Bischof, O., Seeler, J. S., and Dejean, A. (2009). PARP-1 transcriptional activity is regulated by sumoylation upon heat shock. EMBO J *28*, 3534-3548.

Masutani, M., Nakagama, H., and Sugimura, T. (2005). Poly(ADP-ribosyl)ation in relation to cancer and autoimmune disease. Cell Mol Life Sci *62*, 769-783.

Masutani, M., Nozaki, T., Nishiyama, E., Shimokawa, T., Tachi, Y., Suzuki, H., Nakagama, H., Wakabayashi, K., and Sugimura, T. (1999a). Function of poly(ADP-ribose) polymerase in response to DNA damage: gene-disruption study in mice. Mol Cell Biochem *193*, 149-152.

Masutani, M., Suzuki, H., Kamada, N., Watanabe, M., Ueda, O., Nozaki, T., Jishage, K., Watanabe, T., Sugimoto, T., Nakagama, H*., et al.* (1999b). Poly(ADP-ribose) polymerase gene disruption conferred mice resistant to streptozotocin-induced diabetes. Proc Natl Acad Sci U S A *96*, 2301-2304.

Mathieu, J., Flexor, M., Lanotte, M., and Besancon, F. (2008). A PARP-1/JNK1 cascade participates in the synergistic apoptotic effect of TNFalpha and all-trans retinoic acid in APL cells. Oncogene *27*, 3361-3370.

Mathis, G., and Althaus, F. (1987). Release of core DNA from nucleosomal core particles following (ADP-ribose)n-modification in vitro. Biochem Biophys Res Commun *143*, 1049-1054.

Mendoza-Alvarez, H., and Alvarez-Gonzalez, R. (1993). Poly(ADP-ribose) polymerase is a catalytic dimer and the automodification reaction is intermolecular. J Biol Chem *268*, 22575-22580.

Mendoza-Alvarez, H., and Alvarez-Gonzalez, R. (1999). Biochemical characterization of mono(ADP-ribosyl)ated poly(ADP-ribose) polymerase. Biochemistry *38*, 3948-3953.

Menisser-de Murcia, J., Mark, M., Wendling, O., Wynshaw-Boris, A., and de Murcia, G. (2001). Early embryonic lethality in PARP-1 Atm double-mutant mice suggests a functional synergy in cell proliferation during development. Mol Cell Biol *21*, 1828-1832.

Menissier de Murcia, J., Ricoul, M., Tartier, L., Niedergang, C., Huber, A., Dantzer, F., Schreiber, V., Ame, J. C., Dierich, A., LeMeur, M.*, et al.* (2003). Functional interaction between PARP-1 and PARP-2 in chromosome stability and embryonic development in mouse. EMBO J *22*, 2255-2263.

Messner, S., Schuermann, D., Altmeyer, M., Kassner, I., Schmidt, D., Schar, P., Muller, S., and Hottiger, M. O. (2009). Sumoylation of poly(ADP-ribose) polymerase 1 inhibits its acetylation and restrains transcriptional coactivator function. FASEB J *23*, 3978-3989.

Meyer-Ficca, M. L., Lonchar, J., Credidio, C., Ihara, M., Li, Y., Wang, Z. Q., and Meyer, R. G. (2009). Disruption of poly(ADP-ribose) homeostasis affects spermiogenesis and sperm chromatin integrity in mice. Biol Reprod *81*, 46-55.

Meyer-Ficca, M. L., Meyer, R. G., Coyle, D. L., Jacobson, E. L., and Jacobson, M. K. (2004). Human poly(ADP-ribose) glycohydrolase is expressed in alternative splice variants yielding isoforms that localize to different cell compartments. Exp Cell Res *297*, 521-532.

Meyer-Ficca, M. L., Meyer, R. G., Jacobson, E. L., and Jacobson, M. K. (2005a). Poly(ADP-ribose) polymerases: managing genome stability. Int J Biochem Cell Biol *37*, 920-926.

Meyer-Ficca, M. L., Scherthan, H., Burkle, A., and Meyer, R. G. (2005b). Poly(ADP-ribosyl)ation during chromatin remodeling steps in rat spermiogenesis. Chromosoma *114*, 67-74.

Min, W., and Wang, Z. Q. (2009). Poly (ADP-ribose) glycohydrolase (PARG) and its therapeutic potential. Front Biosci *14*, 1619-1626.

Miwa, M., Hanai, S., Poltronieri, P., Uchida, M., and Uchida, K. (1999). Functional analysis of poly(ADP-ribose) polymerase in Drosophila melanogaster. Mol Cell Biochem *193*, 103-107.

Morrison, C., Smith, G. C., Stingl, L., Jackson, S. P., Wagner, E. F., and Wang, Z. Q. (1997). Genetic interaction between PARP and DNA-PK in V(D)J recombination and tumorigenesis. Nat Genet *17*, 479-482.

Munoz-Gamez, J. A., Martin-Oliva, D., Aguilar-Quesada, R., Canuelo, A., Nunez, M. I., Valenzuela, M. T., Ruiz de Almodovar, J. M., De Murcia, G., and Oliver, F. J. (2005). PARP inhibition sensitizes p53-deficient breast cancer cells to doxorubicin-induced apoptosis. Biochem J *386*, 119-125.

Nasta, F., Laudisi, F., Sambucci, M., Rosado, M. M., and Pioli, C. (2010). Increased Foxp3+ regulatory T cells in poly(ADP-Ribose) polymerase-1 deficiency. J Immunol *184*, 3470-3477.

Nossa, C. W., Jain, P., Tamilselvam, B., Gupta, V. R., Chen, L. F., Schreiber, V., Desnoyers, S., and Blanke, S. R. (2009). Activation of the abundant nuclear factor poly(ADP-ribose) polymerase-1 by Helicobacter pylori. Proc Natl Acad Sci U S A *106*, 19998-20003.

Nozaki, T., Fujihara, H., Watanabe, M., Tsutsumi, M., Nakamoto, K., Kusuoka, O., Kamada, N., Suzuki, H., Nakagama, H., Sugimura, T., and Masutani, M. (2003). Parp-1 deficiency implicated in colon and liver tumorigenesis induced by azoxymethane. Cancer Sci *94*, 497-500.

Nusinow, D. A., Hernandez-Munoz, I., Fazzio, T. G., Shah, G. M., Kraus, W. L., and Panning, B. (2007). Poly(ADP-ribose) polymerase 1 is inhibited by a histone H2A variant, MacroH2A, and contributes to silencing of the inactive X chromosome. J Biol Chem *282*, 12851-12859.

Oei, S. L., and Ziegler, M. (2000). ATP for the DNA ligation step in base excision repair is generated from poly(ADP-ribose). J Biol Chem *275*, 23234-23239.

Ogino, H., Nozaki, T., Gunji, A., Maeda, M., Suzuki, H., Ohta, T., Murakami, Y., Nakagama, H., Sugimura, T., and Masutani, M. (2007). Loss of Parp-1 affects gene expression profile in a genome-wide manner in ES cells and liver cells. BMC Genomics *8*, 41.

Oka, S., Kato, J., and Moss, J. (2006). Identification and characterization of a mammalian 39-kDa poly(ADP-ribose) glycohydrolase. J Biol Chem *281*, 705-713.

Okuda, T., Yoshida, T., and Hatano, T. (2000). Correlation of oxidative transformations of hydrolyzable tannins and plant evolution. Phytochemistry *55*, 513-529.

Oliver, A. W., Ame, J. C., Roe, S. M., Good, V., de Murcia, G., and Pearl, L. H. (2004). Crystal structure of the catalytic fragment of murine poly(ADP-ribose) polymerase-2. Nucleic Acids Res *32*, 456-464.

Oliver, F. J., Menissier-de Murcia, J., Nacci, C., Decker, P., Andriantsitohaina, R., Muller, S., de la Rubia, G., Stoclet, J. C., and de Murcia, G. (1999). Resistance to endotoxic shock as a consequence of defective NF-kappaB activation in poly (ADP-ribose) polymerase-1 deficient mice. Embo J *18*, 4446-4454.

Orsburn, B., Escudero, B., Prakash, M., Gesheva, S., Liu, G., Huso, D. L., and Franco, S. (2010). Differential requirement for H2AX and 53BP1 in organismal development and genome maintenance in the absence of poly(ADP)ribosyl polymerase 1. Mol Cell Biol *30*, 2341-2352.

Otto, H., Reche, P. A., Bazan, F., Dittmar, K., Haag, F., and Koch-Nolte, F. (2005). In silico characterization of the family of PARP-like poly(ADP-ribosyl)transferases (pARTs). BMC Genomics *6*, 139.

Panda, S., Poirier, G. G., and Kay, S. A. (2002). tej defines a role for poly(ADP-ribosyl)ation in establishing period length of the arabidopsis circadian oscillator. Dev Cell *3*, 51-61.

Patel, N. S., Cortes, U., Di Poala, R., Mazzon, E., Mota-Filipe, H., Cuzzocrea, S., Wang, Z. Q., and Thiemermann, C. (2005). Mice lacking the 110-kD isoform of poly(ADP-ribose) glycohydrolase are protected against renal ischemia/reperfusion injury. J Am Soc Nephrol *16*, 712-719.

Pavri, R., Lewis, B., Kim, T. K., Dilworth, F. J., Erdjument-Bromage, H., Tempst, P., de Murcia, G., Evans, R., Chambon, P., and Reinberg, D. (2005). PARP-1 determines specificity in a retinoid signaling pathway via direct modulation of mediator. Mol Cell *18*, 83-96.

Pero, R. W., Roush, G. C., Markowitz, M. M., and Miller, D. G. (1990). Oxidative stress, DNA repair, and cancer susceptibility. Cancer Detect Prev *14*, 555-561.

Petesch, S. J., and Lis, J. T. (2008). Rapid, transcription-independent loss of nucleosomes over a large chromatin domain at Hsp70 loci. Cell *134*, 74-84.

Pieper, A. A., Brat, D. J., Krug, D. K., Watkins, C. C., Gupta, A., Blackshaw, S., Verma, A., Wang, Z. Q., and Snyder, S. H. (1999). Poly(ADP-ribose) polymerase-deficient mice are protected from streptozotocin-induced diabetes. Proc Natl Acad Sci U S A *96*, 3059-3064.

Pillai, J., Isbatan, A., Imai, S.-I., and Gupta, M. (2005). Poly(ADP-ribose) Polymerase-1-dependent cardiac myocyte cell death during heart failure is mediated by NAD+ depletion and reduced Sir2α deacetylase activity. J Biol Chem *280*, 43121-43130.

Pleschke, J. M., Kleczkowska, H. E., Strohm, M., and Althaus, F. R. (2000). Poly(ADP-ribose) binds to specific domains in DNA damage checkpoint proteins. J Biol Chem *275*, 40974-40980.

Poirier, G., de Murcia, G., Jongstra-Bilen, J., Niedergang, C., and Mandel, P. (1982). Poly(ADP-ribosyl)ation of polynucleosomes causes relaxation of chromatin structure. Proc Natl Acad Sci USA *79*, 3423-3427.

Quenet, D., El Ramy, R., Schreiber, V., and Dantzer, F. (2009a). The role of poly(ADP-ribosyl)ation in epigenetic events. Int J Biochem Cell Biol *41*, 60-65.

Quenet, D., Gasser, V., Fouillen, L., Cammas, F., Sanglier-Cianferani, S., Losson, R., and Dantzer, F. (2008). The histone subcode: poly(ADP-ribose) polymerase-1 (Parp-

1) and Parp-2 control cell differentiation by regulating the transcriptional intermediary factor TIF1beta and the heterochromatin protein HP1alpha. FASEB J *22*, 3853-3865.

Quenet, D., Mark, M., Govin, J., van Dorsselear, A., Schreiber, V., Khochbin, S., and Dantzer, F. (2009b). Parp2 is required for the differentiation of post-meiotic germ cells: identification of a spermatid-specific complex containing Parp1, Parp2, TP2 and HSPA2. Exp Cell Res *315*, 2824-2834.

Rajamohan, S. B., Pillai, V. B., Gupta, M., Sundaresan, N. R., Birukov, K. G., Samant, S., Hottiger, M. O., and Gupta, M. P. (2009). SIRT1 promotes cell survival under stress by deacetylation-dependent deactivation of poly(ADP-ribose) polymerase 1. Mol Cell Biol *29*, 4116-4129.

Rapizzi, E., Fossati, S., Moroni, F., and Chiarugi, A. (2004). Inhibition of poly(ADP-ribose) glycohydrolase by gallotannin selectively up-regulates expression of proinflammatory genes. Mol Pharmacol *66*, 890-898.

Reale, A., Matteis, G. D., Galleazzi, G., Zampieri, M., and Caiafa, P. (2005). Modulation of DNMT1 activity by ADP-ribose polymers. Oncogene *24*, 13-19.

Rolli, V., Ruf, A., Augustin, A., Schulz, G. E., Ménissier-de Murcia, J., and de Murcia, G. (2000). Poly(ADP-ribose) polymerase: structure and function. In From DNA Damage and Stress Signalling to Cell Death: Poly ADP-Ribosylation Reactions, G. de Murcia, and S. Shall, eds. (New York, Oxford Ubiversity Press), pp. 35-79.

Rongvaux, A., Andris, F., Van Gool, F., and Leo, O. (2003). Reconstructing eukaryotic NAD metabolism. Bioessays *25*, 683-690.

Rossi, M. N., Carbone, M., Mostocotto, C., Mancone, C., Tripodi, M., Maione, R., and Amati, P. (2009). Mitochondrial localization of PARP-1 requires interaction with mitofilin and is involved in the maintenance of mitochondrial DNA integrity. J Biol Chem *284*, 31616-31624.

Rouleau, M., Patel, A., Hendzel, M. J., Kaufmann, S. H., and Poirier, G. G. (2010). PARP inhibition: PARP1 and beyond. Nat Rev Cancer *10*, 293-301.

Ruf, A., de Murcia, G., and Schulz, G. E. (1998). Inhibitor and NAD+ binding to poly(ADP-ribose) polymerase as derived from crystal structures and homology modeling. Biochemistry *37*, 3893-3900.

Ruf, A., Mennissier de Murcia, J., de Murcia, G., and Schulz, G. E. (1996). Structure of the catalytic fragment of poly(AD-ribose) polymerase from chicken. Proc Natl Acad Sci U S A *93*, 7481-7485.

Saenz, L., Lozano, J. J., Valdor, R., Baroja-Mazo, A., Ramirez, P., Parrilla, P., Aparicio, P., Sumoy, L., and Yelamos, J. (2008). Transcriptional regulation by poly(ADP-ribose) polymerase-1 during T cell activation. BMC Genomics *9*, 171.

Sala, A., La Rocca, G., Burgio, G., Kotova, E., Di Gesu, D., Collesano, M., Ingrassia, A. M., Tulin, A. V., and Corona, D. F. (2008). The nucleosome-remodeling ATPase ISWI is regulated by poly-ADP-ribosylation. PLoS Biol *6*, e252.

Schreiber, V., Ame, J. C., Dolle, P., Schultz, I., Rinaldi, B., Fraulob, V., Menissier-de Murcia, J., and de Murcia, G. (2002). Poly(ADP-ribose) polymerase-2 (PARP-2) is required for efficient base excision DNA repair in association with PARP-1 and XRCC1. J Biol Chem *277*, 23028-23036.

Schreiber, V., Dantzer, F., Ame, J. C., and de Murcia, G. (2006). Poly(ADP-ribose): novel functions for an old molecule. Nat Rev Mol Cell Biol *7*, 517-528.

Schuler, W., Weiler, I. J., Schuler, A., Phillips, R. A., Rosenberg, N., Mak, T. W., Kearney, J. F., Perry, R. P., and Bosma, M. J. (1986). Rearrangement of antigen receptor genes is defective in mice with severe combined immune deficiency. Cell *46*, 963-972.

Shall, S. (1975). Proceedings: Experimental manipulation of the specific activity of poly(ADP-ribose) polymerase. J Biochem (Tokyo) *77*, 2p.

Shall, S., and de Murcia, G. (2000). Poly(ADP-ribose) polymerase-1: what have we learned from the deficient mouse model? Mutat Res *460*, 1-15.

Shibata, A., Kamada, N., Masumura, K., Nohmi, T., Kobayashi, S., Teraoka, H., Nakagama, H., Sugimura, T., Suzuki, H., and Masutani, M. (2005). Parp-1 deficiency causes an increase of deletion mutations and insertions/rearrangements in vivo after treatment with an alkylating agent. Oncogene *24*, 1328-1337.

Shirato, M., Tozawa, S., Maeda, D., Watanabe, M., Nakagama, H., and Masutani, M. (2007). Poly(etheno ADP-ribose) blocks poly(ADP-ribose) glycohydrolase activity. Biochem Biophys Res Commun *355*, 451-456.

Simbulan-Rosenthal, C. M., Haddad, B. R., Rosenthal, D. S., Weaver, Z., Coleman, A., Luo, R., Young, H. M., Wang, Z. Q., Ried, T., and Smulson, M. E. (1999). Chromosomal aberrations in PARP(-/-) mice: genome stabilization in immortalized cells by reintroduction of poly(ADP-ribose) polymerase cDNA. Proc Natl Acad Sci U S A *96*, 13191-13196.

Simbulan-Rosenthal, C. M., Ly, D. H., Rosenthal, D. S., Konopka, G., Luo, R., Wang, Z. Q., Schultz, P. G., and Smulson, M. E. (2000). Misregulation of gene expression in primary fibroblasts lacking poly(ADP-ribose) polymerase. Proc Natl Acad Sci U S A *97*, 11274-11279.

Simbulan-Rosenthal, C. M., Rosenthal, D. S., Luo, R., Samara, R., Espinoza, L. A., Hassa, P. O., Hottiger, M. O., and Smulson, M. E. (2003). PARP-1 binds E2F-1 independently of its DNA binding and catalytic domains, and acts as a novel coactivator of E2F-1-mediated transcription during re-entry of quiescent cells into S phase. Oncogene *22*, 8460-8471.

Slama, J. T., Aboul-Ela, N., Goli, D. M., Cheesman, B. V., Simmons, A. M., and Jacobson, M. K. (1995a). Specific inhibition of poly(ADP-ribose) glycohydrolase by adenosine diphosphate (hydroxymethyl)pyrrolidinediol. J Med Chem *38*, 389-393.

Slama, J. T., Aboul-Ela, N., and Jacobson, M. K. (1995b). Mechanism of inhibition of poly(ADP-ribose) glycohydrolase by adenosine diphosphate (hydroxymethyl)pyrrolidinediol. J Med Chem *38*, 4332-4336.

Smith, S., Giriat, I., Schmitt, A., and de Lange, T. (1998). Tankyrase, a poly(ADP-ribose) polymerase at human telomeres. Science *282*, 1484-1487.

St-Laurent, J. F., Gagnon, S. N., Dequen, F., Hardy, I., and Desnoyers, S. (2007). Altered DNA damage response in Caenorhabditis elegans with impaired poly(ADP-ribose) glycohydrolases genes expression. DNA Repair (Amst) *6*, 329-343.

Stilmann, M., Hinz, M., Arslan, S. C., Zimmer, A., Schreiber, V., and Scheidereit, C. (2009). A nuclear poly(ADP-ribose)-dependent signalosome confers DNA damage-induced IkappaB kinase activation. Mol Cell *36*, 365-378.

Susin, S. A., Lorenzo, H. K., Zamzami, N., Marzo, I., Snow, B. E., Brothers, G. M., Mangion, J., Jacotot, E., Costantini, P., Loeffler, M.*, et al.* (1999). Molecular characterization of mitochondrial apoptosis-inducing factor. Nature *397*, 441-446.

Suto, M. J., Turner, W. R., Arundel-Suto, C. M., Werbel, L. M., and Sebolt-Leopold, J. S. (1991). Dihydroisoquinolinones: the design and synthesis of a new series of potent inhibitors of poly(ADP-ribose) polymerase. Anticancer Drug Des *6*, 107-117.

Tanuma, S., Sakagami, H., and Endo, H. (1989a). Inhibitory effect of tannin on poly(ADP-ribose) glycohydrolase from human placenta. Biochem Int *18*, 701-708.

Tanuma, S., Tsai, Y. J., Sakagami, H., Konno, K., and Endo, H. (1989b). Lignin inhibits (ADP-ribose)n glycohydrolase activity. Biochem Int *19*, 1395-1402.

Tao, M., Park, C. H., Bihovsky, R., Wells, G. J., Husten, J., Ator, M. A., and Hudkins, R. L. (2006). Synthesis and structure-activity relationships of novel poly(ADP-ribose) polymerase-1 inhibitors. Bioorg Med Chem Lett *16*, 938-942.

Tao, Z., Gao, P., Hoffman, D. W., and Liu, H. W. (2008). Domain C of human poly(ADP-ribose) polymerase-1 is important for enzyme activity and contains a novel zinc-ribbon motif. Biochemistry *47*, 5804-5813.

Tentori, L., Leonetti, C., Scarsella, M., d'Amati, G., Portarena, I., Zupi, G., Bonmassar, E., and Graziani, G. (2002a). Combined treatment with temozolomide and poly(ADP-ribose) polymerase inhibitor enhances survival of mice bearing hematologic malignancy at the central nervous system site. Blood *99*, 2241-2244.

Tentori, L., Leonetti, C., Scarsella, M., Muzi, A., Vergati, M., Forini, O., Lacal, P. M., Ruffini, F., Gold, B., Li, W.*, et al.* (2005). Poly(ADP-ribose) glycohydrolase inhibitor as chemosensitiser of malignant melanoma for temozolomide. Eur J Cancer *41*, 2948-2957.

Tentori, L., Portarena, I., and Graziani, G. (2002b). Potential clinical applications of poly(ADP-ribose) polymerase (PARP) inhibitors. Pharmacol Res *45*, 73-85.

Timinszky, G., Till, S., Hassa, P. O., Hothorn, M., Kustatscher, G., Nijmeijer, B., Colombelli, J., Altmeyer, M., Stelzer, E. H., Scheffzek, K.*, et al.* (2009). A

macrodomain-containing histone rearranges chromatin upon sensing PARP1 activation. Nat Struct Mol Biol *16*, 923-929.

Tong, W. M., Hande, M. P., Lansdorp, P. M., and Wang, Z. Q. (2001). DNA strand break-sensing molecule poly(ADP-Ribose) polymerase cooperates with p53 in telomere function, chromosome stability, and tumor suppression. Mol Cell Biol *21*, 4046-4054.

Tong, W. M., Ohgaki, H., Huang, H., Granier, C., Kleihues, P., and Wang, Z. Q. (2003). Null mutation of DNA strand break-binding molecule poly(ADP-ribose) polymerase causes medulloblastomas in p53(-/-) mice. Am J Pathol *162*, 343-352.

Tong, W. M., Yang, Y. G., Cao, W. H., Galendo, D., Frappart, L., Shen, Y., and Wang, Z. Q. (2007). Poly(ADP-ribose) polymerase-1 plays a role in suppressing mammary tumourigenesis in mice. Oncogene *26*, 3857-3867.

Trucco, C., Oliver, F. J., de Murcia, G., and Menissier-de Murcia, J. (1998). DNA repair defect in poly(ADP-ribose) polymerase-deficient cell lines. Nucleic Acids Res *26*, 2644-2649.

Tsai, Y. J., Abe, H., Maruta, H., Hatano, T., Nishina, H., Sakagami, H., Okuda, T., and Tanuma, S. (1991). Effects of chemically defined tannins on poly (ADP-ribose) glycohydrolase activity. Biochem Int *24*, 889-897.

Tsai, Y. J., Aoki, T., Maruta, H., Abe, H., Sakagami, H., Hatano, T., Okuda, T., and Tanuma, S. (1992). Mouse mammary tumor virus gene expression is suppressed by oligomeric ellagitannins, novel inhibitors of poly(ADP-ribose) glycohydrolase. J Biol Chem *267*, 14436-14442.

Tsutsumi, M., Masutani, M., Nozaki, T., Kusuoka, O., Tsujiuchi, T., Nakagama, H., Suzuki, H., Konishi, Y., and Sugimura, T. (2001). Increased susceptibility of poly(ADP-ribose) polymerase-1 knockout mice to nitrosamine carcinogenicity. Carcinogenesis *22*, 1-3.

Tulin, A., Chinenov, Y., and Spradling, A. (2003). Regulation of chromatin structure and gene activity by poly(ADP-ribose) polymerases. Curr Top Dev Biol *56*, 55-83.

Tulin, A., Naumova, N. M., Menon, A. K., and Spradling, A. C. (2005). Drosophila poly(ADP-ribose) glycohydrolase (Parg) mediates chromatin structure and Sir2-dependent silencing. Genetics.

Tulin, A., and Spradling, A. (2003). Chromatin loosening by poly(ADP)-ribose polymerase (PARP) at Drosophila puff loci. Science *299*, 560-562.

Tulin, A., Stewart, D., and Spradling, A. C. (2002). The Drosophila heterochromatic gene encoding poly(ADP-ribose) polymerase (PARP) is required to modulate chromatin structure during development. Genes Dev *16*, 2108-2119.

Tuma, R. S. (2009). PARP inhibitors: will the new class of drugs match the hype? J Natl Cancer Inst *101*, 1230-1232.

Tutt, A., Robson, M., Garber, J. E., Domchek, S. M., Audeh, M. W., Weitzel, J. N., Friedlander, M., Arun, B., Loman, N., Schmutzler, R. K.*, et al.* (2010). Oral poly(ADP-ribose) polymerase inhibitor olaparib in patients with BRCA1 or BRCA2 mutations and advanced breast cancer: a proof-of-concept trial. Lancet *376*, 235-244.

Underhill, C., Toulmonde, M., and Bonnefoi, H. (2010). A review of PARP inhibitors: from bench to bedside. Ann Oncol.

Vanderauwera, S., De Block, M., Van de Steene, N., van de Cotte, B., Metzlaff, M., and Van Breusegem, F. (2007). Silencing of poly(ADP-ribose) polymerase in plants alters abiotic stress signal transduction. Proc Natl Acad Sci U S A *104*, 15150-15155.

Virag, L., and Szabo, C. (2002). The therapeutic potential of poly(ADP-ribose) polymerase inhibitors. Pharmacol Rev *54*, 375-429.

Wacker, D. A., Ruhl, D. D., Balagamwala, E. H., Hope, K. M., Zhang, T., and Kraus, W. L. (2007). The DNA binding and catalytic domains of poly(ADP-ribose) polymerase 1 cooperate in the regulation of chromatin structure and transcription. Mol Cell Biol *27*, 7475-7485.

Wang, Z. Q., Auer, B., Stingl, L., Berghammer, H., Haidacher, D., Schweiger, M., and Wagner, E. F. (1995). Mice lacking ADPRT and poly(ADP-ribosyl)ation develop normally but are susceptible to skin disease. Genes Dev *9*, 509-520.

Wang, Z. Q., Stingl, L., Morrison, C., Jantsch, M., Los, M., Schulze-Osthoff, K., and Wagner, E. F. (1997). PARP is important for genomic stability but dispensable in apoptosis. Genes Dev *11*, 2347-2358.

Wells, G. J., Bihovsky, R., Hudkins, R. L., Ator, M. A., and Husten, J. (2006). Synthesis and structure-activity relationships of novel pyrrolocarbazole lactam analogs as potent and cell-permeable inhibitors of poly(ADP-ribose)polymerase-1 (PARP-1). Bioorg Med Chem Lett *16*, 1151-1155.

Woodhouse, B. C., and Dianov, G. L. (2008). Poly ADP-ribose polymerase-1: an international molecule of mystery. DNA Repair (Amst) *7*, 1077-1086.

Yamagami, T., Miwa, A., Takasawa, S., Yamamoto, H., and Okamoto, H. (1985). Induction of rat pancreatic B-cell tumors by the combined administration of streptozotocin or alloxan and poly(adenosine diphosphate ribose) synthetase inhibitors. Cancer Res *45*, 1845-1849.

Yang, F., Baumann, C., and De La Fuente, R. (2009). Persistence of histone H2AX phosphorylation after meiotic chromosome synapsis and abnormal centromere cohesion in poly (ADP-ribose) polymerase (Parp-1) null oocytes. Dev Biol *331*, 326-338.

Yelamos, J., Monreal, Y., Saenz, L., Aguado, E., Schreiber, V., Mota, R., Fuente, T., Minguela, A., Parrilla, P., de Murcia, G.*, et al.* (2006). PARP-2 deficiency affects the survival of CD4+CD8+ double-positive thymocytes. EMBO J *25*, 4350-4360.

Ying, W., Sevigny, M. B., Chen, Y., and Swanson, R. A. (2001). Poly(ADP-ribose) glycohydrolase mediates oxidative and excitotoxic neuronal death. Proc Natl Acad Sci U S A *98*, 12227-12232.

Ying, W., and Swanson, R. A. (2000). The poly(ADP-ribose) glycohydrolase inhibitor gallotannin blocks oxidative astrocyte death. Neuroreport *11*, 1385-1388.

Yu, S. W., Wang, H., Poitras, M. F., Coombs, C., Bowers, W. J., Federoff, H. J., Poirier, G. G., Dawson, T. M., and Dawson, V. L. (2002). Mediation of poly(ADP-ribose) polymerase-1-dependent cell death by apoptosis-inducing factor. Science *297*, 259-263.

Yu, W., Ginjala, V., Pant, V., Chernukhin, I., Whitehead, J., Docquier, F., Farrar, D., Tavoosidana, G., Mukhopadhyay, R., Kanduri, C., *et al.* (2004). Poly(ADP-ribosyl)ation regulates CTCF-dependent chromatin insulation. Nat Genet *36*, 1105-1110.

Zampieri, M., Passananti, C., Calabrese, R., Perilli, M., Corbi, N., De Cave, F., Guastafierro, T., Bacalini, M. G., Reale, A., Amicosante, G., *et al.* (2009). Parp1 localizes within the Dnmt1 promoter and protects its unmethylated state by its enzymatic activity. PLoS One *4*, e4717.

Zhang, J., Dawson, V. L., Dawson, T. M., and Snyder, S. H. (1994). Nitric oxide activation of poly(ADP-ribose) synthetase in neurotoxicity. Science *263*, 687-689.

Zhang, S., Lin, Y., Kim, Y. S., Hande, M. P., Liu, Z. G., and Shen, H. M. (2007). c-Jun N-terminal kinase mediates hydrogen peroxide-induced cell death via sustained poly(ADP-ribose) polymerase-1 activation. Cell Death Differ *14*, 1001-1010.

Zhang, T., Berrocal, J. G., Frizzell, K. M., Gamble, M. J., Dumond, M. E., Krishnakumar, R., Yang, T., Sauve, A. A., and Kraus, W. L. (2009). Enzymes in the NAD+ Salvage Pathway Regulate SIRT1 Activity at Target Gene Promoters. J Biol Chem *284*, 20408-20417.

Zhang, T., and Kraus, W. L. (2010). SIRT1-dependent regulation of chromatin and transcription: Linking NAD(+) metabolism and signaling to the control of cellular functions. Biochim Biophys Acta *1804*, 1666-1675.

Zingarelli, B., Hake, P. W., O'Connor, M., Denenberg, A., Kong, S., and Aronow, B. J. (2003). Absence of poly(ADP-ribose)polymerase-1 alters nuclear factor-kappa B activation and gene expression of apoptosis regulators after reperfusion injury. Mol Med *9*, 143-153.

Zingarelli, B., Salzman, A. L., and Szabo, C. (1998). Genetic disruption of poly (ADP-ribose) synthetase inhibits the expression of P-selectin and intercellular adhesion molecule-1 in myocardial ischemia/reperfusion injury. Circ Res *83*, 85-94.

Zong, W. X., Ditsworth, D., Bauer, D. E., Wang, Z. Q., and Thompson, C. B. (2004). Alkylating DNA damage stimulates a regulated form of necrotic cell death. Genes Dev *18*, 1272-1282.

CHAPTER 2

Global Analysis of Transcriptional Regulation by Poly(ADP-ribose) Polymerase-1 and Poly(ADP-ribose) Glycohydrolase in MCF-7 Human Breast Cancer Cells*

* This research was published as Frizzell KM, Gamble MJ, Berrocal JG, Zhang T, Krishnakumar R, Cen Y, Sauve AA, and Kraus WL. Global Analysis of Transcriptional Regulation by Poly(ADP-ribose) Polymerase-1 and Poly(ADP-ribose) Glycohydrolase in MCF-7 Human Breast Cancer Cells. *Journal of Biological Chemistry*. 2009; 284(49):33926-33938. Minor modifications have been made. Contributions by other authors to this work were as follows: M.J.G., expression microarray and analyses, and RT-qPCR (Figures 2.3, 2.4, and 2.5); J.G.B., RT-qPCR (Figure 2.5); T.Z., expression microarray analyses (Figures 2.3, 2.4, and 2.5); R.K., assisted with PAR westerns and inhibitor experiments (Figures 2.1 and 2.14); Y.C. and A.A.S., NAD^+ measurements (Figure 2.1).

2.1. Summary

Poly(ADP-ribose) polymerase-1 (PARP-1) and poly(ADP-ribose) glycohydrolase (PARG) are enzymes that modify target proteins in the nucleus by the addition and removal, respectively, of ADP-ribose polymers. Although a role for PARP-1 in gene regulation has been well established, the role of PARG is less clear. To investigate how PARP-1 and PARG coordinately regulate global patterns of gene expression, we used short hairpin RNAs (shRNAs) to stably knockdown PARP-1 or PARG in MCF-7 cells, followed by expression microarray analyses. Correlation analyses showed that the majority of genes affected by the knockdown of one factor were similarly affected by the knockdown of the other factor. That is, the changes generally occurred in the same direction and with similar magnitudes. The most robustly regulated common genes were enriched for stress response and metabolic functions. In chromatin immunoprecipitation assays, PARP-1 and PARG localized to the promoters of both positively and negatively regulated target genes. The levels of chromatin-bound PARG at a given promoter generally correlated with the levels of PARP-1 across the subset of promoters tested. For about half of the genes tested, the binding of PARP-1 at the promoter was dependent on the binding of PARG. Experiments using stable re-expression of shRNA-resistant catalytic mutants showed that PARP-1 and PARG enzymatic activities are required for some, but not all, target genes. Collectively, our results indicate that PARP-1 and PARG, two nuclear enzymes with opposing enzymatic activities, localize to target promoters and act in a similar, rather than antagonistic, manner to regulate gene expression.

2.2. Introduction

Poly(ADP-ribosyl)ation (PAR-ylation) is a post-translational modification involving the polymerization of ADP-ribose (ADPR) units from donor NAD^+ molecules on target proteins (D'Amours et al., 1999; Kim et al., 2005). PARylation occurs on a variety of target proteins in all cellular compartments and plays roles in a wide array of processes, such as stress responses, DNA repair, and transcriptional regulation (D'Amours et al., 1999; Kim et al., 2005). Nuclear targets include core histones, the linker histone H1, and an variety of transcription factors (Kraus and Lis, 2003). The synthesis and degradation of poly(ADP-ribose) (PAR) is catalyzed by two types of enzymes: PAR polymerases (PARPs) and PAR glycohydrolases (PARGs), respectively (Amé et al., 2004; Davidovic et al., 2001). Although recent studies have begun to explore the functional interplay between these two types of enzymes, a clear picture of how they cooperate to regulate cellular processes remains unclear.

PARP-1, a ubiquitous 116 kDa nuclear enzyme, is the founding member of the PARP superfamily (Amé et al., 2004; Kim et al., 2005). It is a highly abundant protein (1 to 2 million molecules per cell) that is likely responsible for the majority of PAR synthesis in cells (D'Amours et al., 1999). PARP-1 has three major structural and functions domains: (i) an amino-terminal DNA binding domain (DBD), (ii) a central automodification domain (AMD), and (iii) a carboxyl-terminal catalytic domain with low basal activity (D'Amours et al., 1999; Rolli et al., 2000). The catalytic activity of PARP-1 is potently allosterically activated by the binding of PARP-1 to certain forms of DNA (Kun et al., 2004; Kun et al., 2002; Lonskaya et al., 2005; Potaman et al., 2005), nucleosomes (Kim et al., 2004; Wacker et al., 2007a; Wacker et al., 2007b), and protein binding partners (Ju et al., 2006; Ju et al., 2004; Oei and Shi, 2001). In vivo, PARP-1 is the major target for PARP-1-mediated PARylation

through an automodification reaction involving the AMD (D'Amours et al., 1999; Ogata et al., 1981), although an array of other nuclear targets has been described (D'Amours et al., 1999; Kim et al., 2005; Kraus and Lis, 2003). Its DNA binding, catalytic, and automodification functions allow PARP-1 to modulate a wide variety of cellular processes involving genomic DNA.

Cellular PARG activities in mammals are mediated by multiple PARG isoforms encoded by a single gene (Davidovic et al., 2001; Meyer-Ficca et al., 2004; Meyer-Ficca et al., 2005). The predominant isoforms, all of which have catalytic activity, include: (i) a set of long (~100 to ~110 kDa) isoforms that may shuttle between the nucleus and cytoplasm and (ii) a short (~65 kDa) isoform that resides in the cytoplasm (Meyer-Ficca et al., 2004; Meyer-Ficca et al., 2005). These PARG isoforms catalyze the hydrolysis of PAR to produce ADPR monomers and short ADPR polymers (Davidovic et al., 2001). The longest PARG isoforms contain two major functional domains: (i) a regulatory domain and (ii) a catalytic domain (Davidovic et al., 2001; Kim et al., 2005; Kraus and Lis, 2003). The regulatory domain contains both nuclear localization and nuclear export signals, which mediate shuttling between the nuclear and cytoplasmic compartments (Bonicalzi et al., 2003; Ohashi et al., 2003). The catalytic domain contains the enzyme active site, which confers both endoglycosidic and exoglycosidic activities, allowing for the rapid hydrolysis of PAR (Davidovic et al., 2001).

PARP-1 and PARG play important roles in an overlapping set of biological processes. For example, gene-specific and genomic studies have revealed a clear role for PARP-1 in transcriptional regulation (Hassa and Hottiger, 2002; Kim et al., 2005; Kraus, 2008; Kraus and Lis, 2003; Tulin et al., 2003), and PARP-1 localizes to the promoters of more than 90% of expressed genes in MCF-7 human breast cancer cells (Krishnakumar et al., 2008). Likewise, although more limited, recent gene-specific

studies have also implicated PARG in transcriptional regulation (Kim et al., 2004; Rapizzi et al., 2004; Tulin et al., 2005). Few studies have directly examined the interplay between PARP-1 and PARG in the regulation of their biological endpoints in side-by-side experiments in the same cell type. As such, the means by which PARP-1 and PARG coordinate their enzymatic activities to regulate gene expression across the genome are unknown. Based on the opposing enzymatic activities of PARP-1 and PARG, one might expect PARG to counter the gene regulatory actions of PARP-1 by degrading the PAR chains synthesized by PARP-1. Yet, PARP-1 and PARG have similar effects on many biological endpoints (Cortes et al., 2004; Fisher et al., 2007; Kim et al., 2005; Koh et al., 2004; St-Laurent et al., 2007; Tulin et al., 2003; Tulin et al., 2005; Tulin and Spradling, 2003; Tulin et al., 2002; Wang et al., 1995; Wang et al., 1997), suggesting that this simple model is unlikely to be correct.

In the current studies, we used a series of genomic and gene-specific assays to explore the coordinated regulation of gene expression by PARP-1 and PARG, including the role of their respective enzymatic activities. Our results indicate that PARP-1 and PARG localize to target promoters and act in a similar, rather than antagonistic, manner to regulate global patterns of gene expression.

2.3. Results

Generation of PARP-1 and PARG knockdown cell lines. To explore the role of PARP-1 and PARG in the regulation of gene expression, we used short hairpin RNA (shRNA)-mediated knockdown to deplete each of the proteins individually in MCF-7 human breast cancer cells. Two distinct shRNA sequences targeting either luciferase (Luc, used as a control), PARP-1, or PARG were stably introduced into MCF-7 cells using sequential retrovirus-mediated gene transfer, creating cells doubly targeted for a

given factor. Stably transduced cell populations, rather than clonal lines, for each double knockdown were isolated by appropriate drug selection (see Experimental Procedures) and tested for knockdown by Western blot analysis. The PARP-1 and PARG proteins were depleted by approximately 90 percent and 70 percent, respectively, compared to the Luc control (Figure 2.1A). A Western blot for SIRT1 was included as a loading control. Similar effects were also observed on the levels of PARP-1 and PARG mRNA (Figure 2.1B). Notably, knockdown of either PARP-1 or PARG had no discernable effect on proliferation or cell cycle progression relative to the Luc control for cells in subconfluent growth conditions (Figure 2.2A and 2.2B).

To further characterize these knockdown cell lines, we analyzed PAR (Figure 2.1A and 2.1C) and NAD^+ (Figure 2.1C) levels. Knockdown of PARP-1 in MCF-7 cells reduced, while knockdown of PARG enhanced cellular PAR levels, as determined by Western blot with a PAR-specific antibody. Using a quantitative HPLC/mass spectrometry method with ^{18}O-labeled standards (Yang et al., 2007; Yang and Sauve, 2006; Zhang et al., 2009), we observed an increase in total cellular NAD^+ levels upon PARP-1 knockdown, and a slight decrease upon PARG knockdown. Together, these results demonstrate that depletion of PARP-1 and PARG alters NAD^+ and PAR levels in MCF-7 cells in a predictable manner. Thus, we have generated cell lines with stable shRNA-mediated knockdown of PARP-1 or PARG that can serve as useful models for studying gene regulation by PARP-1 or PARG.

PARP-1 and PARG regulate global patterns of gene expression in MCF-7 cells. To determine the effects of PARP-1 and PARG knockdown on global patterns of gene expression in MCF-7 cells, we isolated total RNA from three control-matched sets of independently generated Luc, PARP-1, and PARG knockdown cell populations. The use of three independently generated populations of cells represents a stringent **Figure**

2.1. shRNA-mediated knockdown of PARP-1 and PARG in MCF-7 cells. *A,* Whole cell lysates collected from Luc, PARP-1, and PARG stable shRNA-mediated knockdown cell lines were subjected to Western blotting analyses for PARP-1 and PARG. SIRT1 was analyzed as a loading control. PAR levels were analyzed by Western blotting using nuclear extracts from the same cell lines. *B,* RT-qPCR analysis confirms the knockdown PARP-1 and PARG mRNA in MCF-7 cells. Total RNA was isolated from Luc, PARP-1, and PARG knockdown cells, reverse transcribed, and subjected to qPCR using gene-specific primers to PARP-1 and PARG. Each bar is the mean + SEM (*error bars*) for three independent RNA isolations. Bars marked with an asterisk are statistically different from the Luc control, as determined by a Student's t-test with a p-value threshold of < 0.05. *C*, Total cellular NAD^+ levels (*black bars*) in Luc, PARP-1, and PARG knockdown cells were measured using a quantitative HPLC/mass spectrometry method with ^{18}O standards. PAR levels (*grey bars*) were quantified from Western blots (from *A*, above) by densitometry. The data are shown as the mean + range or SEM (*error bars*) from two or more independent biological replicates. Bars marked with an asterisk are statistically different from the Luc control, as determined by a Student's t-test with a p-value threshold of < 0.05.

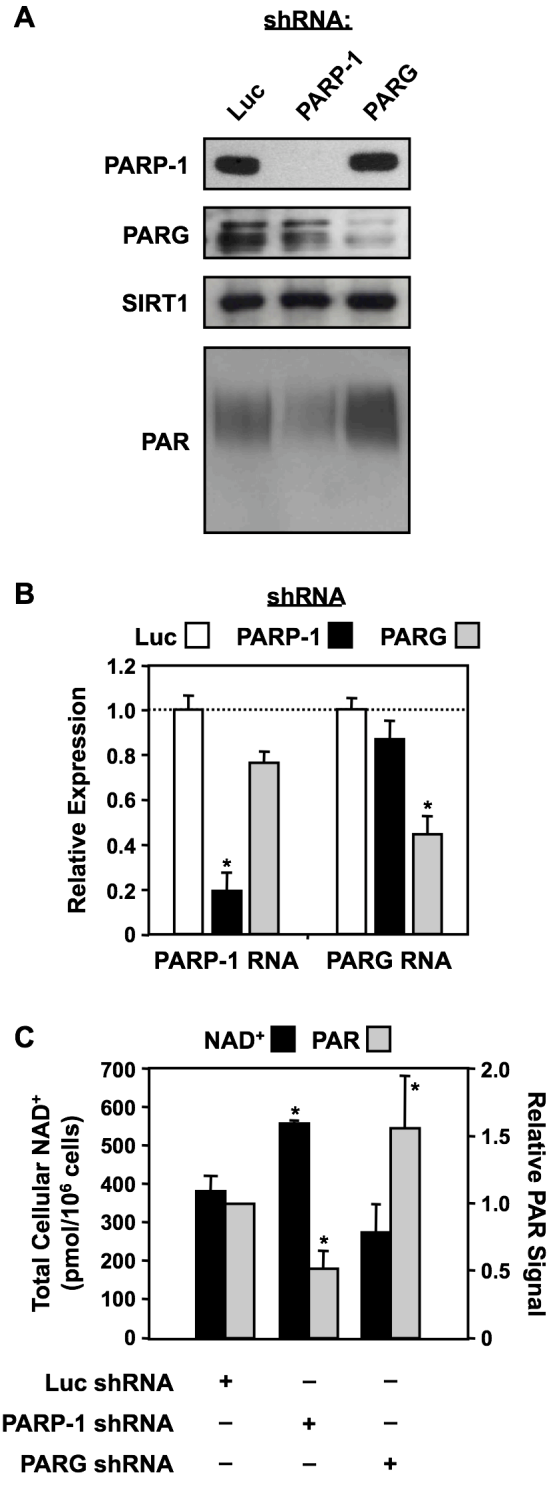
A
shRNA:
Luc
PARP-1
PARG
PARP-1
PARG
SIRT1
PAR
B
shRNA
Luc
PARP-1
PARG
Relative Expression
1.2
1.0
0.8
0.6
0.4
0.2
0
PARP-1 RNA
PARG RNA
C
NAD+
PAR
Total Cellular NAD+ (pmol/10^6 cells)
700
600
500
400
300
200
100
0
2.0
1.5
1.0
0.5
0
Relative PAR Signal
Luc shRNA + – –
PARP-1 shRNA – + –
PARG shRNA – – +

Figure 2.2. PARP-1 or PARG knockdown does not significantly alter MCF-7 cell proliferation or cell cycle progression. *A,* PARP-1 or PARG knockdown does not significantly affect the proliferation of MCF-7 cells. The specified knockdown cell lines were seeded and counted every two days over an 8-day period. Data is shown as the mean ± SEM (*error bars*) for four independent experiments. The significant differences between the samples as determined by ANOVA with a p-value threshold of < 0.05, are indicated by an asterisk (i.e. day 8). All expression and ChIP experiments were conducted 3 to 4 days post plating, as indicated, where growth differences were determined to be insignificant. Stock cells were maintained as subconfluent cultures and passaged at the point indicated. *B,* PARP-1 or PARG knockdown does not significantly affect cell cycle progression. The specified knockdown cell lines were subjected to FACS analysis to determine percent of cells in each cell cycle phase. Data is shown as the mean ± SEM (*error bars*) for four independent experiments. The differences between the samples are not significantly different as determined by ANOVA with a p-value threshold of < 0.05.

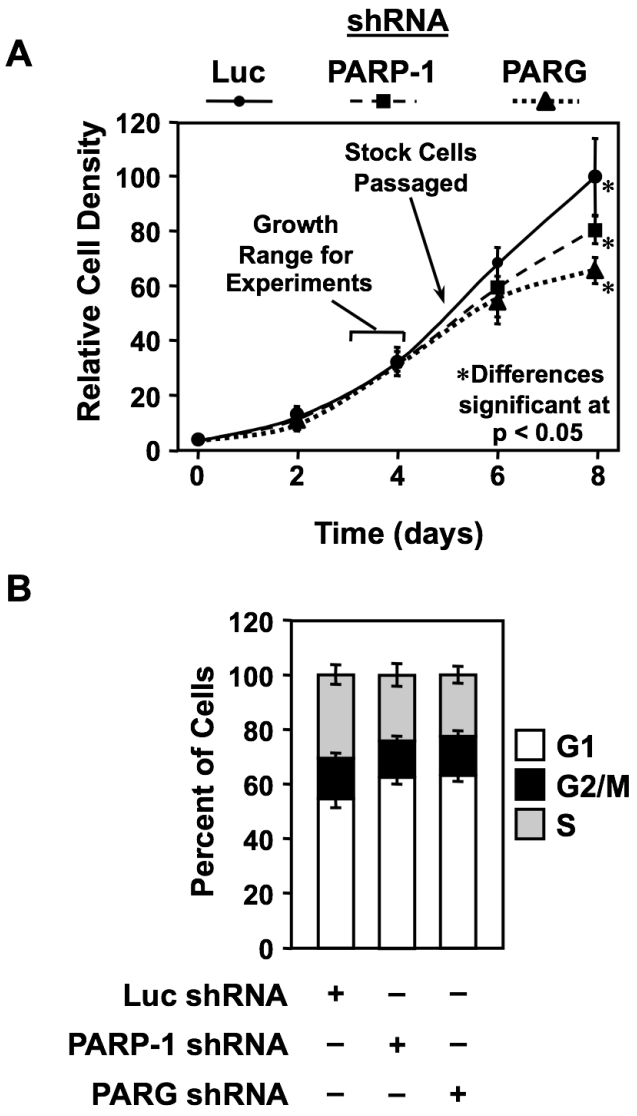
A
shRNA
Luc
PARP-1
PARG
Relative Cell Density
120
100
80
60
40
20
0
Stock Cells Passaged
Growth Range for Experiments
*Differences significant at p < 0.05
0
2
4
6
8
Time (days)
B
Percent of Cells
120
100
80
60
40
20
0
G1
G2/M
S
Luc shRNA + – –
PARP-1 shRNA – + –
PARG shRNA – – +

approach to control for experimental variability and limits the complications that may be observed when using clonally selected lines. Total RNA was isolated, labeled, and hybridized to Affymetrix U133A 2.0 human expression microarrays, which contain more than 22,000 probe sets, including 14,500 well-characterized human genes. The raw data were normalized using Affymetrix GCOS software and adjusted for batch effects using an empirical Bayes method (Johnson et al., 2007). Next, the data were $\log_2$ transformed, median centered, and filtered as described in the Materials and Methods. In our initial analyses, we performed filtering based on (i) a detection call of "present" or "marginal" in two of the three replicates for both Luc and PARP-1/PARG and (ii) a Student's t-test p-value cutoff of < 0.05 (Figure 2.3 and Figure 2.4). In subsequent analyses, we also applied a $\log_2$ fold change cutoff of > 0.5 or < -0.5 (see Figure 2.5). The fully processed and analyzed data yielded lists of genes regulated by PARP-1 or PARG (i.e., genes whose expression changed upon PARP-1 or PARG knockdown; see Tables 2.1, 2.2, and 2.3 for the regulated gene lists). These data sets contain genes both directly regulated (*i.e.*, primary effects) and indirectly regulated (*i.e.,* secondary effects) by PARP-1 or PARG. For the mechanistic studies described herein, we chose a set of target genes based on the criteria discussed below.

The application of a p-value cutoff without a fold change cutoff is one useful approach to define sets of significantly regulated genes in expression microarray experiments (Dow, 2003; Hess and Iyer, 2007; Murphy, 2002). Analysis of our expression microarray data in this manner defined ~1200 genes (~8.7% of all genes tested) regulated by PARP-1 knockdown and ~1100 genes (~8.1% of all genes tested) regulated by PARG knockdown at 95% confidence, with a commonly regulated gene set (*i.e.*, intersection) of ~500 genes (~3.5% of all genes tested) (Figure 2.3A). A heat map representation (Figure 2.3B) and a Spearman correlation analysis (Figure 2.3C) of the PARP-1 and PARG commonly regulated gene set (*i.e.*, intersection) shows that the

majority of genes affected by the knockdown of one factor were similarly affected by the knockdown of the other factor. That is, the changes (*i.e.*, either up- or down-regulated) generally occurred in the same direction and with the same magnitude for both PARP-1 and PARG knockdown (Figures 2.3B and 2.3C). This pattern was also evident in the union of regulated gene sets (Figure 2.4), indicating that even for genes not passing the p-value cutoff in one condition (*i.e.*, PARP-1 or PARG knockdown), the pattern of regulation was similar. Together, these data indicate that PARP-1 and PARG regulate the expression of a common set of genes in a largely similar manner.

Next, to define the sets of genes most robustly regulated by PARP-1 and PARG knockdown (*i.e.*, the top 15% to 20% of the regulated genes), we applied a fold change cutoff ($\log_2$ fold change of > 0.5 or < -0.5) to the data pre-filtered for both detection call and p-value (Figure 2.3A). By these criteria, we identified 204 PARP-1-regulated genes and 217 PARG-regulated genes (Figure 2.5A). About half of each group of the most robustly regulated genes was up-regulated, while the other half was down-regulated (Figure 2.5B). Fifty of the most robustly regulated genes were in both the PARP-1- and PARG-regulated lists (*i.e.*, the intersection). As expected based on Figure 2.3C and Figure 2.4C, the most robustly regulated genes were regulated in the same direction and with the same magnitude, as illustrated by a Spearman correlation analysis (Figure 2.5C). The most robustly regulated genes are listed in Tables 2.1-2.3. Gene-specific mRNA determinations by RT-qPCR were used to confirm the microarray expression data for a subset of genes falling into four classes: (i) up-regulated by both PARP-1 and PARG knockdown, (ii) down-regulated by both PARP-1 and PARG knockdown, (iii) differentially regulated by both PARP-1 and PARG knockdown, and (iv) not regulated by PARP-1 or PARG knockdown (Figure 2.5D). This analysis confirmed a group of more than 20 genes with consistent and well-characterized patterns of regulation in response to PARP-1 and PARG knockdown.

Figure 2.3. PARP-1 and PARG coordinately regulate global patterns of gene expression in MCF-7 cells (Intersection). *A,* Venn diagram of PARP-1- and PARG-regulated genes in MCF-7 cells as defined by shRNA-mediated knockdown and expression microarrays. Genes passing both present call and p-value < 0.05 criteria for at least one factor represent the union (see also Figure 2.4.), whereas genes regulated by both factors represent the commonly regulated genes or intersection). *B,* Heatmap showing the expression profiles of the commonly regulated genes (i.e., intersection; 485 genes) from panel A. The genes are ranked in the heatmap by $\log_2$ fold change in the PARP-1 knockdown cell line (see color scale). *C,* Correlation analysis of the commonly regulated genes (*i.e.*, intersection; 485 genes) from panel A. The Spearman correlation coefficient (c.c.) and p-value are indicated.

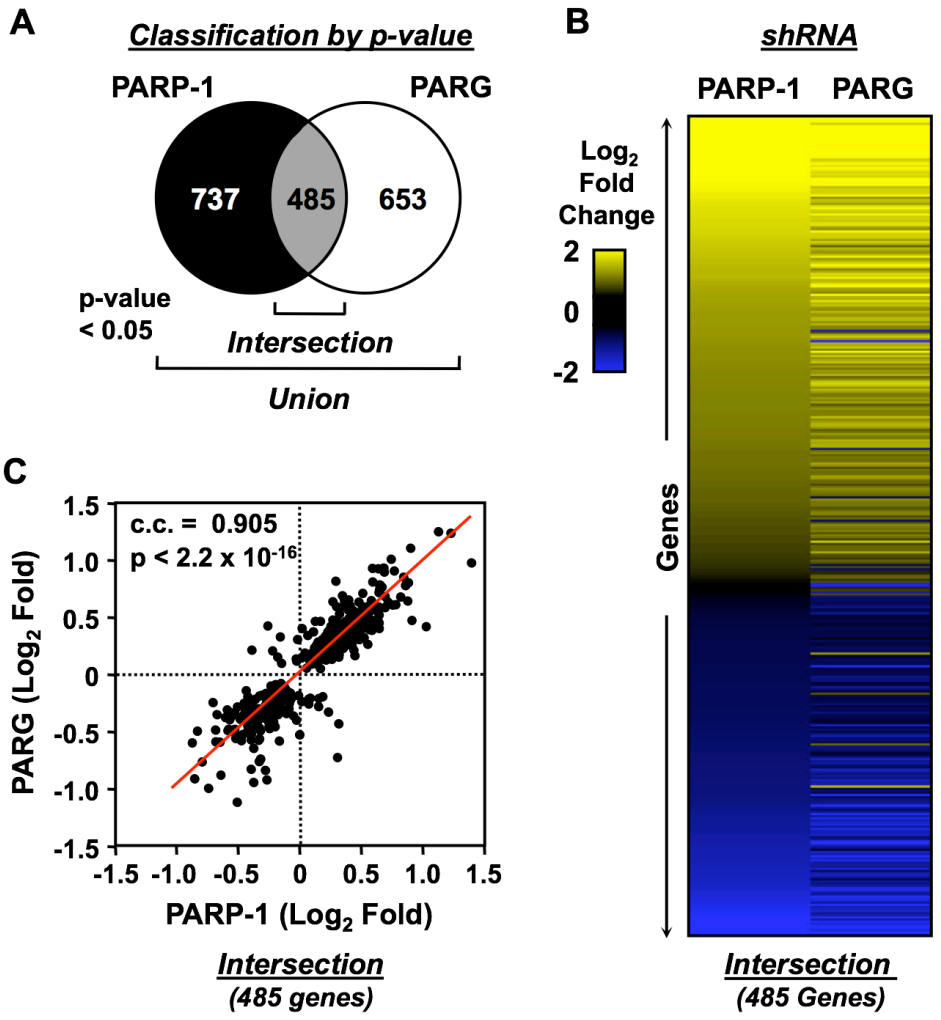
A
Classification by p-value
PARP-1
PARG
737
485
653
p-value
< 0.05
Intersection
Union
B
shRNA
PARP-1
PARG
Log2
Fold
Change
2
0
-2
Genes
Intersection
(485 Genes)
C
c.c. = 0.905
p < 2.2 x 10-16
PARG (Log2 Fold)
PARP-1 (Log2 Fold)
1.5
1.0
0.5
0
-0.5
-1.0
-1.5
Intersection
(485 genes)

F**igure 2.4. PARP-1 and PARG coordinately regulate global patterns of gene expression in MCF-7 cells (Union).** *A,* Venn diagram of PARP-1- and PARG-regulated genes in MCF-7 cells as defined by shRNA-mediated knockdown and expression microarrays. Genes passing both present call and p-value < 0.05 criteria for at least one factor represent the union, whereas genes regulated by both factors represent the commonly regulated genes or intersection (see also Figure 2.3.). *B,* Heatmap showing the expression profiles of the union of regulated genes. The genes are ranked in the heatmap by $\log_2$ fold change in the PARP-1 knockdown cell line (see color scale). *C,* Correlation analysis of the union of regulated genes from panel A. The Spearman correlation coefficient (c.c.) and p-value are indicated.

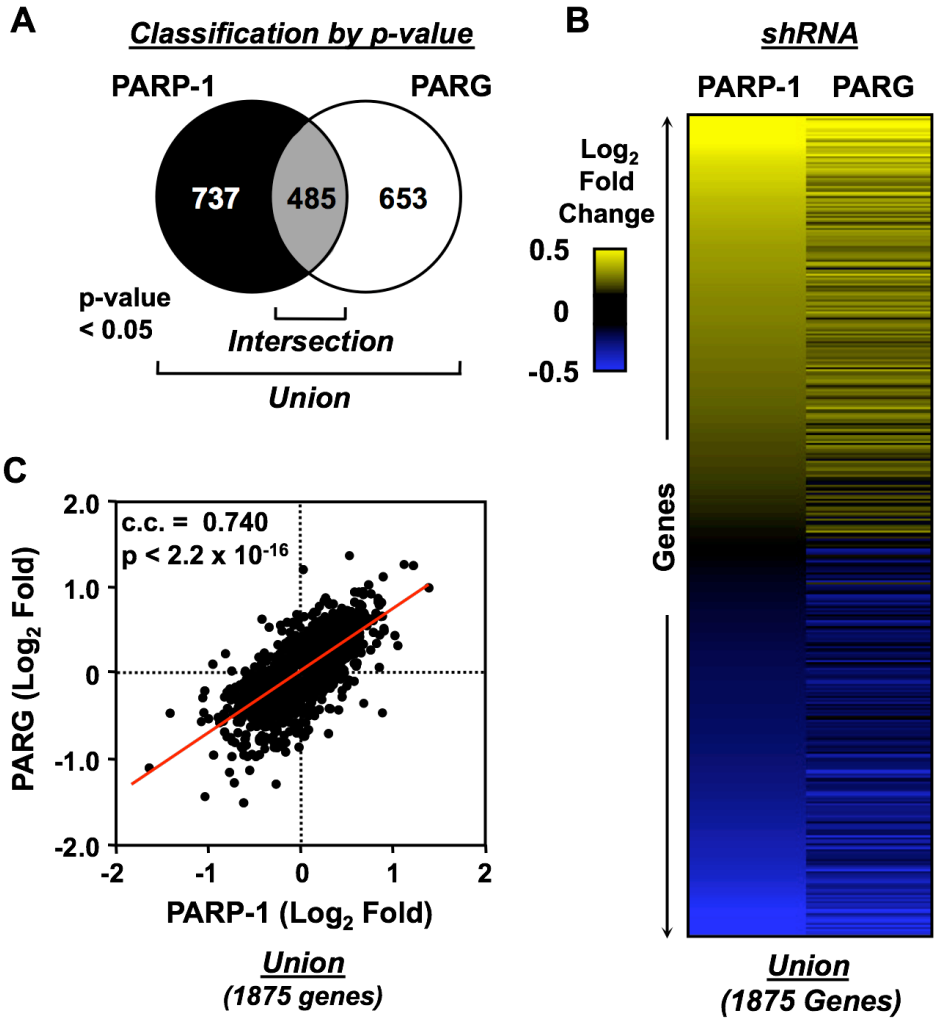
A
Classification by p-value
PARP-1
PARG
737
485
653
p-value
< 0.05
Intersection
Union
B
shRNA
PARP-1
PARG
Log2
Fold
Change
0.5
0
-0.5
Genes
Union
(1875 Genes)
C
c.c. = 0.740
p < 2.2 x 10-16
PARG (Log2 Fold)
PARP-1 (Log2 Fold)
2.0
1.0
0
-1.0
-2.0
-2
-1
0
1
2
Union
(1875 genes)

Figure 2.5. Defining the genes most robustly regulated by PARP-1 and PARG. *A,* Venn diagram of PARP-1- and PARG-regulated genes after applying a fold change cutoff of $\log_2 < -0.5$ or > 0.5. Of the union of 371 genes most robustly regulated by either PARP-1 or PARG, 50 are commonly regulated. *B,* The distribution of the most robustly up-regulated or down-regulated genes upon knockdown of PARP-1 or PARG is indicated. *C,* Correlation analysis comparing the magnitude and direction of regulation of the 371 most robustly regulated genes shown in panels A and B. The Spearman correlation coefficient (c.c.), p-value, and fold change cutoff are indicated. *D,* Gene specific confirmation of the expression microarray results by RT-qPCR. Luc, PARP-1, and PARG knockdown MCF-7 cells were seeded and grown under the same conditions used for the expression microarrays. Total RNA was isolated, reverse transcribed, and subjected to qPCR using gene-specific primers. Genes were considered to be regulated if the $\log_2$ fold change was < -0.5 or > 0.5 (values falling outside of the shaded box). Each bar represents the mean + SEM (*error bars*) from three or more independent determinations. All bars with a mean value falling outside of the shaded box are statistically different than the Luc control, as determined by a Student's t-test with a p-value threshold of < 0.05.

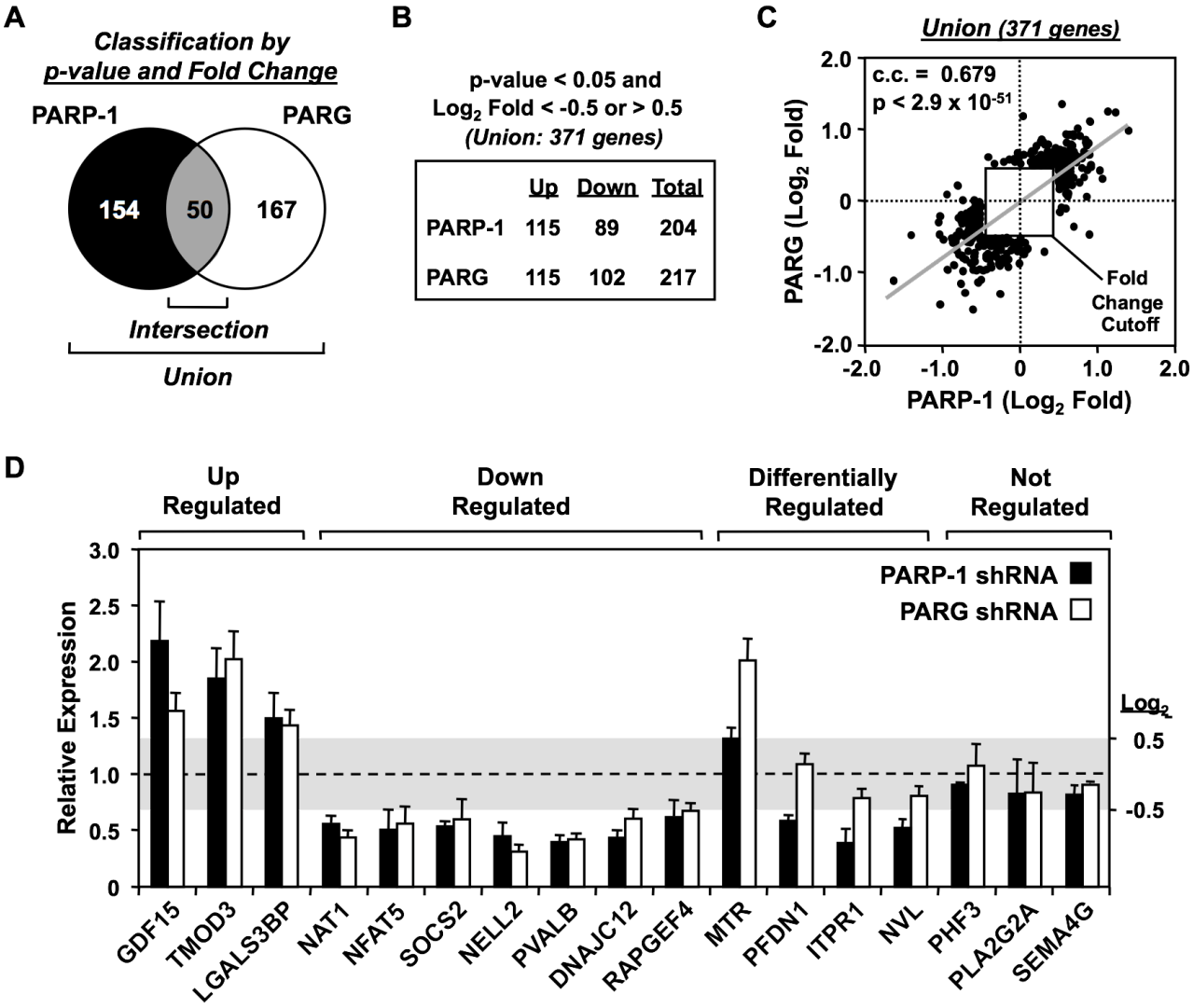
A
Classification by
p-value and Fold Change
PARP-1
PARG
154
50
167
Intersection
Union
B
p-value < 0.05 and
Log2 Fold < -0.5 or > 0.5
(Union: 371 genes)
Up Down Total
PARP-1 115 89 204
PARG 115 102 217
C
Union (371 genes)
c.c. = 0.679
p < 2.9 x 10-51
PARG (Log2 Fold)
PARP-1 (Log2 Fold)
Fold
Change
Cutoff
D
Up
Regulated
Down
Regulated
Differentially
Regulated
Not
Regulated
PARP-1 shRNA
PARG shRNA
Relative Expression
Log2
0.5
-0.5
GDF15
TMOD3
LGALS3BP
NAT1
NFAT5
SOCS2
NELL2
PVALB
DNAJC12
RAPGEF4
MTR
PFDN1
ITPR1
NVL
PHF3
PLA2G2A
SEMA4G

Table 2.1. List of 154 of the most robustly regulated genes affected by PARP-1 knockdown only. List of genes regulated by PARP-1 only (from Figure 2.5A), which include genes passing the present call, p-value, and fold change criteria noted in the text. The degree of change upon PARP-1 knockdown is listed as log_2 fold change relative to the Luc control.

Gene	Log_2 FC	Gene	Log_2 FC
ADAMTSL3	-0.711	DNAJC12	-0.656
ADCK2	0.519	DST	0.503
ALDH5A1	0.519	DUSP2	-0.755
AMY1A	-0.695	DUSP5	0.654
ANKRD17	-0.536	DYNC2LI1	0.641
AQP3	0.919	DZIP3	-0.667
ARL4D	-0.693	EIF2C4	-1.404
ATP2A3	0.651	ELF5	0.584
AVEN	0.522	ENAH	-0.588
BCAT1	0.564	ETS2	0.540
BCORL1	0.511	EXTL2	-0.568
C10orf110	-0.940	F2RL1	0.602
C10orf56	0.837	FADS1	0.572
C10orf84	0.732	FAM117A	-0.587
C11orf32	0.561	FARP1	0.517
C11orf9	-0.514	FHL1	0.604
C18orf25	0.800	FHL2	0.872
C2orf34	0.628	FLJ23172	0.804
C8orf1	-0.575	FZD3	0.501
CALML5	0.921	FZD7	-0.880
CAMK2N1	-0.515	GDF15	1.036
CAV1	-0.744	GNAS	-0.780
CCDC14	-1.631	GP1BA	0.695
CDC42BPB	0.504	GPR30	-0.519
CDC6	0.554	GPR64	-0.554
CEACAM6	1.069	GUSBP1	-0.568
CENPI	-0.610	HADHA	-0.561
CHKB	-0.580	HHEX	0.501
CPM	0.656	HIST1H2AM	0.618
CREB3L1	0.672	HMGA2	-0.787
CRISPLD2	-0.650	HTR2C	-0.656
DBR1	0.576	HYAL2	0.594
DDX19A	0.633	ID1	-0.606
DEGS1	-0.595	ID2	-0.536
DKFZp667G2110	-0.570	ID3	-0.660
DKFZP686A01247	-0.516	INHBB	0.617

Table 2.1. ***(continued)***

Gene	Log_2 FC	Gene	Log_2 FC
IQSEC1	0.584	PFTK1	-0.501
KIAA0040	0.601	PGK1	-0.700
KIAA0367	0.868	PIK3R1	-0.654
KIAA0683	0.532	PLA2G2A	-0.803
KIAA0776	-0.583	PLEKHB1	0.595
KLF4	0.574	PSEN2	-0.675
KPNA5	-0.822	PTGER3	-0.536
LAMC1	-0.531	PTPN3	0.504
LOC92249	-0.617	RAI16	0.594
LRRFIP2	0.533	RAP2C	0.652
LTBP1	0.508	RBM21	0.541
MANEA	0.671	RHBDD3	0.539
MAP3K5	-0.718	RHOBTB3	-0.511
MAP3K9	0.515	RRAGD	0.662
MARS	-0.617	SCAMP1	-0.536
MCAM	-0.618	SCN1A	-1.036
MED6	0.622	SEMA4D	-0.517
MORC4	0.507	SEPP1	-0.524
MUC5AC	0.661	SLC16A2	-0.985
MZF1	-0.663	SLC29A1	0.536
NAV3	-0.555	SLC2A10	0.554
NCKAP1	-0.598	SMOX	0.571
NEK4	0.552	SORD	0.542
NETO2	-0.642	SSBP2	-0.520
NFAT5	-0.808	SSH1	-0.567
NIPSNAP3B	-0.827	SYCP2	-1.048
NMB	-0.550	TBCA	-0.812
NR2F2	0.528	TBCE	0.511
NRF1	0.588	TBX10	0.627
NVL	-0.736	TNRC9	0.901
ODF2	0.597	TPK1	0.602
OSBPL1A	-0.549	TRPC1	-0.733
PADI2	0.698	UBN1	-0.645
PAH	-0.758	UTP18	-0.661
PALMD	-0.662	UTRN	-0.577
PARP1	-2.711	VGLL1	0.903
PARP12	0.775	WASL	0.521
PCGF1	-0.753	YIPF4	0.541
PDLIM7	0.740	ZNF133	-0.519
PER3	-0.574	ZNF35	-0.524
PFDN1	-1.027	ZNF571	-0.55

Table 2.2. List of 167 of the most robustly regulated genes affected by PARG knockdown only. List of genes regulated by PARG only (from Figure 2.5A), which include genes passing the present call, p-value, and fold change criteria noted in the text. The degree of change upon PARG knockdown is listed as log_2 fold change relative to the Luc control.

Gene	Log_2 FC	Gene	Log_2 FC
ABCA5	-0.517	CRISP3	0.551
ABCC4	0.504	CRLF1	-0.584
ABCD1	0.684	CROT	0.519
ACOT2	0.703	DEPDC5	0.611
ACOX1	-0.812	DICER1	-0.627
AGPAT3	0.524	dJ222E13.2	0.521
AMDHD2	-0.660	DLEU2	-0.762
AMPH	-0.779	DTNA	-0.511
AOX1	0.703	EEF1D	-0.720
AP4E1	0.772	EFEMP1	0.834
APH1B	-0.755	EHF	-0.547
ARL4C	-0.615	EMCN	-0.625
ARMC6	0.525	ENPEP	-0.515
ARPC4	0.722	EZH1	-0.681
ATP11A	-0.528	FAM116B	-0.884
ATP11B	0.660	FBXO22	-0.973
AZIN1	-0.618	FBXW7	0.603
BBS1	-0.557	FGFR1	0.719
BCAR3	0.502	FLJ12151	-0.583
BFSP1	-0.519	FLJ21820	-0.561
BHLHB2	-0.903	FLJ22662	0.602
BRAF	-0.818	GALNT12	0.609
C14orf45	-0.617	GDAP1	-0.559
C20orf117	-0.773	GEM	-0.722
C5orf13	0.831	GLE1L	0.586
C9orf156	0.594	GNE	0.871
CARD14	-0.528	GPC5	0.553
CASP2	0.624	GSPT1	0.712
CDC14B	-0.844	GTF2F1	0.614
CDKN2C	-0.509	GULP1	0.654
CES2	-0.707	HLA-A	-0.510
CLIC4	-0.580	HNRPD	-0.552
CLTA	-0.702	H-plk	0.680
CNN2	0.664	HSF1	0.583
COL11A2	0.668	IFT122	-0.872
COQ7	-0.553	INSIG1	0.571

Table 2.2. ***(continued)***

Gene	Log_2 FC	Gene	Log_2 FC
IREB2	0.528	PPP1R9A	-0.630
ITFG2	0.653	PRO0149	0.750
KCNJ5	0.796	PRO1843	-0.537
KIAA0562	0.593	RAB28	0.529
KIAA2010	-0.810	RASL11B	-0.584
KIF14	-0.552	RBM7	0.503
KLF3	0.663	RET	-0.599
KRT86	0.540	RPL23	-0.957
KYNU	0.566	RRM2	-0.545
LIG3	0.530	RXRB	0.657
LOC441296	-0.559	SAV1	0.647
LOC93349	0.567	SF3B3	0.604
LRRC40	-0.954	SIPA1L1	-0.612
LTBP3	0.695	SKIP	-0.562
MAP4	-0.521	SLC6A14	1.362
MARCKS	-0.655	SNRPN	0.935
MAX	-0.815	SOCS2	-0.974
MBNL2	0.608	SPATA2	0.702
MCFD2	0.577	SRGAP3	-0.768
MED6	-1.098	STK3	0.507
MIER2	-0.523	STX6	-0.646
MLF1	-0.578	TAF1	-0.793
MNS1	-0.682	TBC1D5	-0.729
MTSS1	-0.684	TFF1	-0.576
MUM1	1.199	TFF3	-0.869
MYO9B	0.551	TGFB2	0.694
NAT1	-0.857	TMC5	0.640
NCAM2	-0.957	TMCO3	0.824
NEK1	-0.793	TMSL8	-1.295
NEK7	-0.920	TNFSF13	-0.627
NFATC1	0.542	TPM4	0.799
NFYB	0.509	TPR	0.554
NUP62CL	-0.865	TTC12	-0.615
OLR1	0.573	TTC30A	-0.803
OPN3	0.651	TWIST1	-0.586
OR7E37P	-0.738	URG4	-1.281
P18SRP	0.591	USP24	0.583
PARD3	0.545	VAPA	-0.528
PARG	-1.514	VAV3	-0.738
PCP4	0.502	VCX	-0.950
PDCD4	0.523	VCX2	-0.555
PHF3	-0.744	WSB2	-0.661
PHLPPL	-0.658	WTAP	-0.512
PLD3	-0.652	YWHAZ	-0.926
PPAP2B	0.598	ZIC1	0.708
PPFIBP2	-0.754	ZNF165	0.506
PPP1R15A	-0.778	ZNF202	0.614
		ZNF606	-0.73

Table 2.3. List of 50 of the most robustly regulated genes affected by both PARP-1 and PARG knockdown. List of genes regulated by both PARP-1 and PARG (from Figure 2.5A), which include genes passing the present call, p-value, and fold change criteria noted in the text. The degree of change upon PARP-1 or PARG knockdown is listed as $\log_2$ fold change relative to the Luc control.

Gene	PARP-1	PARG	Gene	PARP-1	PARG
ALDH1A3	1.41	0.99	NELL2	-0.54	-1.14
ALOX15	0.70	0.69	NR4A2	0.53	0.53
ANKRD12	-0.51	-0.54	OGFR	0.87	0.79
ATXN10	1.14	1.26	PAQR6	-0.78	-0.74
C10orf97	0.59	0.66	PCCA	0.52	0.61
C14orf78	0.65	0.60	PDLIM5	0.73	0.65
CALM1	0.78	0.92	PGM3	0.66	0.75
CCNA2	0.50	0.56	PPP2R1B	0.56	0.61
CENTD1	-0.87	-0.58	PRODH	0.89	0.82
CTDSPL	0.70	0.91	PRUNE	0.50	0.53
CYB561	0.68	0.78	PVALB	-0.64	-0.57
EPS15	0.66	0.79	QPRT	0.85	0.86
FGFR2	0.65	0.53	RIPK2	0.69	0.94
FLJ11151	1.24	1.25	RPL23AP7	0.75	1.02
GRSF1	0.52	0.72	SERINC3	0.63	0.60
HGD	0.66	0.80	SGK3	0.89	0.66
ITPR1	-0.73	-0.98	SLC35A3	0.65	0.94
KCNK5	0.60	0.94	ST3GAL5	-0.67	-0.57
KIAA0999	0.65	0.73	TARP	-1.03	-1.44
LGALS3BP	0.79	0.62	TBC1D4	0.83	0.69
LYRM1	0.65	0.55	TGOLN2	0.58	0.57
MBOAT2	0.60	0.62	TMOD3	0.91	1.12
MSMB	0.76	0.62	TROVE2	-0.85	-0.89
MTR	0.60	0.82	UBE2B	0.51	0.52
MYB	-0.63	-0.86	ZMYM6	0.70	0.60

Figure 2.6. Comparison of two independent shRNA target sequences for the knockdown of PARP-1 or the knockdown of PARG. *A,* Knockdown of PARP-1 or PARG by two independent shRNA target sequences. Whole cell lysates were collected from Luc, PARP-1, and PARG stable shRNA-mediated single knockdown cell lines. Two independent shRNA sequences (#1 and #2) targeting PARP-1 *(top)* or PARG *(bottom)* were analyzed by Western blotting for their ability to knockdown their cognate proteins relative to the Luc control. *B,* RT-qPCR analysis confirms the knockdown PARP-1 and PARG mRNA in the single knockdown cell lines described in panel A. Total RNA was isolated from Luc, PARP-1, and PARG single knockdown cells, reverse transcribed, and subjected to qPCR using gene-specific primers to PARP-1 and PARG. Each bar is the mean + SEM (*error bars*) for three independent RNA isolations. *C,* Comparable effects on gene expression for single and double PARP-1 knockdown. Luc and PARP-1 single and double knockdown MCF-7 cells were seeded and grown under the conditions described in the text. Total RNA was isolated, reverse transcribed, and subjected to qPCR using gene-specific primers. The effect of single knockdown (PARP-1 shRNA #1 or PARP-1 shRNA#2) and double knockdown were compared for the PARP-1 target genes identified in Figure 2.5 *(left)*. Each bar represents the mean + SEM (*error bars*) from three or more independent determinations. A correlation analysis comparing the effects of PARP-1 shRNA #1 and PARP-1 shRNA #2 at 40 target genes indicates that both shRNAs produce similar effects on target gene expression. The Spearman correlation coefficient (c.c.) and p-value are indicated *(right)*. *D,* Comparable effects on gene expression for single and double PARG knockdown. Experiments similar to those described for PARP-1 in panel C were performed for PARG.

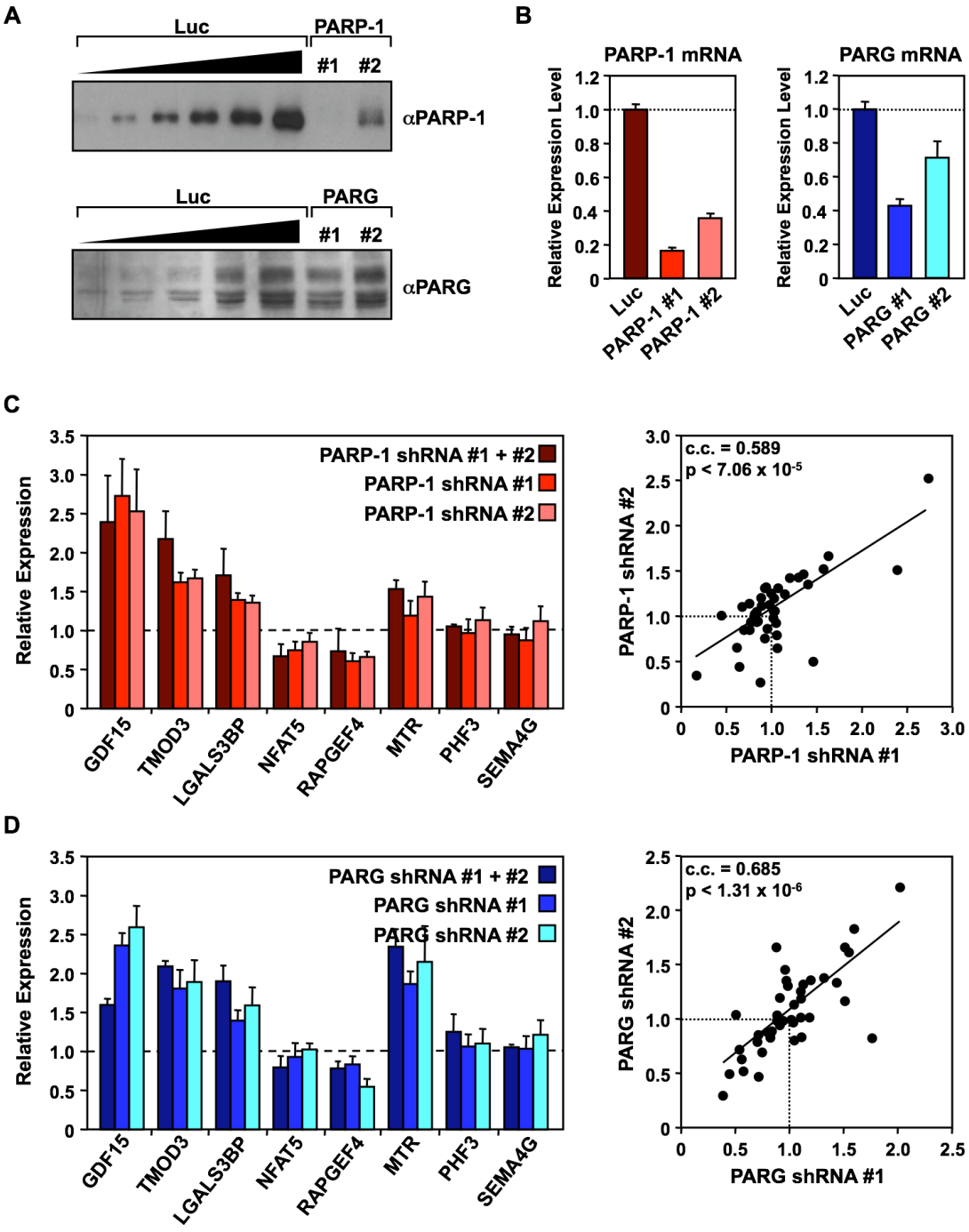
A
Luc
PARP-1
#1 #2
αPARP-1
Luc
PARG
#1 #2
αPARG
B
PARP-1 mRNA
Relative Expression Level
Luc
PARP-1 #1
PARP-1 #2
PARG mRNA
Relative Expression Level
Luc
PARG #1
PARG #2
C
Relative Expression
PARP-1 shRNA #1 + #2
PARP-1 shRNA #1
PARP-1 shRNA #2
GDF15
TMOD3
LGALS3BP
NFAT5
RAPGEF4
MTR
PHF3
SEMA4G
c.c. = 0.589
p < 7.06 x 10-5
PARP-1 shRNA #2
PARP-1 shRNA #1
D
Relative Expression
PARG shRNA #1 + #2
PARG shRNA #1
PARG shRNA #2
GDF15
TMOD3
LGALS3BP
NFAT5
RAPGEF4
MTR
PHF3
SEMA4G
c.c. = 0.685
p < 1.31 x 10-6
PARG shRNA #2
PARG shRNA #1

We focused on these confirmed genes for further analysis in the experiments described below. Additional gene-specific RT-qPCR assays comparing gene expression profiles from single knockdown cell populations indicate that the gene regulatory effects of the shRNAs used in our assays are unlikely to be due to off target effects (Figure 2.6).

Genes commonly regulated by PARP-1 and PARG are enriched in metabolism and stress response functions. To explore the function of the genes most robustly regulated by PARP-1 and PARG knockdown, we performed gene ontology (GO) analyses using the DAVID Bioinformatics Database Resource (Table 2.4). Both the PARP-1- and PARG-regulated genes from Figure 2.5A (*i.e.*, genes passing the present call, p-value, and fold change criteria noted above) are enriched in cell structure and metabolism functions (*e.g.*, *ITPR1* for PARP-1, *SOCS2* and *MTR* for PARG). The 50 commonly regulated genes are enriched in stress response and metabolism functions (*e.g.*, *LGALS3BP*), consistent with the stress- and metabolic-related phenotypes of PARP-1 and PARG knockout mice or cells from the knockout animals grown in culture (Cortes et al., 2004; Koh et al., 2004; Wang et al., 1995; Wang et al., 1997).

Exploring the mechanisms of PARP-1- and PARG-mediated gene expression at target gene promoters. After examining the control of global patterns of gene expression in MCF-7 cells by PARP-1 and PARG, we sought to determine the underlying mechanisms of regulation at specific target gene promoters. We considered a variety of criteria that might help us identify target genes for mechanistic studies. Ultimately, we focused on a set of genes (i) showing the most robust alterations in gene expression upon knockdown of PARP-1 and PARG (*i.e.*, from the list of the 50 most robustly regulated genes; see Figure 2.5A and Table 2.3), (ii) exhibiting binding of PARP-1 and PARG at their promoters by ChIP assays (see the

next section), and (iii) whose expression can be complemented by re-expression of PARP-1 or PARG in the corresponding knockdown cell lines (see below). We also considered other existing evidence of regulation at the promoters of possible target genes, including changes in chromatin composition (*e.g.*, linker histone binding) and structure (promoter chromatin architecture; see Discussion section). Together, these criteria were used as a set of parameters to identify targets for further analysis.

PARP-1 and PARG localize to the promoters of target genes and can affect each other's binding. Previous studies have shown that PARP-1 localizes (and in some cases, is recruited in a signal-dependent manner) to the promoters of target genes (Ju et al., 2006; Ju et al., 2004; Krishnakumar et al., 2008; Pavri et al., 2005). In fact, a recent genomic analysis from our lab has shown that PARP-1 localizes to the promoters of most expressed genes in the genome of MCF-7 cells (Krishnakumar et al., 2008). Whether PARG also localizes to target genes has not been determined.

To address this question, we first needed to validate the use of a new custom PARG antibody for chromatin immunoprecipitation (ChIP) assays. ChIP coupled with Western blotting of the immunoprecipitated material (*i.e.*, "ChIP-Western"), demonstrated that our previously validated PARP-1 antibody (Krishnakumar et al., 2008), as well as a new custom PARG antibody, specifically immunoprecipitate PARP-1 and PARG, respectively, under ChIP conditions (Figure 2.7A). Notably, while our custom antibody recognizes many of the known PARG isoforms in a whole cell lysate (*i.e.*, ChIP Input), it specifically enriches for two isoforms in a ChIP assay (Figure 2.7A). The longest of the PARG isoforms is 110 kDa and is nuclear, while other slightly shorter isoforms are both nuclear and cytoplasmic (Meyer-Ficca et al., 2004; Meyer-Ficca et al., 2005). Our ChIP-Western results demonstrate that the

longest PARG isoforms are chromatin-bound. Thus, these antibodies are useful for exploring the localization of PARP-1 and PARG at native promoters in ChIP assays.

We then used the gene expression data from Figures 2.2 through 2.5, as well as our existing PARP-1 genomic localization data set from MCF-7 cells (Krishnakumar et al., 2008), to identify genes for further examination in ChIP-qPCR assays for PARP-1 and PARG. Our analyses showed that both PARP-1 and PARG localize to the promoters of genes from Figure 2.5D with signals of ~5- to ~20-fold over the "no antibody" (NA) control, but not to the promoter of an unregulated gene (i.e., *SEMA4G*) (Figure 2.8). Specificity was demonstrated by a reduction of the ChIP signals upon PARP-1 or PARG knockdown (Figures 2.7B and 2.7C). PARP-1 and PARG occupy the promoters of both up-regulated and down-regulated target genes, indicating gene-specific effects for transcriptional regulation by these factors. Interestingly, the levels of PARG were proportional to the levels of PARP-1 across the genes we examined (Figure 2.8). That is, a higher PARG signal corresponded to a higher PARP-1 signal (Spearman correlation coefficient of 0.645, p-value < 0.05), even for genes that were regulated by knockdown of one factor, but not the other (*e.g.*, *ITPR1* and *NVL*). This latter result fits well with the striking correlation between the patterns of gene regulation by PARP-1 and PARG in the microarray expression experiments (Figures 2.3C, 2.4C and 2.5C).

Our previous genomic study showed that PARP-1 is enriched at promoters, with regions containing high levels of binding and regions containing low levels of binding (Krishnakumar et al., 2008). ChIP-qPCR analyses in "off-peak" regions confirmed this pattern of binding for both PARP-1 and PARG at selected target gene promoters (e.g., the TSS for *PVALB*) (Figure 2.9A). ChIP "tiling" through the *LGALS3BP* and *PVALB* promoter regions further confirmed this pattern of binding for both PARP-1 and PARG (Figure 2.9B). Together, these results indicate that PARG,

Table 2.4. Gene ontology of PARP-1-, PARG-, and commonly-regulated genes in MCF-7 cells. The PARP-1- and PARG-regulated gene lists from Fig. 2.5A and Tables 2.1, 2.2, and 2.3, which include genes passing the present call, p-value, and fold change criteria noted in the text, were subjected to GO analyses using the DAVID Bioinformatics Database Resource. Resulting terms were grouped together under each category and duplicate probe sets were removed for accurate percentage representation of individual genes. Only those GO terms yielding a p-value < 0.05 by a Fisher exact test were considered significantly enriched in each gene list.

Category	Count	Percent of Total	p-value	Example[8]
A. PARP-1-Regulated Genes				
Cell Structure[1]	33	16%	< 0.045	*ITPR1**
Metabolism[2]	24	12%	< 0.049	*ALDH5A1*
B. PARG-Regulated Genes				
Cell Structure[3]	49	23%	< 0.049	*SOCS2*, TMOD3**
Metabolism[4]	24	11%	< 0.028	*MTR*, NAT1**
GTPase Regulation[5]	9	4%	< 0.046	*VAV3*
C. Commonly-Regulated Genes				
Stress Response[6]	8	16%	< 0.033	*LGALS3BP**
Metabolism[7]	8	16%	< 0.049	*PRODH*

[1] GO Terms: plasma membrane

[2] GO Terms: organic acid metabolism, carboxylic acid metabolism, amine metabolism, nitrogen compound metabolism, aromatic compound metabolism, and regulation of transferase activity

[3] GO Terms: actin binding, cytoplasmic membrane-bound vesicle, cytoplasmic vesicle, membrane-bound vesicle, vesicle, cytoskeletal protein binding, cytoskeleton, endomembrane system, cell organization and biogenesis, and nuclear envelope

[4] GO Terms: amino sugar metabolism, amine metabolism, cofactor biosynthesis, coenzyme metabolism, nitrogen compound metabolism, cofactor metabolism, carboxylic acid metabolism, and organic acid metabolism

[5] GO Terms: GTPase regulator activity, GTPase activator activity

[6] GO Terms: Response to stress

[7] GO Terms: amine metabolism, nitrogen compound metabolism, carboxylic acid metabolism, organic acid metabolism, amino acid metabolism, and amino acid and derivative metabolism

[8] Examples of representative gene(s) for each ontological category. Those marked with an asterisk are genes whose expression patterns in the PARP-1 and PARG knockdown cell lines were confirmed by RT-qPCR, as shown in Fig. 2.5D.

Figure 2.7. PARP-1 and PARG antibodies immunoprecipitate their cognate proteins from crosslinked chromatin. *A, (Top)* Crosslinked and sheared chromatin from MCF-7 cells was subjected to ChIP-Western analyses for PARP-1 and PARG, demonstrating the ability of PARP-1 and PARG antibodies to immunoprecipitate their cognate proteins. In, Input; NA, no antibody control; IP, immunoprecipitate. (*Bottom)* A higher resolution Western blot demonstrates the ability of the PARG antibody to specifically enrich for two PARG isoforms, denoted by asterisks, relative to the input material during ChIP. Isoforms not enriched during ChIP are denoted by pluses. *B and C,* ChIP-qPCR analyses demonstrate a reduction in PARP-1 ChIP signal upon knockdown of PARP-1 (panel B) and, likewise, a reduction in PARG ChIP signal upon knockdown of PARG (panel C), indicating that the antibodies specifically recognize their cognate proteins.

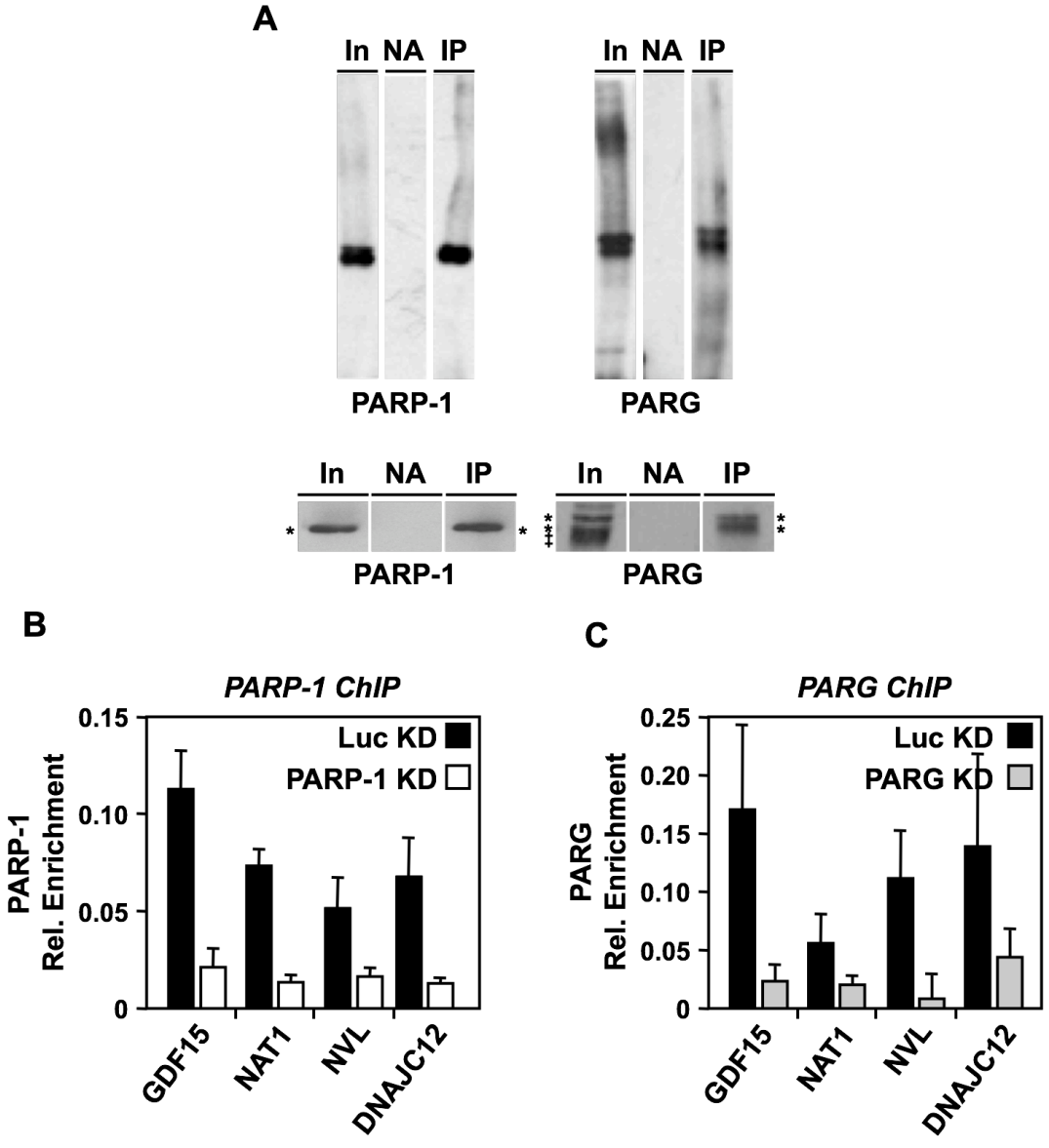
A
In NA IP
In NA IP
PARP-1
PARG
In NA IP
In NA IP
PARP-1
PARG
B
PARP-1 ChIP
PARP-1 Rel. Enrichment
0.15
0.10
0.05
0
Luc KD
PARP-1 KD
GDF15
NAT1
NVL
DNAJC12
C
PARG ChIP
PARG Rel. Enrichment
0.25
0.20
0.15
0.10
0.05
0
Luc KD
PARG KD
GDF15
NAT1
NVL
DNAJC12

Figure 2.8. PARP-1 and PARG localize to the promoters of regulated target genes. *A,* PARP-1 and PARG show similar patterns of localization at the promoters of commonly regulated target genes. The occupancy of PARP-1 (black bars) and PARG (grey bars) at the promoters of co-regulated genes was examined by ChIP analyses. Each bar represents the mean + SEM (*error bars*) from three or more independent determinations. Bars that are not marked with an asterisk are statistically different from the NA control, as determined by a Student's t-test with a p-value threshold of < 0.05. SEMA4G is a gene not regulated by knockdown of PARP-1 or PARG (see Figure 2.5.). The effects of PARP-1 and PARG knockdown (from Figure 2.5.) are indicated for comparison: (1) –, no effect; (2) ⇑, up-regulated by both PARP-1 and PARG knockdown; (3) ⇓, down-regulated by both PARP-1 and PARG knockdown; and (4) ⇑⇓, differentially regulated by PARP-1 and PARG knockdown.

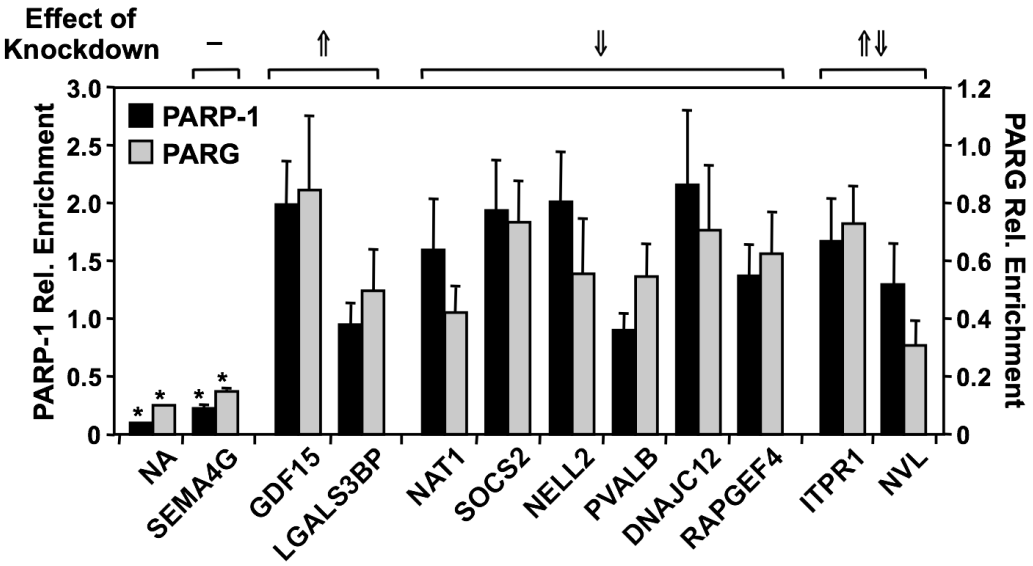
Effect of Knockdown
–
⇑
⇓
⇑⇓
PARP-1
PARG
PARP-1 Rel. Enrichment
PARG Rel. Enrichment
3.0
2.5
2.0
1.5
1.0
0.5
0
1.2
1.0
0.8
0.6
0.4
0.2
0
NA
SEMA4G
GDF15
LGALS3BP
NAT1
SOCS2
NELL2
PVALB
DNAJC12
RAPGEF4
ITPR1
NVL

Figure 2.9. PARP-1 and PARG binding patterns are similar across individual target gene promoters. PARP-1 and PARG binding patterns are similar across individual promoters with both high and low occupancy. *A,* The occupancy of PARP-1 (black bars) and PARG (grey bars) at two regions (~1 kb apart) of the *GDF15*, *PVALB, LGALS3BP, and NELL2* promoters was determined by ChIP analyses. Each bar represents the mean + SEM (*error bars*) from three or more independent determinations. *B,* PARP-1 (solid line) and PARG (dotted line) occupancy was examined by ChIP-tiling analyses over a 2.5 kb region of the *PVALB* and *LGALS3BP* promoters. Each point represents the mean + SEM from three or more independent determinations; all values are statistically different from the "no antibody" control, as determined by a Student's t-test with a p-value threshold of < 0.05.

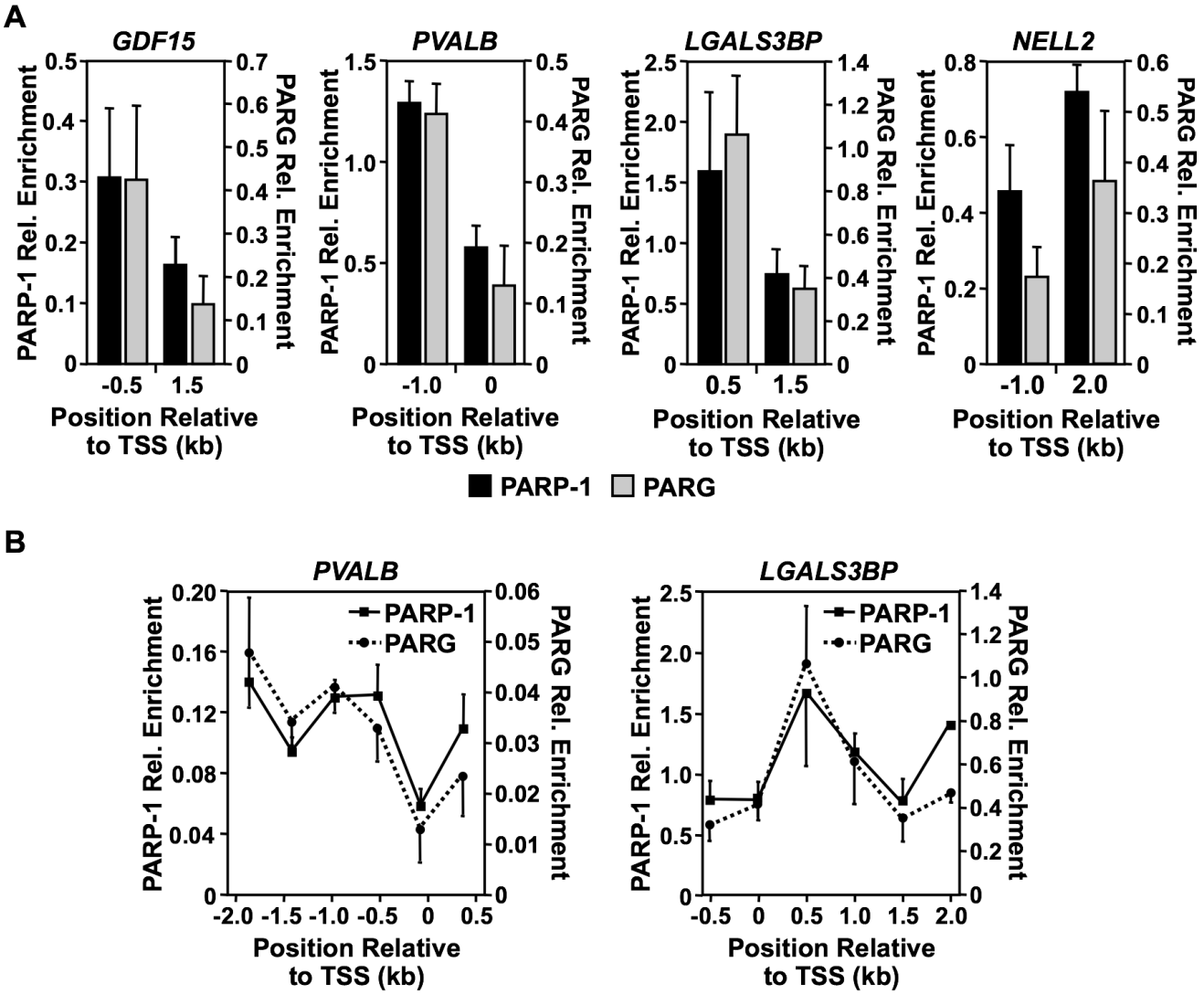
A
GDF15
PVALB
LGALS3BP
NELL2
PARP-1 Rel. Enrichment
PARG Rel. Enrichment
Position Relative to TSS (kb)
PARP-1
PARG
B
PVALB
LGALS3BP
PARP-1
PARG
PARP-1 Rel. Enrichment
PARG Rel. Enrichment
Position Relative to TSS (kb)

like PARP-1, can localize to the promoters of target genes. Furthermore, they show that the localization of PARG correlates with the localization of PARP-1.The similar localization patterns of PARP-1 and PARG at promoters raised the question of whether they might affect each other's binding (*e.g.*, one recruits the other or they bind cooperatively). To address this issue, we examined the effect of knockdown of one protein on the promoter binding of the other in ChIP assays. Our results indicate that PARP-1 and PARG can indeed affect each other's binding, but that they do so in a gene-specific manner (Figure 2.10). For example, we found genes, such as *NAT1*, where the binding of PARP-1 and PARG appear to occur independently; genes, such as *NVL*, where the binding of PARP-1 requires the binding of PARG; and genes, such as *GDF15*, where PARP-1 and PARG require each other for binding. These results support the hypothesis that there is a functional interplay between PARP-1 and PARG at target gene promoters, although, the details of the mechanisms may differ between promoters (see Discussion). Collectively, our ChIP analyses indicate that PARP-1 and PARG localize to promoters of target genes to regulate their expression.

Catalytically inactive mutants of PARP-1 and PARG support the wild-type expression patterns of some, but not all, target genes. Previous studies have provided mixed results about the requirement for PARP-1's enzymatic activity during gene regulation. Some studies have indicated that PARP-1's enzymatic activity is required (Butler and Ordahl, 1999; Ju et al., 2006; Ju et al., 2004; Kim et al., 2004; Miyamoto et al., 1999; Nirodi et al., 2001; Tulin and Spradling, 2003), while others have indicated that it is not (Anderson et al., 2000; Cervellera and Sala, 2000; Hassa et al., 2001; Meisterernst et al., 1997; Pavri et al., 2005). The role of PARG enzymatic activity in the regulation of gene expression has not been examined extensively. To

Figure 2.10. PARP-1 and PARG can affect each other's binding at target gene promoters. To determine if PARP-1 and PARG can affect each other's binding, the occupancy of PARP-1 and PARG was examined by ChIP analyses in the control and knockdown cell line of the opposing factor. *A,* The occupancy of PARP-1 was examined by ChIP analyses in the Luc (black bars) and PARG (grey bars) knockdown cell lines. Each bar represents the mean + SEM (*error bars*) from three or more independent determinations. *B,* The occupancy of PARG was examined by ChIP analyses in the Luc (black bars) and PARP-1 (white bars) knockdown cell lines. Each bar represents the mean + SEM (*error bars*) from three or more independent determinations. The data revealed three groups of PARP-1 and PARG binding patterns, as indicated. All changes in occupancy for PARP-1 (Group I and II) and PARG (Group I) are statistically different between the control and knockdown cell line, as determined by a Student's t-test with a p-value threshold of < 0.05.

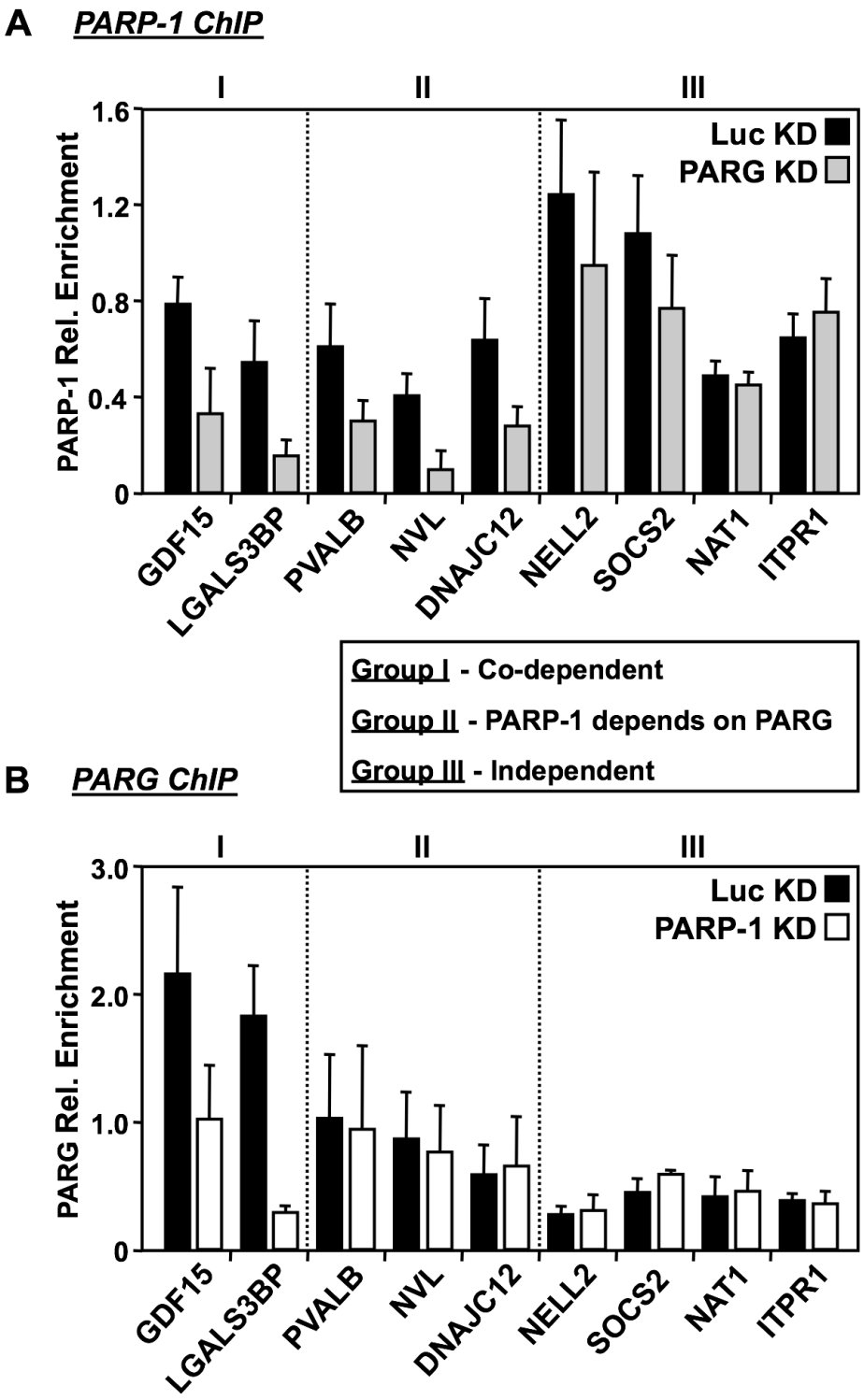
A
PARP-1 ChIP
I
II
III
1.6
1.2
0.8
0.4
0
PARP-1 Rel. Enrichment
Luc KD
PARG KD
GDF15
LGALS3BP
PVALB
NVL
DNAJC12
NELL2
SOCS2
NAT1
ITPR1
Group I - Co-dependent
Group II - PARP-1 depends on PARG
Group III - Independent
B
PARG ChIP
I
II
III
3.0
2.0
1.0
0
PARG Rel. Enrichment
Luc KD
PARP-1 KD
GDF15
LGALS3BP
PVALB
NVL
DNAJC12
NELL2
SOCS2
NAT1
ITPR1

determine the specific requirement of PARP-1 and PARG enzymatic activities in the regulation of target gene expression, we devised a system to stably re-express FLAG-tagged versions of wild-type or catalytically inactive mutants of PARP-1 and PARG in their respective knockdown cell lines using retrovirus-mediated gene transfer. To prevent knockdown of the re-expressed proteins in the PARP-1 and PARG MCF-7 knockdown cell lines, we used shRNA-resistant versions of the PARP-1 and PARG cDNAs (Figures 2.11A and 2.11C; see Experimental Procedures). Using this approach, we were able to restore PARP-1 expression levels to about 20 percent of the levels in parental cells and PARG expression levels to about 10 to 20 times the levels in parental cells (Figures 2.11B and 2.11D). These levels of re-expression were consistent across multiple independent gene transfer experiments. Re-expression of wild-type PARP-1 modestly, but reproducibly, increased total PAR levels above the levels seen in the PARP-1 knockdown cells, while re-expression of the catalytically inactive PARP-1 mutant did not (Figure 2.12A). Similarly, re-expression of wild-type PARG reduced total PAR levels below the levels seen in the PARG knockdown cells, while re-expression of the catalytically inactive PARG mutant did not (Figure 2.12B). These results illustrate that wild-type PARP-1 and PARG and their catalytically inactive mutants alter cellular PAR levels as expected in vivo.

We used these "knockdown/add-back" cell lines to analyze the roles of PARP-1 and PARG catalytic activity in target gene expression. The expression of selected target genes from the gene-specific expression (Figure 2.5D) and ChIP (Figure 2.8) experiments was tested in the knockdown/add-back cell lines. For example, the levels of *LGALS3BP* mRNA, which increased in response to both PARP-1 and PARG knockdown, was largely restored to control levels upon re-expression of either wild-type or catalytically inactive PARP-1 or PARG (Figures 2.13A and 2.13B, left panels). These results suggest that neither PARP-1 nor PARG enzymatic activity is

required for the proper expression of *LGALS3BP*. In contrast, the levels of *NELL2* mRNA, which decreased in response to both PARP-1 and PARG knockdown, was largely restored to control levels upon re-expression of either wild-type or catalytically inactive PARP-1, as well as wild-type PARG, but not catalytically inactive PARG (Figures 2.13A and 2.13B, middle panels). These results suggest that the catalytic activity of PARG, but not PARP-1, is required for the proper expression of *NELL2*. For this gene, PARG may be required to degrade an alternate source of PAR, perhaps from PARP-2, another nuclear PARP enzyme (Amé et al., 2004). Other genes (*e.g.*, *NVL* and *PVALB*) also showed a requirement for PARP-1 or PARG catalytic activity for proper expression (Figures 2.13A and 2.13B, right panels). For the genes not dependent on PARP-1 or PARG catalytic activity, dominant negative effects of the catalytically inactive mutants may contribute to the gene expression outcomes.

The results for *LGALS3BP* and *NELL2* were explored further using chemical inhibitors of PARP-1 (*i.e.*, PJ34) and PARG (i.e., gallotannin, GT; a.k.a. common tannic acid). After verifying the efficacy of the inhibitors using autoPARylation of PARP-1 as an endpoint (Figure 2.14A), we examined their effects on gene expression (Figures 2.14B and 2.14C). As expected based on the knockdown/add-back experiments, PJ34 had no effect on the expression of *LGALS3BP* and *NELL2,* verifying that PARP-1 enzymatic activity is not required for the proper expression of these genes. Likewise, gallotannin inhibited proper expression of *NELL2*, but not *LGALS3BP*, verifying the requirement (or lack of requirement) for PARG enzymatic activity (Figures 2.14B and 2.14C). Overall, of the nine PARP-1- or PARG-regulated genes that we tested in detail, about half required the enzymatic activity of the regulating protein **(**Figure 2.13 and data not shown). These results suggest alternate non-enzymatic functions for PARP-1 and PARG (e.g., protein-protein interactions or scaffolding) in some gene contexts may be important, as suggested by other studies

(Anderson et al., 2000; Cervellera and Sala, 2000; Hassa et al., 2001; Meisterernst et al., 1997; Pavri et al., 2005).

2.4. Discussion

Both PARP-1 and PARG, two enzymes functionally linked in the nuclear PAR metabolic pathway, have been implicated in the regulation of gene expression. However, the means by which they coordinate their gene regulatory actions both globally and at specific target genes, as well as the role of their enzymatic activities in the regulation of gene expression, have not been clearly established. In the current study, we used both genomic and gene-specific assays to address both of these questions in MCF-7 cells. Collectively, our results indicate that PARP-1 and PARG, two nuclear enzymes with opposing enzymatic activities, localize to target promoters and generally regulate gene expression in a similar, rather than antagonist, manner.

PARP-1 and PARG act in concert to regulate a largely overlapping gene set in a similar manner. Our microarray experiments have revealed a number of interesting and unexpected facets of global gene regulation by PARP-1 and PARG that were not revealed in previous studies focusing on one factor or the other. First, PARP-1 and PARG regulate the expression of a common gene set generally in the same direction and with the same magnitude (Figures 2.3, 2.4, and 2.5). Based on the seemingly opposing enzymatic activities of PARP-1 and PARG, this result was unexpected. Second, the most robustly regulated common genes are enriched for stress response and metabolic functions (Table 2.4), which fits well with the known biological roles of PARP-1 and PARG from animal studies. Third, PARG localizes to the promoters of its target genes (Figures 2.8 and 2.9), as has been demonstrated previously for PARP-1

Figure 2.11. Stable re-expression of shRNA-resistant PARP-1 and PARG in their cognate knockdown cell lines. *A,* Schematic diagram of the human PARP-1 structural and functional domains. The DNA binding domain (DBD), zinc fingers (Zn Fingers), nuclear localization signal (NLS), third zinc binding domain (Zn3), automodification domain (AMD), and PARP "signature" motif are shown. Open triangles indicate the location of the 21-nucleotide shRNA recognition sequences used for knockdown. Filled circles indicate the location of the silent point mutations engineered into the cDNAs to make them resistant to the shRNAs. The open circle indicates the location of the inactivating point mutation (Glu 988 to Lys) that inhibits PARP-1 enzymatic activity in the catalytically inactive mutant (CatMut). *B,* FLAG-tagged RNAi-resistant wild-type (Wt) or catalytically inactive (CatMut) PARP-1 was stably expressed in MCF-7 PARP-1 knockdown (KD) cell lines. Re-expression was confirmed by Western blotting for PARP-1 and FLAG. An empty vector was used as a control (Empty) in both Luc and PARP-1 knockdown cell lines. *C,* Schematic diagram of the rat PARG structural and functional domains. The regulatory domain, catalytic domain, active site, nuclear localization signal (NLS), and nuclear export signal (NES) are shown. Open triangles indicate the location of the 21-nucleotide shRNA recognition sequences used for knockdown. Filled circles indicate the location of the silent point mutation engineered into the cDNAs to make them resistant to the shRNA. The open circles indicate the location of the inactivating point mutations (Tyr 788 to Phe and Tyr 791 to Ala) that inhibit PARG enzymatic activity in the catalytically inactive mutant (CatMut). *D,* FLAG-tagged RNAi-resistant wild-type (Wt) or catalytically inactive (CatMut) PARG was stably expressed in MCF-7 PARG knockdown (KD) cell lines. Re-expression was confirmed by Western blotting for PARG and FLAG. An empty vector was used as a control (Empty) in both Luc and PARP-1 knockdown cell lines.

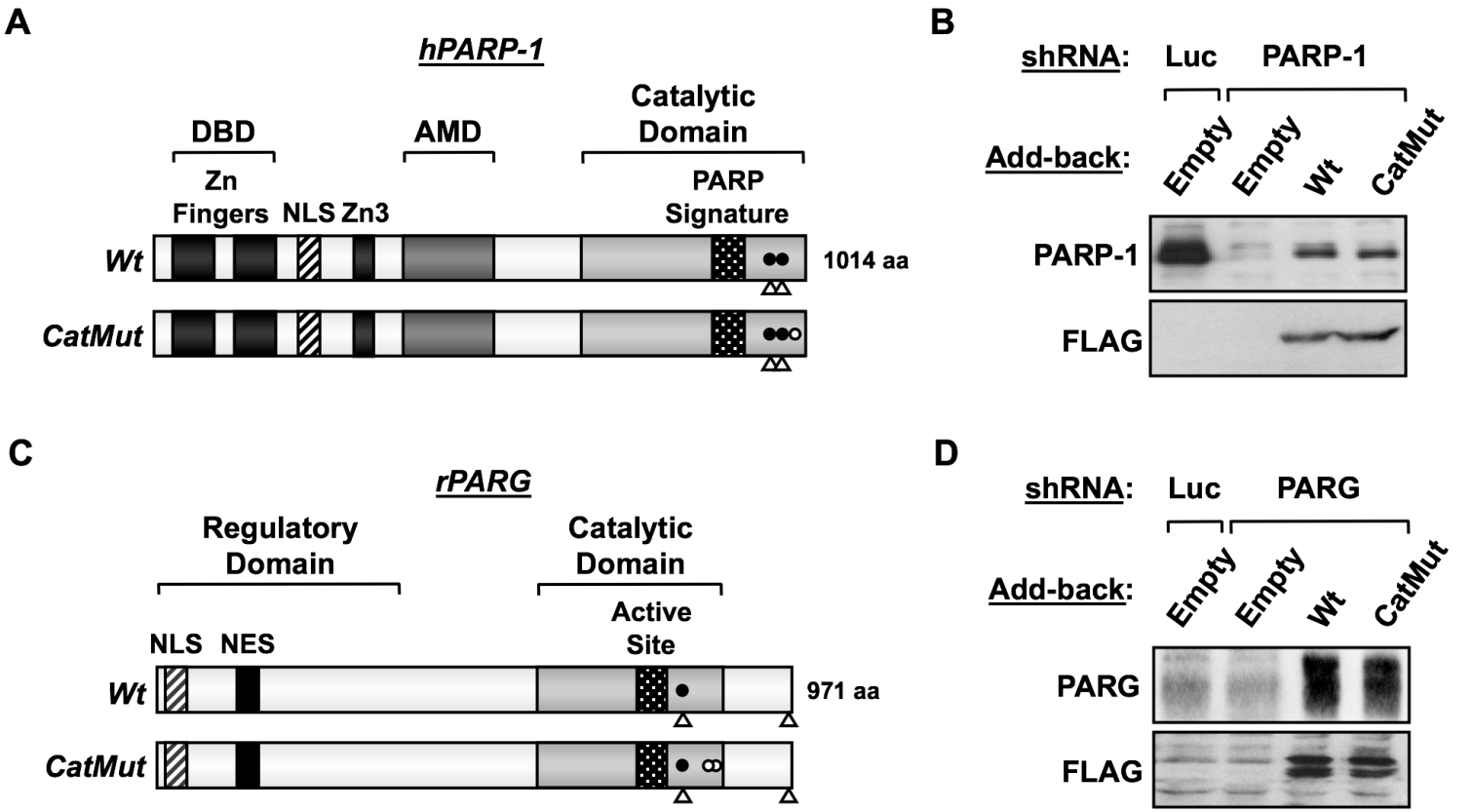
A
hPARP-1
DBD
AMD
Catalytic Domain
Zn Fingers
NLS
Zn3
PARP Signature
Wt
CatMut
1014 aa
B
shRNA:
Luc
PARP-1
Add-back:
Empty
Empty
Wt
CatMut
PARP-1
FLAG
C
rPARG
Regulatory Domain
Catalytic Domain
Active Site
NLS
NES
Wt
CatMut
971 aa
D
shRNA:
Luc
PARG
Add-back:
Empty
Empty
Wt
CatMut
PARG
FLAG

Figure 2.12. Stable re-expression of wild-type PARP-1 or PARG re-establishes cellular PAR levels, while catalytically inactive mutants do not. *A and B,* RNAi-resistant wild-type (Wt) or catalytically inactive (CatMut) PARP-1 (panel A) or PARG (panel B) were stably expressed in their respective MCF-7 knockdown cells, as shown in Figure 2.11. Whole cell lysates from each cell line were isolated and assayed for total cellular PAR levels by Western blot.

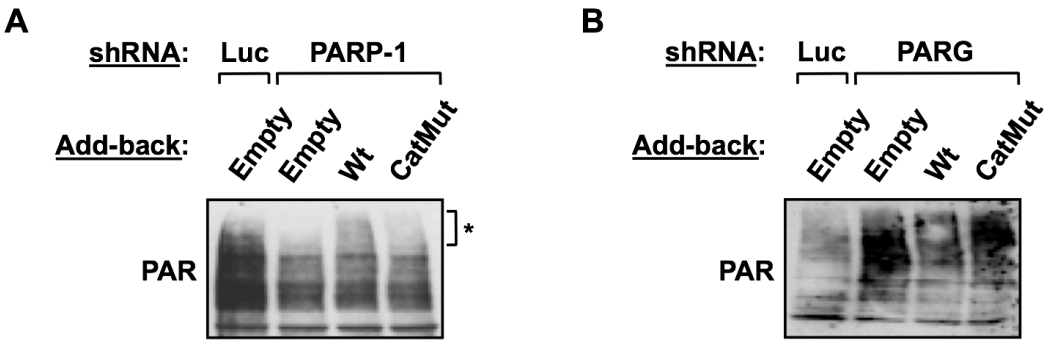
A
shRNA:
Luc
PARP-1
Add-back:
Empty
Empty
Wt
CatMut
PAR
*
B
shRNA:
Luc
PARG
Add-back:
Empty
Empty
Wt
CatMut
PAR

Figure 2.13. Catalytically inactive mutants of PARP-1 and PARG support the wild-type expression patterns of some, but not all, target genes. RNAi-resistant wild-type (Wt) or catalytically inactive (CatMut) PARP-1 and PARG were stably expressed in their respective MCF-7 knockdown cells using retrovirus-mediated gene transfer, as shown in Figure 2.11. Total RNA was isolated from the cells, reverse transcribed, and subjected to qPCR using gene-specific primers. Each bar represents the mean + SEM (*error bars*) from three or more independent determinations. Bars that do not share at least one lower case letter marking (a, b, or c) within each graph are statistically different, as determined by analysis of variance (ANOVA) with a p-value threshold of < 0.05. *A,* Re-expression of PARP-1 after PARP-1 knockdown restores the wild-type expression pattern of some PARP-1 target genes. *B,* Re-expression of PARG after PARG knockdown restores the wild-type expression pattern of some PARG target genes.

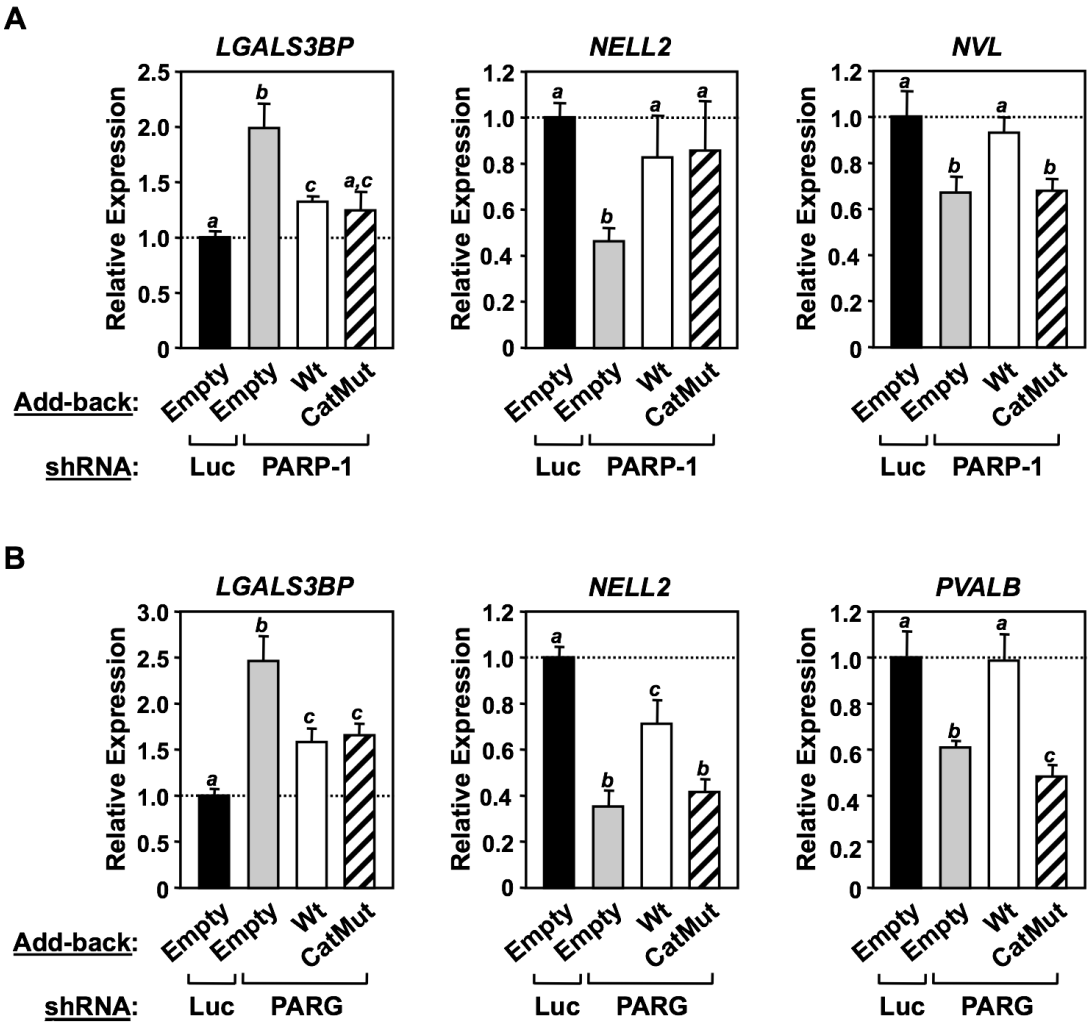
A
LGALS3BP
NELL2
NVL
Relative Expression
Add-back:
Empty
Empty
Wt
CatMut
shRNA:
Luc
PARP-1
B
LGALS3BP
NELL2
PVALB
Relative Expression
Add-back:
Empty
Empty
Wt
CatMut
shRNA:
Luc
PARG

Figure 2.14. Treatment with PARP-1 or PARG chemical inhibitors, PJ34 or Gallotannin (GT), independently confirms that some genes do not require PARP-1 or PARG enzymatic activity for proper gene expression. *A,* PJ34 and GT inhibit and enhance the autoPARylation of PARP-1, respectively, without altering total PARP-1 or PARG levels. Parental MCF-7 cells were seeded and grown to ~80% confluence and subsequently treated with PJ34 (1 μM) or GT (100 μM) for 6 hrs immediately prior to collection of the cells. *(Left)* Whole cell extracts were monitored for PARP-1 and PARG by Western blotting under the treatment conditions noted. U, Untreated; PJ, PJ34-treated; GT, gallotannin-treated. *(Right)* PARP-1 was immunoprecipitated from whole cell extracts *(bottom)* and analyzed for autoPARylation by Western blotting under the treatment conditions noted using a PAR-specific antibody *(top-bracket)*. Oligo(ADP-ribosyl)ated PARP-1 and poly(ADP-ribosyl)ated are indicated. *B and C,* Total RNA was isolated from PJ34- or GT-treated cells, reverse transcribed, and subjected to qPCR using gene-specific primers. Each bar represents the mean + SEM (*error bars*) from three or more independent determinations. Bars that do not share at least one lower case letter marking (a, b, c, or d) with each graph are statistically different, as determined by analysis of variance (ANOVA) with a p-value threshold of < 0.05. *B*, PJ34 has no effect on LGALS3BP or NELL2 gene expression, independently confirming that PARP-1 enzymatic activity is not required to regulate these genes. The knockdown/add-back data is shown for comparison. *C,* GT has no effect on LGALS3BP gene expression, independently confirming that PARG enzymatic activity is not required to regulate this gene. The effect of GT on NELL2 is shown as a control. The knockdown/add-back data is shown for comparison.

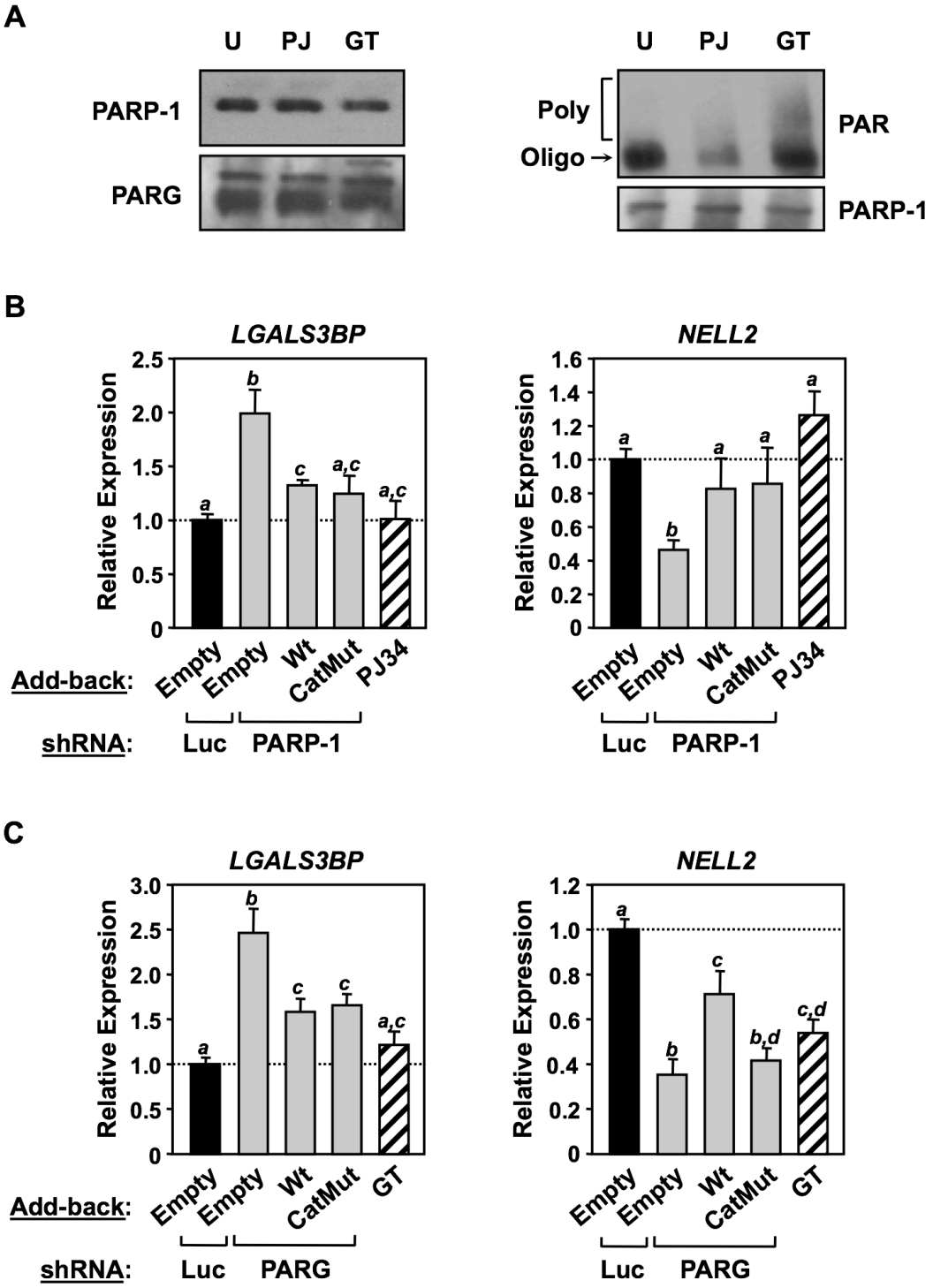
A
U
PJ
GT
PARP-1
PARG
Poly
Oligo
PAR
PARP-1
B
LGALS3BP
NELL2
Relative Expression
Add-back:
Empty
Empty
Wt
CatMut
PJ34
shRNA:
Luc
PARP-1
C
LGALS3BP
NELL2
Relative Expression
Add-back:
Empty
Empty
Wt
CatMut
GT
shRNA:
Luc
PARG

(Ju et al., 2006; Ju et al., 2004; Krishnakumar et al., 2008; Pavri et al., 2005). Furthermore, the levels of chromatin-bound PARG at a given promoter generally correlate with the levels of PARP-1, at least across the subset of promoters tested herein. Finally, PARP-1 and PARG enzymatic activities are required for the regulation of some, but not all, target genes (Figure 2.13).

In a simple model of gene regulation, PARG opposes the actions of PARP-1 by degrading the PAR chains synthesized by PARP-1. With respect to the expression analyses presented herein, this model fails in at least two ways. First, PARP-1 and PARG enzymatic activities are required for the regulation of a subset of target genes (Figure 2.13). Second, as noted above, gene regulation by PARP-1 and PARG generally occurs in the same direction and with the same magnitude. Thus, our results point to concerted, rather than opposing, actions of PARP-1 and PARG in gene regulation. Interestingly, PARP-1 and PARG animal models demonstrate similarities in the biological endpoints analyzed (Cortes et al., 2004; Fisher et al., 2007; Kim et al., 2005; Koh et al., 2004; St-Laurent et al., 2007; Tulin et al., 2003; Tulin et al., 2005; Tulin and Spradling, 2003; Tulin et al., 2002; Wang et al., 1995; Wang et al., 1997). Although they have not yet been explored with respect to gene expression, perhaps the concerted actions of PARP-1 and PARG revealed by our gene expression analyses can provide an explanation to these biological phenomena.

Gene ontology analyses reveal common functions for PARP-1- and PARG-regulated genes. Both PARP-1- and PARG-regulated genes are enriched in cell structure and metabolism functions (e.g., *ITPR1* for PARP-1, *SOCS2* and *MTR* for PARG), with the common genes enriched in stress response and metabolism functions (e.g. *LGALS3BP*) (Table 2.4). These results are consistent with (i) the stress- and metabolic-related phenotypes of PARP-1 and PARG knockout animals (mice, flies,

and worms) or cells from knockout mice grown in culture (Conde et al., 2001; Cortes et al., 2004; Gao et al., 2007; Hanai et al., 2004; Koh et al., 2004; Mabley et al., 2001; Morrison et al., 1997; Oliver et al., 1999; St-Laurent et al., 2007; Tong et al., 2001; Tulin and Spradling, 2003; Tulin et al., 2002; Wang et al., 1995; Wang et al., 1997; Yu et al., 2002; Zong et al., 2004) and (ii) previous gene ontology analyses from microarray expression experiments examining PARP-1-dependent gene regulation. With respect to the latter, PARP-1-regulated genes in mouse embryonic fibroblasts were found to be enriched in functions related to apoptosis, cell cycle control, DNA synthesis/repair, stress and immune responses, chromosomal integrity, and protein processing (Simbulan-Rosenthal et al., 2000; Simbulan-Rosenthal et al., 1999; Zingarelli et al., 2003). Likewise, PARP-1-regulated genes from mouse embryonic stem cells and livers were found to be enriched in functions related to metabolism, signal transduction, cell cycle control, and transcription. (Ogino et al., 2007).

The known functions of the *ITPR1*, *SOCS2*, *MTR*, and *LGALS3BP* gene products fit with the roles of PARP-1 and PARG in cellular physiology. *ITPR1* encodes the type 1 inositol 1,4,5-trisphosphate receptor (Yamada et al., 1994), which plays a critical role in Ca^{2+} signaling in neuronal, immune, and other cell types (deSouza et al., 2007; Inoue et al., 1998). *SOCS2* encodes a cytokine-inducible SH2 protein that functions as a suppressor of cytokine signaling 2 and plays a role in insulin signaling pathways (Dey et al., 1998; Minamoto et al., 1997). *MTR* encodes 5-methyltetrahydrofolate-homocysteine methyltransferase (a.k.a. methionine synthase), an enzyme that catalyzes the remethylation of homocysteine to methionine (Leclerc et al., 1996; Li et al., 1996). Impaired methionine synthase activity leads to elevated levels of plasma homocysteine, which is a risk factor in both birth defects and vascular disease (Watkins and Rosenblatt, 1989). *LGALS3BP* encodes lectin galactoside-binding soluble 3-binding protein (a.k.a. Mac-2-binding protein and tumor-associated

antigen 90K) (Koths et al., 1993), a protein that promotes integrin-mediated cell adhesion and is found in increased levels under pathophysological conditions (e.g., cancer and viral infections) (Tinari et al., 2001). Collectively, our studies indicate a clear role for PARP-1- and PARG-regulated genes in metabolism, stress, DNA repair, and signaling functions, findings corroborated by other studies.

How might PARP-1 and PARG act in concert to regulate gene expression? The specific mechanisms of PARP-1- and PARG-dependent gene regulation are likely to differ depending on the requirement for PARP-1 and PARG catalytic activity at a particular gene. Previous studies have used chemical inhibitors and mutants to explore the roles of PARP-1 and PARG catalytic activities in the regulation of gene expression (Kim et al., 2005; Kraus and Lis, 2003). In some gene-specific studies, PARP-1 enzymatic activity was required for its gene regulatory functions (Butler and Ordahl, 1999; Ju et al., 2006; Ju et al., 2004; Kim et al., 2004; Miyamoto et al., 1999; Nirodi et al., 2001; Tulin and Spradling, 2003), while in others it was not (Anderson et al., 2000; Cervellera and Sala, 2000; Hassa et al., 2001; Meisterernst et al., 1997; Pavri et al., 2005). The results for PARG have also been variable (Kim et al., 2004; Rapizzi et al., 2004; Tulin et al., 2005). These results suggest gene-specific (and perhaps cell type-specific) requirements for the PARP-1 and PARG catalytic activities, a result supported by our observations described herein.

For genes requiring PAR metabolism, the goal of the combined PARP-1 and PARG enzymatic activities may be the production of ADPR, rather than the addition and removal of PAR per se. ADPR may function as a signaling molecule in the nucleus by binding as a small molecule ligand to the macro domain of the histone variant macroH2A1.1 (Karras et al., 2005; Kustatscher et al., 2005), which may act to regulate gene expression in a chromatin-dependent manner. For genes that do not

require PAR metabolism, PARP-1 and PARG may function as classical coregulators, as has been described previously for PARP-1 (Hassa and Hottiger, 1999; Hassa and Hottiger, 2002; Ju et al., 2006; Ju et al., 2004; Pavri et al., 2005). Whether they act within common coregulatory complexes is unknown, although a physical interaction between PARP-1 and PARG has been reported in vitro and in vivo, under certain cellular conditions (Keil et al., 2006). Interestingly, PARP-1 and PARG localize to a similar set of target gene promoters at proportional levels (i.e., higher levels of PARG correspond to higher levels of PARP-1; Figures 2.8 and 2.9). In addition, PARP-1 and PARG facilitate each other's binding to certain promoters (Figure 2.10), which is consistent with the presence of both factors in the same complex. However, we also observe independent binding of PARP-1 and PARG to some promoters, suggesting that these factors are also able to function distinctly in some cases. Unlike PARP-1, PARG does not have a DNA binding domain. Thus, when it binds to chromatin independently of PARP-1, it must do so by binding to histones or through interactions with other DNA- or chromatin-binding proteins.

Our results demonstrating non-enzymatic functions for PARP-1 and PARG suggest that they may also function as scaffolding proteins. Indeed, PARP-1 has been shown to participate as a component of promoter-bound coregulatory complexes, perhaps serving as a protein scaffold or "exchange factor" within those complexes (Hassa and Hottiger, 2002; Kraus, 2008; Pavri et al., 2005). Such a scaffolding role has not yet been described for PARG. Furthermore, PARP-1 and PARG may be subject to post-translational modifications that modulate their gene regulatory actions. For example, PARP-1 is known to be phosphorylated by various cellular kinases that can, in some cases, enhance its DNA-binding or catalytic activity (Gagne et al., 2008; Kauppinen et al., 2006; Mathieu et al., 2008).

The regulation of chromatin structure may also be a common component of PARP-1- and PARG-dependent gene expression outcomes (Kraus, 2008). We have shown previously that PARP-1 can bind specifically to nucleosomes and modulate chromatin structure in the absence of NAD^+ (Kim et al., 2004; Wacker et al., 2007b), although the release of PARP-1 from the nucleosomes, requires its enzymatic activity (Kim et al., 2004; Wacker et al., 2007b). The binding of PARP-1 and PARG at promoters can also affect the binding of other factors. For example, PARP-1 can regulate the binding of the linker histone H1 at target gene promoters. Specifically, we showed that RNAi-mediated knockdown of PARP-1 increases the levels of H1 at the *ITPR1*, *NAT1*, *NELL2*, *PVALB*, and *SOCS2* promoters concomitant with reduced expression of the genes ((Krishnakumar et al., 2008); R.K. and W.L.K., unpublished). Given the inhibitory effect of H1 on transcription, the increase in H1 upon the knockdown of PARP-1 is likely to be accompanied by the formation of less accessible and more repressive chromatin structures. These actions of PARP-1 are consistent with previous biochemical assays, suggesting a role for both PARP-1 and PARG in the regulation of chromatin structure and transcription (Kim et al., 2004).

2.5. Experimental Procedures

Antibodies - The custom rabbit polyclonal antibodies against PARP-1 and PARG used for Western blotting and ChIP assays were generated by using a purified fragment of human PARP-1 (amino-terminal, PARP-N (Kim et al., 2004)) and full-length rat PARG as antigens (Pocono Rabbit Farm and Laboratory, Inc.). The antibodies were screened for: (i) specificity by Western blotting MCF-7 cell extracts, (ii) the ability to immunoprecipitate their cognate antigens from formaldehyde crosslinked chromatin

samples by a ChIP-Western protocol (Kim et al., 2004) (Figure 2.7), and (iii) a reduction in Western blot signal upon knockdown of PARP-1 or PARG (see Figure 2.1). The custom rabbit polyclonal antibody against SIRT1 used for Western blotting was generated by using full-length mouse SIRT1 as an antigen (Zhang et al., 2009). The mouse monoclonal PAR antibody was purchased from Trevigen (4335-AMC-050). The mouse monoclonal FLAG antibody was purchased from Sigma (F3165).

Chemical inhibitors - PJ34 was purchased from Alexis Biochemicals. Gallotannin ("GT"; a.k.a. common tannic acid) was purchased from Sigma Chemical Co. Both inhibitors were dissolved in distilled water, pH-adjusted to approximately 7.5, and added to the cell culture medium for six hours at 1 μM.

Oligonucleotides - The oligonucleotide sequences listed below were used for the shRNA constructs and site-directed mutagenesis. Those sequences denoted with an asterisk (*) were chosen based on priority score described at the website.

shRNA constructs -

Target	Sequence	Source
Luc	5’ - gatatgggctgaatacaaa - 3’	(Reynolds et al., 2004)
hPARP-1 #1	5’ - gggcaagcacagtgtcaaa - 3’	(Ju et al., 2004; Shah et al., 2005)
hPARP-1 #2*	5’ - acacctctctactatataa - 3’	Dharmacon siDESIGN® Center
hPARG #1*	5’ - caataccactcctgaaaca - 3’	Dharmacon siDESIGN® Center
hPARG #2*	5’ - agagaccgctgaccattca - 3’	Dharmacon siDESIGN® Center

Site-directed mutagenesis -

• Primers for site-directed mutagenesis to generate an RNAi-resistant hPARP-1 cDNA:

1. Recognition site #1 (Wt and CatMut)

5’ - caggttacccaagggcaaacatagcgttaaaggtttgggcaaaac - 3’ and

5’ - gttttgcccaaacctttaacgctatgtttgcccttgggtaacctg - 3’

Specific changes relative to the first nucleotide of the first codon:

g2835a, c2838t, t2841c, c2844t

2. Recognition site #2 (Wt)

5’ - ctggtgtgaatgacacgtcgctgctgtataacgagtacattgtc - 3’ and

5’ - gacaatgtactcgttatacagcagcgacgtgtcattcacaccag - 3’

Specific changes relative to the first nucleotide of the first codon:

c2946g, t2949g, a2952g, a2955g

3. Recognition site #2 (CatMut)

5’ - ctggtgtgaatgacacgtcgctgctgtataacaagtacattgtc - 3’ and

5’ - gacaatgtacttgttatacagcagcgacgtgtcattcacaccag - 3’

Specific changes relative to the first nucleotide of the first codon:

c2946g, t2949g, a2952g, a2955g

• Primers for site-directed mutagenesis to generate an RNAi-resistant rPARG cDNA:

1. Recognition site #1 (Wt and CatMut)

5’ - tttgcacccagccaataccgcttctcaagcagaagatgaacc - 3’ and

5’ - ggttcatcttctgcttgagaagcggtattggctgggtgcaaa - 3’

Specific changes relative to the first nucleotide of the first codon:

a1827g, g1833c, a1836g

2. Recognition site #2 (Wt and CatMut) - Not altered

Differences between the human-based PARG shRNA#2 sequence and the rat PARG cDNA abrogated the need to alter the #2 recognition site

PARP-1 and PARG knockdown and expression constructs **-** Short hairpin RNA (shRNA) expression constructs for retroviral-mediated knockdown of PARP-1 and PARG were made using the pSUPER.retro vector (OligoEngine). Double stranded oligonucleotides containing shRNA sequences targeting either luciferase (Luc control), PARP-1, or PARG were cloned into the vector (puromycin or neomycin resistant) using BglII and XhoI restriction sites as described by the manufacturer. The shRNA sequences (one for Luc, two for PARP-1, and two for PARG; listed above) were based on sequences reported in the literature (Ju et al., 2004; Shah et al., 2005) or designed using the Dharmacon siDESIGN® Center software (www.dharmacon.com). All constructs were confirmed by sequencing.

Wild-type and catalytically inactive point mutants of human PARP-1 and rat PARG were used in the studies described herein. The catalytically inactive human PARP-1 contained a change at Glu 988 to Lys (E988K) (Marsischky et al., 1995; Rolli et al., 1997), whereas the catalytically inactive rat PARG contained changes at Tyr 788 and 791 to Phe and Ala, respectively (Y788F/Y791A) (Shimokawa et al., 1999). CMV-based mammalian expression constructs for full-length wild-type or catalytically inactive human PARP-1 (with a carboxyl-terminal 6xHis/FLAG tag) or rat PARG (with a carboxyl-terminal FLAG tag) were generated by PCR-based cloning of the tagged cDNAs into pCMV5. The pCMV5-hPARP-1-His/FLAG and pCMV5-rPARG-FLAG vectors were then used as templates to generate cDNAs resistant to the

shRNAs noted above by site-directed mutagenesis (QuikChange® Site-Directed Mutagenesis Kit from Stratagene). The following nucleotides relative to the first nucleotide of the first codon were changed in the hPARP-1 cDNA: g2835a, c2838t, t2841c, c2844t (for shRNA#1) and c2946g, t2949g, a2952g, a2955g (for shRNA#2). The following nucleotides were changed in the rPARG cDNA: a1827g, g1833c, a1836g (for shRNA#1); note that differences between the human-based PARG shRNA#2 sequence and the rat PARG cDNA eliminated the need to alter the #2 recognition site). Positive clones were identified by sequencing and then cloned into the pQCXIH retroviral expression vector (BD Biosciences; hygromycin resistant) using NotI and BamHI restriction sites.

Generation and culture of MCF-7-derived cell lines - Parental MCF-7 human breast cancer cells, kindly provided by Dr. Benita Katzenellenbogen, were maintained in MEM Eagle medium containing Hanks' salts, L-glutamine, and non-essential amino acids (Sigma) supplemented with 5% bovine calf serum (CS; Sigma), 20 mM HEPES (pH 7.6), 100 units/mL penicillin, 100 μg/mL streptomycin, 25 μg/mL gentamycin, and 0.22 % sodium bicarbonate. The shRNA knockdown ("knockdown") and shRNA knockdown + shRNA-resistant re-expression ("knockdown/add-back") cell lines used in these studies were generated by sequential retroviral infections of parental MCF-7 cells with the appropriate shRNA and cDNA expression vectors (see below). In each case, the final cell line constructions were populations of individual transformants, not clonal lines. A minimum of two independently generated populations were made and tested for each cell line. The Luc, PARP-1, and PARG knockdown cells express two distinct shRNA sequences targeting the intended factor. These same shRNA sequences were tested individually in gene-specific expression studies (Figure 2.6).

Retroviruses were generated by transfection of the pSUPER.retro or pQCXIH vectors described above with an expression vector for the VSV-G envelope protein into Phoenix Ampho cells using GeneJuice transfection reagent (Novagen) according to the manufacturer's protocol. The resulting viruses were collected, filtered through a 0.45 μm syringe filter to remove any remaining cells, and used to infect the parental MCF-7 cells. Stably transduced cells were isolated under appropriate selection with puromycin (Sigma; 0.5 μg/mL), G418 sulfate (Gibco/BRL; 800 μg/mL), or hygromycin (Cellgro; 200 μg/mL), expanded, and frozen in aliquots for future use. The cells were grown under subconfluent conditions for experimental procedures.

For experiments, cells from the various lines were plated in MEM modified Eagle medium with Earle's salts and non-essential amino acids, without phenol red (Sigma), supplemented 5% charcoal/dextran-treated bovine calf serum (CDCS; Sigma) and the other additives noted above. Subconfluent populations of cells were collected for analysis between 3 and 4 days post-plating.

Cell proliferation analyses - For analysis of cell proliferation, stable Luc, PARP-1, and PARG knockdown cells were seeded at ~2 x 10^4 cells per well in 6-well plates in MEM containing 5% CDCS and the additives noted above. Every two days during an 8-day time course, the cells were collected by trypsinization and counted using a hemacytometer. All experiments were conducted a minimum of three times to ensure reproducibility. Analysis of variance (ANOVA) with a p-value threshold of < 0.05 was used to determine the significance of differences between samples.

Cell cycle analyses - For FACS analysis, stable Luc, PARP-1, and PARG knockdown cells were seeded at ~5 x 10^5 cells per 6 cm diameter dish in MEM containing 5% CDCS and the additives noted above. After three days (at ~50 to 60% confluence),

the cells were collected by trypsinization, washed twice with ice-cold PBS, and fixed with 70% ethanol for at least 1 hour at 4°C. The cells were then washed again with ice-cold PBS and stained with a propidium iodide solution (40 μg/mL propidium iodide, 0.1% Triton X-100, 200 μg/mL RNase A). The samples were incubated at 37°C for 30 minutes and analyzed by flow cytometry at Cornell University's Biomedical Sciences Flow Cytometry Laboratory. Briefly, DNA content was measured with a BD Biosciences LSRII (San Jose, CA). Propidium iodide was excited with a 488nm laser and emission collected through a 576/26BP filter. Gating and analysis were done using the BD Biosciences FACSDiVa software. All experiments were conducted a minimum of three times to ensure reproducibility. Analysis of variance (ANOVA) with a p-value threshold of < 0.05 was used to determine the significance of differences between samples.

PAR and NAD^+ Measurements **-** Stable Luc, PARP-1, and PARG knockdown cells were seeded at ~6 x 10^5 cells per 15 cm plate and grown for at least 3 days in MEM containing 5% CDCS and the additives noted above. After three days (at ~60 to 80% confluence), the cells were collected by trypsinization, washed with ice-cold PBS, and frozen in liquid nitrogen. The levels of PAR were determined by Western blotting of whole cell or nuclear extracts prepared in the presence of gallotannin to prevent degradation of the PAR polymers by PARG. The signals were quantified by densitometry using ImageQuant software (Molecular Dynamics). The concentration of NAD^+ in whole cell extracts for each cell line was determined by using a quantitative HPLC/mass spectrometry method (HPLC/MALDI/MS) with ^{18}O Standards (Yang et al., 2007; Yang and Sauve, 2006).

Expression microarrays - Stable Luc, PARP-1, and PARG knockdown cells were seeded at ~8 x 10^5 cells per 10 cm diameter dish and grown for at least 3 days in MEM containing 5% CDCS and the additives noted above. Three independently-generated populations of cells were used for these experiments. The cells were collected and total RNA was isolated using Trizol Reagent (Invitrogen) followed by an RNeasy column (Qiagen) according to the manufacturers' protocols. The RNA quality was assessed using an Agilent Bioanalyzer 2100, and suitable RNA was analyzed for global patterns of gene expression at Cornell University's Microarray Core Facility. Briefly, 7 mg of total RNA was labeled using Affymetrix's standard one-cycle amplification and labeling protocol. The labeled cRNA was then hybridized to Affymetrix Human U133A 2.0 GeneChips, which were scanned using a GeneChip Scanner 3000. The raw array data was processed by Affymetrix GeneChip Operating Software (GCOS) to obtain detection calls and signal values. The signals were normalized by scaling to a target value of 500 using GCOS. To adjust for batch effects due to day-to-day differences in RNA isolations, the empirical Bayes method was applied to the data set (Johnson et al., 2007). After adjusting any values less than 0.01 to 0.01, the data was $\log_2$ transformed, median centered for each array, and median centered for each individual probe set. The criteria for a gene to be considered regulated by PARP-1 or PARG was: (i) detection call flagged as present or marginal in 2 out of 3 array replicates for both control and factor knockdown cell lines and (ii) significance of values between control and knockdown cell lines for any given gene had a two-tailed Student's t-test with a p-value < 0.05 (see Figure 2.3A, Union). To determine the genes most robustly regulated by PARP-1 or PARG, we added a fold change criterion between 0.5 and -0.5 compared to the Luc control knockdown cells (the final gene lists can be found in Tables 2.1, 2.2, and 2.3. The heatmaps used to

visualize the microarray expression data (Figures 2.3B and 2.4B) were generated using Java Treeview (http://www. jtreeview.sourceforge.net/) (Saldanha, 2004).

Gene ontology analyses - Gene ontology (GO) analyses of the microarray expression data were performed using the Database for Annotation, Visualization and Integrated Discovery (DAVID) Bioinformatics Database Resource website for gene ontology analysis (http://david. abcc.ncifcrf.gov/) (Dennis et al., 2003). PARP-1- and PARG-regulated gene lists (consisting of 204 and 217 genes, respectively; see Figure 2.5A and 2.5B) were generated according to the present call, p-value, and fold change criteria as noted above. The commonly regulated gene list (50 genes) represents the overlap between the PARP-1- and PARG-regulated gene lists. Affymetrix gene ID numbers for each list were entered into DAVID website for gene ontology analysis. Resulting terms were grouped together under each category and duplicate probe sets were removed. Only those GO terms yielding a p-value < 0.05 using a Fisher exact test were considered significantly enriched in each gene list.

mRNA expression analyses by RT-qPCR - For gene-specific mRNA expression analyses, "knockdown" or "knockdown/ add-back" MCF-7 cells were grown under standard conditions (see above). For experiments, the cells were seeded at ~1.5 x 10^5 cells per well in 6-well plates and grown for 3 days in MEM containing 5% CDCS and the additives noted above. Total RNA was isolated using Trizol Reagent (Invitrogen), reverse transcribed, and subjected to real-time quantitative PCR using gene specific primers. All target gene transcripts were normalized to the β-actin transcript, which was unaffected by PARP-1 or PARG knockdown (data not shown). All experiments were conducted a minimum of three times with independent RNA isolations.

Chromatin immunoprecipitation assays **-** Parental or knockdown MCF-7 cells were seeded at ~6 x 10^5 cells per 15 cm plate and grown for at least 3 days in MEM containing 5% CDCS and the additives noted above. The cells were crosslinked with 1% formaldehyde in PBS at 37°C for 10 min immediately prior to harvesting. ChIP assays were performed as described previously (Kininis et al., 2007; Krishnakumar et al., 2008) using polyclonal antibodies against PARP-1 and PARG (see above), as well as "no antibody" controls. The "no antibody" signals from the ChIP assays are comparable to pre-immune sera in both ChIP-Western and ChIP-qPCR assays (data not shown). The resulting ChIP DNA material was used in gene-specific qPCR analyses (see below for description and primer sequences). For ChIP-Western analysis (FIgure 2.7), a small aliquot was removed from the input and ChIP samples prior to reversing the crosslinks for conventional Western blotting.

Quantitative PCR analyses (RT-qPCR and ChIP-qPCR) **-** Gene-specific mRNA expression and ChIP analyses were analyzed by quantitative PCR in a similar manner. Briefly, reactions containing DNA from either source, 1x SYBR Green PCR master mix, and forward and reverse primers (500 nM) were used in 40-45 cycles of amplification (95°C for 15 sec, 60°C for 1 min) using an MJ Research DNA Engine Opticon 2 (96-well) or an Applied Biosystems 7900 HT Sequence Detection System (384-well) following an initial 10 min incubation at 95°C. Melting curve analysis was performed to ensure that only the targeted amplicon was amplified.

Verification of PARP-1 and PARG inhibitor activity **-** To verify the inhibitory activities of PJ34 and GT, we monitored autoPARylation of PARP-1 by using an immunoprecipitation-Western blotting protocol. Briefly, parental MCF-7 cells were seeded at ~4 x 10^5 cells per 10 cm diameter plate and grown for at least 3 days in

MEM containing 5% CDCS and the additives noted above. At ~80% confluence, the cells were treated with PJ34 (1 μM) or GT (100 μM) for 6 hrs immediately prior to collection of the cells for analysis. The cells were then rinsed with ice-cold PBS, collected into ice-cold PBS (containing PJ34 or GT where appropriate), and pelleted by centrifugation. The cell pellets were resuspended in 300 mL of lysis buffer [25 mM Tris•HCl (pH 7.5), 150 mM NaCl, 10% glycerol, 0.1 mM EDTA, 0.1% NP-40, 1 mM DTT, and a protease inhibitor cocktail (Roche Molecular Biochemicals)]. The samples were mixed at 4°C for 30 minutes and centrifuged at 12,000 rpm for 20 min at 4°C in a microcentrifuge. The resulting supernatants were used for immunoprecipitation of PARP-1, which was performed for 2 hrs at 4°C using the PARP-1 polyclonal antibody described in the main text. Immune complexes were collected by the addition of 40 μL of a 50% protein A-agarose slurry with an additional 2 hr incubation at 4°C. The agarose beads were washed three times for 5 min each in wash buffer [25 mM Tris•HCl (pH 7.5), 300 mM NaCl, 10% glycerol, 0.1 mM EDTA, 0.1% NP-40, and 1 mM DTT]. Bound proteins were eluted by boiling in SDS loading solution and analyzed by Western blotting for PARP-1 and PAR.

Effect of PARP-1 and PARG inhibition on gene expression - Parental MCF-7 cells were treated with PJ34 (1 μM) or GT (100 μM) for 6 hrs immediately prior to collection of the cells for analysis. The cells were seeded at ~1.5 x 10^5 cells per well in 6-well plates and grown for 3 days in MEM containing 5% CDCS and the additives noted in the main text. Total RNA was isolated using Trizol Reagent (Invitrogen), reverse transcribed, and subjected to real-time quantitative PCR using gene specific primers. All target gene transcripts were normalized to the β-actin transcript. All experiments were conducted a minimum of three times with independent RNA

isolations to ensure reproducibility. Analysis of variance (ANOVA) with a p-value threshold of < 0.05 was used to determine significant differences between samples.

Statistical analyses - For the NAD^+ measurements in Figure 2.1, the ChIP-qPCR assays in Figures 2.8, 2.9, and 2.10, and the RT-qPCR assays in Figures 2.1B and 2.5C, a paired Students' t-test with a p-value threshold of < 0.05 was used to determine the significance of differences between the control and experimental samples. For the gene-specific expression analyses in Figures 2.13 and 2.14, analysis of variance (ANOVA) with a p-value threshold of < 0.05 was used to determine the significance of differences between samples.

Primer Sequences – The primer sequences listed below were used for the RT-qPCR and ChIP-qPCR amplification reactions.

RT-qPCR -

Gene Name	**Primer Sequence**
β-ACTIN Fwd	5'-AGCTACGAGCTGCCTGAC-3'
β-ACTIN Rvs	5'-AAGGTAGTTTCGTGGATGC-3'
DNAJC12 Fwd	5'-GAATGTCACCCAGACAAGC-3'
DNAJC12 Rvs	5'-GAATGGCATCGACATCTG-3'
GAPDH Fwd	5'-CCCAACCACCTGCTGCTTTAACCTG-3'
GAPDH Rvs	5'-TGGCTTTGGAGTTGGAGATTTTTGG-3'
GDF15 Fwd	5'-CTACAATCCCATGGTGCTCA-3'
GDF15 Rvs	5'-TATGCAGTGGCAGTCTTTGG-3'
ITPR1 Fwd	5'- TGCCTCCACAATTCTACG-3'
ITPR1 Rvs	5'- TGAATGTCCCACAGTTGC-3'

LGALS3BP Fwd	5’-AATGTCACCATGAGTGTGG-3’
LGALS3BP Rvs	5’-ACTGACGACAGGGTGATG-3’
MTR Fwd	5’-ACAACAGCCTATGTCCTCTG-3’
MTR Rvs	5’-CCATCATAGAAGGCGTTTC-3’
NAT1 Fwd	5’-CTTCACCCTCACCCATAGGA-3’
NAT1 Rvs	5’-TTTGGGCACAAGCTTTCTCT-3’
NELL2 Fwd	5’-TGAAGGGAACCACCTACC-3’
NELL2 Rvs	5’-ATTTGCCATCCACATACG-3’
NFAT5 Fwd	5’-ACCTCTTCCAGCCCTACCAT-3’
NFAT5 Rvs	5’-CCTCTTCGGTGTTGATGGAT-3’
NVL Fwd	5’-ACGAAGAATTGTAGCCCAAC-3’
NVL Rvs	5’-CGAGTCTGGTCGATTAGTAGC-3’
PARP-1 Fwd	5’-GTGTGGGAAGACCAAAGGAA-3’
PARP-1 Rvs	5’-TTCAAGAGCTCCCATGTTCA-3’
PARG Fwd	5’-GACGCAATCTCTTCCACACA-3’
PARG Rvs	5’-TGAGTCAGGATGGAGGGAGT-3’
PFDN1 Fwd	5’-TGCCTTCTCCCATACATTCC-3’
PFDN1 Rvs	5’-CAGGATTATGGCGTCCATCT-3’
PHF3 Fwd	5’- AATTCCACACCCTCTTGTG-3’
PHF3 Rvs	5’- TGCTGTCGCTTCAGTTTC-3’
PLA2G2A Fwd	5’- GATCCAGGGAGCATTCAC-3’
PLA2G2A Rvs	5’- TGTTTGTTCTGCACTCCTG-3’
PVALB Fwd	5’-CTGAACGCTGAGGACATC-3’
PVALB Rvs	5’-TTCACATCATCCGCACTC-3’
RAPGEF4 Fwd	5’-ATGGAAACGGGCTCTAAC-3’
RAPGEF4 Rvs	5’-AGCAGGACGAAGAGGAAC-3’

SEMA4G Fwd	5’-TGGGGGTCTTGTTAGTCTGG-3’
SEMA4G Rvs	5’-GTGAGGATGCTGAGGAGGAG-3’
SOCS2 Fwd	5’-ACACGTCAGCACCATCTCTG-3’
SOCS2 Rvs	5’-TGGCACCGGTACATTTGTTA-3’
TMOD3 Fwd	5’-GGAAGTAGTAATGGTGTTGACC-3’
TMOD3 Rvs	5’-GCTCATCAAATACCGGAAG-3’

ChIP-qPCR -

Gene Name	**Primer Sequence**
DNAJC12 promoter Fwd	5’-GCTATGTGGAACATGCTGCT-3’
DNAJC12 promoter Rvs	5’-GTCCTTCTTCCCTCGGAAAC-3’
GDF15 -500 Fwd	5’-ACACATCAAGGTTGCCCTTC-3’
GDF15 -500 Rvs	5’-TGGTGAAAAACAAAGGAAGCA-3’
GDF15 0 Fwd (promoter)	5’-CTCAGATGCTCCTGGTGTTG-3’
GDF15 0 Rvs (promoter)	5’-CTCGGAATCTGGAGTCTTCG-3’
GDF15 1500 Fwd	5’-TTTGACTGCCAGAAGAAAAGC-3’
GDF15 1500 Rvs	5’-AGGCAGCCTGAGATTCCAAC-3’
ITPR1 promoter Fwd	5’-ACTGAGGTCGCGGTTTGTAT-3’
ITPR1 promoter Rvs	5’-AAGGAGCCGTGTTGTGACTT-3’
LGALS3BP -500 Fwd (promoter)	5’-GGGCACCCCTCTCTCTACAC-3’
LGALS3BP -500 Rvs (promoter)	5’-TGATTGTTGCTGGACTCAGG-3’
LGALS3BP 0 Fwd	5’-GGGGCATTTCAGAGATGAGA-3’
LGALS3BP 0 Rvs	5’-GTTTGGGGTAGAGGCACAAA-3’
LGALS3BP 500 Fwd	5’-ACAGAAACCCCAGCATCATC-3’
LGALS3BP 500 Rvs	5’-CTCTGCACTCCTGTCCTTCC-3’
LGALS3BP 1000 Fwd	5’- CTCAGTGAGGCAATCAGCAG-3’

LGALS3BP 1000 Rvs	5’-CAAGGCTCATCCAGAACCAT-3’
LGALS3BP 1500 Fwd	5’-TCCACCCTCTCTGTGCTCTT-3’
LGALS3BP 1500 Rvs	5’-GACAGTGCCATGCAACCTT-3’
LGALS3BP 2000 Fwd	5’-GACTGGTCCTTTGACCCAGA-3’
LGALS3BP 2000 Rvs	5’-CCAATCCCGGAAGACATCTA-3’
NAT1 promoter Fwd	5’-CCGGCTGAAATAACCTGGTA-3’
NAT1 promoter Rvs	5’-TATGTGCCAGCCACACTTTC-3’
NELL2 promoter Fwd	5’-TCCCCGGAGGAGCAGTCT-3’
NELL2 promoter Rvs	5’-CGCCCGAACCTGTTGTAAAG-3’
NVL promoter Fwd	5’-TGCAACCAAACGGATCAATA-3’
NVL promoter Rvs	5’-TGAATTAAGTATTAGATTTCCCACTCA-3’
PVALB -1000 Fwd (promoter)	5’-GCTCCCCTATCTGCACACTC-3’
PVALB -1000 Rvs (promoter)	5’-CAAAGGCTGTTTGGAAGCTC-3’
PVALB 0 Fwd	5’-CTGCTGCATCCCTCTATCCT-3’
PVALB 0 Rvs	5’-CTCACTTCCCGACAGGACTT-3’
RAPGEF4 promoter Fwd	5’-GTAACTCCCGACGACAGCTC-3’
RAPGEF4 promoter Rvs	5’-CTGTCACAGCCTGGAAACAA-3’
SEMA4G promoter Fwd	5’-AAACGGACCTCAGAAAACCA-3’
SEMA4G promoter Rvs	5’-CCATGGTGAGAGGGAGTTGT-3’
SOCS2 promoter Fwd	5’-TTCAAGCTTTCGAGCAGTGA-3’
SOCS2 promoter Rvs	5’-CCCTTAACAATCACGGGAAA-3’

REFERENCES

Amé, J. C., Spenlehauer, C., and de Murcia, G. (2004). The PARP superfamily. Bioessays *26*, 882-893.

Anderson, M. G., Scoggin, K. E., Simbulan-Rosenthal, C. M., and Steadman, J. A. (2000). Identification of poly(ADP-ribose) polymerase as a transcriptional coactivator of the human T-cell leukemia virus type 1 Tax protein. J Virol *74*, 2169-2177.

Bonicalzi, M. E., Vodenicharov, M., Coulombe, M., Gagne, J. P., and Poirier, G. G. (2003). Alteration of poly(ADP-ribose) glycohydrolase nucleocytoplasmic shuttling characteristics upon cleavage by apoptotic proteases. Biol Cell *95*, 635-644.

Butler, A. J., and Ordahl, C. P. (1999). Poly(ADP-ribose) polymerase binds with transcription enhancer factor 1 to MCAT1 elements to regulate muscle-specific transcription. Mol Cell Biol *19*, 296-306.

Cervellera, M. N., and Sala, A. (2000). Poly(ADP-ribose) polymerase is a B-MYB coactivator. J Biol Chem *275*, 10692-10696.

Conde, C., Mark, M., Oliver, F. J., Huber, A., de Murcia, G., and Menissier-de Murcia, J. (2001). Loss of poly(ADP-ribose) polymerase-1 causes increased tumour latency in p53-deficient mice. Embo J *20*, 3535-3543.

Cortes, U., Tong, W. M., Coyle, D. L., Meyer-Ficca, M. L., Meyer, R. G., Petrilli, V., Herceg, Z., Jacobson, E. L., Jacobson, M. K., and Wang, Z. Q. (2004). Depletion of the 110-kilodalton isoform of poly(ADP-ribose) glycohydrolase increases sensitivity to genotoxic and endotoxic stress in mice. Mol Cell Biol *24*, 7163-7178.

D'Amours, D., Desnoyers, S., D'Silva, I., and Poirier, G. G. (1999). Poly(ADP-ribosyl)ation reactions in the regulation of nuclear functions. Biochem J *342 (Pt 2)*, 249-268.

Davidovic, L., Vodenicharov, M., Affar, E. B., and Poirier, G. G. (2001). Importance of poly(ADP-ribose) glycohydrolase in the control of poly(ADP-ribose) metabolism. Exp Cell Res *268*, 7-13.

Dennis, G., Jr., Sherman, B. T., Hosack, D. A., Yang, J., Gao, W., Lane, H. C., and Lempicki, R. A. (2003). DAVID: Database for Annotation, Visualization, and Integrated Discovery. Genome Biol *4*, P3.

deSouza, N., Cui, J., Dura, M., McDonald, T. V., and Marks, A. R. (2007). A function for tyrosine phosphorylation of type 1 inositol 1,4,5-trisphosphate receptor in lymphocyte activation. J Cell Biol *179*, 923-934.

Dey, B. R., Spence, S. L., Nissley, P., and Furlanetto, R. W. (1998). Interaction of human suppressor of cytokine signaling (SOCS)-2 with the insulin-like growth factor-I receptor. J Biol Chem *273*, 24095-24101.

Dow, G. S. (2003). Effect of sample size and P-value filtering techniques on the detection of transcriptional changes induced in rat neuroblastoma (NG108) cells by mefloquine. Malar J *2*, 4.

Fisher, A. E., Hochegger, H., Takeda, S., and Caldecott, K. W. (2007). Poly(ADP-ribose) polymerase 1 accelerates single-strand break repair in concert with poly(ADP-ribose) glycohydrolase. Mol Cell Biol *27*, 5597-5605.

Gagne, J. P., Moreel, X., Gagne, P., Labelle, Y., Droit, A., Chevalier-Pare, M., Bourassa, S., McDonald, D., Hendzel, M. J., Prigent, C., and Poirier, G. G. (2008). Proteomic Investigation of Phosphorylation Sites in Poly(ADP-ribose) Polymerase-1 and Poly(ADP-ribose) Glycohydrolase. J Proteome Res.

Gao, H., Coyle, D. L., Meyer-Ficca, M. L., Meyer, R. G., Jacobson, E. L., Wang, Z. Q., and Jacobson, M. K. (2007). Altered poly(ADP-ribose) metabolism impairs cellular responses to genotoxic stress in a hypomorphic mutant of poly(ADP-ribose) glycohydrolase. Exp Cell Res *313*, 984-996.

Hanai, S., Kanai, M., Ohashi, S., Okamoto, K., Yamada, M., Takahashi, H., and Miwa, M. (2004). Loss of poly(ADP-ribose) glycohydrolase causes progressive neurodegeneration in Drosophila melanogaster. Proc Natl Acad Sci U S A *101*, 82-86.

Hassa, P. O., Covic, M., Hasan, S., Imhof, R., and Hottiger, M. O. (2001). The enzymatic and DNA binding activity of PARP-1 are not required for NF-kappa B coactivator function. J Biol Chem *276*, 45588-45597.

Hassa, P. O., and Hottiger, M. O. (1999). A role of poly (ADP-ribose) polymerase in NF-kappaB transcriptional activation. Biol Chem *380*, 953-959.

Hassa, P. O., and Hottiger, M. O. (2002). The functional role of poly(ADP-ribose)polymerase 1 as novel coactivator of NF-kappaB in inflammatory disorders. Cell Mol Life Sci *59*, 1534-1553.

Hess, A., and Iyer, H. (2007). Fisher's combined p-value for detecting differentially expressed genes using Affymetrix expression arrays. BMC Genomics *8*, 96.

Inoue, T., Kato, K., Kohda, K., and Mikoshiba, K. (1998). Type 1 inositol 1,4,5-trisphosphate receptor is required for induction of long-term depression in cerebellar Purkinje neurons. J Neurosci *18*, 5366-5373.

Johnson, W. E., Li, C., and Rabinovic, A. (2007). Adjusting batch effects in microarray expression data using empirical Bayes methods. Biostatistics *8*, 118-127.

Ju, B. G., Lunyak, V. V., Perissi, V., Garcia-Bassets, I., Rose, D. W., Glass, C. K., and Rosenfeld, M. G. (2006). A topoisomerase IIbeta-mediated dsDNA break required for regulated transcription. Science *312*, 1798-1802.

Ju, B. G., Solum, D., Song, E. J., Lee, K. J., Rose, D. W., Glass, C. K., and Rosenfeld, M. G. (2004). Activating the PARP-1 sensor component of the groucho/ TLE1 corepressor complex mediates a CaMKinase IIdelta-dependent neurogenic gene activation pathway. Cell *119*, 815-829.

Karras, G. I., Kustatscher, G., Buhecha, H. R., Allen, M. D., Pugieux, C., Sait, F., Bycroft, M., and Ladurner, A. G. (2005). The macro domain is an ADP-ribose binding module. Embo J *24*, 1911-1920.

Kauppinen, T. M., Chan, W. Y., Suh, S. W., Wiggins, A. K., Huang, E. J., and Swanson, R. A. (2006). Direct phosphorylation and regulation of poly(ADP-ribose) polymerase-1 by extracellular signal-regulated kinases 1/2. Proc Natl Acad Sci U S A *103*, 7136-7141.

Keil, C., Grobe, T., and Oei, S. L. (2006). MNNG-induced cell death is controlled by interactions between PARP-1, poly(ADP-ribose) glycohydrolase, and XRCC1. J Biol Chem *281*, 34394-34405.

Kim, M. Y., Mauro, S., Gevry, N., Lis, J. T., and Kraus, W. L. (2004). NAD+-dependent modulation of chromatin structure and transcription by nucleosome binding properties of PARP-1. Cell *119*, 803-814.

Kim, M. Y., Zhang, T., and Kraus, W. L. (2005). Poly(ADP-ribosyl)ation by PARP-1: 'PAR-laying' NAD+ into a nuclear signal. Genes Dev *19*, 1951-1967.

Kininis, M., Chen, B. S., Diehl, A. G., Isaacs, G. D., Zhang, T., Siepel, A. C., Clark, A. G., and Kraus, W. L. (2007). Genomic analyses of transcription factor binding, histone acetylation, and gene expression reveal mechanistically distinct classes of estrogen-regulated promoters. Mol Cell Biol *27*, 5090-5104.

Koh, D. W., Lawler, A. M., Poitras, M. F., Sasaki, M., Wattler, S., Nehls, M. C., Stoger, T., Poirier, G. G., Dawson, V. L., and Dawson, T. M. (2004). Failure to degrade poly(ADP-ribose) causes increased sensitivity to cytotoxicity and early embryonic lethality. Proc Natl Acad Sci U S A *101*, 17699-17704.

Koths, K., Taylor, E., Halenbeck, R., Casipit, C., and Wang, A. (1993). Cloning and characterization of a human Mac-2-binding protein, a new member of the superfamily defined by the macrophage scavenger receptor cysteine-rich domain. J Biol Chem *268*, 14245-14249.

Kraus, W. L. (2008). Transcriptional control by PARP-1: chromatin modulation, enhancer-binding, coregulation, and insulation. Curr Opin Cell Biol *20*, 294-302.

Kraus, W. L., and Lis, J. T. (2003). PARP goes transcription. Cell *113*, 677-683.

Krishnakumar, R., Gamble, M. J., Frizzell, K. M., Berrocal, J. G., Kininis, M., and Kraus, W. L. (2008). Reciprocal binding of PARP-1 and histone H1 at promoters specifies transcriptional outcomes. Science *319*, 819-821.

Kun, E., Kirsten, E., Mendeleyev, J., and Ordahl, C. P. (2004). Regulation of the enzymatic catalysis of poly(ADP-ribose) polymerase by dsDNA, polyamines, Mg2+, Ca2+, histones H1 and H3, and ATP. Biochemistry *43*, 210-216.

Kun, E., Kirsten, E., and Ordahl, C. P. (2002). Coenzymatic activity of randomly broken or intact double-stranded DNAs in auto and histone H1 trans-poly(ADP-

ribosylation), catalyzed by poly(ADP-ribose) polymerase (PARP I). J Biol Chem *277*, 39066-39069.

Kustatscher, G., Hothorn, M., Pugieux, C., Scheffzek, K., and Ladurner, A. G. (2005). Splicing regulates NAD metabolite binding to histone macroH2A. Nat Struct Mol Biol *12*, 624-625.

Leclerc, D., Campeau, E., Goyette, P., Adjalla, C. E., Christensen, B., Ross, M., Eydoux, P., Rosenblatt, D. S., Rozen, R., and Gravel, R. A. (1996). Human methionine synthase: cDNA cloning and identification of mutations in patients of the cblG complementation group of folate/cobalamin disorders. Hum Mol Genet *5*, 1867-1874.

Li, Y. N., Gulati, S., Baker, P. J., Brody, L. C., Banerjee, R., and Kruger, W. D. (1996). Cloning, mapping and RNA analysis of the human methionine synthase gene. Hum Mol Genet *5*, 1851-1858.

Lonskaya, I., Potaman, V. N., Shlyakhtenko, L. S., Oussatcheva, E. A., Lyubchenko, Y. L., and Soldatenkov, V. A. (2005). Regulation of poly(ADP-ribose) polymerase-1 by DNA structure-specific binding. J Biol Chem *280*, 17076-17083.

Mabley, J. G., Suarez-Pinzon, W. L., Hasko, G., Salzman, A. L., Rabinovitch, A., Kun, E., and Szabo, C. (2001). Inhibition of poly (ADP-ribose) synthetase by gene disruption or inhibition with 5-iodo-6-amino-1,2-benzopyrone protects mice from multiple-low-dose-streptozotocin-induced diabetes. Br J Pharmacol *133*, 909-919.

Marsischky, G. T., Wilson, B. A., and Collier, R. J. (1995). Role of glutamic acid 988 of human poly-ADP-ribose polymerase in polymer formation. Evidence for active site similarities to the ADP-ribosylating toxins. J Biol Chem *270*, 3247-3254.

Mathieu, J., Flexor, M., Lanotte, M., and Besancon, F. (2008). A PARP-1/JNK1 cascade participates in the synergistic apoptotic effect of TNFalpha and all-trans retinoic acid in APL cells. Oncogene *27*, 3361-3370.

Meisterernst, M., Stelzer, G., and Roeder, R. G. (1997). Poly(ADP-ribose) polymerase enhances activator-dependent transcription in vitro. Proc Natl Acad Sci U S A *94*, 2261-2265.

Meyer-Ficca, M. L., Meyer, R. G., Coyle, D. L., Jacobson, E. L., and Jacobson, M. K. (2004). Human poly(ADP-ribose) glycohydrolase is expressed in alternative splice variants yielding isoforms that localize to different cell compartments. Exp Cell Res *297*, 521-532.

Meyer-Ficca, M. L., Meyer, R. G., Jacobson, E. L., and Jacobson, M. K. (2005). Poly(ADP-ribose) polymerases: managing genome stability. Int J Biochem Cell Biol *37*, 920-926.

Minamoto, S., Ikegame, K., Ueno, K., Narazaki, M., Naka, T., Yamamoto, H., Matsumoto, T., Saito, H., Hosoe, S., and Kishimoto, T. (1997). Cloning and functional analysis of new members of STAT induced STAT inhibitor (SSI) family: SSI-2 and SSI-3. Biochem Biophys Res Commun *237*, 79-83.

Miyamoto, T., Kakizawa, T., and Hashizume, K. (1999). Inhibition of nuclear receptor signalling by poly(ADP-ribose) polymerase. Mol Cell Biol *19*, 2644-2649.

Morrison, C., Smith, G. C., Stingl, L., Jackson, S. P., Wagner, E. F., and Wang, Z. Q. (1997). Genetic interaction between PARP and DNA-PK in V(D)J recombination and tumorigenesis. Nat Genet *17*, 479-482.

Murphy, D. (2002). Gene expression studies using microarrays: principles, problems, and prospects. Adv Physiol Educ *26*, 256-270.

Nirodi, C., NagDas, S., Gygi, S. P., Olson, G., Aebersold, R., and Richmond, A. (2001). A role for poly(ADP-ribose) polymerase in the transcriptional regulation of the melanoma growth stimulatory activity (CXCL1) gene expression. J Biol Chem *276*, 9366-9374.

Oei, S. L., and Shi, Y. (2001). Transcription factor Yin Yang 1 stimulates poly(ADP-ribosyl)ation and DNA repair. Biochem Biophys Res Commun *284*, 450-454.

Ogata, N., Ueda, K., Kawaichi, M., and Hayaishi, O. (1981). Poly(ADP-ribose) synthetase, a main acceptor of poly(ADP-ribose) in isolated nuclei. J Biol Chem *256*, 4135-4137.

Ogino, H., Nozaki, T., Gunji, A., Maeda, M., Suzuki, H., Ohta, T., Murakami, Y., Nakagama, H., Sugimura, T., and Masutani, M. (2007). Loss of Parp-1 affects gene

expression profile in a genome-wide manner in ES cells and liver cells. BMC Genomics *8*, 41.

Ohashi, S., Kanai, M., Hanai, S., Uchiumi, F., Maruta, H., Tanuma, S., and Miwa, M. (2003). Subcellular localization of poly(ADP-ribose) glycohydrolase in mammalian cells. Biochem Biophys Res Commun *307*, 915-921.

Oliver, F. J., Menissier-de Murcia, J., Nacci, C., Decker, P., Andriantsitohaina, R., Muller, S., de la Rubia, G., Stoclet, J. C., and de Murcia, G. (1999). Resistance to endotoxic shock as a consequence of defective NF-kappaB activation in poly (ADP-ribose) polymerase-1 deficient mice. Embo J *18*, 4446-4454.

Pavri, R., Lewis, B., Kim, T. K., Dilworth, F. J., Erdjument-Bromage, H., Tempst, P., de Murcia, G., Evans, R., Chambon, P., and Reinberg, D. (2005). PARP-1 determines specificity in a retinoid signaling pathway via direct modulation of mediator. Mol Cell *18*, 83-96.

Potaman, V. N., Shlyakhtenko, L. S., Oussatcheva, E. A., Lyubchenko, Y. L., and Soldatenkov, V. A. (2005). Specific binding of poly(ADP-ribose) polymerase-1 to cruciform hairpins. J Mol Biol *348*, 609-615.

Rapizzi, E., Fossati, S., Moroni, F., and Chiarugi, A. (2004). Inhibition of poly(ADP-ribose) glycohydrolase by gallotannin selectively up-regulates expression of proinflammatory genes. Mol Pharmacol *66*, 890-898.

Reynolds, A., Leake, D., Boese, Q., Scaringe, S., Marshall, W. S., and Khvorova, A. (2004). Rational siRNA design for RNA interference. Nat Biotechnol *22*, 326-330.

Rolli, V., O'Farrell, M., Menissier-de Murcia, J., and de Murcia, G. (1997). Random mutagenesis of the poly(ADP-ribose) polymerase catalytic domain reveals amino acids involved in polymer branching. Biochemistry *36*, 12147-12154.

Rolli, V., Ruf, A., Augustin, A., Schulz, G. E., Ménissier-de Murcia, J., and de Murcia, G. (2000). Poly(ADP-ribose) polymerase: structure and function. In From DNA Damage and Stress Signalling to Cell Death: Poly ADP-Ribosylation Reactions, G. de Murcia, and S. Shall, eds. (New York, Oxford Ubiversity Press), pp. 35-79.

Saldanha, A. J. (2004). Java Treeview--extensible visualization of microarray data. Bioinformatics *20*, 3246-3248.

Shah, R. G., Ghodgaonkar, M. M., Affar el, B., and Shah, G. M. (2005). DNA vector-based RNAi approach for stable depletion of poly(ADP-ribose) polymerase-1. Biochem Biophys Res Commun *331*, 167-174.

Shimokawa, T., Masutani, M., Nagasawa, S., Nozaki, T., Ikota, N., Aoki, Y., Nakagama, H., and Sugimura, T. (1999). Isolation and cloning of rat poly(ADP-ribose) glycohydrolase: presence of a potential nuclear export signal conserved in mammalian orthologs. J Biochem *126*, 748-755.

Simbulan-Rosenthal, C. M., Ly, D. H., Rosenthal, D. S., Konopka, G., Luo, R., Wang, Z. Q., Schultz, P. G., and Smulson, M. E. (2000). Misregulation of gene expression in primary fibroblasts lacking poly(ADP-ribose) polymerase. Proc Natl Acad Sci U S A *97*, 11274-11279.

Simbulan-Rosenthal, C. M., Rosenthal, D. S., Iyer, S., Boulares, H., and Smulson, M. E. (1999). Involvement of PARP and poly(ADP-ribosyl)ation in the early stages of apoptosis and DNA replication. Mol Cell Biochem *193*, 137-148.

St-Laurent, J. F., Gagnon, S. N., Dequen, F., Hardy, I., and Desnoyers, S. (2007). Altered DNA damage response in Caenorhabditis elegans with impaired poly(ADP-ribose) glycohydrolases genes expression. DNA Repair (Amst) *6*, 329-343.

Tinari, N., Kuwabara, I., Huflejt, M. E., Shen, P. F., Iacobelli, S., and Liu, F. T. (2001). Glycoprotein 90K/MAC-2BP interacts with galectin-1 and mediates galectin-1-induced cell aggregation. Int J Cancer *91*, 167-172.

Tong, W. M., Hande, M. P., Lansdorp, P. M., and Wang, Z. Q. (2001). DNA strand break-sensing molecule poly(ADP-Ribose) polymerase cooperates with p53 in telomere function, chromosome stability, and tumor suppression. Mol Cell Biol *21*, 4046-4054.

Tulin, A., Chinenov, Y., and Spradling, A. (2003). Regulation of chromatin structure and gene activity by poly(ADP-ribose) polymerases. Curr Top Dev Biol *56*, 55-83.

Tulin, A., Naumova, N. M., Menon, A. K., and Spradling, A. C. (2005). Drosophila poly(ADP-ribose) glycohydrolase (Parg) mediates chromatin structure and Sir2-dependent silencing. Genetics.

Tulin, A., and Spradling, A. (2003). Chromatin loosening by poly(ADP)-ribose polymerase (PARP) at Drosophila puff loci. Science *299*, 560-562.

Tulin, A., Stewart, D., and Spradling, A. C. (2002). The Drosophila heterochromatic gene encoding poly(ADP-ribose) polymerase (PARP) is required to modulate chromatin structure during development. Genes Dev *16*, 2108-2119.

Wacker, D. A., Frizzell, K. M., Zhang, T., and Kraus, W. L. (2007a). Regulation of chromatin structure and chromatin-dependent transcription by poly(ADP-ribose) polymerase-1: possible targets for drug-based therapies. Subcell Biochem *41*, 45-69.

Wacker, D. A., Ruhl, D. D., Balagamwala, E. H., Hope, K. M., Zhang, T., and Kraus, W. L. (2007b). The DNA binding and catalytic domains of poly(ADP-ribose) polymerase 1 cooperate in the regulation of chromatin structure and transcription. Mol Cell Biol *27*, 7475-7485.

Wang, Z. Q., Auer, B., Stingl, L., Berghammer, H., Haidacher, D., Schweiger, M., and Wagner, E. F. (1995). Mice lacking ADPRT and poly(ADP-ribosyl)ation develop normally but are susceptible to skin disease. Genes Dev *9*, 509-520.

Wang, Z. Q., Stingl, L., Morrison, C., Jantsch, M., Los, M., Schulze-Osthoff, K., and Wagner, E. F. (1997). PARP is important for genomic stability but dispensable in apoptosis. Genes Dev *11*, 2347-2358.

Watkins, D., and Rosenblatt, D. S. (1989). Functional methionine synthase deficiency (cblE and cblG): clinical and biochemical heterogeneity. Am J Med Genet *34*, 427-434.

Yamada, N., Makino, Y., Clark, R. A., Pearson, D. W., Mattei, M. G., Guenet, J. L., Ohama, E., Fujino, I., Miyawaki, A., Furuichi, T., and Mikoshiba, K. (1994). Human inositol 1,4,5-trisphosphate type-1 receptor, InsP3R1: structure, function, regulation of expression and chromosomal localization. Biochem J *302 (Pt 3)*, 781-790.

Yang, H., Yang, T., Baur, J. A., Perez, E., Matsui, T., Carmona, J. J., Lamming, D. W., Souza-Pinto, N. C., Bohr, V. A., Rosenzweig, A.*, et al.* (2007). Nutrient-sensitive mitochondrial NAD+ levels dictate cell survival. Cell *130*, 1095-1107.

Yang, T., and Sauve, A. A. (2006). NAD metabolism and sirtuins: metabolic regulation of protein deacetylation in stress and toxicity. Aaps J *8*, E632-643.

Yu, S. W., Wang, H., Poitras, M. F., Coombs, C., Bowers, W. J., Federoff, H. J., Poirier, G. G., Dawson, T. M., and Dawson, V. L. (2002). Mediation of poly(ADP-ribose) polymerase-1-dependent cell death by apoptosis-inducing factor. Science *297*, 259-263.

Zhang, T., Berrocal, J. G., Frizzell, K. M., Gamble, M. J., Dumond, M. E., Krishnakumar, R., Yang, T., Sauve, A. A., and Kraus, W. L. (2009). Enzymes in the NAD+ Salvage Pathway Regulate SIRT1 Activity at Target Gene Promoters. J Biol Chem *284*, 20408-20417.

Zingarelli, B., Hake, P. W., O'Connor, M., Denenberg, A., Kong, S., and Aronow, B. J. (2003). Absence of poly(ADP-ribose)polymerase-1 alters nuclear factor-kappa B activation and gene expression of apoptosis regulators after reperfusion injury. Mol Med *9*, 143-153.

Zong, W. X., Ditsworth, D., Bauer, D. E., Wang, Z. Q., and Thompson, C. B. (2004). Alkylating DNA damage stimulates a regulated form of necrotic cell death. Genes Dev *18*, 1272-1282.

CHAPTER 3

Role of Poly(ADP-ribose) Polymerase-1 in Mediating the Effects of Estrogen on the Transcriptome of MCF-7 Human Breast Cancer Cells*

* This research was conducted with contributions from Hah, N., Luo, X., Sun, M., Krishnakumar, R., and Danko, C. as follows: N.H. and X.L. assisted with GRO-seq library generation (Figure 3.6); M.S. conducted computational analyses for GRO-seq and ChIP-chip (Figures 3.6-3.10, 3.12, and 3.14-3.16); and R.K. performed and analyzed the ChIP-chip experiments using the custom promoter array (Figure 3.11). C.D. developed all of the computational tools for the GRO-seq data analysis. N.H. also provided GRO-seq data (MCF-7 parental) for comparison analyses (Figures 3.9 and 3.16).

3.1. Summary

Poly(ADP-ribose) Polymerase-1 is a nuclear enzyme that modifies target proteins by the covalent attachment of ADP-ribose polymers. Over the last ten years, a role for PARP-1 in regulating transcription has become apparent in both basal and signal-mediated conditions, including stress response and hormone-mediated transcription. Although considerable attention has been paid investigating the mechanisms of regulation at the gene-specific level, global effects on signal-mediated gene regulation by PARP-1 still remain unclear. I have used a novel method known as Global Run-on Sequencing (GRO-seq) to define the role of PARP-1 on the estrogen-regulated transcriptome. GRO-seq libraries from MCF-7 cells treated with vehicle or 17β-estradiol (E2) under three conditions: (i) a control knockdown; (ii) a control knockdown plus a PARP inhibitor, PJ34; and (iii) a PARP-1 knockdown were produced, sequenced, and compared. I have determined that the estrogen response is highly maintained under PARP-1 knockdown or inhibition. Accordingly, upon estrogen treatment, PARP-1 localization patterns are largely unaffected. However, deeper analyses reveal a small number of genes where PARP-1 knockdown or inhibition reduces the estrogen response at the transcription level (GRO-seq) and at the steady state mRNA level (RT-qPCR).

3.2. Introduction

Poly(ADP-ribose) Polymerase-1 (PARP-1) is a nuclear enzyme that modifies target proteins by the covalent attachment of ADP-ribose polymers, generated from donor nicotinamide adenine dinucleotide (NAD^+) molecules (D'Amours et al., 1999; Kim et al., 2005). This process is known as poly(ADP-ribosyl)ation (PARylation).

PARP-1 is the founding member and most characterized of the PARP superfamily (Ame et al., 2004; Kim et al., 2005) and is responsible for the majority of poly(ADP-ribose) (PAR) synthesis in the cell (D'Amours et al., 1999). PARylation occurs on a variety of target proteins, including transcription factors, histones, DNA repair factors, and PARP-1 itself, all of which play roles in a wide range of cellular processes, such as stress response, DNA damage repair, and transcriptional regulation (D'Amours et al., 1999; Kim et al., 2005; Krishnakumar and Kraus, 2010).

PARP-1 consists of three major domains: (i) an amino-terminal DNA binding domain (DBD), (ii) a central auto-modification domain (AMD), and (iii) a carboxy-terminal catalytic domain (CATD) (Krishnakumar and Kraus, 2010). PARP-1 binding to various forms of DNA (Kun et al., 2004; Kun et al., 2002; Lonskaya et al., 2005; Potaman et al., 2005), nucleosomes (Kim et al., 2004; Wacker et al., 2007a; Wacker et al., 2007b), and interactoring with various proteins (Ju et al., 2006; Ju et al., 2004; Oei and Shi, 2001) can potently stimulate its enzymatic activity (Krishnakumar and Kraus, 2010). The CATD confers NAD^+ binding and ADP-ribosyl transferase activity (D'Amours et al., 1999; Rolli et al., 2000). The combinatorial actions of each of these domains allow PARP-1 to be involved in many cellular processes involving genomic DNA, including transcriptional regulation.

PARP-1 localizes to promoters of the majority of expressed genes in MCF-7 human breast cancer cells (Krishnakumar et al., 2008). This promoter localization is likely to allow for PARP-1 to function in transcriptional regulation. PARP-1 can modulate transcriptional responses in numerous ways, including (i) functioning as a direct DNA binding factor, (ii) regulating the actions of insulators and insulator-binding factors, (iii) functioning as a classical coregulator, and (iv) regulating chromatin structure and composition (reviewed in (Kim et al., 2005; Kraus, 2008; Kraus and Lis, 2003; Tulin et al., 2003)). Importantly, these functions are not

mutually exclusive and may depend on cell-type, specific genes, and the type and strength of the various environmental signals. In this regard, PARP-1 has been show to modulate various types of signal-mediated transcription, involving signals such as heat shock (Tulin et al., 2003), cytokines (Hassa and Hottiger, 1999), and steroid hormones (Ju et al., 2004; Pavri et al., 2005). Although many of these areas have received considerable attention at the gene-specific level, global effects on signal-mediated gene regulation by PARP-1 still remain unclear.

In this study, I have investigated the role of PARP-1 in mediating estrogen-dependent transcription. Estrogen (17β-estradiol, E2; Figure 3.1A) is a naturally produced steroid hormone whose actions are involved in the normal physiology of both males and females, such as reproduction, sexual development, and cardiovascular and neuronal function among various tissues in the body (Couse and Korach, 1999a; Couse and Korach, 1999b; Gruber et al., 2002; Nef and Parada, 2000). In addition, estrogens function to promote various diseases (*i.e.* osteoporosis and breast, uterine, and ovarian cancers), but are also used for medicinal purposes (*i.e.* postmenopausal hormone replacement therapy, contraceptives) (Deroo and Korach, 2006; Foster et al., 2001; Prall et al., 1998; Sommer and Fuqua, 2001). Interestingly, PARP-1 has also been shown to play a role in the progression of various types of cancer, including those of the breast, uterus, and ovary. In fact, treatment of these types of cancers with PARP inhibitors can be detrimental, both in cell models, as well as in clinical settings (Bryant et al., 2005; Farmer et al., 2005; Fong et al., 2009; Inbar-Rozensal et al., 2009; Munoz-Gamez et al., 2005). However, the molecular mechanism of PARP-1 action in the progression of cancer is not clear. For example, we do not understand the contributions of DNA damage repair versus transcriptional regulation by PARP-1. This information would further our understanding of PARP-1 actions, which would enhance the development of more effective inhibitors for therapeutic applications.

Figure 3.1. Estrogen-mediated transcription in the context of chromatin. *A*, Chemical structure of the steroid hormone, 17β-estradiol (estrogen; E2), an estrogen receptor-specific ligand. *B*, Upon binding E2, estrogen receptor (α or β isoform, ER) dimerizes and binds to specific DNA elements, or known as estrogen receptor binding sites (ERBS). This results in the recruitment of multiple coregulators, including bridging factors (*i.e.*, Mediator), histone modifying enzymes (*i.e.*, p300/CBP), and chromatin remodeling complexes (*i.e.*, SWI/SNF), all of which cooperate to regulate the recruitment and activity of RNA polymerase II (RNA Pol II).

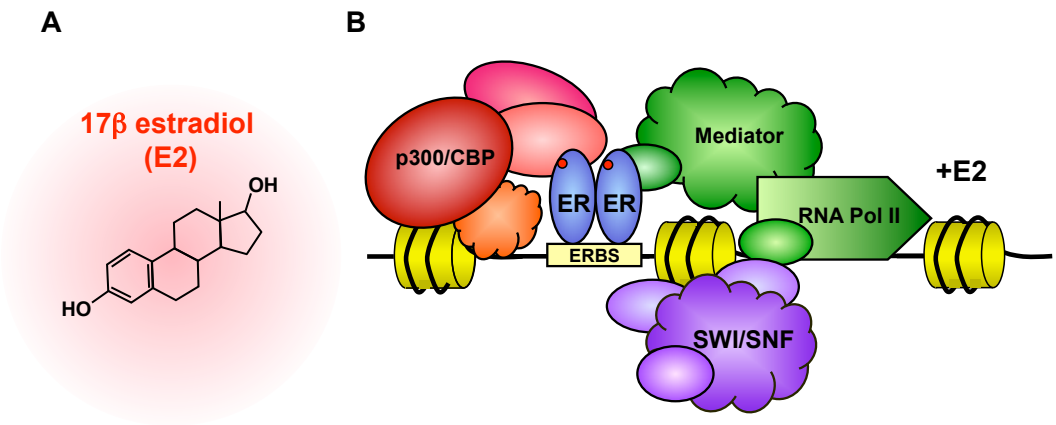
A
17β estradiol
(E2)
OH
HO
B
p300/CBP
Mediator
ER
ER
ERBS
RNA Pol II
+E2
SWI/SNF

Estrogen actions at the molecular level are mediated by estrogen receptors alpha and beta (ERα and β), through both genomic and non-genomic actions (Marino et al., 2006; Ordonez-Moran and Munoz, 2009). In the "classic" view, estrogen-bound ERs bind to specific DNA elements (directly or indirect association through tethering mechanisms) and function to recruit various classes of coregulators to the gene promoters (Kininis and Kraus, 2008). These include bridging factors (*i.e.* Mediator), histone modifying enzymes (*i.e.* p300/CBP), and chromatin remodeling complexes (*i.e.* SWI/SNF), as shown in Figure 3.1B, all of which function to modulate RNA Pol II recruitment and activity. PARP-1 has previously been implicated in regulating estrogen-dependent transcription at the TFF1 promoter (Ju et al., 2006; Lis and Kraus, 2006) by promoting the recruitment of topoisomerase IIβ (TopoIIβ), leading to promoter DNA cleavage, coregulator exchange, and activation of transcription (Ju et al., 2006). However, the mechanisms of PARP-1 action at a single gene are not indicative of global actions on transcription.

In the study described herein, I have used a novel method known as Global Run-on Sequencing (GRO-seq) to define the role of PARP-1 on the estrogen-regulated transcriptome at the level of the nascent transcript. GRO-seq libraries from MCF-7 cells treated with vehicle or 17β-estradiol (E2) under three conditions: (i) a control knockdown; (ii) a control knockdown plus a PARP inhibitor, PJ34; and (iii) a PARP-1 knockdown were produced, sequenced, and compared. I have determined that the estrogen response is highly maintained under PARP-1 knockdown or inhibition. Accordingly, upon estrogen treatment, PARP-1 localization patterns are largely unaffected. However, upon deeper analyses, my data reveal a few genes where PARP-1 knockdown or inhibition reduces the estrogen response at the transcription level (GRO-seq) and at the steady state mRNA level (RT-qPCR).

3.3. Results

GRO-seq experimental design. To explore the role of PARP-1 and PARP activity in the regulation of estrogen-dependent transcription, I designed a Global Run-On sequencing (GRO-seq) experiment under various conditions, including estrogen treatment, PARP-1 knockdown, and PARP inhibition. GRO-seq is a highly sensitive and quantitative methodology that maps the position, orientation, and amount of transcriptionally engaged polymerases in the cell (Core et al., 2008). In addition, this method is exceptional in detecting transcriptional changes upon a signal over time (N.H. and W.L.K., unpublished). Importantly, GRO-seq detects transcription, or changes in transcription, at the level of the nascent transcript, rather than at the steady-state mRNA level, giving a direct measure of transcription occurring on the DNA.

I used luciferase (Luc, used as a control) and PARP-1 stably transduced short hairpin RNA (shRNA)-mediated knockdown cell lines, previously described and characterized (Chapter 2; (Frizzell et al., 2009)). The reduction in PARP-1 protein and mRNA levels were previously determined to be approximately 90 percent, compared to the Luc control (Frizzell et al., 2009). To compare the role of PARP-1 protein to PARP activity, I also treated the control cells with a PARP inhibitor, PJ34 (Figure. 3.2A; (Abdelkarim et al., 2001)), previously shown to largely inhibit PARP-1 automodification (Frizzell et al., 2009). Interestingly, this inhibitor was shown to block cell cycle progression and trigger apoptosis in MCF-7 cells at high doses (Inbar-Rozensal et al., 2009). This result was recapitulated in Luc knockdown cells treated with increasing doses of PJ34 over a 48 hour period (Figure 3.2B). MCF-7 cell survival dramatically decreased with increasing doses of PJ34. Interestingly, this effect of PJ34 was not altered upon PARP-1 knockdown, a perplexing result given the fact that the majority of PAR is generated by PARP-1 in the cell (Kim et al., 2005;

Krishnakumar and Kraus, 2010). This indicates that total PARP activity is absolutely required for MCF-7 cell survival. In addition, the lack of reversal of the PJ34 effect by PARP-1 knockdown suggests that more than one PARP is involved in regulating cell cycle progression and cell death pathways, since PJ34 inhibits more than one PARP. To determine the effect of PARP inhibition at the transcription level, which is likely to precede cell cycle arrest and cell death, I determined that short treatment times (1 hr) and low doses (1 μM) of PJ34 would be suitable for my experiment.

I treated Luc and PARP-1 knockdown cells with or without PJ34 for 1 hr, directly followed by treatment with or without 17β-estradiol (estrogen, E2) for 40 minutes (Figure 3.3A). The time of estrogen treatment was determined using previously generated GRO-seq data in the Kraus lab (N.H. and W.L.K., unpublished), as well as previously published genomic and gene-specific analyses (Kininis et al., 2007; Kininis et al., 2009; Kininis and Kraus, 2008). Immediately following estrogen treatment, the cells were collected and used for further experimentation. Examination of whole cell lysates and nuclear extracts by Western blot analysis (Figure 3.3B) showed a reduction in PARP-1 protein levels and PAR modification in the PARP-1 knockdown cell line, as described previously (Frizzell et al., 2009). In addition, treatment with PJ34 completely blocked the production of PAR, without affecting PARP-1 levels, as determined previously (Frizzell et al., 2009). Importantly, PARP-1 and PAR levels were not altered upon estrogen treatment, nor were the levels of estrogen receptor alpha (ERα), the nuclear receptor that mediates estrogen-dependent transcription. A Western blot for Actin was included as a loading control.

Generation of GRO-seq libraries. Nuclei from Luc and PARP-1 knockdown cell lines, treated under the conditions noted above, were isolated and used for GRO-seq library generation, using the methods described in the Experimental Procedures and in

Figure 3.2. PJ34, a PARP inhibitor, causes MCF-7 cell death at high doses. *A*, Chemical structure of the competitive PARP inhibitor, PJ34 (PJ), and the enzymatic reaction that it inhibits. *B*, MCF-7 cell survival decreases with increasing doses of PJ34, irrespective of PARP-1 levels. Stable Luc and PARP-1 shRNA-mediated knockdown cell lines were subjected to treatment with PJ34 at various doses for 48 hours. Cells were trypsinized, collected, and counted to determine percent survival rate. The data are shown as the mean ± SEM (*error bars*) for at least two three independent experiments. All experiments were conducted using the lowest dose of PJ34 (1 μM; denoted by *asterisk*) at short treatment times to avoid cell growth arrest.

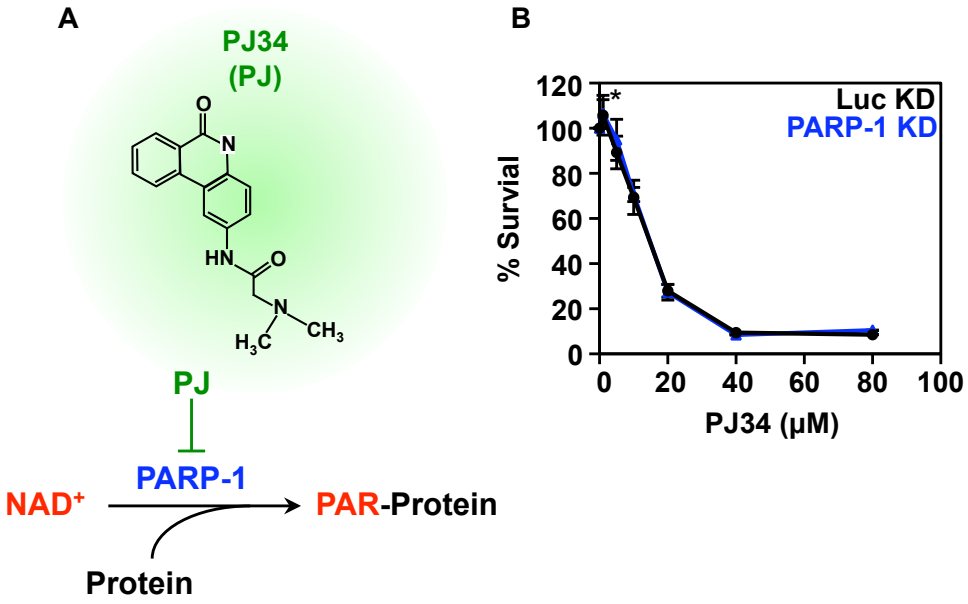
A
PJ34
(PJ)
O
N
HN
O
N
CH3
H3C
PJ
PARP-1
NAD+
PAR-Protein
Protein
B
Luc KD
PARP-1 KD
% Survial
120
100
80
60
40
20
0
0
20
40
60
80
100
PJ34 (μM)

Figure. 3.3. Experimental design and conditions for GRO-seq experiment. *A*, Schematic of cell lines and treatments conditions for GRO-seq. Stable Luc and PARP-1 shRNA-mediated knockdown cell lines were grown in estrogen-free medium for at least three days prior to conditional treatments. Cells were then treated with vehicle or PJ34 (1 μM) for 1 hour, directly followed by treatment with vehicle or E2 (100 nM) for 40 minutes, as indicated. The cells were immediately collected and nuclei were isolated, frozen, and stored as described in the Experimental Procedures. The GRO-seq experiment was conducted using two independently isolated replicates for each condition. *B*, Western blot analysis confirms PARP-1 knockdown and inhibition by PJ34. Whole cell lysates collected from Luc and PARP-1 knockdown cells under the conditions described in (A) were subjected to Western blotting analyses for PARP-1 and ERα. Actin was also analyzed as a loading control. PAR levels were analyzed by Western blotting using nuclear extracts from the same cell lines and treatment conditions.

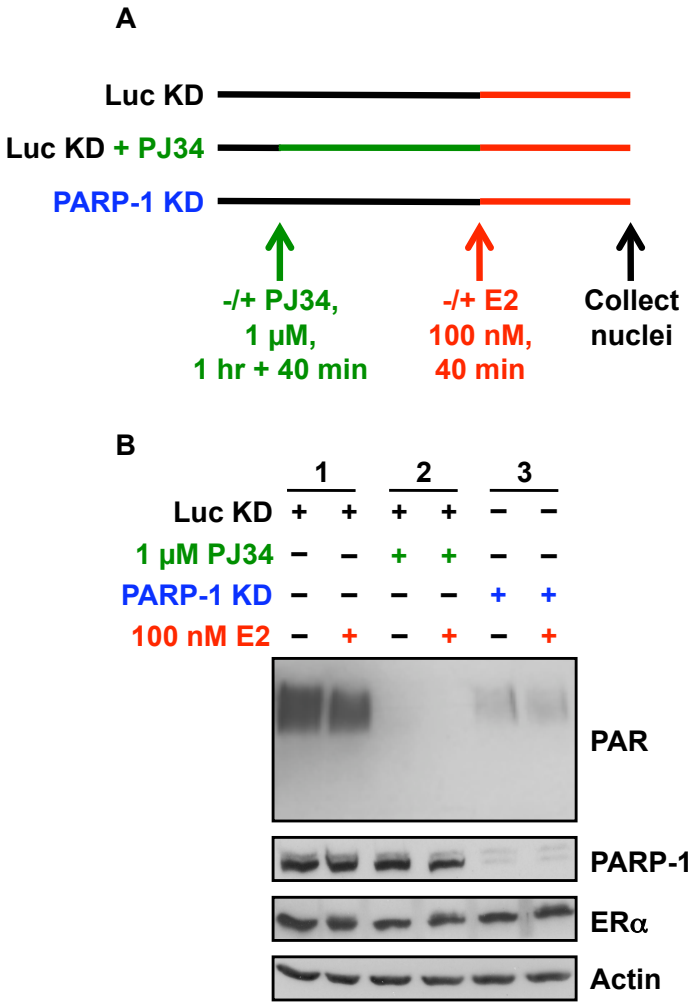
A
Luc KD
Luc KD + PJ34
PARP-1 KD
-/+ PJ34,
1 μM,
1 hr + 40 min
-/+ E2
100 nM,
40 min
Collect
nuclei
B
1
2
3
Luc KD + + + + – –
1 μM PJ34 – – + + – –
PARP-1 KD – – – – + +
100 nM E2 – + – + – +
PAR
PARP-1
ERα
Actin

Core *et al* (Figure 3.4; (Core et al., 2008)). The experiment was conducted using two biological replicates for each condition. Briefly, an *in vitro* run-on reaction was performed in the presence of sarkosyl (to inhibit non-engaged polymerases from re-engaging) and the NTP-analog, Bromo-UTP (Br-UTP; to allow for isolation/purification of nascent RNA). The NTP-analog, α^{32}P-CTP, was also included for the purpose of tracking the RNAs by autoradiography. RNA polymerases were allowed to run-on ~100 bases, using conditions previously determined (Core et al., 2008). The nuclear run-on RNA (NRO RNA) was then isolated, hydrolyzed to ~100 bases, and enriched using α-BrdUTP-conjugated agarose beads. The bound RNAs were washed several times and eluted, the 5' RNA caps were removed, and the ends repaired for subsequent adapter ligation steps. Small RNA adapters (Illumina) were ligated to the 5' end, followed by a second bead-binding enrichment. These two steps were repeated for the 3' adapter. An example of bead binding and elution of base-hydrolyzed Br-UTP-incorporated RNA to α-BrdUTP beads is shown in Figure 3.5A. To assess the efficiency of bead binding, equivalent amounts of the Input (I), flow through (Unbound, U), and eluted (Bound, B) fractions for each bead binding step were run on a denaturing PAGE and visualized by autoradiography. With each bead-binding step, the enrichment of NRO RNAs over the unbound fraction is dramatically enhanced (~5-15X). The resulting RNAs were reverse transcribed and PCR amplified using adapter-specific primers at an overall size of ~170 bases in length (Figure 3.5B). The cDNA libraries were then PAGE purified (Figure 3.5C) and sequenced from the 5' end on the Illumina 1G genome analyzer.

An average of 42 million reads were generated for each experimental condition (summed reads of biological replicates for each condition), approximately 70% of which were uniquely mapped to the human genome (Figure 3.6A). Notably, estrogen treatment, PJ34 treatment, and PARP-1 knockdown had no discernable effect on the

Figure 3.4. GRO-seq method. Nuclei isolated from Luc and PARP-1 knockdown cell lines, under the treatment conditions described in Figure 3.3, were subjected to GRO-seq methodology. Briefly, RNA polymerases were allowed to run-on ~100 bases in the presence of sarkosyl and the NTP-analog, Bromo-UTP (Br-UTP). The RNA was then isolated, hydrolyzed to ~100 bases, and bound to α-BrdUTP-conjugated agarose beads. The 5' RNA caps were removed and the ends repaired for subsequent adapter ligation steps. Small RNA adapters (Illumina) were ligated to the 5' and 3' ends, each step followed by a second bbead-binding enrichment. These two steps were repeated for the 3' adapter. The resulting RNAs were reverse transcribed and PCR amplified. The cDNA libraries were then PAGE purified and sequenced from the 5' end on the Illumina 1G genome analyzer. This figure was taken from Core *et al* (Core et al., 2008).

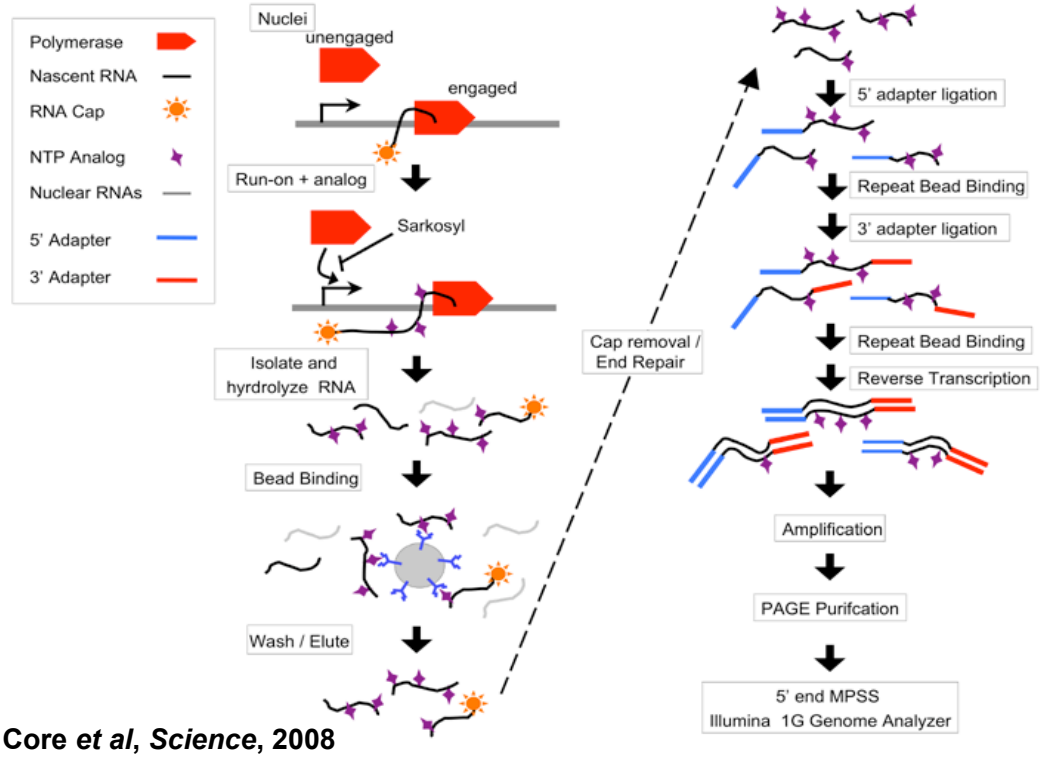

Core *et al*, *Science*, 2008

Figure 3.5. Bead-binding, PCR amplification, and PAGE purification of GRO-seq libraries. *A,* Example of binding and elution of base-hydrolyzed Br-UTP-RNA to α-BrdUTP beads. Isolated RNA from a nuclear run-on containing Br-UTP and α^{32}P-CTP was base hydrolyzed to ~100-120 bases (compare to marker, M), bound to α-BrdUTP-conjugated agarose beads, washed several times, and eluted from the resin. Equivalent amounts of the Input (I), flow through (Unbound, U), and eluted (Bound, B) fractions from each of the three bead-binding enrichment steps (1, 2, and 3) were run on a 6% denaturing PAGE and visualized by autoradiography to assess the efficiency of bead binding. *B*, Example of PCR amplification of NRO RNA. After the third bead-binding, the isolated NRO RNA was subjected to reverse transcription and subsequently amplified by 15-17 cycles of PCR. The resulting cDNA was visualized on an agarose gel to assess the size and quantity. *C*, Example of PAGE-purified cDNA libraries. After PCR amplification, the cDNA was run on a 6% non-denaturing acrylamide gel, the library was cut from the gel, and the cDNA was eluted and purified. A small fraction was the run on a 6% non-denaturing gel to assess the size, quantity, and quality of the gel-excised material.

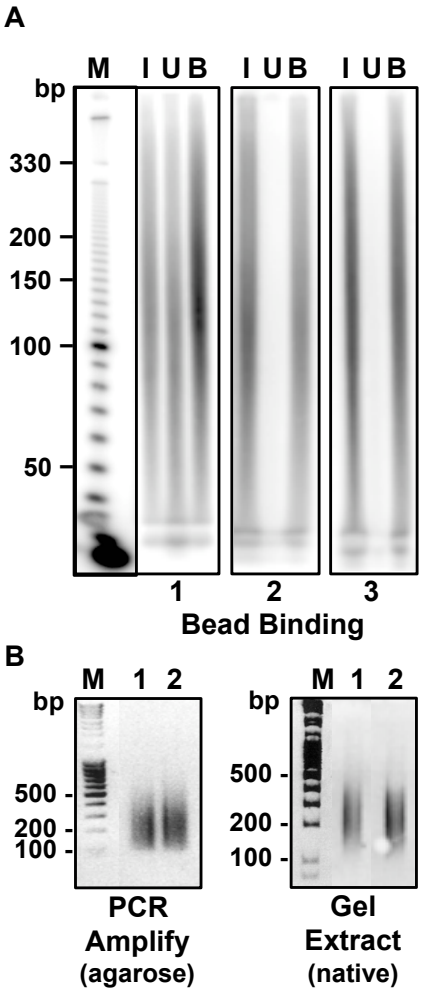
A
M I U B I U B I U B
bp
330
200
150
100
50
1 2 3
Bead Binding
B
M 1 2
bp
500
200
100
PCR
Amplify
(agarose)
M 1 2
bp
500
200
100
Gel
Extract
(native)

resulting library read counts. To determine the variability among libraries, a Pearson correlation analysis was performed between individual biological replicates for uniquely mapped reads from +1 to +13 kb relative to the TSS for annotated RefSeq genes (Figure 3.6B). Biological replicates for any given condition (grey boxes, diagonal) were among the highest correlations values. Upon estrogen treatment, the correlations between samples were reduced (*i.e.* Luc KD –E2 compared to Luc KD + E2), indicative of changes in gene expression. This effect was also seen in previously generated data sets from the Kraus lab (N.H. and W.L.K., unpublished). Notably, PJ34 treatment and PARP-1 knockdown did not have a discernable effect on the correlations between samples (unlike E2 treatment).

As a control, I compared the GRO-seq data to RT-qPCR data for previously identified PARP-1-regulated genes (Figure 3.7; (Frizzell et al., 2009)). For each gene, the GRO-seq reads were summed throughout the entire transcription unit (Figure 3.7A) and RT-qPCR analysis was performed (Figure 3.7B) for each of the three conditions (i) Luc KD, (ii) Luc KD + PJ34, and (iii) PARP-1 KD. Overall, the raw GRO-seq data matches well with the RT-qPCR measurements, an example of which is shown in Figure 3.7C. This suggests that, at the most basic level, the GRO-seq data set is reflective of changes seen at the mRNA level for gene-specific analyses.

Defining the estrogen-regulated transcriptome. After all the GRO-seq reads were mapped to the genome, I focused my analyses on annotated RefSeq genes. I plotted the sum of reads at each position (weighted by expression level and normalized to both number of genes and total reads) and centered the data at the TSS for each condition examined for all RefSeq genes (Figure 3.8). The resulting metagene profiles display reads on the sense strand moving toward the right (red), and antisense strand (blue) moving toward the left. This analysis revealed interesting aspects of my data.

Figure 3.6. Total read counts and correlations among GRO-seq libraries. *A*, The reads from biological replicates were summed to yield the total reads from Illumina sequencing for each condition. Also listed are the read counts that mapped uniquely to the human genome (hg19 assembly) and the overall percentage of mapped reads, relative to the total. *B*, Correlation analysis between individual biological replicates for each condition. Uniquely mapped reads from +1 to +13 kb relative to the TSS were used for Pearson correlation analyses for all condition combinations. Values in grey boxes represent the correlation between biological replicates in each condition.

A

	E2	All Reads Total	Mapped Reads Total	Mapped Reads %
Luc KD	–	37,782,246	28,749,124	76.09
	+	41,806,857	30,635,200	73.28
Luc KD + PJ34	–	47,264,167	34,918,448	73.88
	+	43,049,008	29,479,605	68.48
PARP-1 KD	–	45,578,219	27,208,690	59.70
	+	38,730,112	21,712,706	56.06

B

Rep. 1 ↓ / Rep. 2 →	E2	Luc KD –	Luc KD +	Luc KD + PJ34 –	Luc KD + PJ34 +	PARP-1 KD –	PARP-1 KD +
Luc KD	–	**0.93**	0.78	0.94	0.74	0.92	0.72
	+	0.69	**0.94**	0.69	0.97	0.77	0.96
Luc KD + PJ34	–	0.90	0.76	**0.90**	0.76	0.93	0.76
	+	0.68	0.94	0.68	**0.97**	0.76	0.96
PARP-1 KD	–	0.90	0.74	0.91	0.70	**0.90**	0.69
	+	0.67	0.91	0.67	0.94	0.76	**0.93**

Figure 3.7. GRO-seq data confirms PARP-1-regulated genes defined by expression microarray and RT-qPCR. *A*, The relative number of GRO-seq reads per transcription unit was summed and plotted for eight previously characterized PARP-1-regulated genes (Frizzell et al., 2009) for the basal conditions of the GRO-seq experiment (*i.e.*, Luc KD, Luc KD + PJ34, and PARP-1 KD; non-estrogen treated). *B*, RT-qPCR analysis reflects similar trends to the GRO-seq data for the same gene set. Total RNA was isolated from Luc and PARP-1 knockdown cell lines in the absence or presence of PJ34, reverse transcribed, and subjected to qPCR using gene-specific primers. Each bar is the mean + SEM (*error bars*) for three or more independent RNA isolations. The data for Luc KD and PARP-1 KD is exactly as published previously (Chapter 2; (Frizzell et al., 2009)). *C*, An example of GRO-seq data at a PARP-1 down-regulated gene, *ITPR1*, whose expression is not affected by PJ34 treatment, is shown via the University of California Santa Cruz (UCSC) Genome Browser. Each graph has identical x- and y-axes and only the plus strand is depicted.

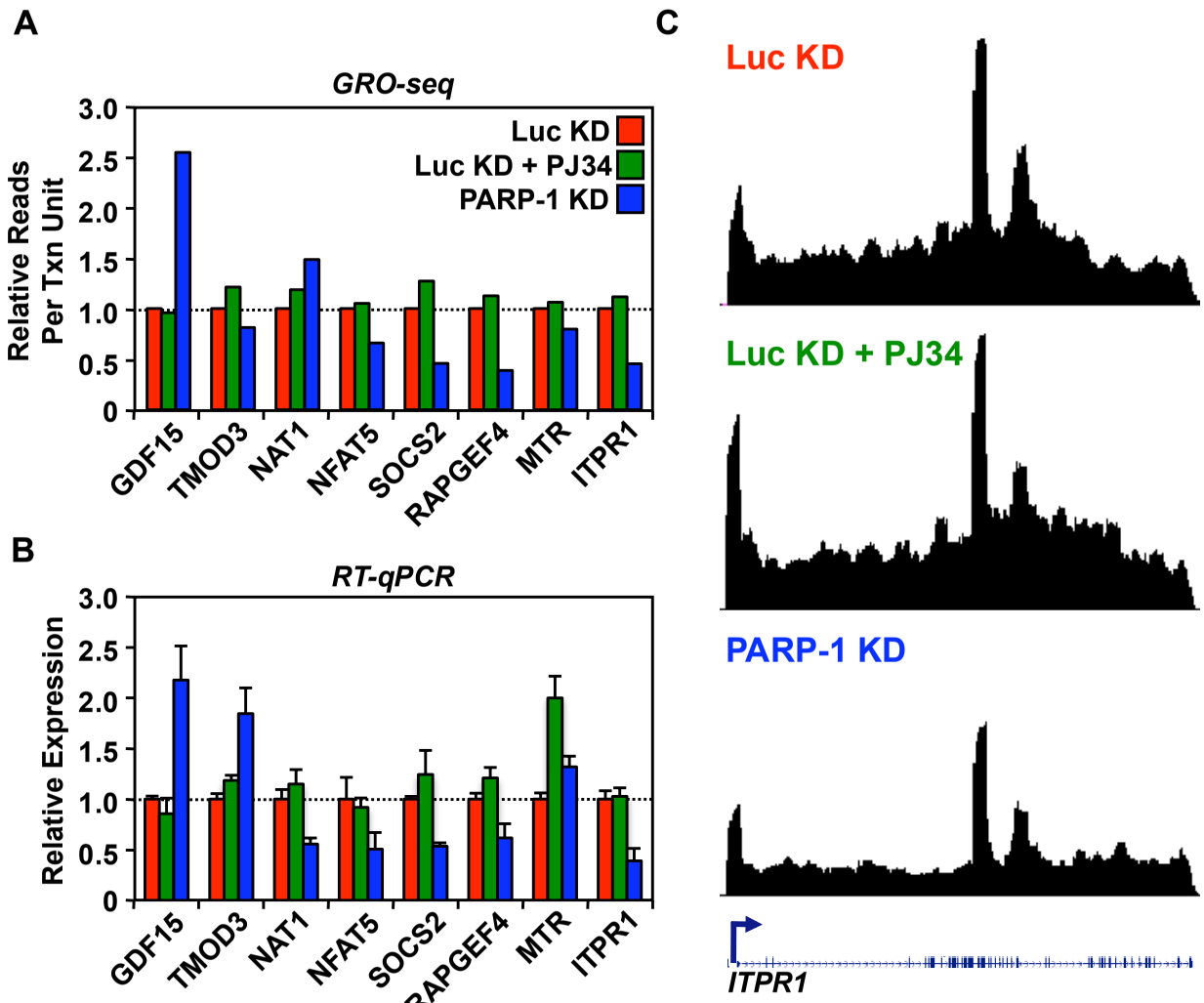
A
GRO-seq
Relative Reads Per Txn Unit
3.0
2.5
2.0
1.5
1.0
0.5
0
Luc KD
Luc KD + PJ34
PARP-1 KD
GDF15
TMOD3
NAT1
NFAT5
SOCS2
RAPGEF4
MTR
ITPR1
B
RT-qPCR
Relative Expression
3.0
2.5
2.0
1.5
1.0
0.5
0
GDF15
TMOD3
NAT1
NFAT5
SOCS2
RAPGEF4
MTR
ITPR1
C
Luc KD
Luc KD + PJ34
PARP-1 KD
ITPR1

Primarily, PJ34 treatment and PARP-1 knockdown does not seem to have a dramatic effect in overall gene transcription. In addition, changes in the height of the paused polymerase peak at the TSS are altered upon estrogen treatment, as well as with PJ34 treatment and PARP-1 knockdown. For example, upon estrogen treatment, the height of the paused peak increases in the Luc knockdown condition (Figure 3.8A and B), a result also seen in the previously generated GRO-seq data set in the Kraus lab (N.H. and W.L.K., unpublished). Notably, further analyses suggest that while the estrogen-dependent increase in RNA Pol II pausing is a consistent effect, the PJ34- and PARP-1 knockdown-dependent increase in RNA Pol II pausing is not statistically significant. Finally, the average peak position of the paused polymerase is altered upon PJ34 treatment, PARP-1 knockdown, and even estrogen treatment, which may coincide with the increase in the paused polymerase. Further analysis is required to determine if this positional element is a genuine effect.

In order to compare the estrogen-regulated transcriptome in each of the three conditions (i) Luc KD, (ii) Luc KD + PJ34, and (iii) PARP-1 KD, the total reads from +1 to +13 kb relative to the TSS for all 12 samples (all pairs of biological replicates) were used as input into the EdgeR software package (Robinson et al., 2010). The EdgeR software quantile normalizes all the reads within the given window, forcing the distribution of all samples to be equal, and calculates the parameters for a negative binomial distribution based on all pairs of biological replicates. For each gene, the read counts are compared between pair-wise conditions using an exact test, the p-value of which is corrected for multiple hypothesis testing using a false discovery rate (FDR) cut-off (*i.e.* 0.1%), defining the change as significantly different (or not) from the control. This analysis can be used for any pair-wise condition comparison (*i.e.* vehicle and estrogen treatment, or control and knockdown). The resulting data is plotted as the Log_{10} (gene body reads/total reads) for one condition versus another

Figure 3.8. Metagene profiles for all Ref-seq genes for each GRO-seq condition. *A through F*, The metagene profiles for vehicle and E2-treated samples are shown for Luc KD (*A and B*), Luc KD + PJ34 (*C and D*), and PARP-1 KD (*E and F*) conditions. The data are aligned at the TSS of all Ref-seq genes, and normalized as described in the text. The reads on the + strand (red) and – strand (blue) are shown.

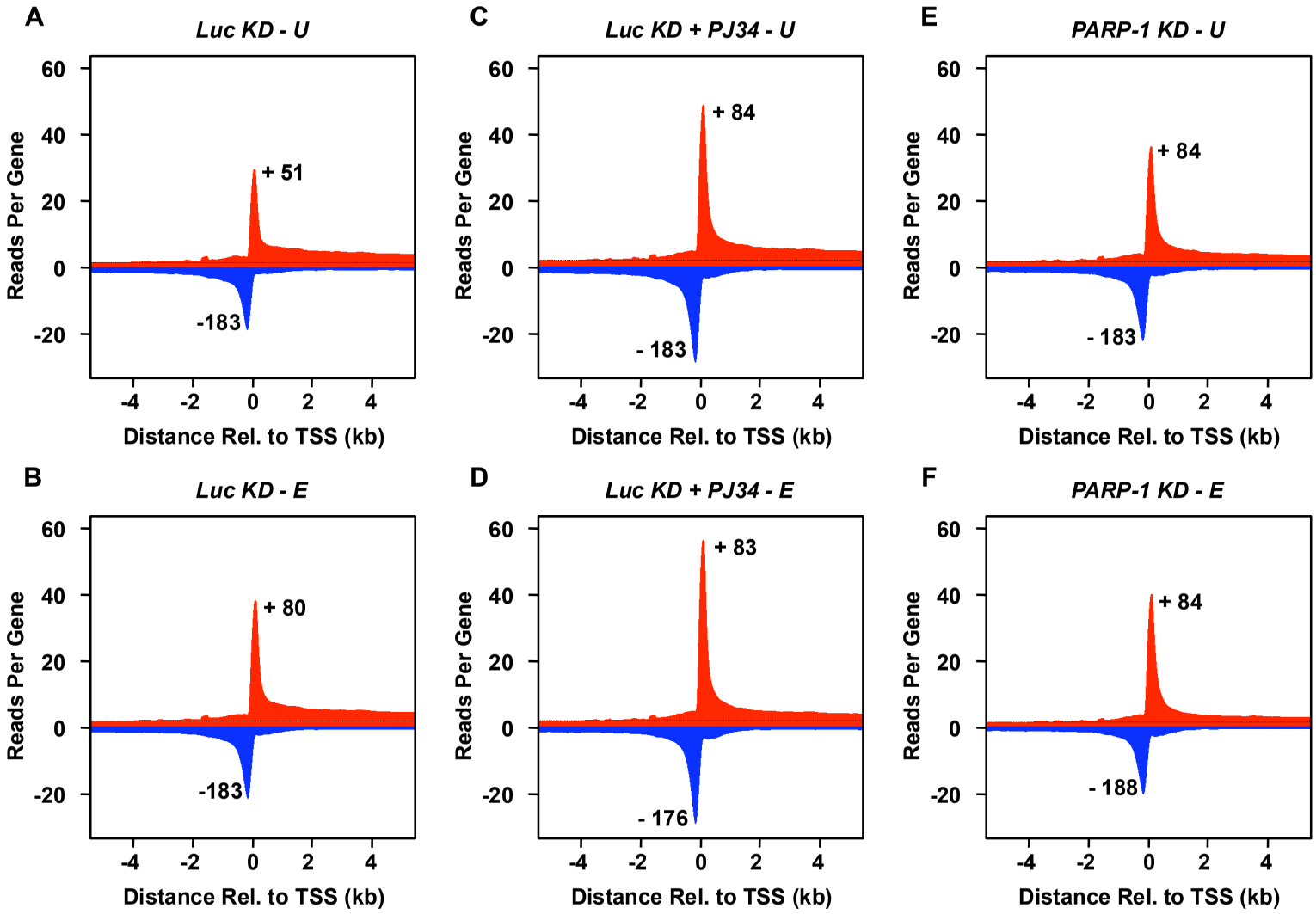
A
Luc KD - U
+ 51
-183
C
Luc KD + PJ34 - U
+ 84
- 183
E
PARP-1 KD - U
+ 84
- 183
B
Luc KD - E
+ 80
-183
D
Luc KD + PJ34 - E
+ 83
- 176
F
PARP-1 KD - E
+ 84
- 188
Reads Per Gene
60
40
20
0
-20
-4
-2
0
2
4
Distance Rel. to TSS (kb)

(Figures 3.9, 3.13, and 3.15). Black circles represent genes whose change between the two conditions is not statistically different, while red circles represent genes whose change between the two conditions is statistically different.

Using this analysis (0.1% FDR), I identified 1055 genes significantly regulated by estrogen in the Luc KD control condition (Figures 3.9A). Importantly, ~75% of these genes were previously identified to be regulated by estrogen in GRO-seq experiments in the Kraus lab (Figure 3.9B), conducted under nearly identical conditions (N.H. and W.L.K., unpublished). In that study, MCF-7 parental cells were grown and treated with estrogen for 40 minutes, much like the conditions in this study. However, there are a few important differences between them. First, although the experimental conditions are similar, the Luc knockdown cells in my study have undergone two independent shRNA integrations and are maintained under puromycin and G418 drug selection. This may interfere with basal as well as estrogen-mediated transcription. In addition, separate individuals performed the two studies at separate times. Due to these major differences, it is not uncommon to identify genes regulated in one study and not in another. However, of the nearly 800 genes that were defined as regulated in both studies, the estrogen response is highly reproducible, as determined using a Spearman's correlation analysis (Figure 3.9C; correlation coefficient = 0.88, p-value < 2.2×10^{-16}).

PARP-1 promoter localization is maintained upon estrogen treatment. In order to determine how PARP-1 might be altering the estrogen response, I asked whether or not PARP-1 protein localization was altered upon estrogen treatment. Using an antibody specific for PARP-1, I performed ChIP-chip experiments in MCF-7 cells using the high density tiling Niblegen platform (HD2) previously described (Gamble et al., 2010; Krishnakumar and Kraus, 2010), representing nearly 23,000 promoters

Figure 3.9. Comparison of E2-regulated genes in Luc knockdown and parental MCF-7 cells. *A*, Defining E2-regulated genes in Luc KD cells. Gene body reads (from +1 to +13 kb relative to the TSS) normalized to total reads in vehicle (U) and E2-treated (E) samples were compared in the Luc KD condition using the method and parameters described in the text. Each circle represents the degree of change upon E2 treatment for a single gene; black indicates no significant change, red indicates a significant change (0.1% FDR). Red circles below the diagonal represent a down-regulation upon E2-treatment, while those that are above the diagonal represent an up-regulation upon E2-treatment. *B*, Venn diagram of the unique E2-regulated genes in Luc KD and parental MCF-7 cells (unpublished data, N.H. and W.L.K). *C*, Correlation analysis of the commonly regulated genes (intersection) from panel B. The Spearman correlation coefficient and p-value are indicated.

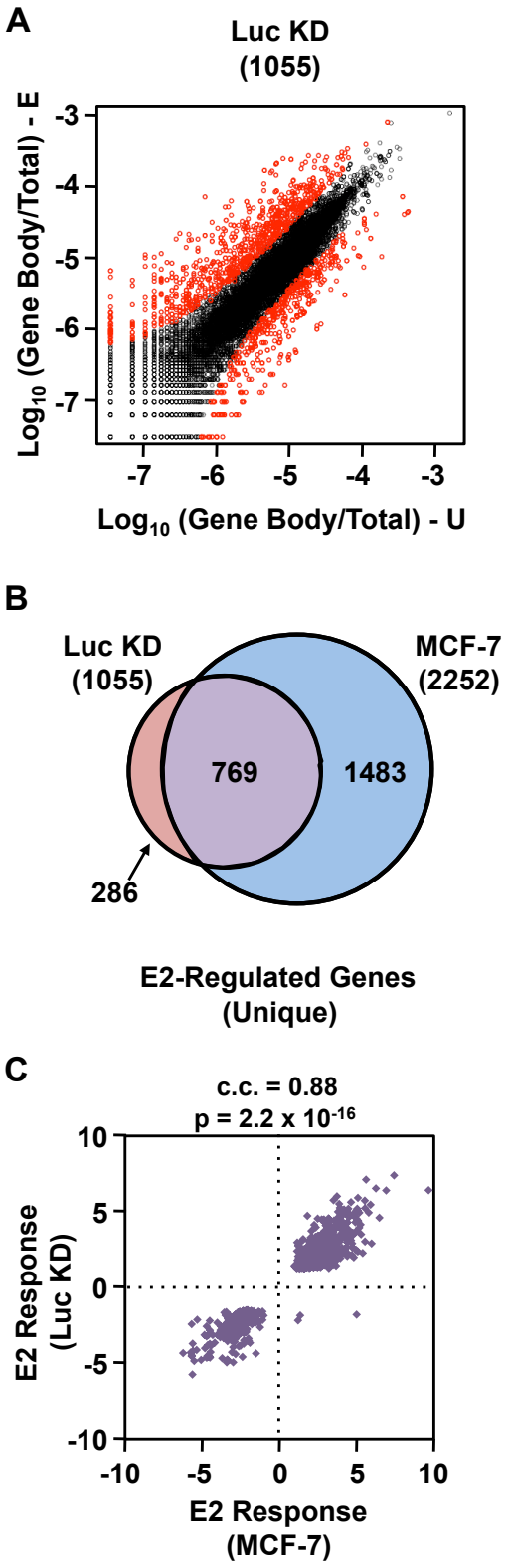
A
Luc KD
(1055)
Log10 (Gene Body/Total) - E
-3
-4
-5
-6
-7
-7
-6
-5
-4
-3
Log10 (Gene Body/Total) - U
B
Luc KD
(1055)
MCF-7
(2252)
769
1483
286
E2-Regulated Genes
(Unique)
C
c.c. = 0.88
p = 2.2 x 10-16
E2 Response
(Luc KD)
10
5
0
-5
-10
-10
-5
0
5
10
E2 Response
(MCF-7)

tiled from -7 to +3 kb surrounding the TSSs. Using previously defined criteria (Gamble et al., 2010; Krishnakumar et al., 2008; Krishnakumar and Kraus, 2010), I determined the promoter localization of PARP-1 in the absence and presence of estrogen. To determine if PARP-1 localization patterns changed upon estrogen treatment, I depicted the ChIP-chip data sets for each condition as a heat map in which each row corresponds to the ChIP-chip signal from -3 to +3 kb relative to the TSS for each gene represented on the array (Figure 3.10A). When the data are ordered for increasing average intensity of PARP-1 in the vehicle-treated condition (U), an obvious correspondence for PARP-1 in the E2-treated condition (E) is evident. An averaging analysis for all genes represented on the ChIP-chip array clearly displays the same result (Figure 3.10B). Furthermore, for estrogen-regulated genes defined by the GRO-seq analysis for which ChIP-chip data exists, the PARP-1 localization patterns do not change upon estrogen treatment (Figure 3.10C), regardless of direction of gene regulation (Figure 3.10D-F). These results are also seen for the same gene categories using a custom-designed Nimblegen platform previously described (Gamble et al., 2010; Krishnakumar et al., 2008), representing 4.14 Mb of genomic DNA including 1829 gene promoters typically tiled from -25 to +5 kb surrounding the TSSs (Figure 3.11B-E). Importantly, the PARP-1 profiles are nearly identical between the two platforms, albeit with differences in overall signal, and the overall histone levels are not altered upon E2-treatment (Figure 3.11A). Taken together, the results of my PARP-1 ChIP-chip experiments using two independent array platforms show that PARP-1 localization patterns are unaltered upon estrogen treatment.

PJ34 treatment and PARP-1 knockdown reduces the magnitude of the estrogen response. To determine the effect of PJ34 treatment and PARP-1 knockdown on estrogen-regulated genes, I first aligned my GRO-seq data to categories of estrogen-

Figure 3.10. PARP-1 localization is unaltered upon E2-treatment. *A*, Heat maps showing PARP-1 ChIP-chip data across ~23,000 promoters, tiled from -3 to +3 kb surrounding the transcription start sites (TSS). Parental MCF-7 cells were grown in estrogen-free medium for a minimum of three days, treated with vehicle (U) or estrogen (100 nM, E) for 40 minutes, crosslinked with formaldehyde, and subjected to a ChIP assay using the PARP-1 antibody, as described in the Experimental Procedures. The data in both panels are ordered for the average PARP-1 intensity in the U condition. *B*, Averaging analysis of the Log_2 enrichment ratios for PARP-1 under vehicle (blue) and E2 (red) treated MCF-7 cells in shown for all genes represented on the array. *C, D, E, and F,* For genes defined as E2-regulated by GRO-seq in the Luc KD condition, described in Figure 3.9, the average Log_2 enrichment ratios for the corresponding PARP-1 ChIP-chip data is plotted. The PARP-1 profile in vehicle (blue) and E2 (red) treated MCF-7 cells in shown for all E2-regulated genes (C) for which ChIP-chip data exists, only up-regulated genes (D), non-regulated genes (E), and only down-regulated genes (F).

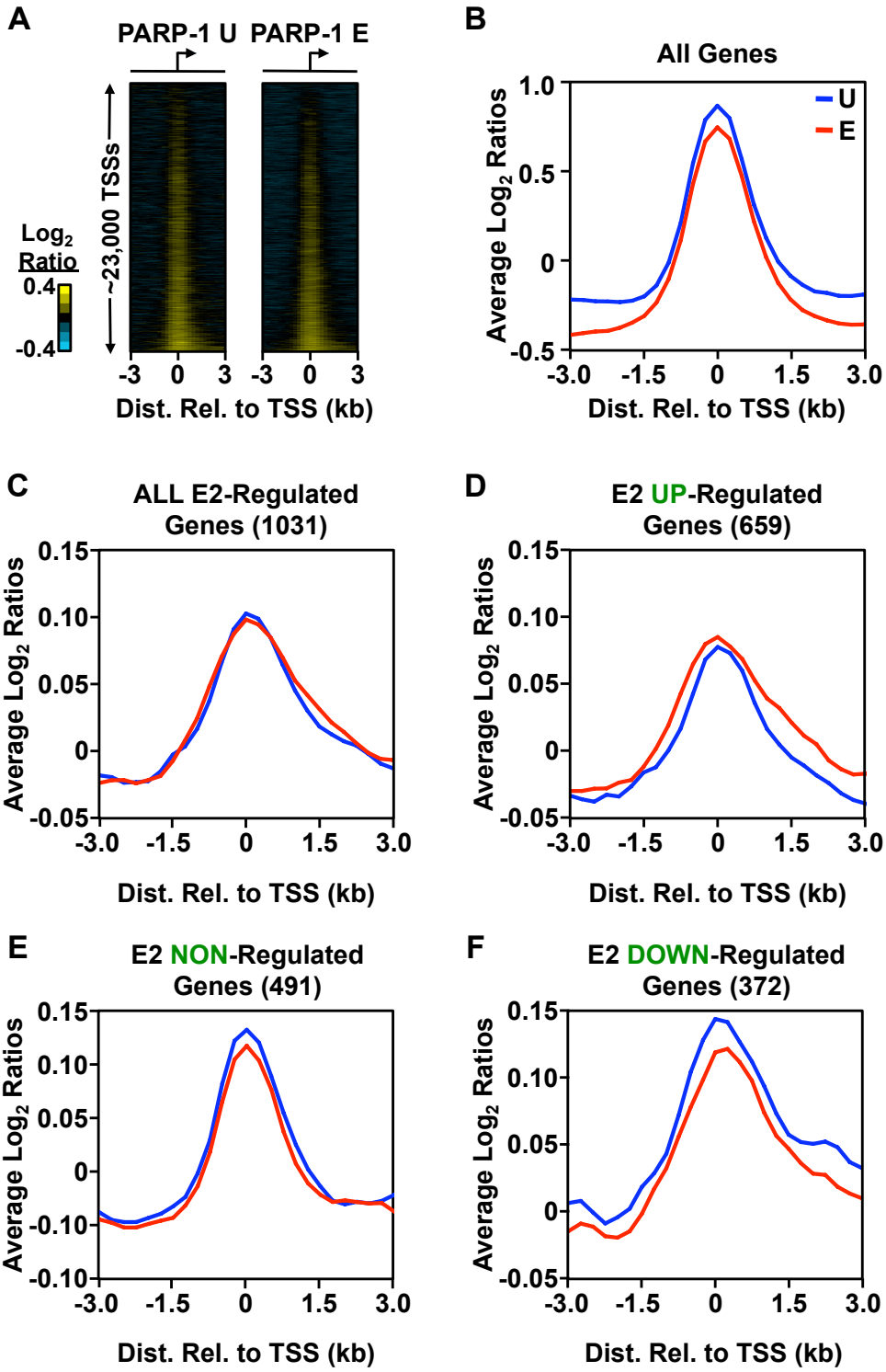
A
PARP-1 U
PARP-1 E
~23,000 TSSs
Log2 Ratio
0.4
-0.4
-3
0
3
Dist. Rel. to TSS (kb)
B
All Genes
U
E
Average Log2 Ratios
1.0
0.5
0
-0.5
-3.0
-1.5
1.5
3.0
C
ALL E2-Regulated Genes (1031)
D
E2 UP-Regulated Genes (659)
E
E2 NON-Regulated Genes (491)
F
E2 DOWN-Regulated Genes (372)

Figure 3.11. Comparison of PARP-1 ChIP-chip data across platforms. *A*, Averaging analysis of the Log_2 enrichment ratios for PARP-1 under vehicle (blue, light blue) and E2 (red, orange) treated MCF-7 cells for the 1401 genes represented on both the Nimblegen HD2 and custom-designed array platforms. H3 ChIP-chip data (custom platform only) is shown for comparison. *B, D, D, and E,* For genes defined as E2-regulated by GRO-seq in the Luc KD condition, described in Figure 3.9, the average Log_2 enrichment ratios for the corresponding PARP-1 ChIP-chip data (custom platform only) is plotted. The PARP-1 profile in vehicle (light blue) and E2 (orange) treated MCF-7 cells in shown for all E2-regulated genes (B) for which ChIP-chip data exists, only up-regulated genes (C), non-regulated genes (D), and only down-regulated genes (E). Although the number of genes in each category is smaller, the overall trends of PARP-1 localization remain consistent between platforms.

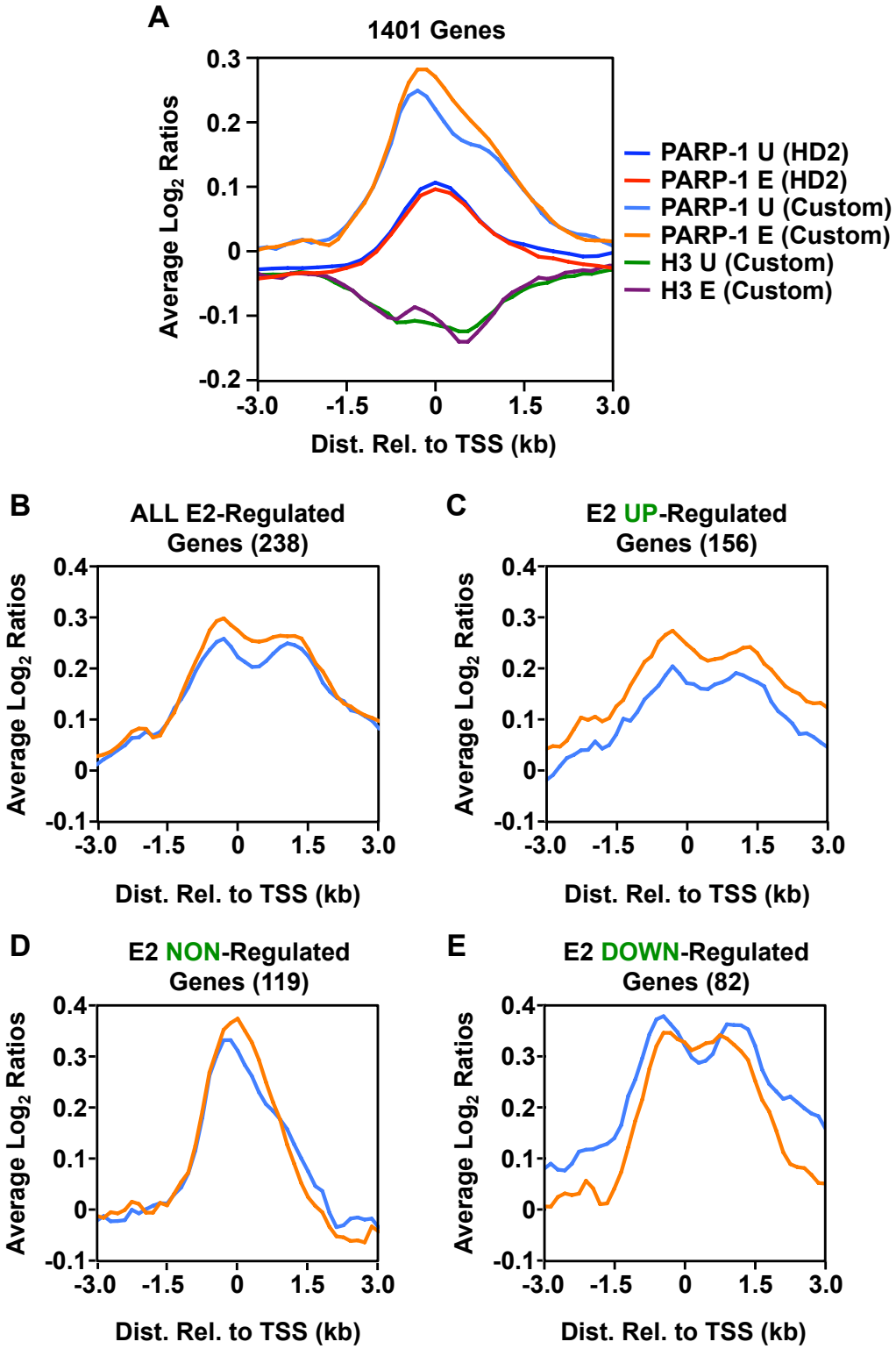
A
1401 Genes
Average Log2 Ratios
0.3
0.2
0.1
0
-0.1
-0.2
-3.0
-1.5
0
1.5
3.0
Dist. Rel. to TSS (kb)
PARP-1 U (HD2)
PARP-1 E (HD2)
PARP-1 U (Custom)
PARP-1 E (Custom)
H3 U (Custom)
H3 E (Custom)
B
ALL E2-Regulated Genes (238)
C
E2 UP-Regulated Genes (156)
D
E2 NON-Regulated Genes (119)
E
E2 DOWN-Regulated Genes (82)

regulated genes previously identified from GRO-seq experiments in parental MCF-7 cells (Figure 3.12; N.H. and W.L.K., unpublished). For genes that are up-regulated (peak at 40 min E2; Figure 3.12A) or down-regulated (at 10, 40, or 160 min E2; Figure 3.12B) by estrogen, I plotted the sum of reads at each position (weighted by expression level and normalized to both number of genes and total reads) and centered the data at the TSS. Regardless of the cell line or treatment condition, the overall trends for estrogen up-regulated and down-regulated genes are largely similar.

Using the analysis and parameters described above, I identified the estrogen-regulated genes in all three of my experimental conditions: (i) Luc KD, (ii) Luc KD + PJ34, and (iii) PARP-1 KD (Figure 3.13A). PJ34 treatment slightly increased the total number of estrogen-responsive genes, while PARP-1 knockdown slightly reduced the total number of estrogen-responsive genes. However, most of the genes (nearly 90%) in any of the three conditions were also regulated in at least one other condition (Figure 3.13B). This result indicates that the general estrogen response is highly maintained upon PARP inhibition and specific depletion of PARP-1, an effect noted using estrogen-regulated genes in MCF-7 parental cells (Figure 3.12). And, although I have identified approximately 12% of genes in each condition that are regulated by estrogen in *only* that condition, many of these genes contain low read counts, which may be indicative of noise, rather than effective regulation. Thus, these classes need to be interpreted with caution. In support of this result, only the largest class of genes is significantly enriched in gene ontological categories that are indicative of estrogen signaling pathways (Table 3.1), while the outlying classes are not. In addition, PARP-1 localization patterns are similar across all classes in the Venn diagram (Figure 3.14). Importantly, there are very few genes regulated by PJ34 treatment and PARP-1 knockdown as compared to the Luc knockdown control (Figure 3.15), indicating that basal transcription is not significantly altered. Therefore, any alterations in the

Figure 3.12. Metagene profiles of previously defined estrogen-regulated genes for each GRO-seq condition. *A and B*, The metagene profiles for vehicle (blue, light blue) and E2-treated (red, pink) samples are shown for Luc KD, Luc KD + PJ34, and PARP-1 KD conditions. The genes shown in each panel are estrogen up-regulated (A), which peak at 40 min of estrogen treatment, and estrogen down-regulated (B), as defined by GRO-seq time-course experiments (unpublished data, N.H. and W.L.K.). The data are aligned at the TSS and normalized as described in the text. The reads on the + strand (red, blue) and – strand (pink, light blue) are shown.

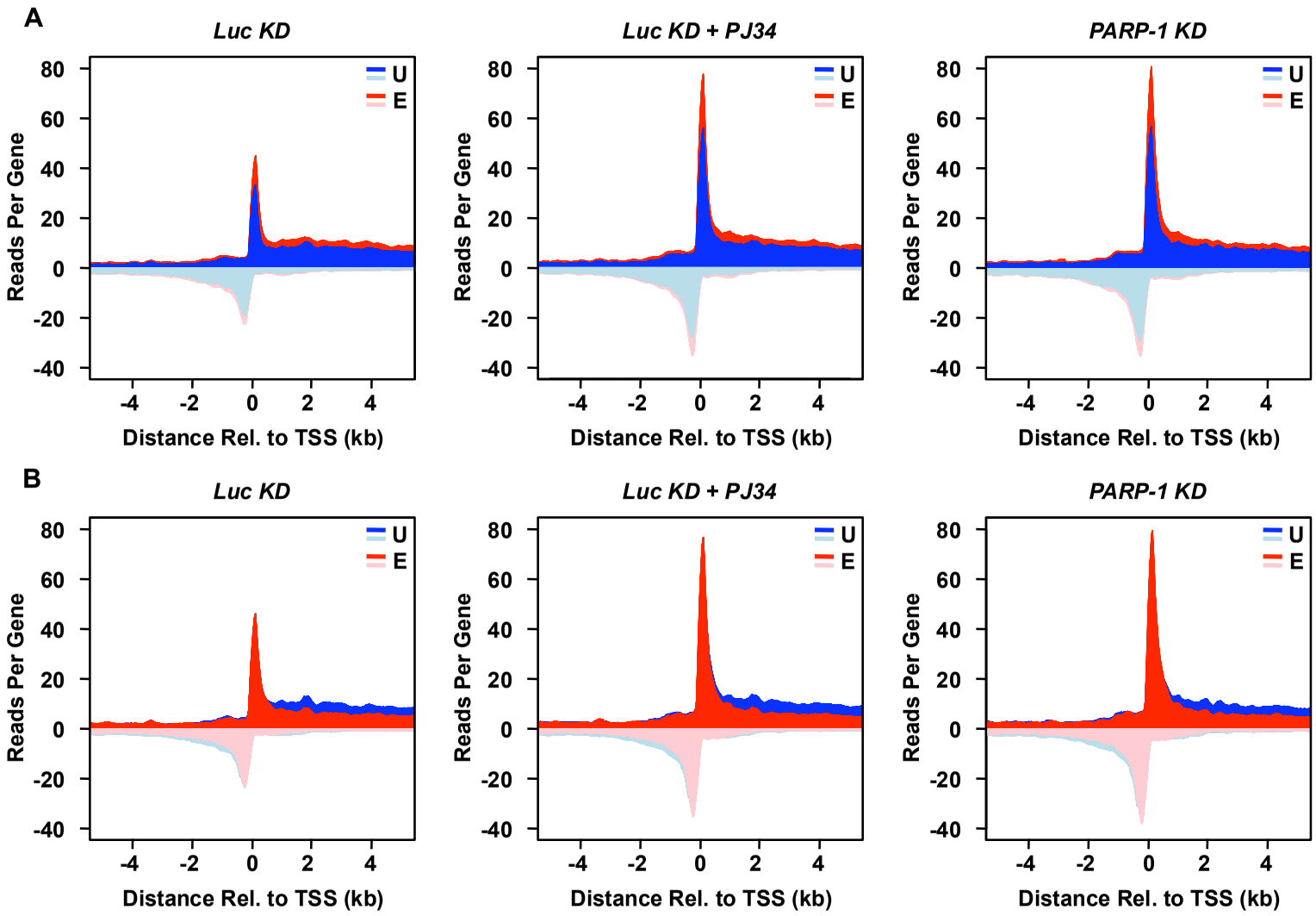
A
Luc KD
Luc KD + PJ34
PARP-1 KD
B
Luc KD
Luc KD + PJ34
PARP-1 KD
U
E
Reads Per Gene
80
60
40
20
0
-20
-40
-4
-2
0
2
4
Distance Rel. to TSS (kb)

Figure 3.13. The estrogen response is highly maintained upon PJ34 treatment and PARP-1 knockdown. *A*, Defining E2-regulated genes in Luc KD, PJ34-treated, and PARP-1 KD cells. Gene body reads (from +1 to +13 kb relative to the TSS) normalized to total reads in all biological replicates were compared the methods and parameters described in the text. The vehicle (U) treated and E2-treated (E) samples were compared in Luc KD, Luc KD + PJ34, and PARP-1 KD conditions. Each circle represents the degree of change upon E2 treatment for a single gene; black indicates no significant change, red indicates a significant change (0.1% FDR). Red circles below the diagonal represent a down-regulation upon E2-treatment, while those that are above the diagonal represent an up-regulation upon E2-treatment. The total number of unique genes regulated upon E2 treatment is listed. *B*, Venn diagram comparing E2-regulated genes in the three experimental conditions.

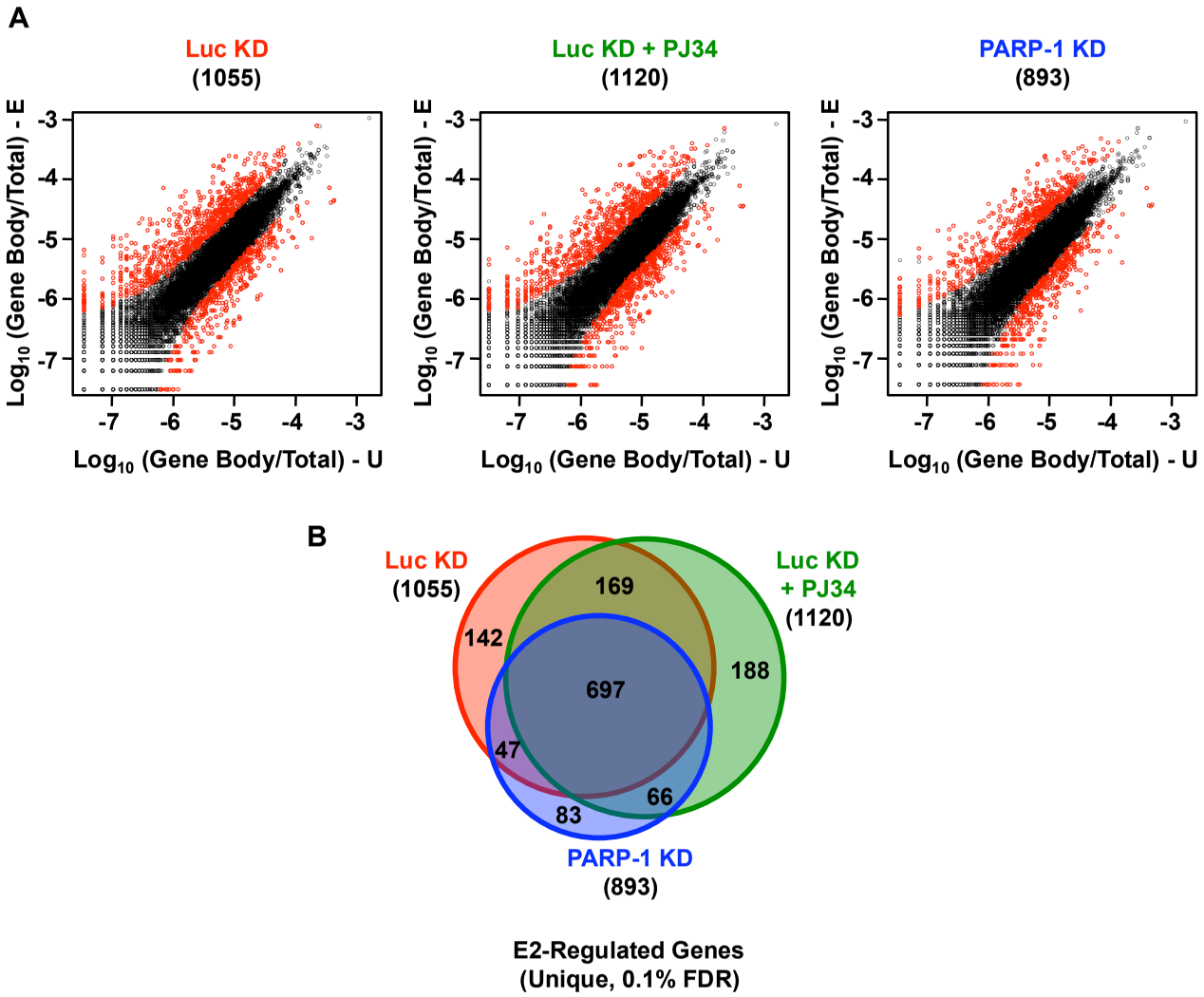
A
Luc KD
(1055)
Luc KD + PJ34
(1120)
PARP-1 KD
(893)
Log10 (Gene Body/Total) - E
Log10 (Gene Body/Total) - U
-3
-4
-5
-6
-7
B
Luc KD
(1055)
Luc KD
+ PJ34
(1120)
PARP-1 KD
(893)
142
169
188
697
47
66
83
E2-Regulated Genes
(Unique, 0.1% FDR)

Table 3.1. Summary of the most significant gene ontology terms enriched in each Venn diagram class shown in Figure 3.12. The enrichment of gene ontology terms in estrogen regulated genes in one, two, or three GRO-seq conditions (*i.e.* each category in the Venn diagram shown in Figure 3.12) was compared to all RefSeq genes in the human genome for all three ontology aspects. Only those categories with significant GO terms (p-value < 0.0001) are represented.

Gene Ontology Term[a]	Aspect[b]	*P*-value
Luc KD (142 genes)		
Membrane	CC	7.65×10^{-5}
Luc KD and Luc KD + PJ34 (169 genes)		
Membrane	CC	5.45×10^{-5}
Luc KD and Luc KD + PJ34 and PARP-1 KD (687 genes)		
Membrane	CC	5.01×10^{-13}
Cell part	CC	5.75×10^{-13}
Cell	CC	5.86×10^{-13}
Cytoplasm	CC	5.75×10^{-9}
Plasma membrane	CC	7.38×10^{-8}
Intracellular	CC	1.48×10^{-7}
Membrane part	CC	1.87×10^{-7}
Plasma membrane part	CC	2.83×10^{-6}
Intracellular part	CC	4.18×10^{-6}
Cell surface	CC	1.14×10^{-5}
Insoluble fraction	CC	6.49×10^{-5}
Cell fraction	CC	8.54×10^{-5}
Protein binding	MF	1.68×10^{-14}
Binding	MF	2.16×10^{-12}
PDZ domain binding	MF	1.75×10^{-7}
Protein domain specific binding	MF	2.85×10^{-6}
Enzyme regulator activity	MF	2.02×10^{-5}
Multicellular organismal development	BP	5.20×10^{-20}
Developmental process	BP	6.89×10^{-20}
System development	BP	8.76×10^{-20}
Anatomical structure development	BP	4.51×10^{-18}
Biological regulation	BP	5.13×10^{-17}
Multicellular organismal process	BP	7.34×10^{-17}
Organ development	BP	8.50×10^{-17}
Regulation of cellular process	BP	2.96×10^{-16}
Regulation of biological process	BP	1.65×10^{-15}
Signaling	BP	9.43×10^{-15}
Signaling pathway	BP	4.69×10^{-14}
Cellular process	BP	1.20×10^{-12}
Cell differentiation	BP	1.26×10^{-12}
Negative regulation of biological process	BP	2.27×10^{-12}
Cellular developmental process	BP	3.11×10^{-12}
Negative regulation of cellular process	BP	9.69×10^{-12}
Signaling process	BP	6.92×10^{-11}
Signal transmission	BP	1.34×10^{-10}
Regulation of multicellular organismal process	BP	1.79×10^{-10}
Signal transduction	BP	2.35×10^{-10}
Anatomical structure morphogenesis	BP	3.70×10^{-10}
Organ morphogenesis	BP	2.57×10^{-9}
Cell communication	BP	3.98×10^{-9}
Tissue development	BP	7.63×10^{-9}

Table 3.1 (cont'd)

Intracellular signaling pathway	BP	1.14×10^{-8}
Regulation of signaling pathway	BP	3.23×10^{-8}
Response to chemical stimulus	BP	4.32×10^{-8}
Cell surface receptor linked signaling pathway	BP	4.98×10^{-8}
Regulation of developmental process	BP	9.30×10^{-8}
Regulation of cell communication	BP	1.66×10^{-7}
Cell migration	BP	2.34×10^{-7}
Regulation of cell differentiation	BP	2.48×10^{-7}
Intracellular signal transduction	BP	2.85×10^{-7}
Positive regulation of biological process	BP	3.65×10^{-7}
Nervous system development	BP	3.93×10^{-7}
Regulation of cellular component movement	BP	4.19×10^{-7}
Cell development	BP	5.26×10^{-7}
Regulation of localization	BP	5.50×10^{-7}
Cell proliferation	BP	6.30×10^{-7}
Regulation of cell migration	BP	8.74×10^{-7}
Regulation of phosphorylation	BP	1.48×10^{-6}
Positive regulation of cellular process	BP	1.81×10^{-6}
Regulation of phosphate metabolic process	BP	1.87×10^{-6}
Regulation of phosphorus metabolic process	BP	1.87×10^{-6}
Cell motility	BP	1.91×10^{-6}
Localization of cell	BP	1.91×10^{-6}
Regulation of biological quality	BP	5.48×10^{-6}
Regulation of multicellular organismal development	BP	7.55×10^{-6}
Regulation of locomotion	BP	8.54×10^{-6}
Response to steroid hormone stimulus	BP	8.87×10^{-6}
Regulation of metabolic process	BP	9.75×10^{-6}
Regulation of cell proliferation	BP	1.25×10^{-5}
Response to estrogen stimulus	BP	1.78×10^{-5}
Response to hormone stimulus	BP	2.14×10^{-5}
Lipid metabolic process	BP	2.54×10^{-5}
Cellular response to chemical stimulus	BP	3.58×10^{-5}
Localization	BP	3.65×10^{-5}
Cellular component movement	BP	3.77×10^{-5}
Enzyme linked receptor protein signaling pathway	BP	3.81×10^{-5}
Response to endogenous stimulus	BP	4.39×10^{-5}
Positive regulation of macromolecule metabolic process	BP	4.46×10^{-5}
Negative regulation of signaling pathway	BP	5.35×10^{-5}
Regulation of signaling process	BP	5.77×10^{-5}
Cell morphogenesis involved in differentiation	BP	6.39×10^{-5}
Regulation of primary metabolic process	BP	7.05×10^{-5}
Regulation of cellular metabolic process	BP	8.29×10^{-5}

Figure 3.14. PARP-1 localization is unaltered upon E2-treatment among each Venn diagram category. *A-G*, Averaging analysis of the Log_2 enrichment ratios for PARP-1 under vehicle (blue) and E2 (red) treated MCF-7 cells is shown for genes within each Venn diagram category, described in Figure 3.12, for which ChIP-chip data exists. PARP-1 profiles are plotted for genes regulated by estrogen in only one condition (A, B, and C), two conditions (D, E, and F), and three conditions (G).

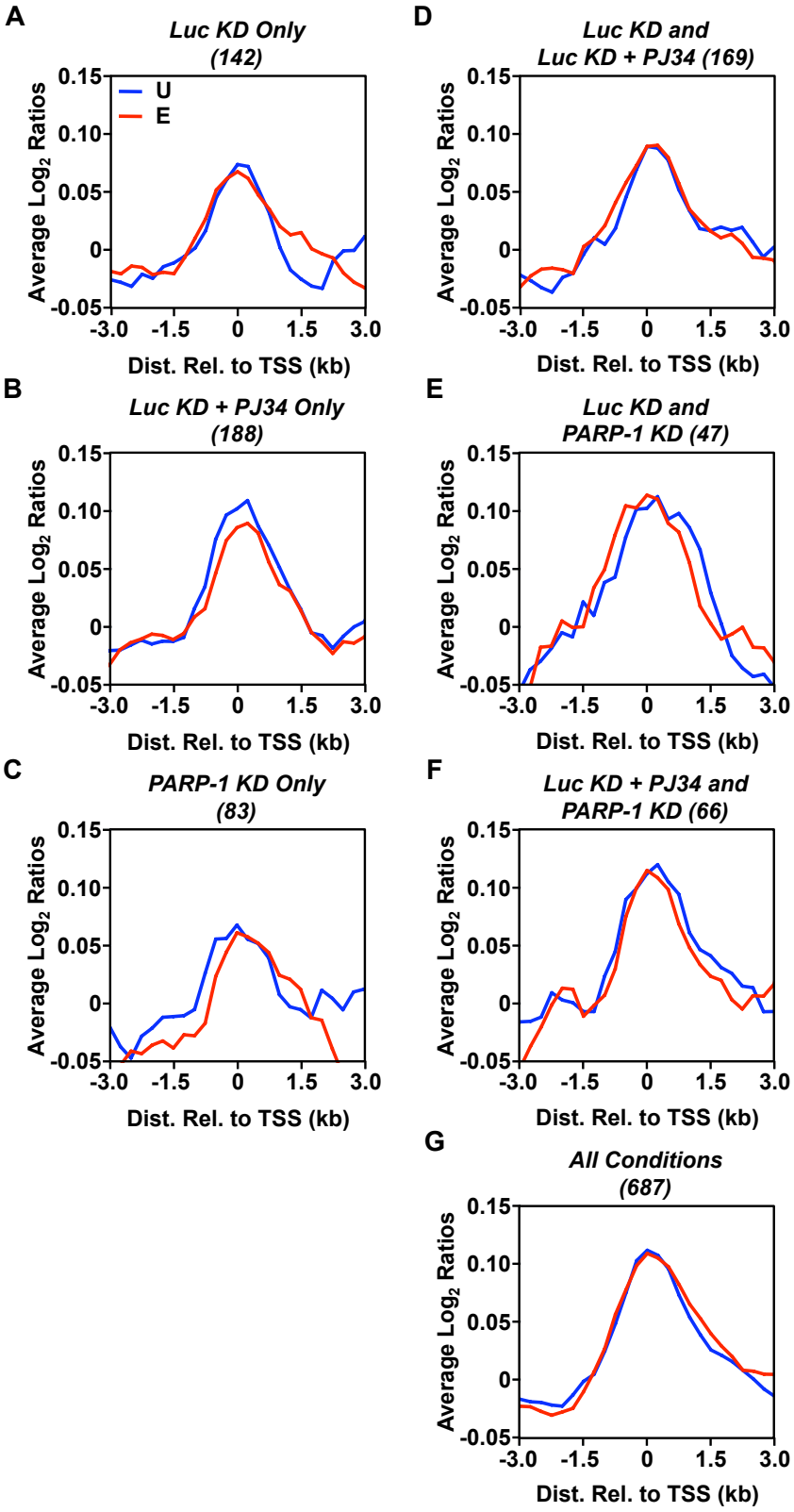
A
Luc KD Only
(142)
U
E
Average Log2 Ratios
0.15
0.10
0.05
0
-0.05
-3.0
-1.5
0
1.5
3.0
Dist. Rel. to TSS (kb)
B
Luc KD + PJ34 Only
(188)
C
PARP-1 KD Only
(83)
D
Luc KD and
Luc KD + PJ34 (169)
E
Luc KD and
PARP-1 KD (47)
F
Luc KD + PJ34 and
PARP-1 KD (66)
G
All Conditions
(687)

estrogen response can be attributed to changes in the treated condition, rather than the untreated condition. While this basal comparison is seemingly different than the expression microarray and qPCR analyses previously reported (Figure 3.7 and Chapter 2; (Frizzell et al., 2009)), one should use caution in this interpretation. This GRO-seq analysis is performed using stringent statistical criteria, incorporating the data and variation of at least 6 samples. Thus, global analyses are not as useful for detecting subtle changes that can be detected at the gene-specific level. Finally, the GRO-seq data reflects events occurring on the genomic DNA level, while RT-qPCR analyses reflect stead-state levels of mRNA, two independent measurements.

My results indicate that PJ34 treatment and PARP-1 knockdown does not dramatically change the genes that are responsive to estrogen. To answer this question with regard to the fold estrogen response at each gene, I compared the PJ34 treated or PARP-1 knockdown condition to the Luc knockdown control, plotting the fold estrogen response (Figure 3.16A and B, respectively). Only those genes that are considered regulated by estrogen in at least one of the two conditions is plotted. Overall, the correlations are tight, with some variation. By applying a fold change cut-off (Log_2 FC >2 or <-2 in one condition and Log_2 FC >-1 or <1 in the other condition), I identified only a few genes regulated by estrogen in one condition, but not in the other (shown in red). Two of the nine genes were tested in gene-specific RT-qPCR assays (Figure 3.16C), and confirm this result.

However, this analysis does not indicate whether the overall magnitude of the estrogen response is enhanced or reduced by PARP inhibition or PARP-1 knockdown, although there was some variation in the graphical representation (Figure 3.16B, for example). In order to determine if the magnitudes of estrogen-responsive genes are changed under these conditions, I compared the 697 genes defined to be estrogen-regulated in all three conditions examined (Figure 3.13B). Of these, ~1/3 of the genes

Figure 3.15. PJ34 treatment and PARP-1 knockdown does not alter basal transcription in MCF-7 cells. *A and B*, Gene body reads (from +1 to +13 kb relative to the TSS) normalized to total reads in Luc KD and Luc KD + PJ34 (A) or PARP-1 KD (B) samples were compared using the method and parameters described in the text. Each circle represents the degree of change upon PJ34-treatment or PARP-1 KD for a single gene; black indicates no significant change, red indicates a significant change (0.1% FDR). Red circles below the diagonal represent a down-regulation upon PJ34-treatment or PARP-1 KD, while those that are above the diagonal represent an up-regulation upon PJ34-treatment or PARP-1 KD. The two genes that are considered statistically different than Luc KD are indicated in each panel.

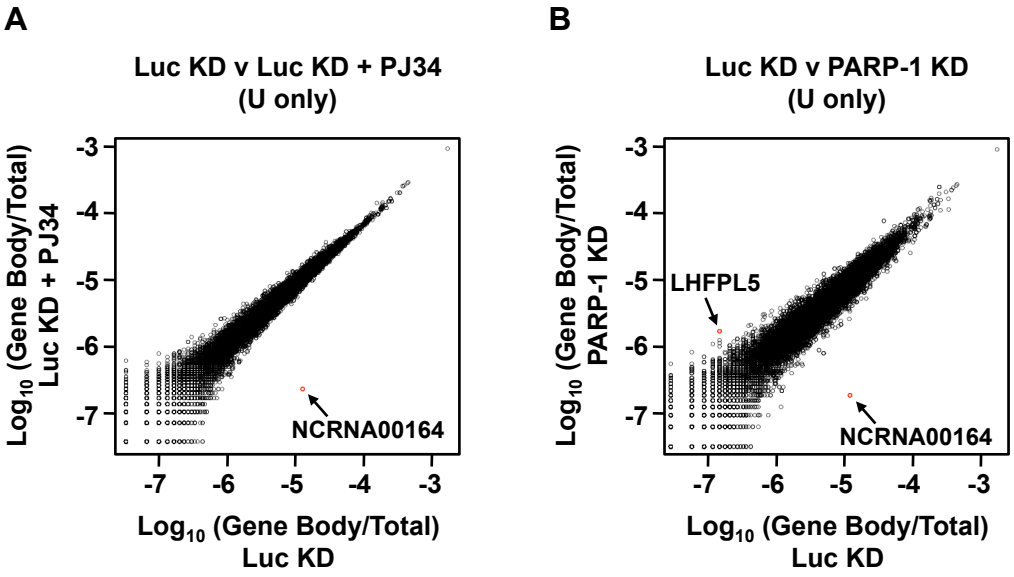
A
Luc KD v Luc KD + PJ34
(U only)
Log10 (Gene Body/Total)
Luc KD + PJ34
-3
-4
-5
-6
-7
NCRNA00164
-7
-6
-5
-4
-3
Log10 (Gene Body/Total)
Luc KD
B
Luc KD v PARP-1 KD
(U only)
Log10 (Gene Body/Total)
PARP-1 KD
LHFPL5
NCRNA00164
Log10 (Gene Body/Total)
Luc KD

Figure 3.16. Few genes are estrogen responsive in only one GRO-seq condition. *A and B*, The Log_2 estrogen response relative to the vehicle treated (E/U) in Luc KD and Luc KD + PJ34 (A) or PARP-1 KD (B) samples were compared using the method and parameters described in the text. Only those genes displaying a significant estrogen response in at least one of the two conditions is shown. Each circle represents the degree of change upon E2-treatment for a single gene. Black indicates significant changes in both conditions; red indicates a significant change in one condition but not the other (Log_2 fold change > 2 or < -2 in one condition and Log_2 fold change > -1 and < 1 for the other condition; 0.1% FDR). Only a few genes are considered regulated by estrogen in only Luc KD, Luc KD + PJ34, or PARP-1 KD. *C*, RT-qPCR analysis for two genes identified from the analysis in panels A and B. Total RNA was isolated from Luc and PARP-1 knockdown cell lines in the absence or presence of PJ34 and E2 for the time points indicated, reverse transcribed, and subjected to qPCR using gene-specific primers for *ABCA4* and *CALCR*. Each point is the mean + SEM (*error bars*) for four independent RNA isolations.

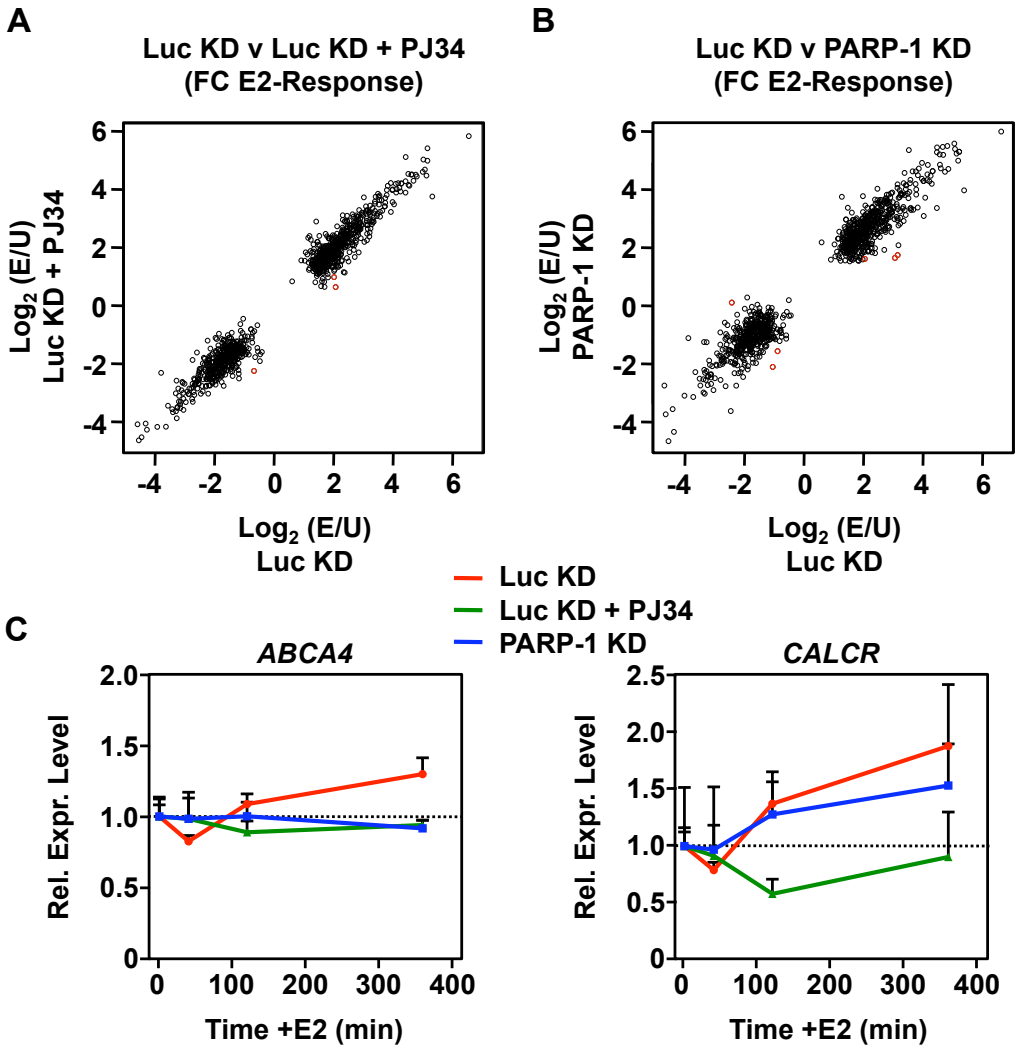
A
Luc KD v Luc KD + PJ34
(FC E2-Response)
Log2 (E/U)
Luc KD + PJ34
Log2 (E/U)
Luc KD
B
Luc KD v PARP-1 KD
(FC E2-Response)
Log2 (E/U)
PARP-1 KD
Log2 (E/U)
Luc KD
Luc KD
Luc KD + PJ34
PARP-1 KD
C
ABCA4
Rel. Expr. Level
Time +E2 (min)
CALCR
Rel. Expr. Level
Time +E2 (min)

are down-regulated in response to estrogen, while ~2/3 are up-regulated in response to estrogen (defined by the E2-response in the Luc KD condition). For the E2 down-regulated genes (Figure 3.17A), PJ34 treatment and PARP-1 knockdown have little effect on the median and overall dynamic range of the estrogen response. However, for the E2 up-regulated genes (Figure 3.17B), PJ34 treatment and PARP-1 knockdown seemingly quenches the overall dynamic range of the estrogen response. An example of this result is depicted in Figure 3.17C at the *HSPB8* gene.

Interestingly, further analysis revealed that the most up-regulated and most down-regulated genes have the largest degree of change in the estrogen response upon PJ34 treatment and PARP-1 knockdown (Figure 3.18A and B). In both cases, the effective estrogen response is reduced and PARP-1 knockdown has a greater effect than PJ34 treatment. Notably, regardless of the degree of estrogen response, PARP-1 levels remain unchanged upon estrogen treatment (Figure 3.19A and B). For up-regulated genes, PARP-1 knockdown also affects genes with the lowest basal expression level, many of which also have the highest estrogen responses. Again, regardless of expression level in the basal state, PARP-1 remains unchanged upon estrogen treatment (Figure 3.19C and D). However, the overall levels are different between low expressed and high expressed gene classes, a result previously reported (Krishnakumar et al., 2008). I tested ~50 of the most E2 up- and down-regulated genes that are affected by PJ34 treatment and/or PARP-1 knockdown from this analysis in gene-specific RT-qPCR assays (Figures 3.20 and 3.21). For the most part, at the mRNA level, the effect of PJ34 or PARP-1 knockdown on these genes is minimal, if not negligible. Together, my results indicate that both PARP-1 protein and activity are important for a complete estrogen response at a subset of genes.

Figure 3.17. The magnitude of the estrogen response is slightly reduced upon PJ34 treatment or PARP-1 knockdown. *A and B,* Box plots of the estrogen response for the overlapping E2 down-regulated (A) and up-regulated (B) genes in Luc KD, Luc KD + PJ34, and PARP-1 KD conditions. *C*, An example of GRO-seq data at an estrogen up-regulated gene, *HSPB8*, whose expression is slightly reduced by PJ34 treatment and PARP-1 knockdown. The data was visualized using the University of California Santa Cruz (UCSC) Genome Browser. Each graph has identical x- and y-axes and both the plus (red) and minus (blue) strands are depicted.

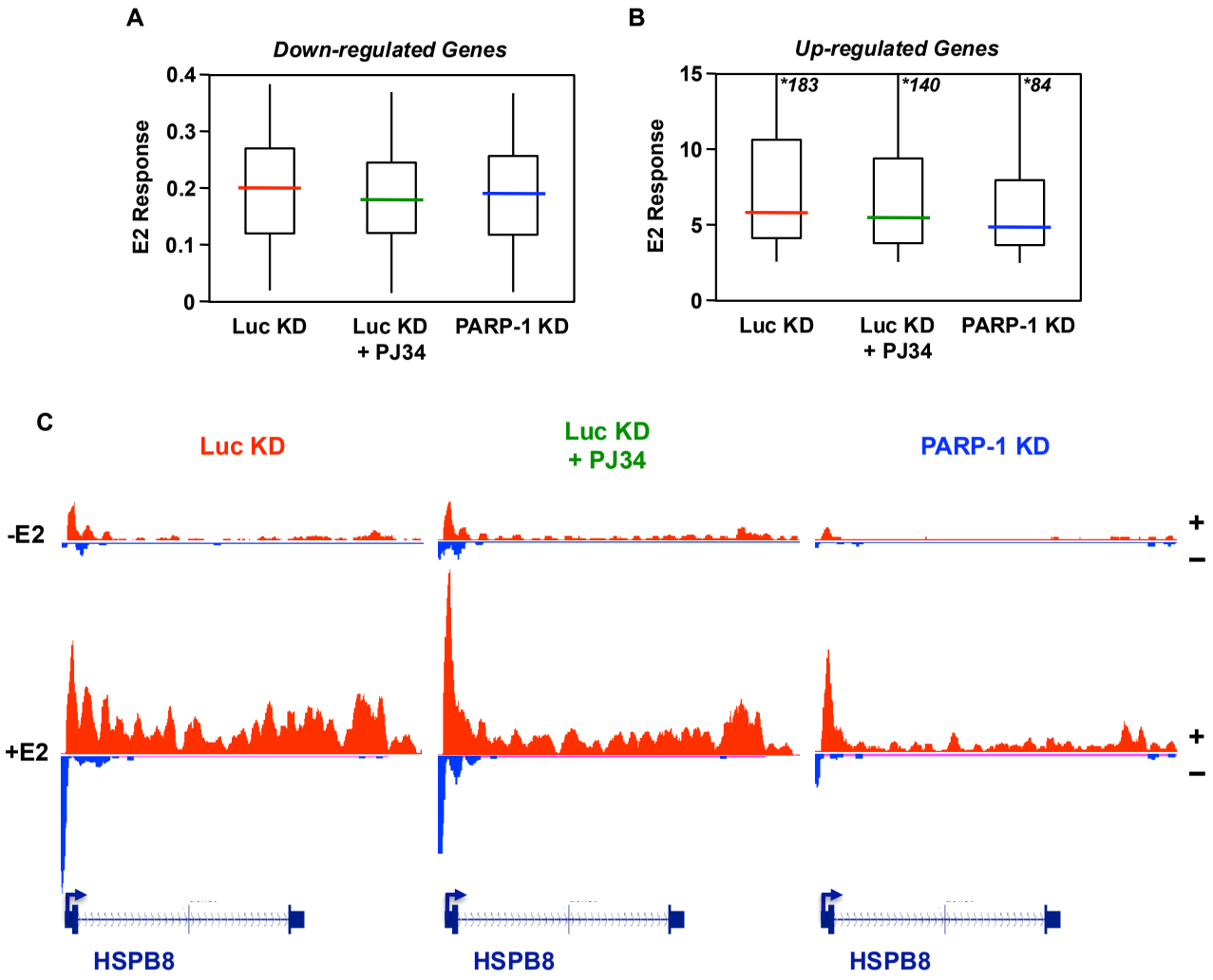
A
Down-regulated Genes
E2 Response
0.4
0.3
0.2
0.1
0
Luc KD
Luc KD + PJ34
PARP-1 KD
B
Up-regulated Genes
E2 Response
15
10
5
0
*183
*140
*84
Luc KD
Luc KD + PJ34
PARP-1 KD
C
Luc KD
Luc KD + PJ34
PARP-1 KD
-E2
+E2
+
−
HSPB8
HSPB8
HSPB8

Figure 3.18. The magnitude of the estrogen response is reduced upon PJ34 treatment or PARP-1 knockdown at the most up- and down-regulated genes. *A and B,* The average degree of change in the E2 response is plotted for PJ34 treatment (green) and PARP-1 KD (blue) among pentiles of down-regulated genes (A) and up-regulated genes (B), defined in Figure 3.17. Pentiles are defined by the degree of estrogen response. *C and D*, Same as in A and B. Pentiles are defined by the level of expression (GRO-seq read count) in the basal (vehicle-treated) condition.

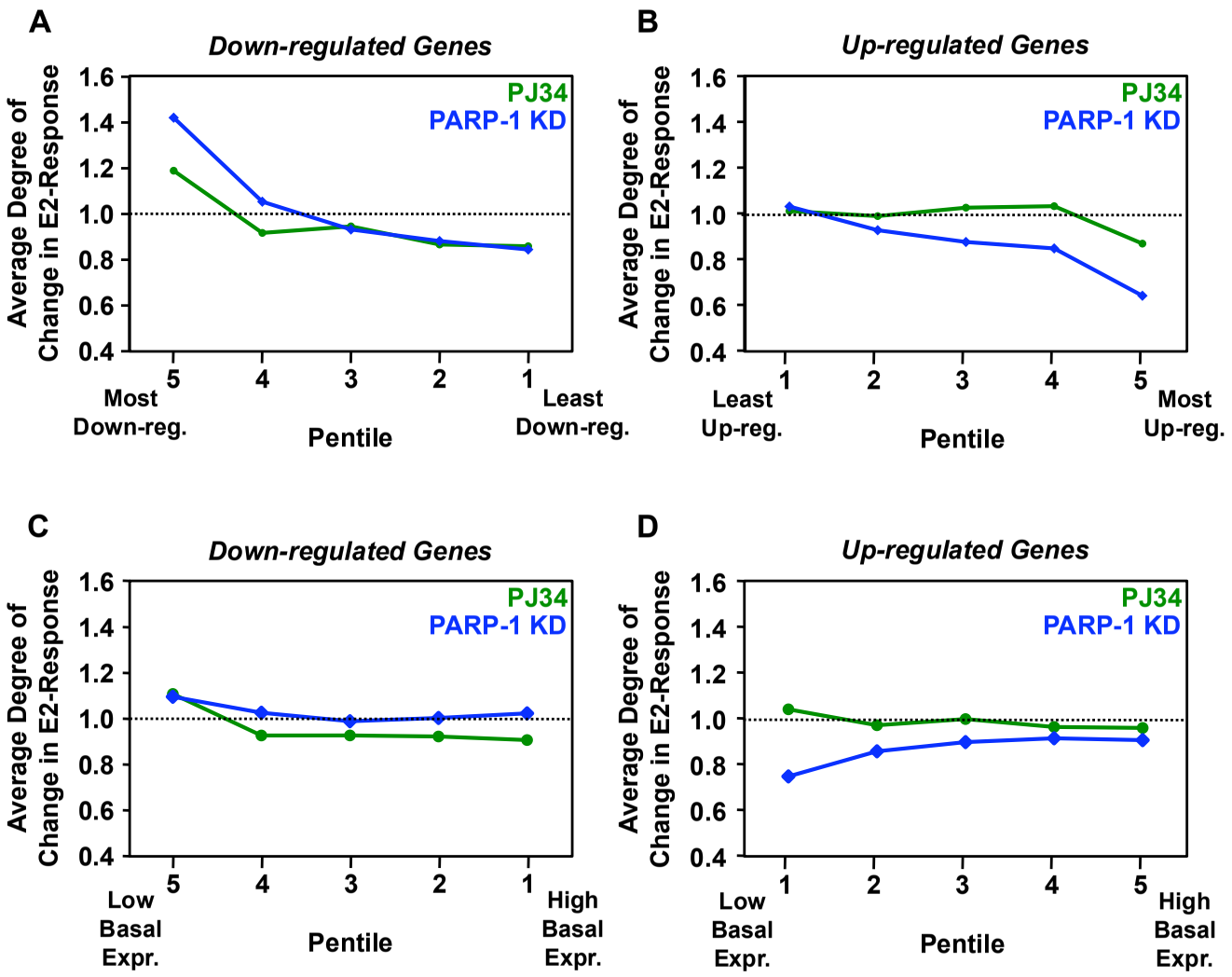
A
Down-regulated Genes
Average Degree of Change in E2-Response
1.6
1.4
1.2
1.0
0.8
0.6
0.4
PJ34
PARP-1 KD
5
4
3
2
1
Most Down-reg.
Least Down-reg.
Pentile
B
Up-regulated Genes
Average Degree of Change in E2-Response
PJ34
PARP-1 KD
1
2
3
4
5
Least Up-reg.
Most Up-reg.
Pentile
C
Down-regulated Genes
Average Degree of Change in E2-Response
PJ34
PARP-1 KD
5
4
3
2
1
Low Basal Expr.
High Basal Expr.
Pentile
D
Up-regulated Genes
Average Degree of Change in E2-Response
PJ34
PARP-1 KD
1
2
3
4
5
Low Basal Expr.
High Basal Expr.
Pentile

Figure 3.19. PARP-1 localization is unaltered upon E2-treatment regardless of degree of estrogen response or basal expression level. *A-D*, Averaging analysis of the Log_2 enrichment ratios for PARP-1 under vehicle (blue, light blue) and E2 (red, orange) treated MCF-7 cells is shown for genes within pentiles 1 and 5 from each panel in Figure 3.18, for which ChIP-chip data exists. PARP-1 profiles are plotted for genes down-regulated by estrogen in (A and C) and up-regulated by estrogen (B and D). For genes with either a high or low estrogen response (A and B), PARP-1 localization patterns are unaltered upon estrogen treatment. For genes with either a high or low basal expression level, PARP-1 localization patterns are unaltered upon estrogen treatment. Notably, genes with a low expression level have a lower amount of PARP-1, compared to genes with a higher expression level.

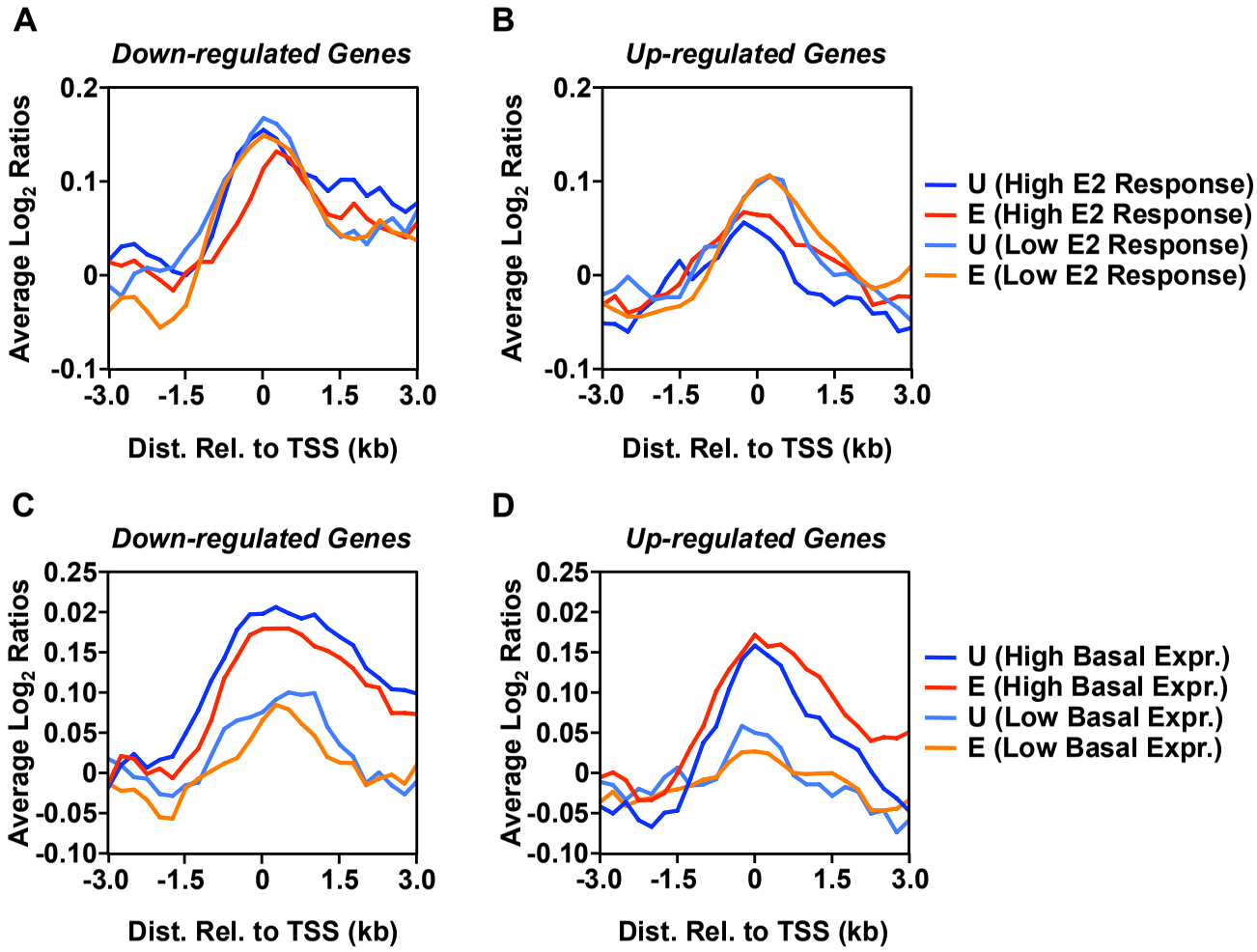
A
Down-regulated Genes
Average Log2 Ratios
0.2
0.1
0
-0.1
-3.0
-1.5
0
1.5
3.0
Dist. Rel. to TSS (kb)
B
Up-regulated Genes
Average Log2 Ratios
Dist. Rel. to TSS (kb)
U (High E2 Response)
E (High E2 Response)
U (Low E2 Response)
E (Low E2 Response)
C
Down-regulated Genes
Average Log2 Ratios
0.25
0.02
0.15
0.10
0.05
0
-0.05
-0.10
Dist. Rel. to TSS (kb)
D
Up-regulated Genes
Average Log2 Ratios
Dist. Rel. to TSS (kb)
U (High Basal Expr.)
E (High Basal Expr.)
U (Low Basal Expr.)
E (Low Basal Expr.)

Figure 3.20. PJ34 treatment and PARP-1 knockdown only mildly alter estrogen-dependent changes in steady-state mRNA levels. *A and B*, Total RNA was isolated from Luc and PARP-1 knockdown cell lines in the absence or presence of PJ34 and E2 for the time points indicated, reverse transcribed, and subjected to qPCR using gene-specific primers. Each point is the mean + SEM (*error bars*) for four independent RNA isolations. Of the 51 genes up-regulated or down-regulated by estrogen that were tested from the categories most affected by PJ34 treatment or PARP-1 knockdown, only a few confirmed this result (A), while others did not (B).

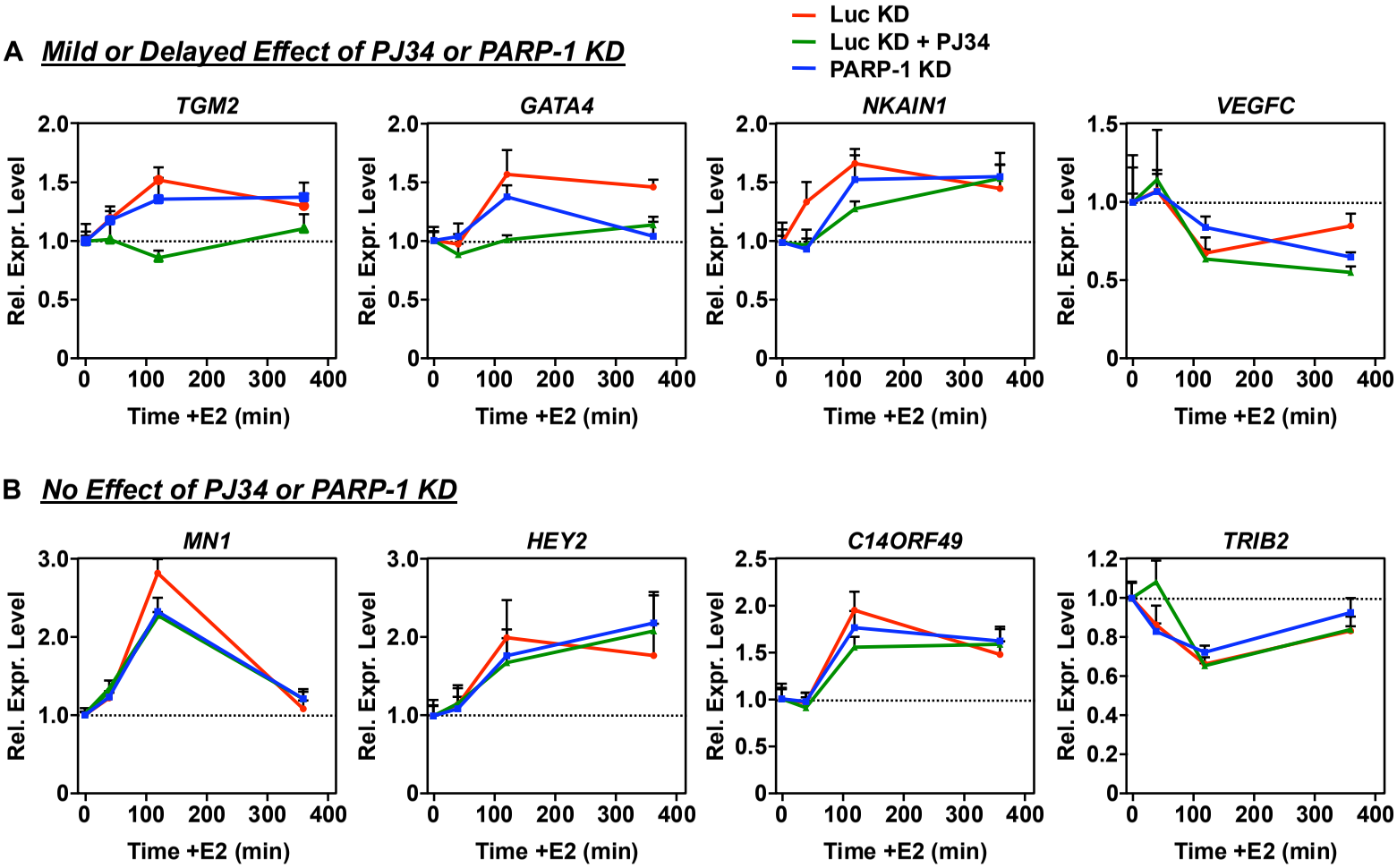
A Mild or Delayed Effect of PJ34 or PARP-1 KD
Luc KD
Luc KD + PJ34
PARP-1 KD
TGM2
GATA4
NKAIN1
VEGFC
Rel. Expr. Level
Time +E2 (min)
B No Effect of PJ34 or PARP-1 KD
MN1
HEY2
C14ORF49
TRIB2

Figure 3.21. Graphs showing all estrogen-regulated genes that were tested for PJ34- or PARP-1-dependent changes at the steady-state mRNA level. Total RNA was isolated from Luc and PARP-1 knockdown cell lines in the absence or presence of PJ34 and E2 for the time points indicated, reverse transcribed, and subjected to qPCR using gene-specific primers. Each point is the mean + SEM (*error bars*) for four independent RNA isolations. 51 genes up-regulated or down-regulated by estrogen were tested (including Figure 3.20) from the categories most affected by PJ34 treatment or PARP-1 knockdown. Of those that confirmed a change in mRNA level upon estrogen treatment, most were not affected by PARP-1 perturbation.

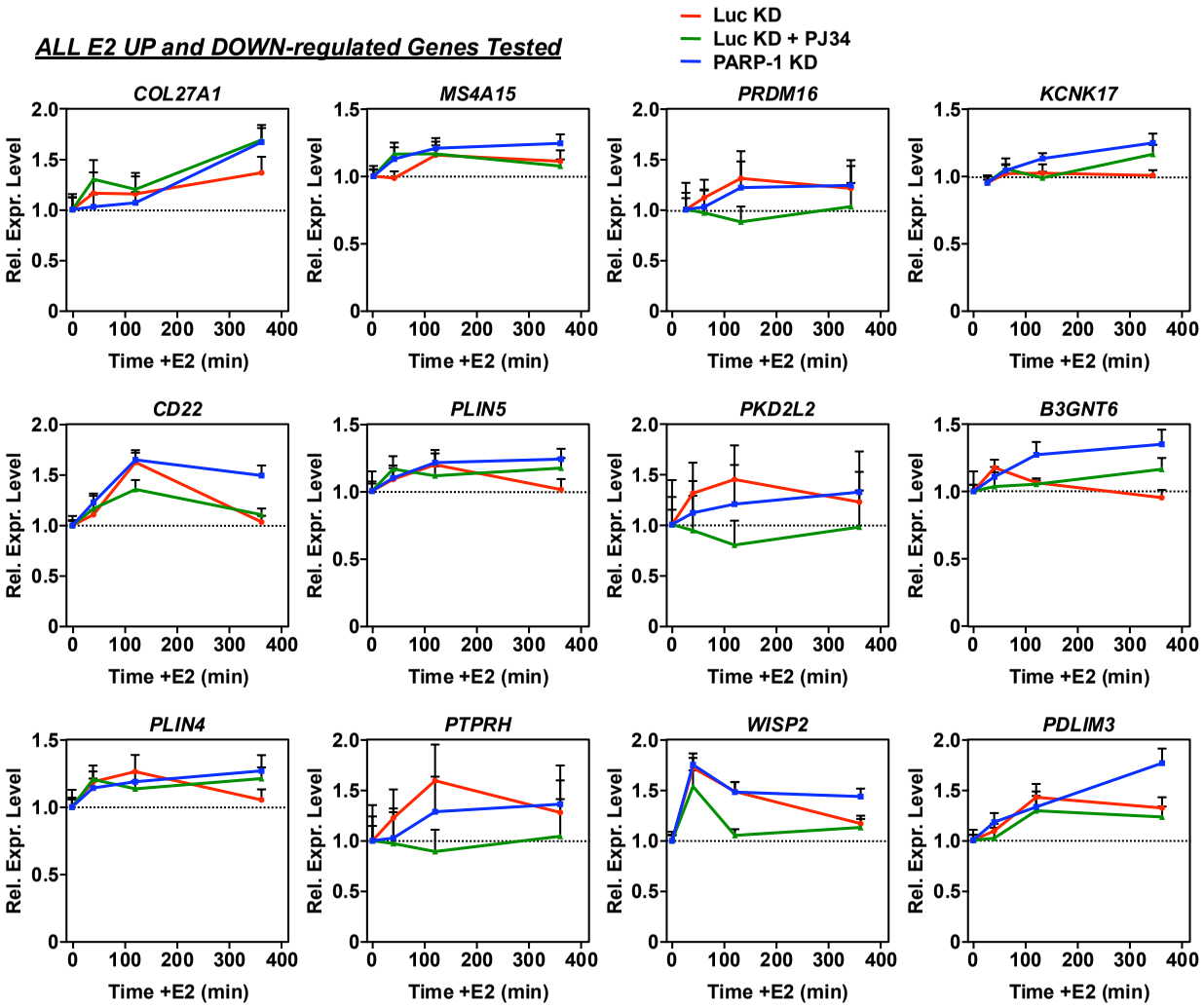
ALL E2 UP and DOWN-regulated Genes Tested
Luc KD
Luc KD + PJ34
PARP-1 KD
COL27A1
MS4A15
PRDM16
KCNK17
CD22
PLIN5
PKD2L2
B3GNT6
PLIN4
PTPRH
WISP2
PDLIM3
Rel. Expr. Level
Time +E2 (min)

Figure 3.21 (cont'd)

ALL E2 UP and DOWN-regulated Genes Tested

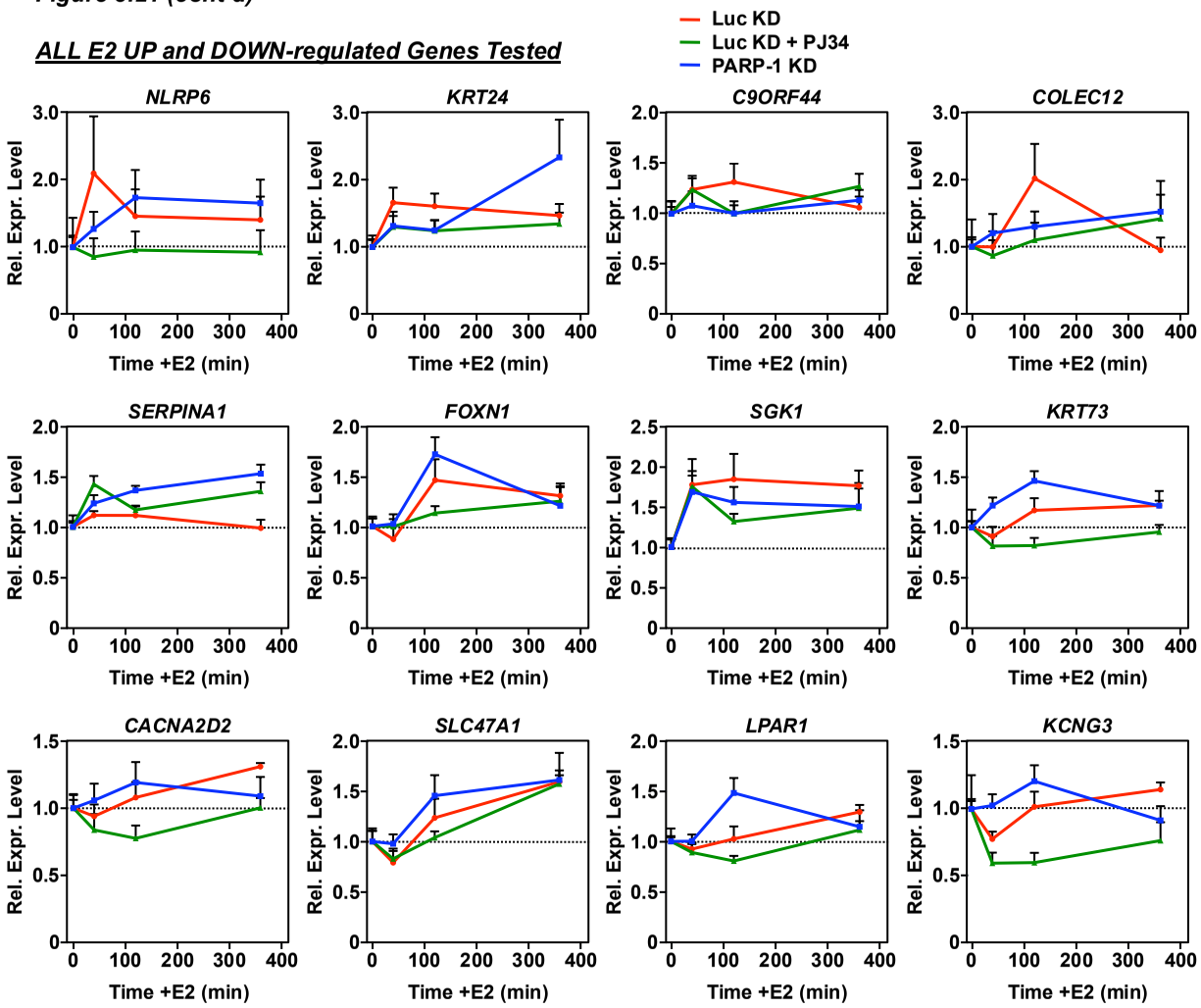

Figure 3.21 (cont'd)

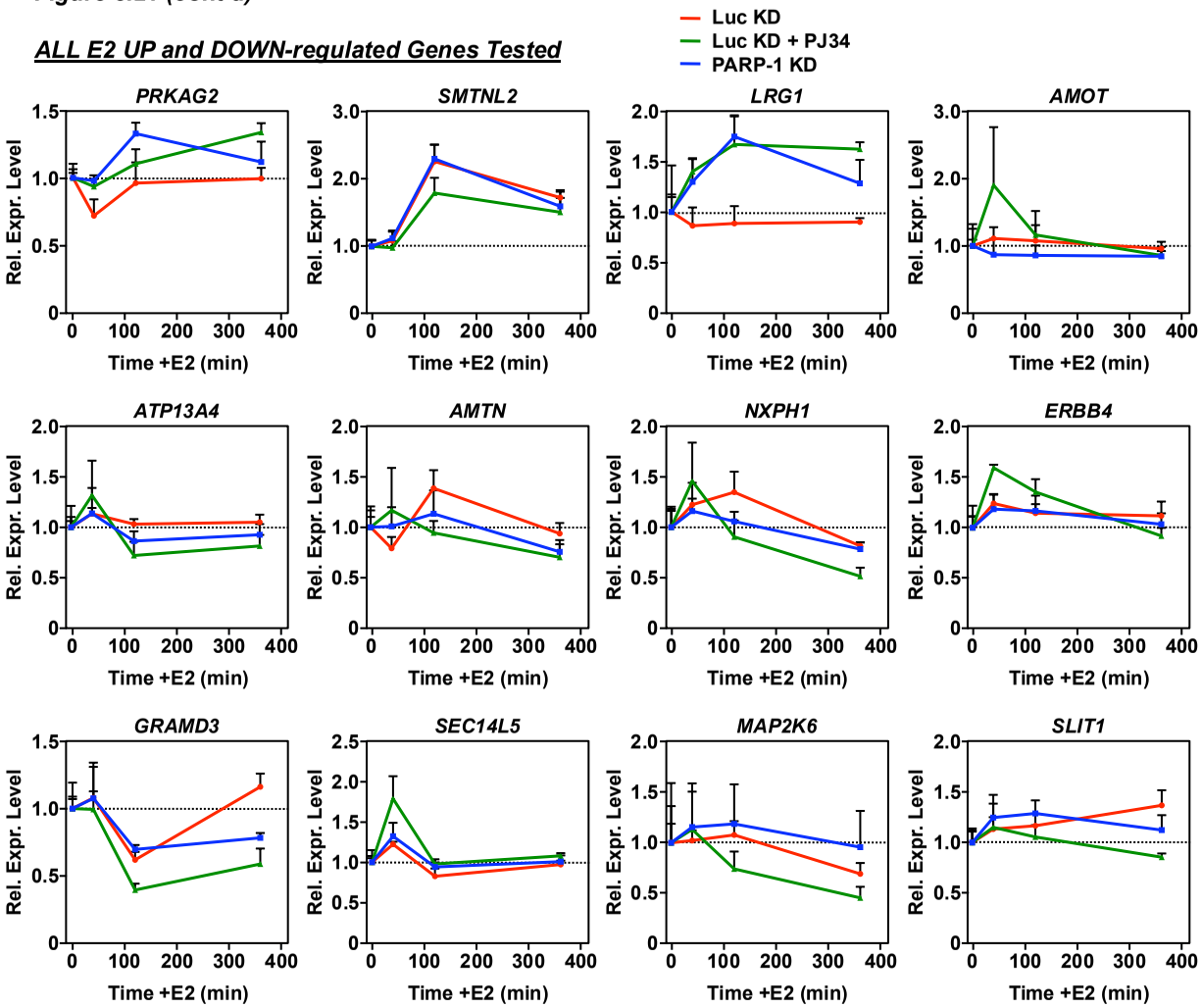

Figure 3.21 (cont'd)

ALL E2 UP and DOWN-regulated Genes Tested

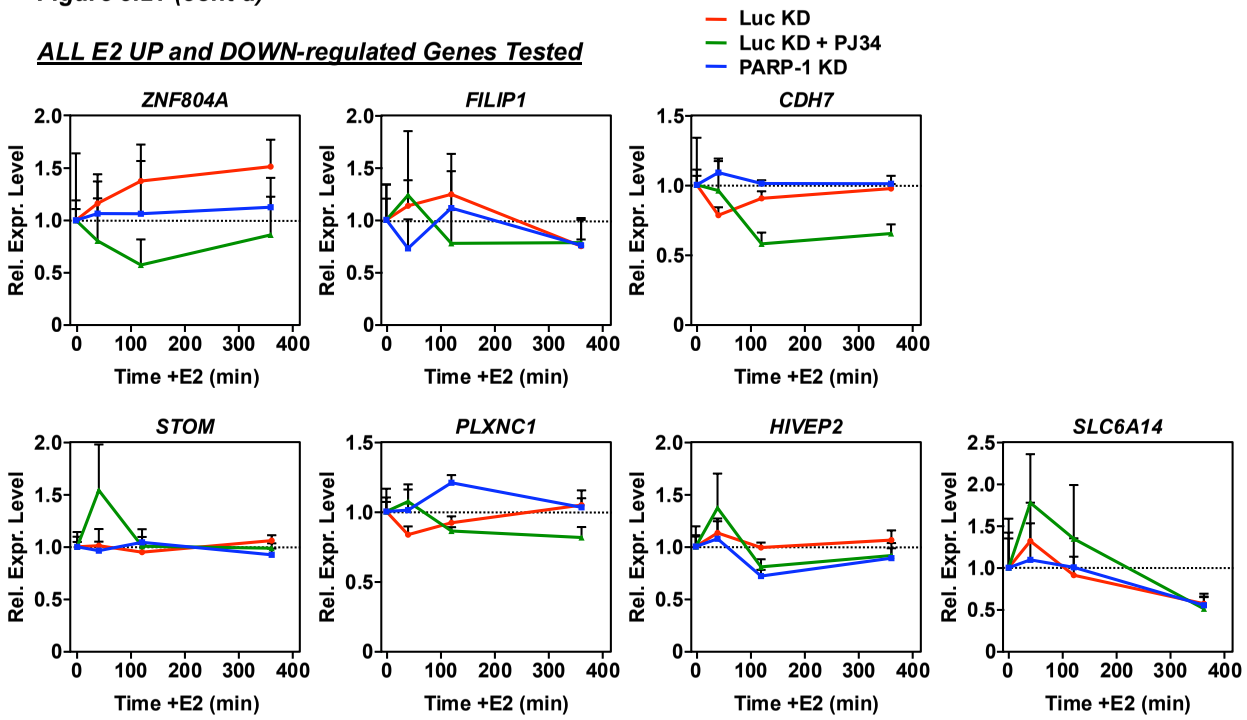

3.4. Discussion

Poly(ADP-ribose) Polymerase-1 is a nuclear enzyme that has been implicated in signal-mediated transcriptional regulation, including that modulated by estrogen. However, global effects on estrogen-dependent gene regulation by PARP-1 have not been established. In the current study, I have used GRO-seq to define the role of PARP-1 and PARP activity on the estrogen-regulated transcriptome. Collectively, my results suggest that the estrogen response is highly maintained under PARP-1 knockdown or inhibition at both the transcription and steady-state mRNA levels.

PARP-1 is required for a complete estrogen response. The data described herein have revealed unexpected facets of PARP-1 action in estrogen-dependent gene regulation. First, PJ34 treatment and PARP-1 knockdown largely do not affect the estrogen response in MCF-7 cells (Figures 3.12, 3.13, and 3.16). Based on previously published data (Ju et al., 2006), this result was somewhat unexpected. In fact, my data did not recapitulate that previously reported for the TFF1 gene.

Second, even though the majority of genes are still regulated by E2 under PJ34 treatment and PARP-1 knockdown, these conditions seemingly quench the spectrum of the estrogen response. That is, PARP inhibition and PARP-1 knockdown reduce the degree of estrogen regulation for the top 10-20% of up-regulated and down-regulated genes (Figure 3.18). At the gene-specific level, most GRO-seq-defined effects of PARP-1 inhibition or knockdown were not confirmed. However, this could be a result of (i) the difference in GRO-seq transcription versus steady-state mRNA levels, (ii) the subtlety of the effects, resulting in low confirmation rate, or (iii) a high false positive/negative rate in the GRO-seq data itself.

Third, PARP-1 promoter localization is largely unaltered upon estrogen treatment at estrogen-regulated genes, regardless of direction of regulation or magnitude of the response. In fact, PARP-1 localization patterns are not changed at the top 10-20% of up-regulated and down-regulated genes. At these genes, it is possible that PARP-1 might be regulating the chromatin structure or the recruitment of a protein at these estrogen-regulated promoters, such as histone modifying enzymes.

Basal transcription is unaffected by PJ34 treatment and PARP-1 knockdown. Another result gained from my GRO-seq experiment is that PJ34 treatment and PARP-1 knockdown to do alter basal transcription in MCF-7 cells (Figure 3.15). Given that PARP-1 knockdown changes the expression levels of over 1000 genes in the same cell line as shown by expression microarray experiments (Frizzell et al., 2009), this result was unexpected. How is it possible that a GRO-seq detects minimal changes in the basal state, but mRNA levels change upon PARP-1 knockdown? One possible explanation is that the statistical criteria used to make "changes in transcript" calls, is too stringent to detect subtle changes, as noted above. However, the raw read counts at specific genes seemingly matches that of RT-qPCR analyses (Figure 3.7), indicating that those changes are reflected in the raw data.

Another explanation is that PARP-1 may be functioning as an RNA processing factor at promoters, or participating in mRNA stability. This is not an unreasonable hypothesis given that PARP-1 interacts with factors involved in RNA processing and export from the nucleus (*i.e.* nucleolin, nucleophosmin; (Fu and Fenselau, 2005; Isabelle et al., 2010; Meder et al., 2005)) and localizes with those factors in the nucleolus (Meder et al., 2005). In addition, many other PARP-1-interacting factors localize to the nucleolus, such as XRCC1 and CTCF (Kotoglou et al., 2009; Torrano et al., 2006). Interestingly, it was recently shown that PARP-1 can regulate

inflammatory gene expression by increasing the mRNA stability of target genes via modulating proper p38/MAPK signaling cascades (Galbis-Martinez et al., 2010). Further experiments are required to prove such hypotheses.

In conclusion, my studies reveal that while PARP-1 and its activity may be important at a subset of estrogen responsive genes, they are largely dispensable for estrogen-mediated transcriptional outcomes in MCF-7 human breast cancer cells.

2.5. Experimental Procedures

Antibodies - The custom rabbit polyclonal antibody against PARP-1 used for Western blotting, ChIP-chip, and ChIP-qPCR assays was generated by using a purified fragment of human PARP-1 (amino-terminal, PARP-N (Kim et al., 2004)) (Pocono Rabbit Farm and Laboratory, Inc.). The antibody was previously screened for: (i) specificity by Western blotting MCF-7 cell extracts, (ii) the ability to immunoprecipitate its cognate antigen from formaldehyde-crosslinked chromatin samples by a ChIP-Western protocol (Kim et al., 2004), and (iii) a reduction in Western blot signal upon PARP-1 knockdown (Chapter 2; (Frizzell et al., 2009)). The custom rabbit polyclonal antibody against ERα used for Western blotting was generated by using a purified fragment of human ERα (Pocono Rabbit Farm and Laboratory, Inc.) (Kim et al., 2006). The rabbit polyclonal H3 antibody used for ChIP-chip was purchased from Abcam. The mouse monoclonal PAR antibody used for Western blotting was purchased from Trevigen. The mouse monocolonal β-Actin antibody used for Western blotting was purchased from Sigma-Aldrich.

Culture and treatment of MCF-7-derived cell lines – Luciferase (Luc) and PARP-1 knockdown MCF-7 cell lines (generated and previously characterized, Chapter 2; (Frizzell et al., 2009)) were maintained in MEM Eagle medium containing Hanks' salts, L-glutamine, and non-essential amino acids (Sigma) supplemented with 5% bovine calf serum (CS; Sigma), 20 mM HEPES (pH 7.6), 100 units/mL penicillin, 100 μg/mL streptomycin, 25 μg/mL gentamycin, and 0.22 % sodium bicarbonate. The medium was supplemented with puromycin (Sigma; 0.5 μg/mL) and G418 sulfate (Gibco/BRL; 800 μg/mL) for stock cultures.

For experiments, cells were plated in MEM modified Eagle medium with Earle's salts and non-essential amino acids, without phenol red (Sigma), supplemented 5% charcoal/dextran-treated bovine calf serum (CDCS; Sigma) and the other additives noted above. Subconfluent populations of cells were treated as indicated in the figure legends and collected for analysis between 3 and 4 days post-plating.

The PARP-1 chemical inhibitor, PJ34, was purchased from Alexis Biochemicals, dissolved in distilled water, pH-adjusted to approximately 7.5. PJ34 (1 μM, unless otherwise noted) or dH_2O (vehicle) was added to the cell culture medium for 1 hr at 37°C prior to treatment with estrogen (was not removed during estrogen treatment). 17β-estradiol (E2) was purchased from Sigma and dissolved in ethanol. E2 (100 nM) or ethanol (vehicle) was added to the cell culture medium for 40 min at 37°C prior to collecting the cells, unless otherwise indicated.

Cell survival assay - For analysis of cell survival, stable Luc and PARP-1 knockdown cells were seeded at ~5 x 10^5 cells per well in 6-well plates in MEM containing 5% CS and the additives noted above. After 24 hours, the cells were treated with increasing doses of PJ34 for a period of 48 hours. The cells were collected by trypsinization,

stained with trypan-blue, and surviving cells were counted using a hemacytometer. Experiments were conducted a minimum of three times to ensure reproducibility.

Global Run-on Sequencing (GRO-seq) - The GRO-seq methodology was performed essentially as described previously (Core et al., 2008), with minor modifications.

Isolation of MCF-7 Nuclei - Luc or PARP-1 knockdown MCF-7 cells were seeded at ~6 x 10^5 cells per 15 cm plate and grown for at least 3 days in MEM containing 5% CDCS and the additives noted above. After at least three days of estrogen deprivation and at nearly 100% confluence, cells were treated with or without PJ34 and E2 at the indicated concentrations and times noted above. Cells were washed directly on the plate three times with ice-cold PBS. 10 mL of ice-cold lysis buffer [10 mM Tris•HCl (pH 7.4), 2 mM $MgCl_2$, 3 mM $CaCl_2$, 10% Glycerol, 0.5% NP-40, 1 mM DTT, a protease inhibitor cocktail (Roche Molecular Biochemicals), and 2 U/mL SUPERase-Inhibitor (Ambion)] was added directly on the plate and allowed to incubate on ice for 5 min. Cells were scraped using a plastic scraper, collected into a 15-mL conical tube, and pelleted for 10 min at 4°C using setting 4 in a clinical centrifuge. The cell pellets were resuspended in 1.5 mL of lysis buffer and gently pipetted up and down ~30 times using a cut p1000 pipette tip to reduce shearing. The volume was then brought to 10 mL with lysis buffer, inverted gently to mix, and pelleted again. The nuclei pellet was again resuspended in 1 mL of lysis buffer and gently pipetted to resuspend fully. The samples were transferred to a 1.7 mL tube and centrifuged at 3,000 rpm for 5 min at 4°C in a microcentrifuge. The nuclei were then resuspended in freezing buffer [50 mM Tris•HCl (pH 8.3), 5 mM $MgCl_2$, 40% Glycerol, 0.1 mM EDTA (pH 8.0), and 4 U/mL SUPERase-Inhibitor] and centrifuged at 13,000 rpm for 1 min at 4°C in a microcentrifuge. Nuclei were resuspended in freezing buffer and stored in aliquots of

~5 x 10^6 nuclei per 100 μL at -80°C. All stock buffers and solutions were made with DEPC-treated water (for RNA work, Fisher) and filtered to avoid RNA degradation.

Library Generation – Construction of the nuclear run on (NRO) library consists of multiple steps: (i) Run-on reaction; (ii) Base Hydrolysis; (iii) Immuno-purification; (iv) End Repair; (v) 5'- and 3'-adapter ligation; (vi) Reverse transcription and PCR amplification; and (vii) PAGE purification. All stock buffers and solutions were made with DEPC-treated water (for RNA work, Fisher) to avoid RNA degradation. At each major step, 1.25-2.5% of each reaction was removed for analysis on a 6% PAGE-urea gel, followed by autoradiographic analysis using a PhosphorImager (Molecular Dynamics) and visualized using ImageQuant software.

(i) Run-on reactions were conducted exactly as described in Core *et al* (Core et al., 2008), except for the amount of RQ1 RNase free DNase I used (5 μL, rather than 10 μL). Each reaction used ~5 x 10^6 MCF-7 Luc or PARP-1 knockdown nuclei (100 μL) either treated with PJ34 and/or E2, as described above.

(ii) Base hydrolysis of NRO RNA was conducted exactly as described in Core *et al* (Core et al., 2008), except for (a) the time of hydrolysis (20 min, rather than 30 min), and (b) the amount of EDTA stopping the reaction (2 mM, rather than 10 mM).

(iii) Immuno-purification of NRO RNA was conducted using Anti-deoxyBrU beads (Santa Cruz Biotechnology), which were blocked for at least 1 hour rotating (10-15 rotations per minute) at room temperature using blocking buffer [1X SSPE, 1 mM EDTA, 0.1% Tween, 0.1 % PVP, and 1 mg/ml Ultrapure BSA (Ambion)]. 100 μL of NRO RNA was heated to 70°C for 5 min, followed by 2 min on ice, and

subsequently added to 60 μL beads (washed twice with binding buffer), in a total reaction volume of 500 μL supplemented with binding buffer [0.25X SSPE, 1 mM EDTA, 0.05 % Tween, and 37.5 mM NaCl]. The NRO RNAs were allowed to bind for 1 hour while rotating at room temperature. The beads were then washed (5 min each, rotating at room temperature) once in binding buffer, once in low salt buffer [0.25X SSPE, 1 mM EDTA, and 0.1% Tween], once in high salt buffer [0.25X SSPE, 1 mM EDTA, 0.1% Tween, and 150 mM NaCl], and twice in TET buffer [1x TE and 0.1% Tween]. The BrU RNA was then eluted two times using 125 μL and once using 250 μL of elution buffer [20 mM DTT, 300 mM NaCl, 50 mM Tris•HCl (pH 7.5), 1 mM EDTA, and 0.1% SDS]. The elutions were then combined, extracted and precipitated exactly as described in Core *et al* (Core et al., 2008). All buffers were supplemented with 1 μL SUPERase-Inhibitor per 5 mL of buffer.

(iv) End repair of the enriched RNAs was conducted exactly as described in Core *et al* (Core et al., 2008), except for (a) the amount of Tobacco acid pyrophosphatase (TAP, 1.5 μL, rather than 2.5 μL), (b) the time of incubation with TAP enzyme (1.5 hrs, rather than 1 hr), (c) the amount of $MgCl_2$ added to the kinase reaction (0.3 μL of 1 M $MgCl_2$, rather than 0.5 μL of 5 mM $MgCl_2$), (d) the amount of polynucleotide kinase (PNK, 2 μL, rather than 1 μL), and (e) the amount of EDTA used to stop the reaction (5 μL, rather than 10 μL).

(v) Adapter ligation reactions were conducted directly after end repair (5') and after the 2nd Br-U enrichment step (3'). The RNA was resuspended in 8.5 μL prior to the adapter ligation step, directly mixed with 1.5 μL of 10 μM adapter oligo (Illumina Small RNA Isolation Kit) and 6 μL 50% PEG, and subsequently heated to 70°C for 5 min followed by 2 min on ice. 1 μL of SUPERase-Inhibitor, 2 μL 10X RNA ligation

buffer, and 1.5 μL of T4 RNA ligase (NEB) were added and the reactions were incubated on the bench top for 4 hours (5') or 6 hours (3'). The reactions were stopped with a mixture of 2 μL 500 mM EDTA and 28 μL DEPC water. The reactions were then enriched over anti-deoxyBrU beads, as described above.

(vi) Reverse transcription of enriched RNAs were conducted in a single 20 μL reaction. RNAs were combined with 1 μL of 100 μM RT Primer (Illumina Small RNA Isolation Kit) and subsequently heated to 70°C for 5 min followed by 2 min on ice. 4 μL of 5X First Strand buffer, 2 μL 10 mM dNTPs, 2 μL 100 mM DTT, and 1 μL SUPERase-Inhibitor were added and incubated at 48°C for 3 minutes. 2 μL of SSIII RT enzyme (Invitrogen) was added and RNA was reverse transcribed by incubating at 44°C for 20 minutes followed by 52°C for 45 minutes. RNAs were then degraded by addition of RNAse cocktail (Ambion) and RNase H (Ambion) for 15 min at 37°C, followed by extraction and precipitation as described above. DNA was then amplified in duplicate 50 μL reactions for 15 cycles using Phusion high fidelity DNA polymerase (Finnzymes) and the PCR primers specified by Illumina. After confirming the amplification by agarose gel electrophoresis, cDNAs were extracted and precipitated as described previously above.

(vii) NRO cDNA libraries were purified using a non-denaturing acrylamide gel exactly as described in Core *et al* (Core et al., 2008), except for using a 6% acrylamide gel, rather than 8%. Libraries were quantified and sequenced at the Cornell University's Fee-for-service Core Sequencing Facility using the Illumina 1G Genome Analyzer. A single lane was sequenced for each biological replicate.

GRO-seq Analyses - The GRO-seq analyses were performed using the statistical programming language R (R Development Core Team). The general protocols for each of the following sections were followed from Core *et al* (Core et al., 2008).

Alignment of GRO-seq Reads to the Human Genome - Alignments of each 43-bp read to the hg19 assembly of the human genome were performed with the Short Oligonucleotide Alignment Package (SOAP) alignment tool (Li et al., 2008). Alignments allowed up to three mismatches per sequence to account for sequencing errors and SNPs between the cell line and the sequenced genome. Since sequencing was performed from the 5' end of the library, the 5' coordinate of each read was used as the position of engaged polymerase for all future analyses.

Correlation Analyses - A Pearson correlation analysis was performed between individual biological replicates for uniquely mapped reads from +1 to +13 kb relative to the TSS. All pair-wise comparisons were made for all conditions.

Defining Changes in Expression - To define changes in gene expression among any pair-wise comparisons, the total reads from +1 to +13 kb relative to the TSS for all 12 samples (all pairs of biological replicates) were used as input into the EdgeR software package (Robinson et al., 2010). The EdgeR software quantile normalizes all the reads within the given window, forcing the distribution of all samples to be equal, and calculates the parameters for a negative binomial distribution based on all pairs of biological replicates. For each gene, the read counts are compared between pair-wise conditions using an exact test, the p-value of which is corrected for multiple hypothesis testing using a false discovery rate (FDR) cut-off of 0.1%, defining the change as significantly different (or not) between two conditions. The resulting data is

plotted as the Log_{10} (gene body reads/total reads) for one condition versus another (as in Figures 3.9, 3.13, and 3.15). Black circles represent genes whose change between the two conditions is not statistically different, while red circles represent genes whose change between the two conditions is statistically different.

Metagene Profiles - The sum of reads at each position (weighted by expression level and normalized to both number of genes and total reads) and centered the data at the TSS for each condition examined for all Ref-seq (Figures 3.8) or estrogen-regulated (Figure 3.12) genes. The resulting metagene profiles display reads on the sense strand moving toward the right (red), and antisense strand (blue) moving toward the left.

mRNA expression analyses by RT-qPCR - For gene-specific mRNA expression analyses, total RNA was isolated from Luc and PARP-1 knockdown cells treated with vehicle, PJ34 (1 μM, 1 hr) or E2 (100 nM, 3 hrs) using Trizol Reagent (Invitrogen), reverse transcribed, and subjected to real-time quantitative PCR using a set of gene specific primers. All target gene transcripts were normalized to the β-actin transcript, which was unaffected by estrogen treatment, PJ34 treatment, or PARP-1 knockdown (data not shown). All experiments were conducted a minimum of three times with independent RNA isolations to ensure reproducibility.

Quantitative PCR analyses (RT-qPCR) - Gene-specific mRNA expression analyses were analyzed by quantitative PCR in a similar manner. Briefly, reactions containing DNA from either source, 1x SYBR Green PCR master mix, and forward and reverse primers (250 nM for ChIP, 500 nM for expression) were used in 40-45 cycles of amplification (95°C for 15 sec, 60°C for 1 min) using a Roche LightCycler® 480

System (384-well) following an initial 10 min incubation at 95°C. Melting curve analysis was performed to ensure that only the targeted amplicon was amplified.

Chromatin immunoprecipitation assays - ChIP assays were performed essentially as described previously (Gamble et al., 2010; Krishnakumar et al., 2008). The immunoprecipitations were performed from crosslinked knockdown MCF-7 cells with antibodies against PARP-1 or histone H3, using "no antibody" as a control. The resulting Input and ChIP DNA material was used for ChIP-chip analyses.

ChIP-chip - The ChIP-chip sample processing and analysis were done essentially as described previously (Gamble et al., 2010; Krishnakumar et al., 2008). Briefly, PARP-1-specific immunoprecipitated genomic DNA and reference DNA was blunted, amplified by ligation-mediated PCR (LM-PCR), labeled with Cy5 and Cy3, respectively, and used to probe a custom human oligonucleotide genomic array (HD2 Platform or custom-designed, Nimblegen) (Gamble et al., 2010; Krishnakumar et al., 2008). The PARP-1 ChIP-chip was run in duplicate to ensure reproducibility and H3 ChIP-chip was run only on the custom-designed platform.

ChIP-chip Analyses - The Genomic data analyses for the PARP-1 ChIP-chip were performed as described previously (Gamble et al., 2010; Krishnakumar et al., 2008), using the statistical programming language R (R Development Core Team).

Primer Sequences – The primer sequences listed below were used for RT-qPCR.

Gene Name	**Primer Sequence**
β-ACTIN forward	5'-AGCTACGAGCTGCCTGAC-3'

β-ACTIN reverse	5’-AAGGTAGTTTCGTGGATGC-3’
ABCA4 forward	5’-CAGCCAGAAAGGAACTCTGG-3’
ABCA4 reverse	5’-CATGCTCCTCGTGTGTTTGT-3’
AMOT forward	5’-TAAACGGCCAAATCAAGAGC-3’
AMOT reverse	5’-CCTTGTCCTCACCCTCAAAA-3’
AMTN forward	5’-CAGTGGCACAGATGACGACT-3’
AMTN reverse	5’-CCAAATTCGAGGCAGCTTAG-3’
ATP13A4 forward	5’-GGACTTGGCAAATGACCCTA-3’
ATP13A4 reverse	5’-GCATGTCAGAGTGGGAGGTT-3’
B3GNT6 forward	5’-TACATCCTGGCTCCATCTCC-3’
B3GNT6 reverse	5’-ATTCGCATCACTGGAGGAAC-3’
C14ORF49 forward	5’-CGCTACCAGTGGATGCTGTA-3’
C14ORF49 reverse	5’-CTCCCCTGGAGAACTTTGTG-3’
C9ORF44 forward	5’-GGACTCCTCTTGGCTGTGAC-3’
C9ORF44 reverse	5’-TGCACCTGATTAGGGCTCTT-3’
CACNA2D2 forward	5’-GCAGAGACTGACCAACACCA-3’
CACNA2D2 reverse	5’-GTATCGCGGTCTCTGCACTA-3’
CALCR forward	5’-CTGGCGACATCCCAATTTAC-3’
CALCR reverse	5’-GCTGGTTCATTCCTCAGCTC-3’
CD22 forward	5’-AGTGGGCGACTATGAGAACG-3’
CD22 reverse	5’-TGAATCCCCTCATCTTCTGG-3’
CDH7 forward	5’-GACATGGCTGCACTGAGAAA-3’
CDH7 reverse	5’-AAAGCTGGTCGACTCAGGAA-3’
COL27A1 forward	5’-TGGACAGACGTGTCTCAAGC-3’
COL27A1 reverse	5’-AGCTTAGCAGGTGCAGGAAA-3’
COLEC12 forward	5’-TGGAACGATTTCCAATGTGA-3’

COLEC12 reverse	5’-GGAGTGTCCTTTGCCTTTGA-3’
ERBB4 forward	5’-AGGCCGAGGATGAGTATGTG-3’
ERBB4 reverse	5’-GTTGGCAAAGGTGTTGAGGT-3’
FILIP1 forward	5’-ACCCGCATTCCTATGTCAAA-3’
FILIP1 reverse	5’-GGTCAGATTTCCTGCTCCTG-3’
FOXN1 forward	5’-ATGCCATCAATCCCTCACTC-3’
FOXN1 reverse	5’-AGGGCCAAGCTATCATCCTT-3’
GATA4 forward	5’-AAATGCAGCTGGCAACTTCT-3’
GATA4 reverse	5’-AGCGGGAAGAGGGATTTTTA-3’
GDF15 forward	5’-CTACAATCCCATGGTGCTCA-3’
GDF15 reverse	5’-TATGCAGTGGCAGTCTTTGG-3’
GRAMD3 forward	5’-TGAGGCGTTTTGTTTGAGTG-3’
GRAMD3 reverse	5’-TCCACATGCAATGTCTGGAT-3’
HEY2 forward	5’-GTACCTGAGCTCCGTGGAAG-3’
HEY2 reverse	5’-CGCAAGTGCTGAGATGAGAC-3’
HIVEP2 forward	5’-CCTTTTCCCTGAGGGTCCTA-3’
HIVEP2 reverse	5’-TGTTGCTGAGAGTGGAGTGG-3’
ITPR1 forward	5’- TGCCTCCACAATTCTACG-3’
ITPR1 reverse	5’- TGAATGTCCCACAGTTGC-3’
KCNG3 forward	5’-CCCGTCACTTCATTGGTCTT-3’
KCNG3 reverse	5’-ACCATCTCTCGGTAGCAACG-3’
KCNK17 forward	5’-TGCTCTTCTCCCACATGGA-3’
KCNK17 reverse	5’-AGGGTGATGAAGGCGAAGTA-3’
KRT24 forward	5’-GGAAGCTGTTCTGGTCAAGG-3’
KRT24 reverse	5’-GCCATCCACCAACTCCTCTA-3’
KRT73 forward	5’-AGCTCTAAGCTCACCCACCA-3’

KRT73 reverse	5’-TGGGCTGTGTTGCACTTTTA-3’
LPAR1 forward	5’-ACTCCTACCGCGACAAAGAA-3’
LPAR1 reverse	5’-TGTGAACTCCAGCCAAGATG-3’
LRG1 forward	5’-GAACCAGTTGGAGACCTTGC-3’
LRG1 reverse	5’-TGCCGTTCAGGAAGAGGTAG-3’
MAP2K6 forward	5’-CGGTTGACCCTACTGTGGAT-3’
MAP2K6 reverse	5’-TGGGAGAGAAAACCCTCTGA-3’
MN1 forward	5’-GGTCTGAGTCTGCGGTTCTC-3’
MN1 reverse	5’-GCTTTGTCTGCCCTCTGAAG-3’
MS4A15 forward	5’-CTCTGGCATTCCACAGAGGT-3’
MS4A15 reverse	5’-ATGGATGTGGCAACAGATGA-3’
MTR forward	5’-ACAACAGCCTATGTCCTCTG-3’
MTR reverse	5’-CCATCATAGAAGGCGTTTC-3’
NAT1 forward	5’-CTTCACCCTCACCCATAGGA-3’
NAT1 reverse	5’-TTTGGGCACAAGCTTTCTCT-3’
NFAT5 forward	5’-ACCTCTTCCAGCCCTACCAT-3’
NFAT5 reverse	5’-CCTCTTCGGTGTTGATGGAT-3’
NKAIN1 forward	5’- GCGGCTTTGACTCCTACG -3’
NKAIN1 reverse	5’-ACAGAGGCTGCAGCTGTAAA-3’
NLRP6 forward	5’-GTCTGCCGAGACCTTTCTGA-3’
NLRP6 reverse	5’-TCACTCAGCATACGCAGTCC-3’
NXPH1 forward	5’-CACAGACTTTTCGTGGCAAA-3’
NXPH1 reverse	5’-CAGTCCCAGAGGTCTTGCTC-3’
PDLIM3 forward	5’-GATAAGTACCGGCACCCTGA-3’
PDLIM3 reverse	5’-CCCTTTTGCTTGAGGTTGAG-3’
PKD2L2 forward	5’- GGCAGAAGGCTAGATTTTGAA -3’

PKD2L2 reverse	5’- GCTTGTTCAGCCAAATCTCC -3’
PLIN4 forward	5’-TACAGTGGCCTGGTCTCCA-3’
PLIN4 reverse	5’-CGATGCCATAGAGCTCACAG-3’
PLIN5 forward	5’-CCAGGCAGAGCTGGAGAC-3’
PLIN5 reverse	5’-TGGACTCCAGAGCCTCTACC-3’
PLXNC1 forward	5’-TGAAGAAGTGGCCTTGACAG-3’
PLXNC1 reverse	5’-CCAGCCCTCGTTCTCTTTCT-3’
PRDM16 forward	5’-GCGGTCTGTTAGCTTTGGAG-3’
PRDM16 reverse	5’-CCTGCCTGCACAGTGTATGT-3’
PRKAG2 forward	5’-TGGTGGTGGTAAATGAAGCA-3’
PRKAG2 reverse	5’-GTTCTCCTCCTAGGGCGTCT-3’
PTPRH forward	5’-CGTTGATGGTGCAGACTGAG-3’
PTPRH reverse	5’-CGACATCCTCATACGGGACT-3’
RAPGEF4 forward	5’-ATGGAAACGGGCTCTAAC-3’
RAPGEF4 reverse	5’-AGCAGGACGAAGAGGAAC-3’
SEC14L5 forward	5’-CATAGCAGCTCCCTGGTCTC-3’
SEC14L5 reverse	5’-GCTGGCTTCTCATTCTGGAC-3’
SERPINA1 forward	5’-TGGAGGAGGAATGAAGAAAGCA-3’
SERPINA1 reverse	5’-AGCAGGACCCCAAATTCTGA-3’
SGK1 forward	5’-GCAGAAGGACAGGACAAAGC-3’
SGK1 reverse	5’-TTTGGGTTAAAAGGGGGAGT-3’
SLC47A1 forward	5’-CGAACGATGTTGGAAAGACA-3’
SLC47A1 reverse	5’-CCAGCTGTTTCCTGGACAAT-3’
SLC6A14 forward	5’-GCAGTGGGATTAGGAAATG-3’
SLC6A14 reverse	5’-GCAAATTGTCCCAGTGAAC-3’
SLIT1 forward	5’-GGACTTTCACCAGGTCCAGA-3’

SLIT1 reverse	5’-GTGAACTTCCTCCGCTTCAG-3’
SMTNL2 forward	5’-GAATCTGGCCAACTGTGAGC-3’
SMTNL2 reverse	5’-CATCACCATCATGTCCTCCA-3’
SOCS2 forward	5’-ACACGTCAGCACCATCTCTG-3’
SOCS2 reverse	5’-TGGCACCGGTACATTTGTTA-3’
STOM forward	5’-CACCATTGCTGCTGAGAAAA-3’
STOM reverse	5’-TTTGCCCCTATGATTCCTTG-3’
TGM2 forward	5’-ACCCTTCAGACCCCAGTTCT-3’
TGM2 reverse	5’-CAGCTAAGGCTGTTGGGAAG-3’
TMOD3 forward	5’-GGAAGTAGTAATGGTGTTGACC-3’
TMOD3 reverse	5’-GCTCATCAAATACCGGAAG-3’
TRIB2 forward	5’-GATGATTCCCTCTCCGACAA-3’
TRIB2 reverse	5’-GTAGCTGCCACTGGTGTTCA-3’
VEGFC forward	5’-AAAGAACCTGCCCCAGAAAT-3’
VEGFC reverse	5’-TGGTGGTGGAACTTCTTTCC-3’
WISP2 forward	5’-TGCATGGGACATTCACCAAA-3’
WISP2 reverse	5’-TTCCTTATGGGATTGTTGTGCAT-3’
ZNF804A forward	5’-CAAAGGGAATTTGCTCGAAA-3’
ZNF804A reverse	5’-TTGGAGTGCCTTTTCCTGTT-3’

REFERENCES

Abdelkarim, G. E., Gertz, K., Harms, C., Katchanov, J., Dirnagl, U., Szabo, C., and Endres, M. (2001). Protective effects of PJ34, a novel, potent inhibitor of poly(ADP-ribose) polymerase (PARP) in in vitro and in vivo models of stroke. Int J Mol Med *7*, 255-260.

Ame, J. C., Spenlehauer, C., and de Murcia, G. (2004). The PARP superfamily. Bioessays *26*, 882-893.

Bryant, H. E., Schultz, N., Thomas, H. D., Parker, K. M., Flower, D., Lopez, E., Kyle, S., Meuth, M., Curtin, N. J., and Helleday, T. (2005). Specific killing of BRCA2-deficient tumours with inhibitors of poly(ADP-ribose) polymerase. Nature *434*, 913-917.

Core, L. J., Waterfall, J. J., and Lis, J. T. (2008). Nascent RNA sequencing reveals widespread pausing and divergent initiation at human promoters. Science *322*, 1845-1848.

Couse, J. F., and Korach, K. S. (1999a). Estrogen receptor null mice: what have we learned and where will they lead us? Endocr Rev *20*, 358-417.

Couse, J. F., and Korach, K. S. (1999b). Reproductive phenotypes in the estrogen receptor-alpha knockout mouse. Ann Endocrinol (Paris) *60*, 143-148.

D'Amours, D., Desnoyers, S., D'Silva, I., and Poirier, G. (1999). Poly(ADP-ribosyl)ation reactions in the regulation of nuclear functions. Biochem J *342*, 249-268.

Deroo, B. J., and Korach, K. S. (2006). Estrogen receptors and human disease. J Clin Invest *116*, 561-570.

Farmer, H., McCabe, N., Lord, C. J., Tutt, A. N., Johnson, D. A., Richardson, T. B., Santarosa, M., Dillon, K. J., Hickson, I., Knights, C.*, et al.* (2005). Targeting the DNA repair defect in BRCA mutant cells as a therapeutic strategy. Nature *434*, 917-921.

Fong, P. C., Boss, D. S., Yap, T. A., Tutt, A., Wu, P., Mergui-Roelvink, M., Mortimer, P., Swaisland, H., Lau, A., O'Connor, M. J.*, et al.* (2009). Inhibition of

poly(ADP-ribose) polymerase in tumors from BRCA mutation carriers. N Engl J Med *361*, 123-134.

Foster, J. S., Henley, D. C., Bukovsky, A., Seth, P., and Wimalasena, J. (2001). Multifaceted regulation of cell cycle progression by estrogen: regulation of Cdk inhibitors and Cdc25A independent of cyclin D1-Cdk4 function. Mol Cell Biol *21*, 794-810.

Frizzell, K. M., Gamble, M. J., Berrocal, J. G., Zhang, T., Krishnakumar, R., Cen, Y., Sauve, A. A., and Kraus, W. L. (2009). Global analysis of transcriptional regulation by poly(ADP-ribose) polymerase-1 and poly(ADP-ribose) glycohydrolase in MCF-7 human breast cancer cells. J Biol Chem *284*, 33926-33938.

Fu, Z., and Fenselau, C. (2005). Proteomic evidence for roles for nucleolin and poly[ADP-ribosyl] transferase in drug resistance. J Proteome Res *4*, 1583-1591.

Galbis-Martinez, M., Saenz, L., Ramirez, P., Parrilla, P., and Yelamos, J. (2010). Poly(ADP-ribose) polymerase-1 modulates interferon-gamma-inducible protein (IP)-10 expression in murine embryonic fibroblasts by stabilizing IP-10 mRNA. Mol Immunol *47*, 1492-1499.

Gamble, M. J., Frizzell, K. M., Yang, C., Krishnakumar, R., and Kraus, W. L. (2010). The histone variant macroH2A1 marks repressed autosomal chromatin, but protects a subset of its target genes from silencing. Genes Dev *24*, 21-32.

Gruber, C. J., Tschugguel, W., Schneeberger, C., and Huber, J. C. (2002). Production and actions of estrogens. N Engl J Med *346*, 340-352.

Hassa, P. O., and Hottiger, M. O. (1999). A role of poly (ADP-ribose) polymerase in NF-kappaB transcriptional activation. Biol Chem *380*, 953-959.

Inbar-Rozensal, D., Castiel, A., Visochek, L., Castel, D., Dantzer, F., Izraeli, S., and Cohen-Armon, M. (2009). A selective eradication of human non-hereditary breast cancer cells by phenanthridine derived poly(ADP-ribose) polymerase inhibitors. Breast Cancer Research.

Isabelle, M., Moreel, X., Gagne, J. P., Rouleau, M., Ethier, C., Gagne, P., Hendzel, M. J., and Poirier, G. G. (2010). Investigation of PARP-1, PARP-2, and PARG interactomes by affinity-purification mass spectrometry. Proteome Sci *8*, 22.

Ju, B. G., Lunyak, V. V., Perissi, V., Garcia-Bassets, I., Rose, D. W., Glass, C. K., and Rosenfeld, M. G. (2006). A topoisomerase IIbeta-mediated dsDNA break required for regulated transcription. Science *312*, 1798-1802.

Ju, B. G., Solum, D., Song, E. J., Lee, K. J., Rose, D. W., Glass, C. K., and Rosenfeld, M. G. (2004). Activating the PARP-1 sensor component of the groucho/ TLE1 corepressor complex mediates a CaMKinase IIdelta-dependent neurogenic gene activation pathway. Cell *119*, 815-829.

Kim, M. Y., Mauro, S., Gevry, N., Lis, J. T., and Kraus, W. L. (2004). NAD+-dependent modulation of chromatin structure and transcription by nucleosome binding properties of PARP-1. Cell *119*, 803-814.

Kim, M. Y., Woo, E. M., Chong, Y. T., Homenko, D. R., and Kraus, W. L. (2006). Acetylation of estrogen receptor alpha by p300 at lysines 266 and 268 enhances the DNA binding and transactivation activities of the receptor. Mol Endocrinol.

Kim, M. Y., Zhang, T., and Kraus, W. L. (2005). Poly(ADP-ribosyl)ation by PARP-1: 'PAR-laying' NAD+ into a nuclear signal. Genes Dev *19*, 1951-1967.

Kininis, M., Chen, B. S., Diehl, A. G., Isaacs, G. D., Zhang, T., Siepel, A. C., Clark, A. G., and Kraus, W. L. (2007). Genomic analyses of transcription factor binding, histone acetylation, and gene expression reveal mechanistically distinct classes of estrogen-regulated promoters. Mol Cell Biol *27*, 5090-5104.

Kininis, M., Isaacs, G. D., Core, L. J., Hah, N., and Kraus, W. L. (2009). Postrecruitment regulation of RNA polymerase II directs rapid signaling responses at the promoters of estrogen target genes. Mol Cell Biol *29*, 1123-1133.

Kininis, M., and Kraus, W. L. (2008). A global view of transcriptional regulation by nuclear receptors: gene expression, factor localization, and DNA sequence analysis. Nucl Recept Signal *6*, e005.

Kotoglou, P., Kalaitzakis, A., Vezyraki, P., Tzavaras, T., Michalis, L. K., Dantzer, F., Jung, J. U., and Angelidis, C. (2009). Hsp70 translocates to the nuclei and nucleoli, binds to XRCC1 and PARP-1, and protects HeLa cells from single-strand DNA breaks. Cell Stress Chaperones *14*, 391-406.

Kraus, W. L. (2008). Transcriptional control by PARP-1: chromatin modulation, enhancer-binding, coregulation, and insulation. Curr Opin Cell Biol *20*, 294-302.

Kraus, W. L., and Lis, J. (2003). PARP goes transcription. Cell *113*, 677-683.

Krishnakumar, R., Gamble, M. J., Frizzell, K. M., Berrocal, J. G., Kininis, M., and Kraus, W. L. (2008). Reciprocal binding of PARP-1 and histone H1 at promoters specifies transcriptional outcomes. Science *319*, 819-821.

Krishnakumar, R., and Kraus, W. L. (2010). The PARP side of the nucleus: molecular actions, physiological outcomes, and clinical targets. Mol Cell *39*, 8-24.

Kun, E., Kirsten, E., Mendeleyev, J., and Ordahl, C. P. (2004). Regulation of the enzymatic catalysis of poly(ADP-ribose) polymerase by dsDNA, polyamines, Mg2+, Ca2+, histones H1 and H3, and ATP. Biochemistry *43*, 210-216.

Kun, E., Kirsten, E., and Ordahl, C. P. (2002). Coenzymatic activity of randomly broken or intact double-stranded DNAs in auto and histone H1 trans-poly(ADP-ribosylation), catalyzed by poly(ADP-ribose) polymerase (PARP I). J Biol Chem *277*, 39066-39069.

Li, R., Li, Y., Kristiansen, K., and Wang, J. (2008). SOAP: short oligonucleotide alignment program. Bioinformatics *24*, 713-714.

Lis, J. T., and Kraus, W. L. (2006). Promoter cleavage: a topoIIbeta and PARP-1 collaboration. Cell *125*, 1225-1227.

Lonskaya, I., Potaman, V. N., Shlyakhtenko, L. S., Oussatcheva, E. A., Lyubchenko, Y. L., and Soldatenkov, V. A. (2005). Regulation of poly(ADP-ribose) polymerase-1 by DNA structure-specific binding. J Biol Chem *280*, 17076-17083.

Marino, M., Galluzzo, P., and Ascenzi, P. (2006). Estrogen signaling multiple pathways to impact gene transcription. Curr Genomics *7*, 497-508.

Meder, V. S., Boeglin, M., de Murcia, G., and Schreiber, V. (2005). PARP-1 and PARP-2 interact with nucleophosmin/B23 and accumulate in transcriptionally active nucleoli. J Cell Sci *118*, 211-222.

Munoz-Gamez, J. A., Martin-Oliva, D., Aguilar-Quesada, R., Canuelo, A., Nunez, M. I., Valenzuela, M. T., Ruiz de Almodovar, J. M., De Murcia, G., and Oliver, F. J. (2005). PARP inhibition sensitizes p53-deficient breast cancer cells to doxorubicin-induced apoptosis. Biochem J *386*, 119-125.

Nef, S., and Parada, L. F. (2000). Hormones in male sexual development. Genes Dev *14*, 3075-3086.

Oei, S. L., and Shi, Y. (2001). Transcription factor Yin Yang 1 stimulates poly(ADP-ribosyl)ation and DNA repair. Biochem Biophys Res Commun *284*, 450-454.

Ordonez-Moran, P., and Munoz, A. (2009). Nuclear receptors: genomic and non-genomic effects converge. Cell Cycle *8*, 1675-1680.

Pavri, R., Lewis, B., Kim, T. K., Dilworth, F. J., Erdjument-Bromage, H., Tempst, P., de Murcia, G., Evans, R., Chambon, P., and Reinberg, D. (2005). PARP-1 determines specificity in a retinoid signaling pathway via direct modulation of mediator. Mol Cell *18*, 83-96.

Potaman, V. N., Shlyakhtenko, L. S., Oussatcheva, E. A., Lyubchenko, Y. L., and Soldatenkov, V. A. (2005). Specific binding of poly(ADP-ribose) polymerase-1 to cruciform hairpins. J Mol Biol *348*, 609-615.

Prall, O. W., Rogan, E. M., and Sutherland, R. L. (1998). Estrogen regulation of cell cycle progression in breast cancer cells. J Steroid Biochem Mol Biol *65*, 169-174.

Robinson, M. D., McCarthy, D. J., and Smyth, G. K. (2010). edgeR: a Bioconductor package for differential expression analysis of digital gene expression data. Bioinformatics *26*, 139-140.

Rolli, V., Ruf, A., Augustin, A., Schulz, G. E., Ménissier-de Murcia, J., and de Murcia, G. (2000). Poly(ADP-ribose) polymerase: structure and function. In From DNA Damage and Stress Signalling to Cell Death: Poly ADP-Ribosylation Reactions, G. de Murcia, and S. Shall, eds. (New York, Oxford Ubiversity Press), pp. 35-79.

Sommer, S., and Fuqua, S. A. (2001). Estrogen receptor and breast cancer. Semin Cancer Biol *11*, 339-352.

Torrano, V., Navascues, J., Docquier, F., Zhang, R., Burke, L. J., Chernukhin, I., Farrar, D., Leon, J., Berciano, M. T., Renkawitz, R.*, et al.* (2006). Targeting of CTCF to the nucleolus inhibits nucleolar transcription through a poly(ADP-ribosyl)ation-dependent mechanism. J Cell Sci *119*, 1746-1759.

Tulin, A., Chinenov, Y., and Spradling, A. (2003). Regulation of chromatin structure and gene activity by poly(ADP-ribose) polymerases. Curr Top Dev Biol *56*, 55-83.

Wacker, D. A., Frizzell, K. M., Zhang, T., and Kraus, W. L. (2007a). Regulation of chromatin structure and chromatin-dependent transcription by poly(ADP-ribose) polymerase-1: possible targets for drug-based therapies. Subcell Biochem *41*, 45-69.

Wacker, D. A., Ruhl, D. D., Balagamwala, E. H., Hope, K. M., Zhang, T., and Kraus, W. L. (2007b). The DNA binding and catalytic domains of poly(ADP-ribose) polymerase 1 cooperate in the regulation of chromatin structure and transcription. Mol Cell Biol *27*, 7475-7485.

CHAPTER 4

The Histone Variant macroH2A1 Regulates Target Gene Expression in Part by Recruiting the Transcriptional Coregulator PELP1*

***** Contributions by other authors to this work were as follows: M.J.G., GST-pull downs, PELP1 ChIP-chip, and computational analyses, ChIP-qPCR, and RT-qPCR (Figures 4.1-4.6 and 4.10-4.12); E.P., GST-pull downs (Figures 4.1 and 4.2); C.Y., PELP1 knockdown cell line generation and RT-qPCR (Figures 4.8-4.10); N.H., MCF-7 TetR cell line generation (Figure 4.9 and data not shown); H.E-B. and P.T., MS/MS analyses (Figure 4.1).

4.1. Summary

MacroH2A1 is a distinct histone variant harboring a ~30 kDa carboxyl-terminal macro domain. Due to its enrichment on the inactive X chromosome, macroH2A1 has long been thought to play a role in transcriptional repression. However, recent studies have begun to shed light on a more complex role for macroH2A1. That is, macroH2A1 occupies autosomal chromatin and regulates genes in a context-specific manner. The globular macro domain protruding from the nucleosome core may be a major player in the modulation of gene expression outcomes via physical interactions with effector proteins, which may depend on the ability of the macro domain to bind NAD^+ metabolite ligands. Here, we identify Proline, glutamate, and leucine rich protein 1 (PELP1), a chromatin-associated factor and classic transcriptional coregulator, as a novel ligand-independent macro domain-interacting factor. We used chromatin immunoprecipitation coupled with tiling microarrays (ChIP-chip) to determine the genomic localization of PELP1 in MCF-7 human breast cancer cells. Our data reveal that PELP1 genomic localization is highly correlated with that of macroH2A1. Additionally, PELP1 positively correlates with heterochromatic chromatin marks and negatively correlates with active transcription marks, much like macroH2A1. We show that macroH2A1 specifically recruits PELP1 to the promoters of macroH2A1 target genes, but macroH2A1 deposition occurs independent of PELP1. Furthermore, we demonstrate that this recruitment allows for macroH2A1 and PELP1 to cooperatively regulate gene expression outcomes.

4.2. Introduction

The canonical nucleosome architecture, two copies each of histones H2A, H2B, H3, and H4, organizes the genomes of Eukaryotes and is locally modified in a multitude of ways for various regulatory purposes. These modifications include the post-translational modification of histones, changes in nucleosome positioning, and the replacement of canonical histones with their histone variant counterparts.

MacroH2A1 is one such histone variant that can substitute for at least one copy of H2A in a subset of nucleosomes in vertebrates. At three times the size of histone H2A, macroH2A1 is made up of an amino-terminal histone like regions with 64% identity to H2A and a carboxyl-terminal ~30 kDa macro domain. Based largely on the observation that macroH2A1 is enriched on the transcriptionally silent inactive X chromosome (*Xi*) (Costanzi and Pehrson, 1998; Mietton et al., 2009), macroH2A1 was originally hypothesized to play a role in transcriptional repression (reviewed in (Ladurner, 2003)). However, later studies demonstrated that macroH2A1 is not required for the initiation or maintenance of X-inactivation (Changolkar et al., 2007; Csankovszki et al., 1999; Rasmussen et al., 2001; Wutz et al., 2002), casting doubt on a general role for macroH2A in transcriptional repression.

Recent work from our lab and others has determined that macroH2A1 is not only a component of chromatin on the *Xi*, it occupies approximately a quarter of the autosomal genome (Buschbeck et al., 2009; Gamble et al., 2010). Additionally, macroH2A1 is generally associated with transcriptionally repressive heterochromatin across autosomes where it co-localizes with other heterochromatin marks such as histone H3 lysine 27 trimethylation (H3K27me3) (Buschbeck et al., 2009; Gamble et al., 2010). However, while macroH2A1 is a component of autosomal heterochromatin, it is not generally required for the repression of genes found in

macroH2A1-containing domains (Gamble et al., 2010), similar to the lack of a general requirement for macroH2A1 in the transcriptional repression of genes on the *Xi*. A growing body of evidence suggests that macroH2A1 can play either a positive or negative role in regulating the transcription of genes found in its domains in a context-specific manner (Agelopoulos and Thanos, 2006; Buschbeck et al., 2009; Changolkar et al., 2007; Changolkar et al., 2008; Gamble et al., 2010; Gamble and Kraus, 2010).

MacroH2A1-containing nucleosomes and canonical nucleosomes are structurally similar. They both organize the same amount of DNA and their crystal structures are also highly comparable (Abbott et al., 2004; Chang et al., 2005; Changolkar and Pehrson, 2002). However, the macro domain protruding from the nucleosome core has important biochemical consequences for macroH2A1-containing nucleosomes. For example, macroH2A1-containing nucleosomes display increased nuclease protection near the dyad of symmetry (Changolkar and Pehrson, 2002). Some transcription factors cannot bind to their DNA sites specifically when they are incorporated into a macroH2A1-containing nucleosome (Agelopoulos and Thanos, 2006; Angelov et al., 2003). Additionally, macroH2A1-containing nucleosomes are poor substrates for ATP-dependent chromatin remodeling enzymes, in the absence of histone chaperones (Angelov et al., 2006; Angelov et al., 2003; Chang et al., 2008).

Macro domains are ancient domains that have been identified in proteins from bacteria to humans (Pehrson and Fuji, 1998). In macroH2A1-containing nucleosomes, this extra 30-kDa globular domain may be responsible for recruiting additional effector proteins to macroH2A1-containing chromatin in order to facilitate the regulation of gene expression (Chakravarthy et al., 2005; Hernandez-Munoz et al., 2005; Nusinow et al., 2007; Ouararhni et al., 2006). Recent work from Ladurner's group and others suggest that most macro domains are ligand binding domains for NAD^+ metabolites such as poly(ADP-ribose) (PAR), a post-translational modification

catalyzed by a family of PAR polymerases (PARPs), monomeric ADP-ribose, and O-acetyl-ADP-ribose, produced as a by-product of sirtuin family deacetylase reactions (Ahel et al., 2009; Gottschalk et al., 2009; Karras et al., 2005; Kraus, 2009; Kustatscher et al., 2005; Timinszky et al., 2009). Ligand binding by macro domains appears to have two functions that have been identified thus far. First, ligand binding can alter the affinity of some proteins to interact with macro domains. For example, the macro domain of macroH2A1.1 interacts specifically with automodified PARP-1, in a manner that requires the ability of the macro domain to bind PAR (Nusinow et al., 2007; Timinszky et al., 2009). Second, macro domains can mediate the recruitment of factors that contain these domains to genomic sites of PAR accumulation (Ahel et al., 2009; Gottschalk et al., 2009; Timinszky et al., 2009).

Here, we report the identification of the transcriptional coactivator Proline-, glutamic acid-, and leucine-rich protein 1 (PELP1) as a novel factor that interacts with the macro domain of macroH2A1. PELP1, otherwise known as modulator of the non-genomic activities of estrogen receptor (MNAR), has been shown to promote estrogen receptor-dependent transcription as both a classical coactivator and through a controversial plasma membrane signaling mechanism (Cheskis et al., 2008; Vadlamudi et al., 2001). PELP1 is also a chromatin-associated factor that has been shown to interact with a variety of transcription factors (i.e. AR, GR), covalently modified histone H3, and the linker histone H1 (Choi et al., 2004; Khan et al., 2006; Nair et al., 2007; Nair et al., 2004; Nair et al., 2010). Recently, PELP1 has been shown to stimulate transcription by displacing the linker histone H1 and/or by recruiting the lysine demethylase KDM1 to demethylate H3K9me2 (Nair et al., 2010). Taken together, these studies suggest that PELP1 is multifunctional protein that can regulate chromatin-dependent transcriptional processes through many mechanisms.

In the studies described herein, we document the physical and functional interactions of macroH2A1 with PELP1, using a series of biochemical, genomic, and gene-specific analyses. We demonstrate that PELP1 and macroH2A1 interact in a manner that is independent of macroH2A1's ability to bind NAD^+ metabolites. Using ChIP-chip, we show that macroH2A1 and PELP1 are highly correlated in their genomic localization patterns. Furthermore, we demonstrate that macroH2A1 specifically recruits PELP1 to a subset of macroH2A1 target gene promoters to cooperatively modulate gene expression outcomes.

4.3. Results

A GST pull-down using the macro domain of the histone variant macroH2A1.1 reveals interactions with a multitude of nuclear proteins. Our previous work demonstrated that macroH2A1-containing chromatin can both positively and negatively regulate the expression of its target genes in a context-specific manner. The histone variant macroH2A1.1, depicted in Figure 4.1A, consists of a canonical histone H2A region, followed by a basic linker and a globular macro domain. The macro domain of macroH2A is the most striking feature differentiating macroH2A1-containing nucleosomes from canonical nucleosomes. At ~30 kDa, the globular macro domain extends near the dyad axis of the nucleosome and makes minimal contact with DNA (Changolkar and Pehrson, 2002), suggesting that the macro domain may make important protein-protein interactions that facilitate the regulation of transcription by macroH2A1. To identify the proteins interacting with this macro domain, we performed a GST pull-down assay using the basic linker and macro domain regions of macroH2A1.1 (GST-macro1.1) as bait (Figure 4.1B). GST alone or GST-macro1.1 was immobilized using glutathione affinity resin and incubated with or

without HeLa nuclear extract. After washing the resin, the bound fraction was eluted from the resin using glutathione. The eluates were separated by SDS-PAGE and visualized by silver staining. GST-macro1.1-specific protein bands were excised from the gel, trypsinized, and protein fragments were identified by mass spectrometry.

The GST-macro1.1-interacting proteins we identified are chromatin-associated and nucleolar components that participate in cellular activities such as transcription, ribosome biogenesis/export, RNA maturation, protein chaperoning, and maintenance of chromatin structure (see supplementary Figure 4.2 and Table 4.1). Notably, both Poly(ADP-ribose) Polymerase-1 (PARP-1) and Proline, glutamate, and leucine rich protein 1 (PELP1) were identified as factors that interact with the macro domain of macroH2A1.1. PARP-1 has previously been identified as a factor that interacts with the macroH2A macro domain (Nusinow et al., 2007; Ouararhni et al., 2006), validating our results. PELP1 is a nuclear protein (~180 kDa) that modulates both genomic and non-genomic activities of nuclear receptors through interactions with nuclear proteins (*i.e.*, HDAC2, SUMO2, ERα, AR, GR, RXRA, STAT3; (Brann et al., 2008; Choi et al., 2004; Khan et al., 2006; Manavathi et al., 2005; Nair et al., 2007; Rosendorff et al., 2006; Singh et al., 2006)) and chromatin components (*i.e.*, H1 and H3; (Nair et al., 2004; Nair et al., 2010)) involved in transcriptional regulation.

Previous reports indicate that the interaction of macroH2A1 and PARP-1 is modulated by the macro domain ligand, ADP-ribose (ADPR) (Timinszky et al., 2009). We hypothesized that macroH2A1 and PELP1 may interact in a similar manner. To test this, the GST pull-down assay was repeated in the presence of the macro domain ligand ADPR or NAD^+ as a control (Figure 4.1C). Using Western blot analyses, we were able to confirm the specific interactions of both PARP-1 and PELP1 with GST-macro1.1, compared to GST alone. As previously shown (Timinszky et al., 2009), PARP-1 binding was lost in the presence of ADPR, but not with NAD^+. However, we

Figure 4.1. PELP1 interacts with the macro domain of the histone variant macroH2A1.1 in an ADPR-independent manner. *A,* Schematic diagram of the histone variant macroH2A1.1 and GST-tagged macro domain. The histone H2A-like region (*H2A*), macro domain, and the basic linker region (*Basic*), are shown. The GST-macro1.1 fusion consists of GST fused to the non-histone regions only. GST alone, used as a control, is shown for comparison. *B,* Silver stain image of GST-macro1.1 interacting proteins from a GST pull-down assay. GST alone or GST-macro1.1 fusion protein were immobilized on glutathione affinity resin and incubated with or without HeLa nuclear extract. Bound fractions were washed, eluted with glutathione, and separated by SDS-PAGE. Resulting eluates were visualized by silver stain. GST-macro1.1-specific protein bands were excised from the gel, trypsinized, and identified by mass spectrometry. Macro domain-interacting proteins, PELP1 and PARP-1, are shown. The full data set of identified proteins can be found in supplementary Figure 4.2 and Table 4.1. *C,* PELP1 and PARP-1 interactions with the macro domain of macroH2A1 are differentially mediated by the macro domain ligand, ADP-ribose (ADPR). The GST pull-down assay described in panel B was repeated in the absence and presence of ADPR or NAD^+, as a control. Western blotting confirms PELP1 and PARP-1 interaction with GST-macro1.1 (*None*). ADPR impedes the interaction of PARP-1 with the macro domain, but not that of PELP1 (*ADPR*).

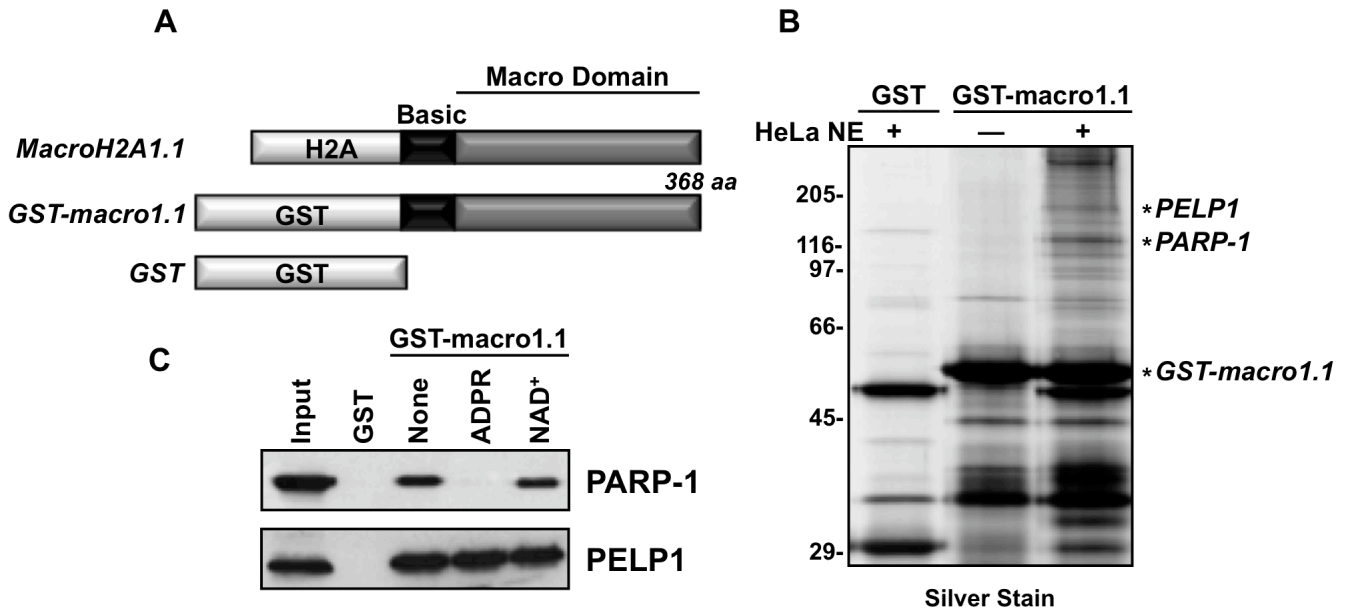
A
Macro Domain
Basic
MacroH2A1.1
H2A
368 aa
GST-macro1.1
GST
GST
GST
B
GST
GST-macro1.1
HeLa NE
+
—
+
205-
116-
97-
66-
45-
29-
*PELP1
*PARP-1
*GST-macro1.1
Silver Stain
C
GST-macro1.1
Input
GST
None
ADPR
NAD+
PARP-1
PELP1

Figure 4.2. The macro domain of the histone variant MacroH2A1.1 interacts with a both chromatin-associated proteins and nucleolar components. *A,* Silver stain image of GST-macro1.1 interacting proteins from a GST pull-down assay. GST alone or GST-macro1.1 fusion protein were immobilized on glutathione affinity resin and incubated with or without HeLa nuclear extract. Bound fractions were washed, eluted with free glutathione, and separated by SDS-PAGE. Resulting eluates were visualized by silver stain. GST-macro1.1-specific protein bands were excised from the gel, trypsinized, and identified by mass spectrometry. All identified macro domain-interacting proteins are described further in Table 4.1. *B,* Western blotting confirms the interaction of GST-macro1.1 with nucleolin and SET.

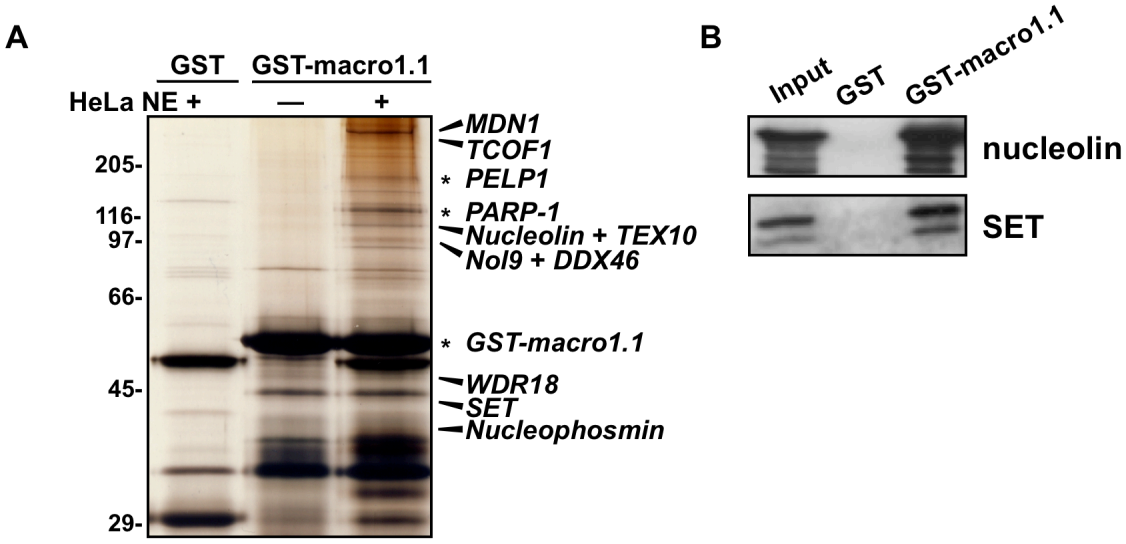
A
GST
GST-macro1.1
HeLa NE +
—
+
205-
116-
97-
66-
45-
29-
MDN1
TCOF1
* PELP1
* PARP-1
Nucleolin + TEX10
Nol9 + DDX46
* GST-macro1.1
WDR18
SET
Nucleophosmin
B
Input
GST
GST-macro1.1
nucleolin
SET

Table 4.1. Proteins identified as interactors of the histone variant macroH2A1 macro domain are categorized as chromatin-associated and nucleolar components. For each identified protein, the gene symbol, protein name, and known cellular functions are listed, based on GeneCards descriptions.

Gene Symbol	Protein Name	GeneCards® Accession No.[a]	Protein Function[b]
Chromatin-Associated Components			
PELP1	Proline, glutamate, and leucine rich protein 1	GC17M004521	Modulator of non-genomic activity of estrogen receptor and other nuclear receptors; Associated with tumorigenesis via interactions with oncogenic proteins (e.g. SRC)
PARP1	Poly(ADP-ribose) Polymerase 1	GC01M224615	Involved in DNA repair and cell death pathways; Modulates chromatin structure and transcription; Associated with various diseases (e.g., cancer, stroke, heart disease, obesity)
WDR18	WD repeat-containing protein 18	GC19P000935	WD repeat protein family member with unknown specific function; WD repeat domain facilitates the formation of multiprotein complexes and is involved in cell cycle progression and death, signal transduction, and transcription
SET	SET nuclear oncogene	GC09P130485	Involved in apoptosis, transcription, nucleosome assembly and histone binding
Nucleolar Components			
TCOF1	Treacher Collins-Franceschetti syndrome 1	GC05P149717	Involved in rDNA transcription via interaction with upstream binding factor (UBF) and nucleolar-cytoplasmic; Associated with Treacher Collins Syndrome by defects in early embryo development
NCL	Nucleolin	GC02M232027	Involved in rDNA transcription, maturation, and ribosomal nuclear export
NPM1	Nucleophosmin	GC05P170747	Involved in ribosome biogenesis, protein chaperoning, histone assembly, cell proliferation, transcription, and centrosome duplication; Associated with acute myeloid leukemia (AML) by genetic mutations
MDN1	Midasin homolog (yeast)	GC06M090352	AAA ATPase family member involved in maturation and export of pre-60S ribosome subunit
DDX46	DEAD (Asp-Glu-Ala-Asp) box polypeptide 46	GC05P134094	RNA helicase involved in RNA splicing; 17S U2 snRNP complex component
TEX10	Testis expressed 10	GC09M102104	Nucleolar membrane component with unknown function
Nol9	Nucleolar Protein 9	GC01M006520	Nucleolus component with unknown function

[a] From GeneCards®, a searchable, integrated database of human genes that provides concise genomic, proteomic, trancriptomic, genetic, and functional information on all known and predicted human genes. http://www.genecards.org/index.shtml

[b] Based on GeneCards® description.

found that the PELP1 interaction with GST-macro1.1 was not interrupted in the presence of either ADPR or NAD^+. These results demonstrate that PELP1 interacts with the macro domain of macroH2A1 in an ADPR-independent manner.

PELP1 occupies large chromatin domains in the MCF-7 genome and is enriched in macroH2A1-bound regions. Recently, our lab reported the genomic localization patterns of macroH2A1 in MCF-7 cells using chromatin immunoprecipitation (ChIP) coupled to genomic tiling microarrays (*i.e.*, ChIP-chip; (Gamble et al., 2010)). Those results indicated that macroH2A1 occupies large chromatin domains and that the boundaries of those occupied regions are near transcription start sites. For a subset of genes, macroH2A1 bound regions occupy the transcribed region. Since our in vitro assay suggested that macroH2A1 and PELP1 interact, we sought to determine if PELP1 associated to the genome in a similar localization pattern to macroH2A1.

Using an antibody specific for PELP1, we performed ChIP-chip experiments in MCF-7 cells using a custom-designed Nimblegen platform previously described (Gamble et al., 2010; Krishnakumar et al., 2008), representing 4.14 Mb of genomic DNA including 1829 gene promoters typically tiled from -25 to +5 kb surrounding the TSSs. Using our previously defined criteria (Gamble et al., 2010), we determined that PELP1 significantly bound over 1953 regions on the array ranging in size from 1.5 to 7.5 kb (average ~1.9 kb) covering ~9% of the genome represented on the array. In total, PELP1 is found within 3 kb of the TSS for 257 (14.1%) genes on the array.

We compared the binding pattern of PELP1 to our previously published macroH2A1 ChIP-chip data set (National Institutes of Health GEO accession number GSE9607). Comparisons across several genomic loci, including all forty-four ENCODE regions (2004), revealed a striking correspondence between the PELP1 and macroH2A1 genomic occupancy (Figure 4.3). In order to determine if macroH2A1

and PELP1 associated with similar genomic regions on a global scale, we depicted each ChIP-chip data set as a heat map in which each row corresponds to the macroH2A1 or PELP1 ChIP-chip signal from -25 kb to +5 kb relative to the TSS for each TSS represented on the array. When the data from both heat maps are ordered for increasing average intensity of PELP1, an obvious correspondence between the two data sets can be observed (Figure 4.4A). This pattern is also clearly evident by an averaging analysis of all TSSs represented on our array (Figure 4.4B). As would be expected from these results, there is a significant correlation between the global localization pattern of macroH2A1 and PELP1 (Spearman correlation coefficient of ~0.53, *P*-value < 10^{-300}). Further analysis indicated that 67.7% of the PELP1-bound regions overlap with macroH2A1-containing domains (Figure 4.4C). In fact, there is over a 27-fold enrichment of PELP1 binding in macroH2A1-containing regions of the genome (*P*-value < 10^{-300}) (Figure 4.4D). Finally, of the 257 genes marked by PELP1 occupancy, 200 (78%) are co-occupied by macroH2A1. Overall, this data indicates that there is a tight statistical association between PELP1 and macroH2A1 binding across the genome in MCF-7 cells. Combined with the interaction data shown in Figure 4.1, this data supports the hypothesis that macroH2A1 and PELP1 are interacting with each other over many regions across the genome.

Despite the strong statistical enrichment of PELP1 in macroH2A1-containing domains, we are not able to detect PELP1 at all sites of macroH2A1 deposition in MCF-7 cells. In fact, PELP1 occupies only 29% of macroH2A1-bound regions (Figure 4.4C). Additionally, 22% of PELP1-bound genes do not contain significant levels of macroH2A1 within 3 kb of the TSS. The lack of complete overlap of PELP1 and macroH2A1 binding may indicate that PELP1 binding functionally distinguishes a subset of macroH2A1-containing regions. Alternatively, these differences could be due to the reduced efficiency of the PELP1 ChIP compared to that of macroH2A1. To

Figure 4.3. A comparison across several genomic loci reveals a striking correspondence between PELP1 and macroH2A1. *A* and *B,* Histograms depicting the Log_2 ratios of PELP1 and macroH2A1 ChIP-chip signals from MCF-7 cells across a representative ENCODE region (A) and a region centered around the SOCS2 promoter (B) represented on our custom-designed ChIP-chip array. The genomic location is shown and the position and orientation of RefSeq genes are depicted below each track. The genes are color-coded according to expression microarray data: green, expressed; blue, unexpressed; grey, ambiguous.

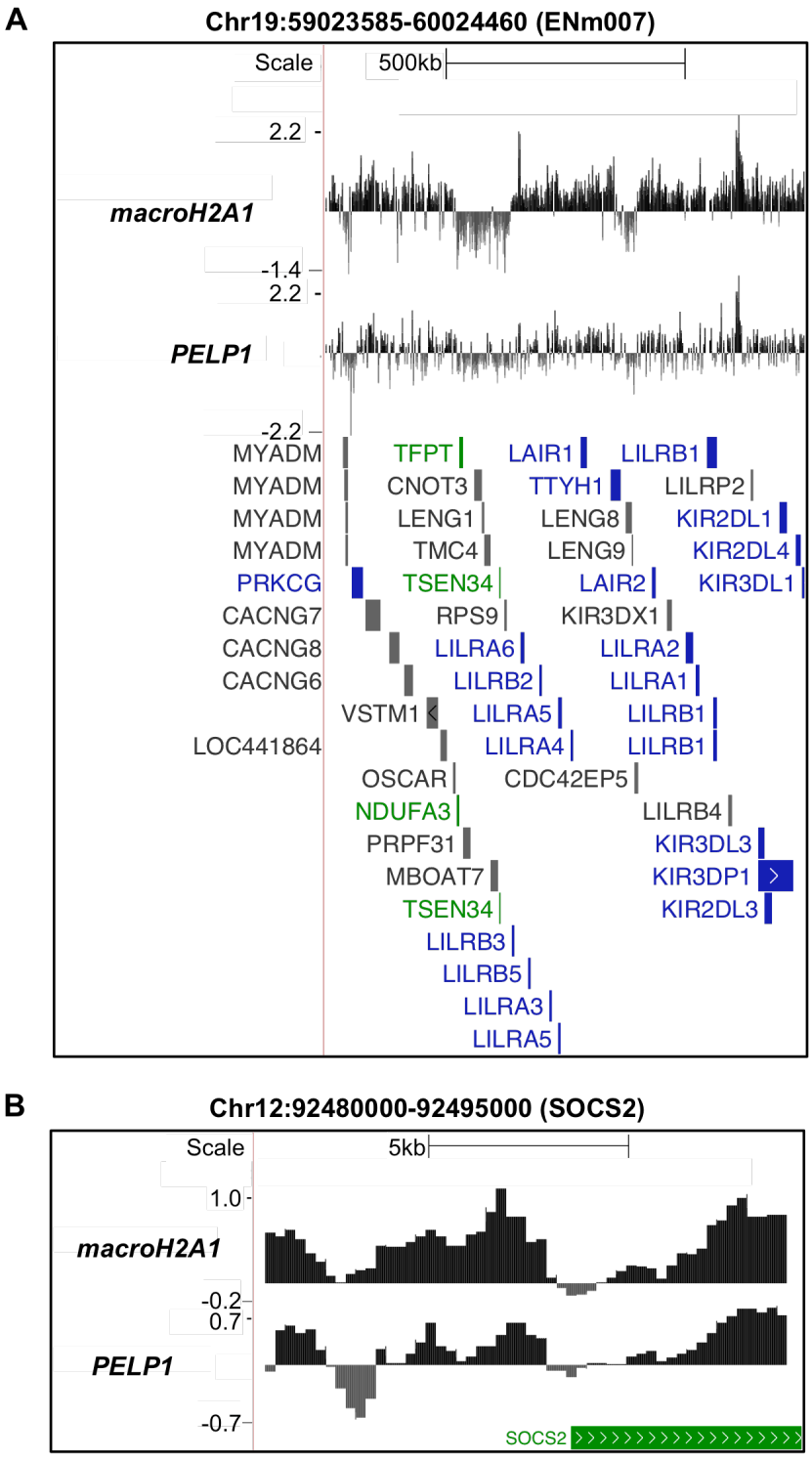
A
Chr19:59023585-60024460 (ENm007)
Scale
500kb
2.2
macroH2A1
-1.4
2.2
PELP1
-2.2
MYADM
MYADM
MYADM
MYADM
PRKCG
CACNG7
CACNG8
CACNG6
LOC441864
TFPT
CNOT3
LENG1
TMC4
TSEN34
RPS9
LILRA6
LILRB2
VSTM1
LILRA5
LILRA4
OSCAR
NDUFA3
PRPF31
MBOAT7
TSEN34
LILRB3
LILRB5
LILRA3
LILRA5
LAIR1
TTYH1
LENG8
LENG9
LAIR2
KIR3DX1
LILRA2
LILRA1
LILRB1
LILRB1
CDC42EP5
LILRB4
KIR3DL3
KIR3DP1
KIR2DL3
LILRB1
LILRP2
KIR2DL1
KIR2DL4
KIR3DL1
B
Chr12:92480000-92495000 (SOCS2)
Scale
5kb
1.0
macroH2A1
-0.2
0.7
PELP1
-0.7
SOCS2

Figure 4.4. PELP1 is significantly enriched in macroH2A1-bound regions and is also negatively correlated with gene expression. *A,* Heat maps showing macroH2A1 and PELP1 ChIP-chip data across 2149 promoters, tiled from -25 to +5 kb surrounding the transcription start sites. The data, ordered for average PELP1 intensity, reveal similar genomic localization patterns for both factors. *B,* Averaging analysis of the Log_2 enrichment ratios (IP/Input) for all windows from macroH2A1 (red) and PELP1 (blue) ChIP-chip data along the 30 kb regions represented on the array. Histone H3 (green) ChIP-chip data is shown for comparison. *C,* Venn diagram representing the number of well-tiled windows bound by macroH2A1, PELP1, or both (*Intersection*). Nearly 23% of macroH2A1 bound windows are also bound by PELP1, while 68% of PELP1 bound windows are also bound by macroH2A1. PELP1 bound "regions" are defined as consecutive windows bound by PELP1. *D,* Histogram depicting the fraction of macroH2A1 bound or unbound regions that are also bound by PELP1. The enrichment value (E) and *P*-value (p) from a Fisher exact test are shown. *E*, Histogram depicting the average Log_2 ratios of PELP1 and macroH2A1 signal within 3 kb of the TSS at genes within each pentile of expression, as determined from MCF-7 expression microarray data. The correlation coefficient (c.c.) and *P*-value (p) for PELP1 and macroH2A1 with gene expression is shown. *mH2A1, macroH2A1.*

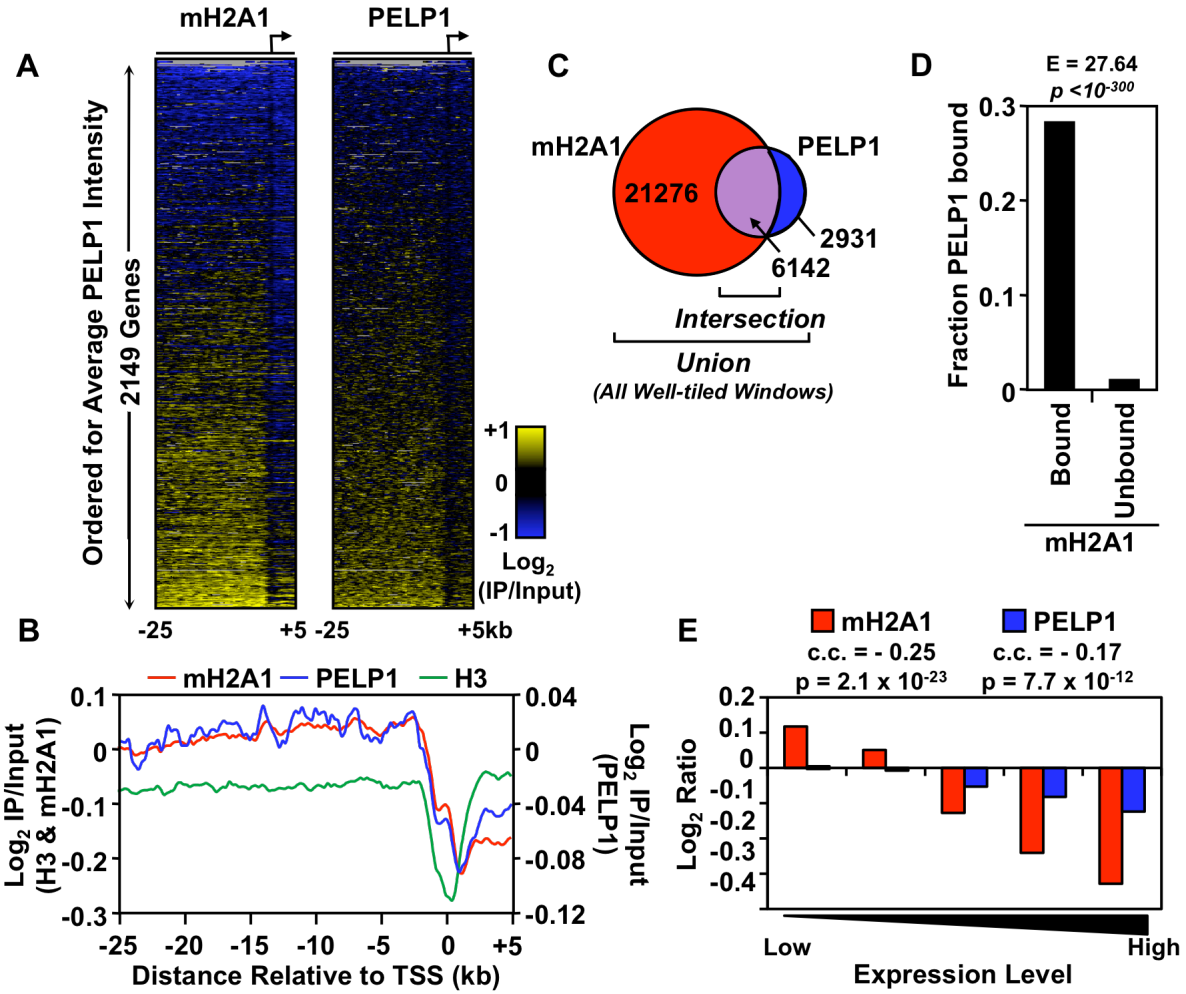
A
mH2A1
PELP1
Ordered for Average PELP1 Intensity
2149 Genes
+1
0
-1
Log2 (IP/Input)
-25
+5
-25
+5kb
B
mH2A1
PELP1
H3
Log2 IP/Input (H3 & mH2A1)
Log2 IP/Input (PELP1)
0.1
0
-0.1
-0.2
-0.3
0.04
-0.04
-0.08
-0.12
-25
-20
-15
-10
-5
0
+5
Distance Relative to TSS (kb)
C
mH2A1
PELP1
21276
2931
6142
Intersection
Union
(All Well-tiled Windows)
D
E = 27.64
p <10-300
Fraction PELP1 bound
0.3
0.2
0.1
0
Bound
Unbound
mH2A1
E
mH2A1
PELP1
c.c. = - 0.25
p = 2.1 x 10-23
c.c. = - 0.17
p = 7.7 x 10-12
Log2 Ratio
0.2
0.1
0
-0.1
-0.2
-0.3
-0.4
Low
High
Expression Level

examine these possibilities we set out to determine if PELP1 has a similar correlation to gene expression and histone marks, as well as gene ontology enrichment as previously observed for macroH2A1 (Gamble et al., 2010).

MacroH2A1 is negatively correlated with gene expression in both IMR90 cells and in MCF-7 cells (Gamble et al., 2010). By calculating the average macroH2A1 and PELP1 ChIP-chip signal within 3 kb of all TSSs and comparing to previously published Affymetrix expression data from MCF-7 cells (Kininis et al., 2007) we determined that similar to macroH2A1 (correlation coefficient of -0.25, *P*-value = 2 x 10^{-23}), PELP1 (correlation coefficient of -0.17, *P*-value = 7.7 x 10^{-12}) is significantly negatively correlated with gene expression (Figure 4.4E).

Previous gene ontology analysis determined that macroH2A1-containing domains are enriched for genes that are involved in developmental processes and signaling events. MacroH2A1-containing genes also often encode proteins that are secreted from the cell (Gamble et al., 2010). We performed a similar gene ontology analysis for PELP1-bound genes, as well as for those genes that are bound by both macroH2A1 and PELP1. We found that PELP1-bound genes are enriched for a similar set of ontological processes (Table 4.2 and Table 4.3).

Previously, we correlated macroH2A1 occupancy to 362 publically available ChIP-chip data sets and determined that macroH2A1 positively correlates with heterochromatic histone marks, including histone H3 lysine 27 trimethylation (H3K27me3), while negatively correlating with active transcription marks, such as RNA Polymerase II (RNA Pol II) (Gamble et al., 2010). By performing a similar analysis for PELP1 (Figure 4.5A), we found that PELP1 correlates with many of the same marks as macroH2A1 (Figure 4.5B), both positively and negatively. In addition, PELP1 correlates with factors and histone marks independent of macroH2A1 (Figure

Table 4.2. Summary of the most significant gene ontology terms enriched in genes with macroH2A1, PELP1, or both within 3kb surrounding the TSS. The enrichment of gene ontology terms in genes with macroH2A1-bound or PELP1-bound regions found within 3kb of the TSS in MCF-7 cells was compared with all other genes represented on the ChIP-chip array for all three ontology aspects.

Gene Ontology Term[a]	Aspect[b]	*P*-value
macroH2A1-bound Genes[c]		
Multicellular organismal process	BP	4.46×10^{-5}
System development	BP	7.44×10^{-5}
Multicellular organismal development	BP	0.00011
Anatomical structure development	BP	0.00087
Developmental process	BP	0.00103
Organ development	BP	0.00288
Regulation of localization	BP	0.00342
Signaling	BP	0.00663
Cell surface receptor linked signaling pathway	BP	0.00948
Extracellular region	CC	2.60×10^{-7}
Extracellular region part	CC	1.82×10^{-5}
Pattern binding	MF	0.00072
Polysaccharide binding	MF	0.00072
Glycosaminoglycan binding	MF	0.00200
PELP1-bound Genes[d]		
Multicellular organismal process	BP	0.00020
Cell surface receptor linked signaling pathway	BP	0.00878
Extracellular region part	CC	0.00071
Proteinaceous extracellular matrix	CC	0.00128
Extracellular matrix	CC	0.00175
macroH2A1- and PELP1-bound Genes[e]		
Multicellular organismal development	BP	4.74×10^{-5}
Organ development	BP	0.00023
Multicellular organismal process	BP	0.00024
Developmental process	BP	0.00026
System development	BP	0.00142
Anatomical structure development	BP	0.00216
Extracellular region part	CC	0.00011
Proteinaceous extracellular matrix	CC	0.00022
Extracellular matrix	CC	0.00023
Extracellular region	CC	0.00645

[a] Gene ontology terms were generated using the Generic Gene Ontology Term Finder (http://go.princeton.edu/cgi-bin/GOTermFinder/GOTermFinder).
[b] The aspects covered include: bp, biological process; cc, cellular component; and mf, molecular function.
[c, d, and e] The genes that correspond to each category can be found listed in Table 4.3.

Table 4.3. Gene lists used for gene ontology analysis. Gene lists consist of significantly bound or unbound macroH2A1 or PELP1, or both and subsequently used for gene ontology analysis, as shown in Table 4.2. (MacroH2A1 ChIP-chip data was accessed from the NCBI GEO website using accession number GSE9607.)

(i) macroH2A1-bound Genes

AADAT	C21orf54	CXCL12	FLJ44054	HOXA11AS	LILRA3
ABHD6	C22orf42	CXCR4	FLNA	HOXA13	LILRA4
ACADL	C3	CXCR7	FLRT2	HOXA2	LILRA5
ACCN4	C3orf54	CYB561	FOS	HOXA3	LILRA6
ACSL6	C5orf13	CYP1A1	FOXG1	HOXA4	LILRB1
ACTA2	C5orf35	CYP1A2	FOXN3	HOXA5	LILRB2
ACTB	C8orf74	DAPK2	FOXP2	HOXA6	LILRB3
ADAM2	CACNA1G	DBP	FST	HOXA7	LILRB4
ADAMTS9	CACNG6	DCLK1	FZD1	HOXA9	LILRB5
ADAMTSL1	CACNG7	DDX18	FZD7	IGF1	LILRP2
ADAMTSL3	CADM1	DEGS1	GAB3	IGF2	LOC100188949
ADIPOQ	CALCR	DES	GADD45A	IGF2AS	LOC26010
ADRB1	CALD1	DHRS3	GALNT12	IGFBP4	LOC284067
ADRBK1	CALML3	DIAPH2	GAS6	IGFBP5	LOC441108
ADSSL1	CALML5	DIRAS1	GATM	IL13	LOC441864
ALDH5A1	CAMK2N1	DKC1	GDF15	IL1R1	LOC91149
AMIGO2	CAPN9	DKFZP434K028	GDF5	IL24	LRIG1
AMMECR1	CAPZA2	DKK1	GEM	INPP5J	LRRC15
AMOTL2	CAV1	DLL4	GLRB	INS-IGF2	LRRK2
ANKRD43	CAV2	DNAJB3	GPC5	IQGAP1	LSP1
ANKRD55	CBFA2T3	DNASE1L3	GPRC5A	IRF1	LTF
ANXA3	CCBP2	DUSP1	GRAMD3	IRX5	LUZP2
APOA1	CCL2	DUSP3	GRB10	ISL1	MAP2K6
APOA4	CCNI2	DUSP4	GREB1	ITGA6	MAP3K1
APOA5	CD209	DYNC2LI1	GRM1	ITGB3	MAPK11
APOC3	CDC2	DYRK2	GRM8	ITGB4	MAPK12
ARAP2	CDC42EP4	EDAR	GTF2A1	ITK	MBNL2
AREG	CDH16	EFEMP1	GULP1	ITPR2	MBOAT7
ARHGAP18	CDH2	EGFR	H19	KCNK1	MCAM
ARHGAP26	CDH29	EGR3	H1FNT	KCNK5	MCF2L
ARHGDIG	CDH5	EIF6	H1FOO	KCNN2	MCM3
ARL14	CDKN2C	ELL2	HAPLN1	KIAA1026	MCTP2
ARL4A	CEACAM4	EMD	HBA1	KIR2DL1	MDFI
ASB13	CEACAM6	ENAH	HBA2	KIR2DL3	MDFIC
ASCL1	CEBPB	ENC1	HBE1	KIR2DL4	MEGF8
ASPH	CEP55	ENPP2	HBM	KIR3DL1	MET
ASZ1	CERK	EPHB2	HBP1	KIR3DL3	METTL9
ATF7IP	CFTR	EPN3	HBZ	KIR3DP1	MGAT3
ATL2	CH25H	ERBB4	HCCA2	KIR3DX1	MICB
AVPR2	CHAC1	ERG	HEY2	KLC3	MIER3
B3GAT2	CIDEC	ESR2	HIGD1A	KLF4	MMP1
BCAS1	CKMT1A	ETS2	HILS1	KLF6	MMP2
BCAT1	CKMT1B	EVX1	HISPPD2A	KLF9	MN1
BCL6	CLEC10A	F10	HIST1H1C	KREMEN2	MPP1
BIRC5	CLEC11A	F13A1	HIST1H1D	KRT13	MPPED2
BMP4	CLEC4M	F2RL1	HIST1H1E	KRT222P	MSL3L2
BMPER	CRAT	F7	HIST1H2AB	KRT81	MSLN
BPIL2	CSGALNACT1	FAM117A	HIST1H2AL	KRT86	MT1A
BRAF	CST5	FAM13A	HIST1H3B	KRTAP5-2	MT1B
BTG2	CSTA	FAS	HIST1H3I	L1CAM	MT1DP
BUB1	CTAG1A	FBN2	HIST1H4B	LACE1	MT1F
C11orf21	CTAG2	FCGR2B	HIST1H4F	LAD1	MT1M
C11orf9	CTDSPL	FER1L4	HIST1H4L	LAIR1	MTSS1
C13orf18	CTGF	FGF1	HMGA2	LAIR2	MYB
C14orf23	CTSD	FGFR2	HMSD	LEFTY1	MYCN
C16orf38	CTTNBP2	FHL2	HOXA1	LHX2	MYCNOS
C1orf107	CTXN2	FLJ32063	HOXA10	LILRA1	MYEF2
C20orf118	CXADR	FLJ43752	HOXA11	LILRA2	MYLK

Table 4.3 (cont'd)

MYO1F	PCDH7	RAB9A	SGCE	TAL1	TRIM6-TRIM34
MYOT	PDE4DIP	RAMP3	SGK1	TARP	TRPM8
NACC2	PDE6A	RAPGEF4	SGK3	TBKBP1	TSC22D3
NCKAP1	PDLIM4	RAPGEF5	SHANK1	TBX3	TSEN34
NCR2	PDLIM5	RARG	SHROOM1	TES	TSPAN32
NDP	PDZD2	RASGRP1	SIRT1	TFAP2A	TSPAN5
NEK1	PEG10	RASGRP2	SIVA1	TFB1M	TTLL7
NELL2	PERP	REEP1	SIX2	TFEB	TTYH1
NFAT5	PFTK1	RET	SLC22A11	TFF1	UBAC1
NFKBIE	PGC	RFPL2	SLC22A12	TFF3	UBASH3A
NISCH	PI4KB	RFPL3S	SLC26A2	TFPI	UBE2D1
NKX2-1	PICALM	RGS10	SLC2A13	TGFBR2	UGT1A1
NMU	PIK3IP1	RHO	SLC5A4	TGFBR3	UGT1A3
NOX3	PKIA	RICH2	SLCO4C1	TGM2	UGT1A4
NPY5R	PLAC1	RNASEH2A	SNX24	TGM3	UGT1A6
NR2E1	PLBD1	RND3	SOBP	TH	UGT1A7
NR4A1	PLCL1	RNF43	SOCS2	THBS1	UGT1A9
NR5A2	PLCL2	RP1L1	SOX1	THOC2	UGT2B15
NRAP	PNRC1	RPL39L	SOX4	TIMP3	UGT8
NRXN2	PPAP2B	RPRM	SOX9	TMEM145	UTRN
NTM	PPARG	RPSAP52	SPEG	TMEM151B	VEGFA
ODAM	PPFIBP2	S100A10	SPP2	TMEM71	VTCN1
OLIG1	PPP2R1B	S1PR1	SPSB1	TMOD3	WDR44
OLIG2	PPP2R2B	SAMD3	ST6GALNAC4	TMPRSS2	WFS1
OPN1LW	PPP2R3A	SATB1	ST7	TMPRSS3	WISP2
OR51A4	PPP2R4	SATB2	ST7OT1	TMSB15A	WNT2
OR51Q1	PRDX2	SAV1	ST7OT4	TNC	WWC1
OR51T1	PRKAG2	SCGB1D2	STATH	TNFRSF11B	YAP1
OR52N4	PRKCA	SCN1A	STC1	TNFSF10	ZC3H14
OR56B1	PRKCG	SEC1	STEAP1	TNNC1	ZCCHC24
OSBPL1A	PRL	SEC14L2	STEAP2	TNNI2	ZIC1
OVGP1	PROM1	SELENBP1	STK3	TNNT3	ZIC4
PADI2	PRSS23	SEMA3G	STMN4	TP53BP1	ZMYND10
PALMD	PRX	SEMA4G	STXBP1	TRAF1	ZNF259
PAPSS2	PTGER3	SENP7	SULT1E1	TRIB2	ZNF462
PAQR4	PTPN21	SERPINA1	SYN2	TRIM22	ZNF711
PARP1	PTPRK	SERPINB2	SYN3	TRIM34	ZNF804A
PARP12	PVALB	SERPINB9	SYT8	TRIM5	ZSCAN2
PBX1	RAB28	SGCA	TACC1	TRIM6	

(ii) PELP1-bound Genes

ABCC4	ARL14	BRIP1	CDC2	CTXN2	EDAR
ACADL	ASB13	BUB1	CDC42EP4	CYP1A1	EFEMP1
ACSL6	ASCL1	C10orf84	CDH16	CYP1A2	EGR3
ACTB	ASPH	C21orf49	CDK3	DAPK2	ELL2
ADAM2	ASZ1	C21orf66	CEBPB	DBP	ENAH
ADAMTS9	ATL2	C22orf42	CFTR	DBT	ENPP2
ADIPOQ	ATP11B	C6orf221	CG030	DCLK1	ERBB4
AGPAT3	AXIN1	CACNG6	CH25H	DDX18	ERG
ANKRD13C	BBS1	CADM1	CHD1	DIAPH2	ETS2
APH1B	BCAS1	CALCR	CRAT	DKK1	F13A1
ARAP2	BCL2A1	CALML3	CSTA	DTNA	FAM117A
AREG	BCL6	CAV1	CTDSPL	DUSP4	FAM13A
ARHGAP18	BMP4	CAV2	CTGF	DYNC2LI1	FAS
ARHGAP26	BMPER	CCL2	CTTNBP2	DYRK2	FHL2

Table 4.3 (cont'd)

FLJ32063	HIST1H2AL	MCAM	OR56B1	SAV1	TNFSF10
FLJ44054	HMGA2	MCFD2	OSBPL1A	SCGB1D2	TRAF1
FLRT2	HMSD	MDFI	PBX1	SCN1A	TRIM34
FOS	HOXA1	MDFIC	PCM1	SEC1	TRIM6
FOXP2	HOXA3	MET	PDE6A	SERPINB2	TRMT5
FRAT1	IGF1	MMP1	PDZD2	SGCE	TRPM8
FST	IGF1R	MMP26	PEG10	SIRT1	TSC22D3
GAB3	IGF2	MPP1	PERP	SLC22A5	TSEN34
GADD45A	IGF2AS	MT1DP	PFTK1	SLC2A2	TTLL7
GALK2	IGFBP5	MT1F	PGC	SLC35A3	UBASH3A
GAS6	IL1R1	MYB	PLA2G16	SLC38A6	UBE2B
GDF9	IL5	MYCN	PPAP2B	SLCO4C1	UCP2
GEM	INPP4A	MYCNOS	PPP2R4	SOBP	UGT1A1
GLRB	IRF1	MYEF2	PRKAG2	SOX4	UGT2B15
GPC5	ITGA6	MYO1F	PRL	ST6GALNAC4	UGT8
GREB1	ITK	NCOA2	PROM1	STEAP2	UPF1
GULP1	KIAA0776	NKX2-1	PTGER3	STMN4	UQCRQ
H19	KIR2DL1	NR0B1	PTPN21	SULT1E1	UTRN
HAPLN1	KIR3DX1	NR5A2	PTPRK	SYTL2	VEGFA
HBA1	KLF9	NRAP	RABL5	TARP	VPS41
HBA2	KRT81	ODAM	RAPGEF5	TFAP2A	WFS1
HBBP1	KRT86	OR51A7	RET	TFDP1	WNT2
HBM	LOC100188949	OR51B2	RFPL3S	TFF1	ZC3H14
HES4	LOC26010	OR51B5	RHO	THBS1	ZIC1
HEY2	LOC441108	OR51F1	RICH2	TIMP3	ZIC4
HHLA3	LSP1	OR51Q1	RND3	TMEM71	ZNF238
HILS1	MANEA	OR51T1	RXRA	TMPRSS3	ZNF711
HIST1H1D	MARCKS	OR51V1	SATB1	TNC	ZNF804A
HIST1H2AB	MBOAT7	OR52R1	SATB2	TNFRSF11B	

<u>(iii) macroH2A1- and PELP1-bound Genes</u>

ACADL	CALCR	DKK1	GAB3	IGF2AS	MYB
ACSL6	CALML3	DUSP4	GADD45A	IGFBP5	MYCN
ACTB	CAV1	DYNC2LI1	GAS6	IL1R1	MYCNOS
ADAM2	CAV2	DYRK2	GEM	IRF1	MYEF2
ADAMTS9	CCL2	EDAR	GLRB	ITGA6	MYO1F
ADIPOQ	CDC2	EFEMP1	GPC5	ITK	NKX2-1
ARAP2	CDC42EP4	EGR3	GREB1	KIR2DL1	NR5A2
AREG	CDH16	ELL2	GULP1	KIR3DX1	NRAP
ARHGAP18	CEBPB	ENAH	H19	KLF9	ODAM
ARHGAP26	CFTR	ENPP2	HAPLN1	KRT81	OR51Q1
ARL14	CH25H	ERBB4	HBA1	KRT86	OR51T1
ASB13	CRAT	ERG	HBA2	LOC100188949	OR56B1
ASCL1	CSTA	ETS2	HBM	LOC26010	OSBPL1A
ASPH	CTDSPL	F13A1	HEY2	LOC441108	PBX1
ASZ1	CTGF	FAM117A	HILS1	LSP1	PDE6A
ATL2	CTTNBP2	FAM13A	HIST1H1D	MBOAT7	PDZD2
BCAS1	CTXN2	FAS	HIST1H2AB	MCAM	PEG10
BCL6	CYP1A1	FHL2	HIST1H2AL	MDFI	PERP
BMP4	CYP1A2	FLJ32063	HMGA2	MDFIC	PFTK1
BMPER	DAPK2	FLJ44054	HMSD	MET	PGC
BUB1	DBP	FLRT2	HOXA1	MMP1	PPAP2B
C22orf42	DCLK1	FOS	HOXA3	MPP1	PPP2R4
CACNG6	DDX18	FOXP2	IGF1	MT1DP	PRKAG2
CADM1	DIAPH2	FST	IGF2	MT1F	PRL

Table 4.3 (cont'd)

PROM1	SATB1	SOBP	TIMP3	TSC22D3	WNT2
PTGER3	SATB2	SOX4	TMEM71	TSEN34	ZC3H14
PTPN21	SAV1	ST6GALNAC4	TMPRSS3	TTLL7	ZIC1
PTPRK	SCGB1D2	STEAP2	TNC	UBASH3A	ZIC4
RAPGEF5	SCN1A	STMN4	TNFRSF11B	UGT1A1	ZNF711
RET	SEC1	SULT1E1	TNFSF10	GT2B15	ZNF804A
RFPL3S	SERPINB2	TARP	TRAF1	UGT8	
RHO	SGCE	TFAP2A	TRIM34	UTRN	
RICH2	SIRT1	TFF1	TRIM6	VEGFA	
RND3	SLCO4C1	THBS1	TRPM8	WFS1	

<u>(iv) macroH2A1-bound and PELP1-unbound Genes (no GO terms)</u>

AADAT	CACNA1G	DLL4	HCCA2	KLF4	MGAT3
ABHD6	CACNG7	DNAJB3	HIGD1A	KLF6	MICB
ACCN4	CALD1	DNASE1L3	HISPPD2A	KREMEN2	MIER3
ACTA2	CALML5	DUSP1	HIST1H1C	KRT13	MMP2
ADAMTSL1	CAMK2N1	DUSP3	HIST1H1E	KRT222P	MN1
ADAMTSL3	CAPN9	EGFR	HIST1H3B	KRTAP5-2	MPPED2
ADRB1	CAPZA2	EIF6	HIST1H3I	L1CAM	MSL3L2
ADRBK1	CBFA2T3	EMD	HIST1H4B	LACE1	MSLN
ADSSL1	CCBP2	ENC1	HIST1H4F	LAD1	MT1A
ALDH5A1	CCNI2	EPHB2	HIST1H4L	LAIR1	MT1B
AMIGO2	CD209	EPN3	HOXA10	LAIR2	MT1M
AMMECR1	CDC2	ESR2	HOXA11	LEFTY1	MTSS1
AMOTL2	CDH2	EVX1	HOXA11AS	LHX2	MYLK
ANKRD43	CDH29	F10	HOXA13	LILRA1	MYOT
ANKRD55	CDH5	F2RL1	HOXA2	LILRA2	NACC2
ANXA3	CDKN2C	F7	HOXA3	LILRA3	NCKAP1
APOA1	CEACAM4	FBN2	HOXA4	LILRA4	NCR2
APOA4	CEACAM6	FCGR2B	HOXA5	LILRA5	NDP
APOA5	CEP55	FER1L4	HOXA6	LILRA6	NEK1
APOC3	CERK	FGF1	HOXA7	LILRB1	NELL2
ARHGDIG	CHAC1	FGFR2	HOXA9	LILRB2	NFAT5
ARL4A	CIDEC	FLJ43752	IGF2	LILRB3	NFKBIE
ATF7IP	CKMT1A	FLNA	IGFBP4	LILRB4	NISCH
AVPR2	CKMT1B	FOXG1	IL13	LILRB5	NMU
B3GAT2	CLEC10A	FOXN3	IL24	LILRP2	NOX3
BCAT1	CLEC11A	FZD1	INPP5J	LOC284067	NPY5R
BIRC5	CLEC4M	FZD7	INS-IGF2	LOC441864	NR2E1
BPIL2	CSGALNACT1	GALNT12	IQGAP1	LOC91149	NR4A1
BRAF	CST5	GATM	IRX5	LRIG1	NRXN2
BTG2	CTAG1A	GDF15	ISL1	LRRC15	NTM
C11orf21	CTAG2	GDF5	ITGB3	LRRK2	OLIG1
C11orf9	CTSD	GPRC5A	ITGB4	LTF	OLIG2
C13orf18	CXADR	GRAMD3	ITPR2	LUZP2	OPN1LW
C14orf23	CXCL12	GRB10	KCNK1	MAP2K6	OR51A4
C16orf38	CXCR4	GREB1	KCNK5	MAP3K1	OR52N4
C1orf107	CXCR7	GRM1	KCNN2	MAPK11	OVGP1
C20orf118	CYB561	GRM8	KIAA1026	MAPK12	PADI2
C21orf54	DEGS1	GTF2A1	KIR2DL3	MBNL2	PALMD
C3	DES	H1FNT	KIR2DL4	MCF2L	PAPSS2
C3orf54	DHRS3	H1FOO	KIR3DL1	MCM3	PAQR4
C5orf13	DIRAS1	HBE1	KIR3DL3	MCTP2	PARP1
C5orf35	DKC1	HBP1	KIR3DP1	MEGF8	PARP12
C8orf74	DKFZP434K028	HBZ	KLC3	METTL9	PCDH7

Table 4.3 (cont'd)

PDE4DIP	PVALB	SEMA4G	ST7	TGFBR3	TTYH1
PDLIM4	RAB28	SENP7	ST7OT1	TGM2	UBAC1
PDLIM5	RAB9A	SERPINA1	ST7OT4	TGM3	UBE2D1
PI4KB	RAMP3	SERPINB9	STATH	TH	UGT1A3
PICALM	RAPGEF4	SGCA	STC1	THOC2	UGT1A4
PIK3IP1	RARG	SGK1	TEAP1	TMEM145	UGT1A6
PKIA	RASGRP1	SGK3	STEAP2	TMEM151B	UGT1A7
PLAC1	RASGRP2	SHANK1	STK3	TMOD3	UGT1A9
PLBD1	REEP1	SHROOM1	STXBP1	TMPRSS2	UGT8
PLCL1	RFPL2	SIVA1	SYN2	TMPRSS3	VTCN1
PLCL2	RGS10	SIX2	SYN3	TMSB15A	WDR44
PNRC1	RNASEH2A	SLC22A11	SYT8	TNNC1	WISP2
PPARG	RNF43	SLC22A12	TACC1	TNNI2	WWC1
PPFIBP2	RP1L1	SLC26A2	TAL1	TNNT3	YAP1
PPP2R1B	RPL39L	SLC2A13	TBKBP1	TP53BP1	ZCCHC24
PPP2R2B	RPRM	SLC5A4	TBX3	TRIB2	ZMYND10
PPP2R3A	RPSAP52	SNX24	TES	TRIM22	ZNF259
PRDX2	S100A10	SOCS2	TFAP2A	TRIM34	ZNF462
PRKCA	S1PR1	SOX1	TFB1M	TRIM5	ZSCAN2
PRKCG	SAMD3	SOX9	TFEB	TRIM6	
PROM1	SEC14L2	SPEG	TFF3	TRIM6-TRIM34	
PRSS23	SELENBP1	SPP2	TFPI	TSPAN32	
PRX	SEMA3G	SPSB1	TGFBR2	TSPAN5	

<u>(v) PELP1-bound and macroH2A1-unbound Genes (no GO terms)</u>

ABCC4	C21orf49	GDF9	MCFD2	PCM1	TRMT5
AGPAT3	C21orf66	HBBP1	MMP26	PLA2G16	UBE2B
ANKRD13C	C6orf221	HES4	NCOA2	RABL5	UCP2
APH1B	CDK3	HHLA3	NR0B1	RXRA	UPF1
ATP11B	CG030	IGF1R	OR51A7	SLC22A5	UQCRQ
AXIN1	CHD	IL5	OR51B2	SLC2A2	VPS41
BBS1	DBT	INPP4A	OR51B5	SLC35A3	ZNF238
BCL2A1	DTNA	KIAA0776	OR51F1	SLC38A6	
BRIP1	FRAT1	MANEA	OR51V1	SYTL2	
C10orf84	GALK2	MARCKS	OR52R1	TFDP1	

4.5C), e.g. histone 3 lysine 9 trimethylation (H3K9me3), while negatively correlating with active transcription marks and factors.

Overall, these analyses demonstrate that PELP1 and macroH2A1 have a highly similar pattern of genomic occupancy. While bound to a subset of macroH2A1-containing regions, PELP1 genomic association correlates with gene expression, histone marks, and functional classes of genes in a manner that is highly similar to that of macroH2A1. Taken together, the results from our biochemical GST pull-down and genomic ChIP-chip analyses indicate that PELP1 and macroH2A1 interact with each other and co-localize across the genome of MCF-7 cells.

PELP1 is recruited to the genome by macroH2A1, but macroH2A1 deposition is independent of PELP1. The high degree of coincidence between macroH2A1 and PELP1 genomic occupancy led us to explore the hypothesis that macroH2A1 functions in recruiting PELP1 to the genome. In order to determine the effect of macroH2A1 knockdown on the localization of PELP1, we took advantage of the shRNA-mediated stable macroH2A1 knockdown cell line described previously (Gamble et al., 2010). MacroH2A1 knockdown did not alter the overall levels of PELP1 in MCF-7 cells (Figure 4.6A) compared to the luciferase (Luc) knockdown control. For our ChIP assays, we focused on gene promoters previously shown to contain and be regulated by macroH2A1 (Gamble et al., 2010). At these promoters, knockdown of macroH2A1 significantly decreased macroH2A1 levels, as would be expected (Figure 4.6B). We were able to confirm the occupancy of PELP1 at these gene promoters, as predicted from the ChIP-chip data. Interestingly, at all regions tested, we observed that PELP1 genomic occupancy decreased upon macroH2A1 knockdown (Figure 4.6C), a finding independent of nucleosome loss (Figure 4.7), suggesting that macroH2A1 is required to recruit PELP1 to chromatin.

Figure 4.5. PELP1 occupancy correlates with heterochromatic chromatin marks and negatively correlates with active chromatin marks. *A,* Volcano plot of Spearman's correlation coefficients for the PELP1 ChIP-chip data with each of 362 ChIP-chip data sets versus the corresponding significance score ($-\text{Log}_2$ *P*-value). The grey box depicts those data sets that positively or negatively correlate with PELP1 occupancy using a correlation coefficient of ±0.20 and *P*-value of $< 10^{-100}$ as cutoffs of significance. *B and C*, Average Log_2 ratios (IP/Input) in PELP1-bound (*black bars*) or unbound (*grey bars*) regions for the factors correlating positively or negatively with both PELP1 and macroH2A1 (B) or with PELP1 only (C). The corresponding data for macroH2A1 is shown for comparison (*right*). The correlating factor and cell line source are listed. *mH2A1, macroH2A1.*

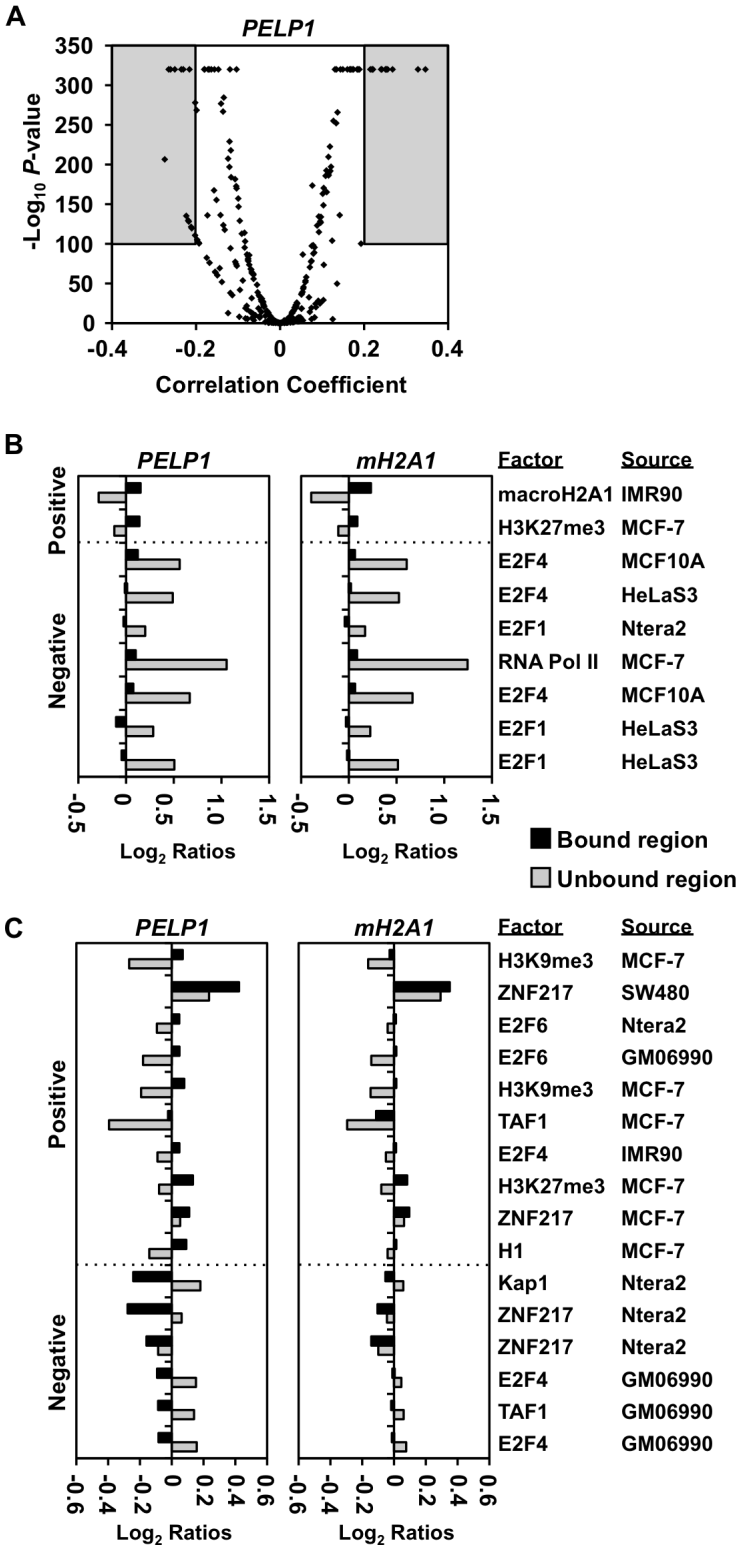
A
PELP1
-Log10 P-value
Correlation Coefficient
B
PELP1
mH2A1
Factor
Source
Positive
Negative
macroH2A1 IMR90
H3K27me3 MCF-7
E2F4 MCF10A
E2F4 HeLaS3
E2F1 Ntera2
RNA Pol II MCF-7
E2F4 MCF10A
E2F1 HeLaS3
E2F1 HeLaS3
Log2 Ratios
Bound region
Unbound region
C
PELP1
mH2A1
Factor
Source
H3K9me3 MCF-7
ZNF217 SW480
E2F6 Ntera2
E2F6 GM06990
H3K9me3 MCF-7
TAF1 MCF-7
E2F4 IMR90
H3K27me3 MCF-7
ZNF217 MCF-7
H1 MCF-7
Kap1 Ntera2
ZNF217 Ntera2
ZNF217 Ntera2
E2F4 GM06990
TAF1 GM06990
E2F4 GM06990
Log2 Ratios

Figure 4.6. PELP1 is recruited to gene promoters by macroH2A1. *A,* Western blot showing the shRNA-mediated depletion of macroH2A1 in MCF-7 cells compared to luciferase (Luc) knockdown cells. Total cellular levels of PELP1 is unaffected by macroH2A1 knockdown. β-actin and histone H3 were also analyzed as loading controls. *B and* C*,* MacroH2A1 and PELP1 occupancy is reduced upon macroH2A1 depletion at gene promoters. The occupancy of macroH2A1 (B) and PELP1 (C) was examined by ChIP analyses in the Luc (*black bars*) and macroH2A1 (*white bars*) knockdown cell lines. Each bar represents the mean + SEM (*error bars*) from three or more independent determinations. All changes in occupancy for macroH2A1 (B) and PELP1 (C) upon macroH2A1 knockdown are statistically different then the control cell line, as determined by a Student's *t*-test with a *P*-value threshold of < 0.05. *Luc, luciferase; mH2A1, macroH2A1; KD, knockdown.*

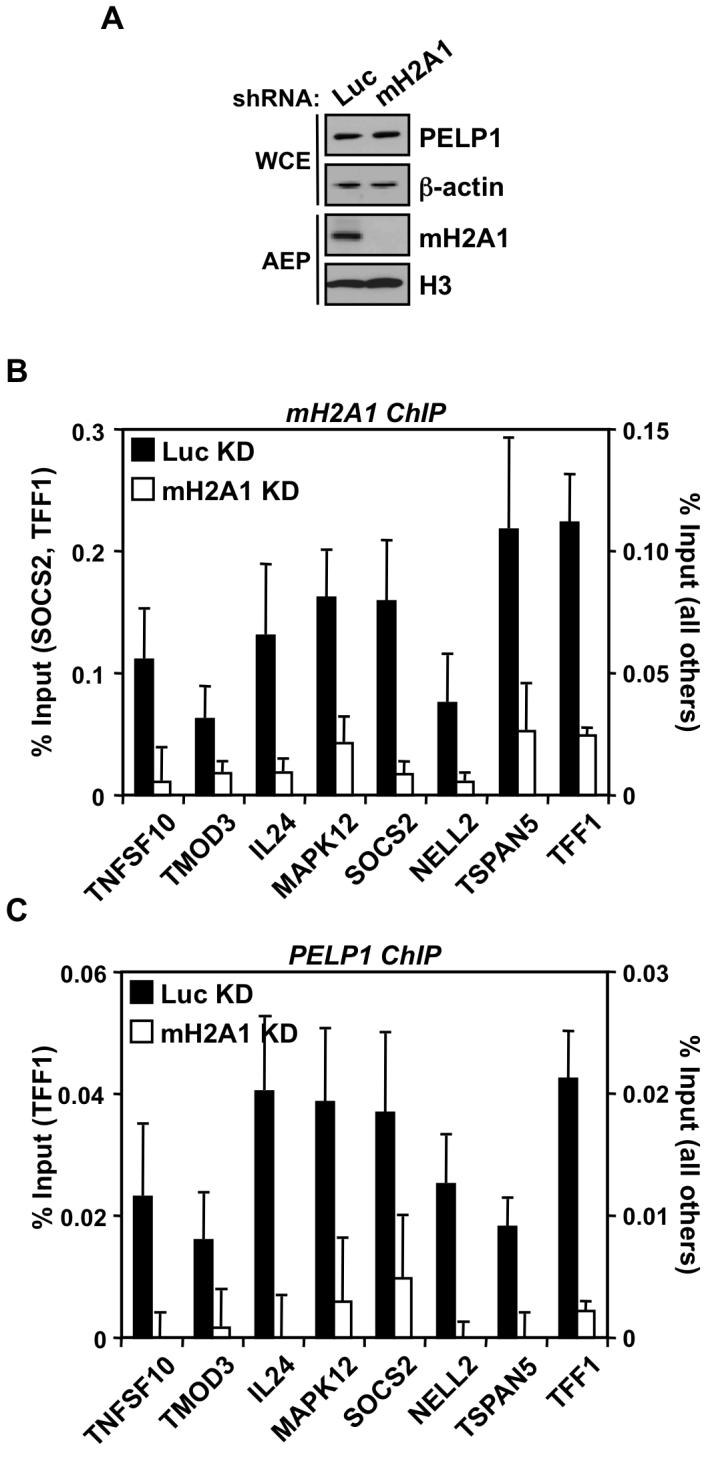
A
shRNA: Luc mH2A1
WCE
PELP1
β-actin
AEP
mH2A1
H3
B
mH2A1 ChIP
Luc KD
mH2A1 KD
% Input (SOCS2, TFF1)
% Input (all others)
0.3
0.2
0.1
0
0.15
0.10
0.05
0
TNFSF10
TMOD3
IL24
MAPK12
SOCS2
NELL2
TSPAN5
TFF1
C
PELP1 ChIP
Luc KD
mH2A1 KD
% Input (TFF1)
% Input (all others)
0.06
0.04
0.02
0
0.03
0.02
0.01
0
TNFSF10
TMOD3
IL24
MAPK12
SOCS2
NELL2
TSPAN5
TFF1

Figure 4.7. Reductions in both mH2A1 and PELP1 upon mH2A1 depletion is not due to loss of nucleosomes. The occupancy of histone H3 was examined by ChIP analyses in the Luc (*black solid bars*) and mH2A1 (*black striped bars*) knockdown cell lines. Each bar represents the mean + SEM (*error bars*) from two independent determinations. All changes in occupancy for H3 are not statistically different then the control cell line, as determined by a Student's *t*-test with a *P*-value threshold of < 0.05. *Luc, luciferase; mH2A1, macroH2A1; KD, knockdown.*

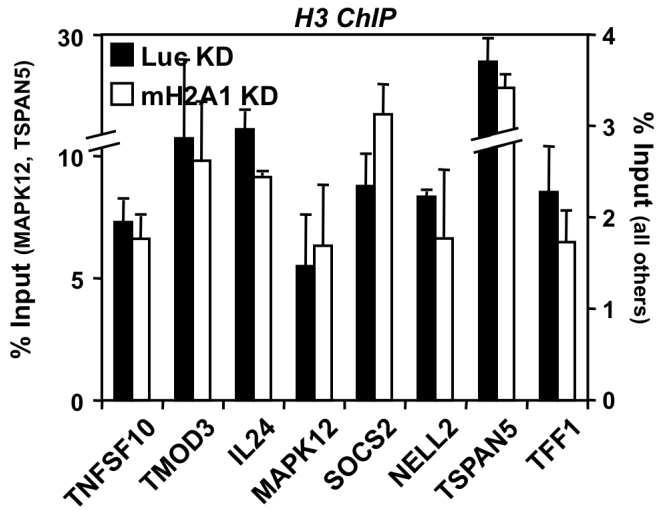
H3 ChIP
Luc KD
mH2A1 KD
% Input (MAPK12, TSPAN5)
% Input (all others)
30
10
5
0
4
3
2
1
0
TNFSF10
TMOD3
IL24
MAPK12
SOCS2
NELL2
TSPAN5
TFF1

To determine whether macroH2A1 deposition was reciprocally dependent on PELP1, we used an analogous set of experiments. We developed a PELP1 knockdown cell line in MCF-7 cells to compare macroH2A1 promoter occupancy in control versus PELP1 knockdown. Our initial attempts to create a stable cell line using shRNA-mediated knockdown of PELP1, much like that shown above for macroH2A1, were unsuccessful, as PELP1 expression reverted to wild type levels after only a couple of passages (data not shown). In an alternative approach, we developed a "Tet-on" inducible knockdown system where treatment of doxycycline induced the expression of shRNA in MCF-7 cells via a Tet-responsive promoter. Using this system, we created MCF-7 cells stably expressing both the Tet Repressor (TetR) and either a doxycycline (dox) responsive Luc or PELP1 shRNA.

The resulting inducible knockdown cell lines, Luc_i and $PELP1_i$, were treated with or without dox (see Experimental Procedures) and tested for cellular PELP1 levels by Western blot analysis. As expected, dox treatment induced shRNA expression, leading to a decrease in PELP1 mRNA levels and PELP1 protein by ~80% compared to the Luc control (Figure 4.8A and Figure 4.9). Notably, PELP1 knockdown did not have an effect on total cellular levels of macroH2A1 (Figure 4.8A and Figure 4.9). We performed ChIP assays at the same promoter regions using our inducible knockdown cell lines to determine if macroH2A1 localization was altered in response to PELP1 depletion. Upon PELP1 knockdown, macroH2A1 recruitment remained constant, even though PELP1 levels at the promoters were significantly reduced (Figure 4.8B and 4.8C). These results demonstrate that while macroH2A1 deposition into nucleosomes occurs independent of PELP1 recruitment, it is necessary in order to recruit PELP1 to the chromatin.

Figure 4.8. macroH2A1 deposition is independent of PELP1. *A,* Western blot showing the doxycycline-inducible shRNA-mediated depletion of PELP1 in MCF-7 cells compared to luciferase (Luc) knockdown cells. Cellular levels of macroH2A1 is unaffected by PELP1 knockdown. β-actin and histone H3 were also analyzed as loading controls. Only the + dox condition (those marked with an *asterisk*; *) for Luc_i and $PELP1_i$ was analyzed for gene-specific experiments. *B and* C, MacroH2A1 occupancy is unaffected by PELP1 depletion at gene promoters. The occupancy of macroH2A1 (B) and PELP1 (C) was examined by ChIP analyses in the Luc_i (*dark grey bars*) and $PELP1_i$ (*light grey bars*) inducible knockdown cell lines. Each bar represents the mean + SEM (*error bars*) from three or more independent determinations. All changes in occupancy for PELP1 (C) upon PELP1 knockdown are statistically different then the control cell line, as determined by a Student's *t*-test with a *P*-value threshold of < 0.05. *Luc, luciferase; mH2A1, macroH2A1; KD, knockdown; dox, doxycycline; i, inducible.*

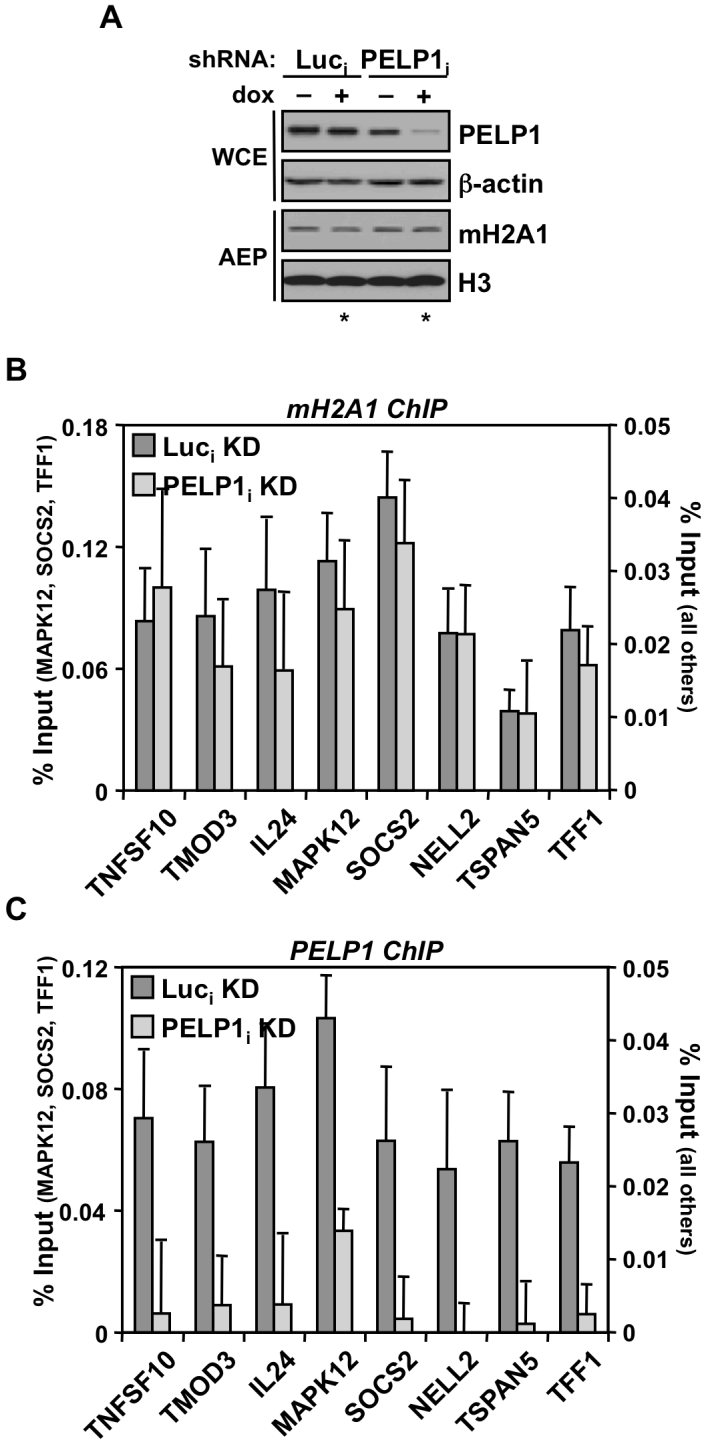
A
shRNA: Luc$_i$ PELP1$_j$
dox – + – +
WCE
PELP1
β-actin
AEP
mH2A1
H3
* *
B
mH2A1 ChIP
Luc$_i$ KD
PELP1$_i$ KD
% Input (MAPK12, SOCS2, TFF1)
% Input (all others)
0.18
0.12
0.06
0
0.05
0.04
0.03
0.02
0.01
0
TNFSF10
TMOD3
IL24
MAPK12
SOCS2
NELL2
TSPAN5
TFF1
C
PELP1 ChIP
Luc$_i$ KD
PELP1$_i$ KD
% Input (MAPK12, SOCS2, TFF1)
% Input (all others)
0.12
0.08
0.04
0
0.05
0.04
0.03
0.02
0.01
0
TNFSF10
TMOD3
IL24
MAPK12
SOCS2
NELL2
TSPAN5
TFF1

Figure 4.9. Comparison of two independent shRNA target sequences for the inducible knockdown of PELP1. *A,* Knockdown of PELP1 by two independent shRNA target sequences. Whole cell lysates or acid extracted pellets (for mH2A1, *e.g.*) were collected from doxycycline-treated Luc_i or $PELP1_i$ stable shRNA-mediated knockdown cell lines. Two independent shRNA sequences (#1 and #2) targeting PELP1 were analyzed by Western blotting for their ability to knockdown PELP1 relative to the Luc control. PARP-1 and β-actin were also analyzed as loading controls. *B,* RT-qPCR analysis confirms the knockdown of PELP1 mRNA in the knockdown cell lines described in (A). Total RNA was isolated from Luc_i and $PELP1_i$ knockdown cells, reverse transcribed, and subjected to RT-qPCR using gene-specific primers to PELP1. Each bar is the mean + SEM (*error bars*) for three independent RNA isolations. *C,* Comparable effects on gene expression for each $PELP1_i$ shRNA sequence. Total RNA was isolated from Luc_i and $PELP1_i$ knockdown cells, reverse transcribed, and subjected to RT-qPCR using gene-specific primers. The effect of each knockdown (PELP1 shRNA #1 or PELP1 shRNA#2) was compared for a subset of target genes identified in Fig. 5. Each bar represents the mean + SEM (*error bars*) from three or more independent determinations. *D,* A correlation analysis comparing the effects of PELP1 shRNA #1 and PELP1 shRNA #2 at 22 genes indicates that both shRNAs produce similar effects on gene expression. The Spearman correlation coefficient (c.c.) and *P*-value are indicated. For all other experiments, only shRNA #2 was used. *Luc, luciferase.*

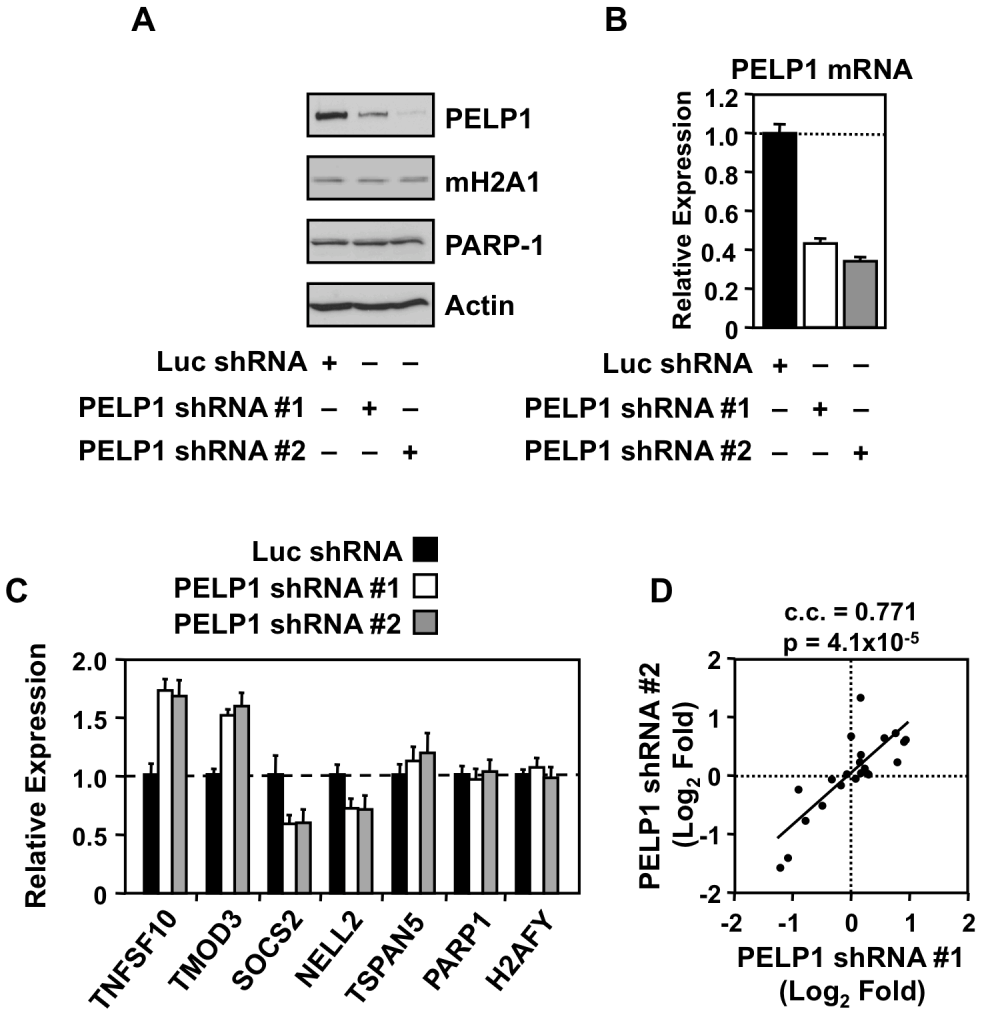
A
PELP1
mH2A1
PARP-1
Actin
Luc shRNA + – –
PELP1 shRNA #1 – + –
PELP1 shRNA #2 – – +
B
PELP1 mRNA
Relative Expression
1.2
1.0
0.8
0.6
0.4
0.2
0
Luc shRNA + – –
PELP1 shRNA #1 – + –
PELP1 shRNA #2 – – +
C
Luc shRNA
PELP1 shRNA #1
PELP1 shRNA #2
Relative Expression
2.0
1.5
1.0
0.5
0
TNFSF10
TMOD3
SOCS2
NELL2
TSPAN5
PARP1
H2AFY
D
c.c. = 0.771
p = 4.1x10-5
PELP1 shRNA #2 (Log2 Fold)
PELP1 shRNA #1 (Log2 Fold)
2
1
0
-1
-2

Figure 4.10. PELP1 knockdown alters the mRNA levels of a subset of macroH2A1-regulated genes in a similar manner to macroH2A1. Previously identified macroH2A1-regulated genes (Gamble et al., 2010) were analyzed for changes in mRNA levels upon $PELP1_i$ knockdown (*grey bars*). Total RNA from Luc_i or $PELP1_i$ knockdown cells (+ dox) was isolated, reverse-transcribed, and subjected to qPCR using gene-specific primers. The effect of macroH2A1 knockdown (from Gamble *et al* (Gamble et al., 2010), *black bars*) is shown for comparison. Each bar represents the mean + SEM (*error bars*) from three or more independent determinations. Bars marked with an *asterisk* are statistically different from the luciferase knockdown control, as determined by a Student's *t*-test with at *P*-value threshold of < 0.05. *mH2A1, macroH2A1.*

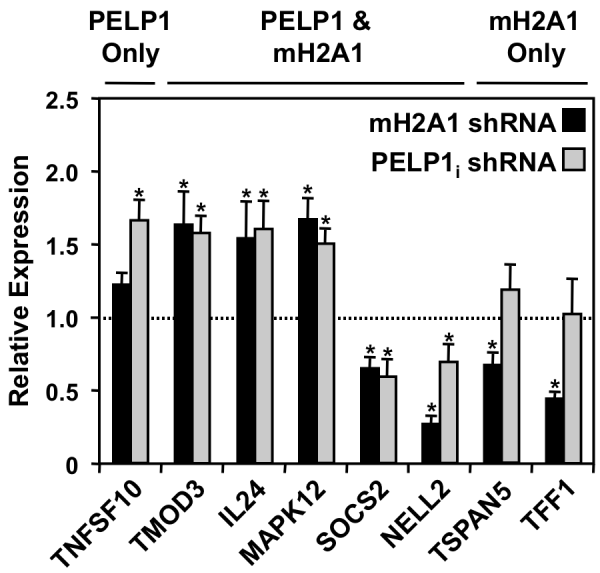
PELP1 Only
PELP1 & mH2A1
mH2A1 Only
mH2A1 shRNA
PELP1i shRNA
Relative Expression
2.5
2.0
1.5
1.0
0.5
0
TNFSF10
TMOD3
IL24
MAPK12
SOCS2
NELL2
TSPAN5
TFF1

PELP1 regulates a subset of macroH2A1-regulated genes in a similar manner to macroH2A1 in both basal and signal-regulated transcription. Thus far, our results demonstrate that macroH2A1 interacts with PELP1 and is responsible for the recruitment of PELP1 to target gene promoters. We hypothesized that these genes, previously shown to be regulated by macroH2A1 (Gamble et al., 2010), would also be regulated by PELP1. We examined the expression levels of macroH2A1-regulated genes in Luc_i and $PELP1_i$ knockdown cell lines by RT-qPCR. Our analyses show that PELP1 knockdown alters the expression levels of a subset of macroH2A1-regulated genes (Figure 4.10). Interestingly, the direction of regulation is similar to that of macroH2A1 knockdown, which is shown for comparison (data from Gamble *et al* (Gamble et al., 2010)). This result suggests that both macroH2A1 and PELP1 are required for proper expression of a subset of genes.

We previously reported that macroH2A1 could also participate in signal-regulated transcription. As a model, we investigated both serum starvation and TPA signaling systems and showed that macroH2A1 can function both positively and negatively in regulated signal-induced transcription (Gamble et al., 2010; Gamble and Kraus, 2010). Specifically, macroH2A1 potentiates the response of serum starvation-induced genes found in macroH2A1 domains. Additionally, macroH2A1 abrogates the expression of TPA-responsive genes found in these domains. We asked whether PELP1 could modulate transcription in the same signaling pathways. To test this, we considered TPA- or serum starvation-induced genes whose expression pattern was altered upon macroH2A1 knockdown (Figure 4.11A and Figure 4.12). We assayed the mRNA levels of these genes upon Luc_i and $PELP1_i$ knockdown. PELP1 involvement in signal-regulated transcription was limited to a subset of genes, as shown under resting conditions. For example, knockdown of PELP1 further enhanced the expression of the TPA-induced *CCL2* gene similarly to macroH2A1 knockdown,

Figure 4.11. PELP1 acts to repress the transcriptional induction of the TPA-responsive gene, *CCL2*. *A,* macroH2A1 and PELP1 knockdown results in further induction of the TPA-responsive gene, *CCL2*. Luc and macroH2A1 knockdown cells and Luc_i and $PELP1_i$ knockdown cells (+ dox) were treated with vehicle (–) or 100 nM TPA (+) for 3 hrs. Total RNA was isolated, reverse-transcribed, and subjected to qPCR using gene-specific primers. *AREG* is shown as a control, as it is only modulated by macroH2A1. Each bar represents the mean + SEM (*error bars*) from three or more independent determinations. Bars marked with an *asterisk* are statistically different from the corresponding luciferase knockdown control (Luc, in the case of macroH2A1; Luc_i in the case of $PELP1_i$), as determined by a Student's *t*-test with at *P*-value threshold of < 0.05. The Luc and macroH2A1 knockdown data for *AREG* is taken from Gamble and Kraus (Gamble et al., 2010). *B,* macroH2A1 and PELP1 occupancy are reduced downstream of the *CCL2* TSS upon TPA treatment. MacroH2A1 and PELP1 ChIP assays were performed from parental MCF-7 cells were treated with vehicle (–) or 100 nM TPA (+) for 1.5 hrs. Primers were designed to regions upstream and downstream of the TSS. Each bar represents the mean + SEM (*error bars*) from three or more independent determinations. Bars marked with an *asterisk* are statistically different from the vehicle treated control, as determined by a Student's *t*-test with at *P*-value threshold of < 0.05. The macroH2A1 ChIP data for *AREG* is taken from Gamble and Kraus (Gamble and Kraus, 2010). *Luc, luciferase; mH2A1, macroH2A1; i, inducible; U, upstream of the TSS; D, downstream of the TSS.*

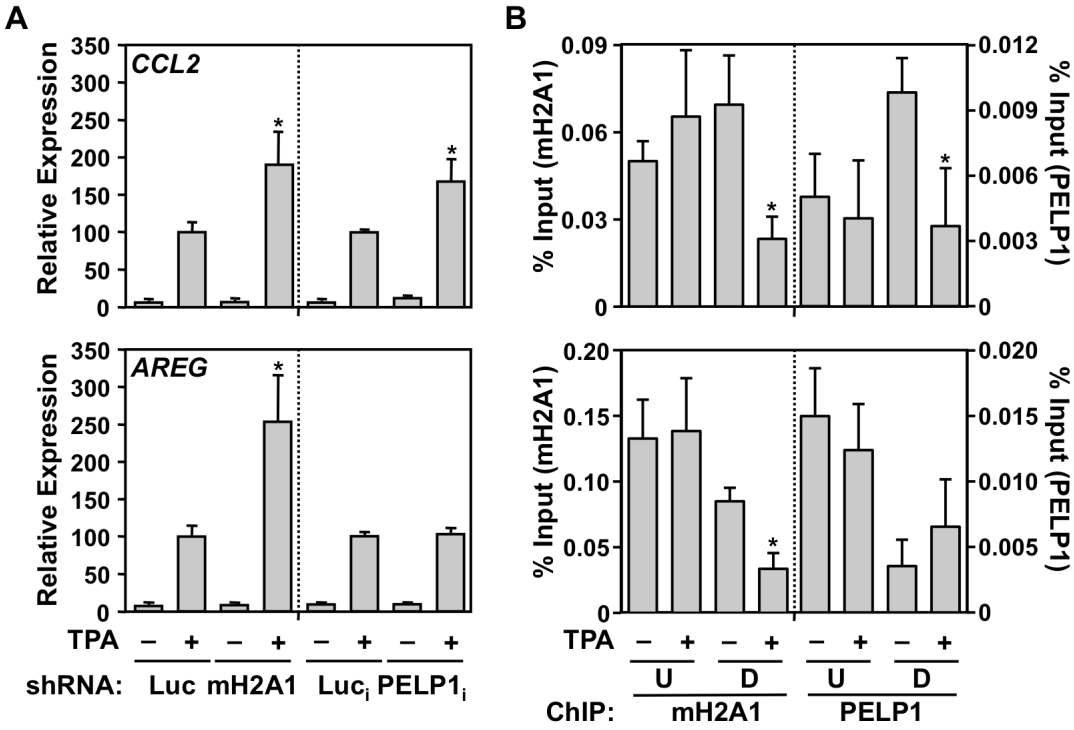
A
CCL2
AREG
Relative Expression
350
300
250
200
150
100
50
0
TPA – + – + – + – +
shRNA: Luc mH2A1 Luc$_i$ PELP1$_i$
B
% Input (mH2A1)
% Input (PELP1)
0.09
0.06
0.03
0
0.012
0.009
0.006
0.003
0.20
0.15
0.10
0.05
0.020
0.015
0.010
0.005
U D U D
ChIP: mH2A1 PELP1

Figure 4.12. PELP1 acts to potentiate the transcriptional induction of the serum starvation-responsive gene, *SOCS2*. *A,* macroH2A1 and PELP1 knockdown represses the induction of the serum starvation-responsive gene, *SOCS2*. Luc and macroH2A1 knockdown cells and Luc_i and $PELP1_i$ knockdown cells (+ dox) were cultured with serum (+) or serum deprivation (–) for 24 hrs. Total RNA was isolated, reverse-transcribed, and subjected to qPCR using gene-specific primers. *ASCL1* is shown as a control, as it is only modulated by macroH2A1. Each bar represents the mean + SEM (*error bars*) from three or more independent determinations. Bars marked with an *asterisk* are statistically different from the corresponding luciferase knockdown control (Luc, in the case of macroH2A1; Luc_i in the case of $PELP1_i$), as determined by a Student's *t*-test with at *P*-value threshold of < 0.05. The Luc and macroH2A1 knockdown data for *SOCS2* and *ASCL1* is taken from Gamble *et al* (Gamble et al., 2010). *B,* macroH2A1 and PELP1 occupancy are unaltered at the promoters of serum starvation-responsive genes. MacroH2A1 and PELP1 ChIP assays were performed from parental MCF-7 cells were cultured with serum (+) or serum deprivation (–) for 24 hrs. Primers were designed to regions upstream and downstream of the TSS. Each bar represents the mean + SEM (*error bars*) from three or more independent determinations. The macroH2A1 ChIP data for *SOCS2* and *ASCL1* is taken from Gamble et al (Gamble et al., 2010). *Luc, luciferase; mH2A1, macroH2A1; i, inducible; U, upstream of the TSS; D, downstream of the TSS.*

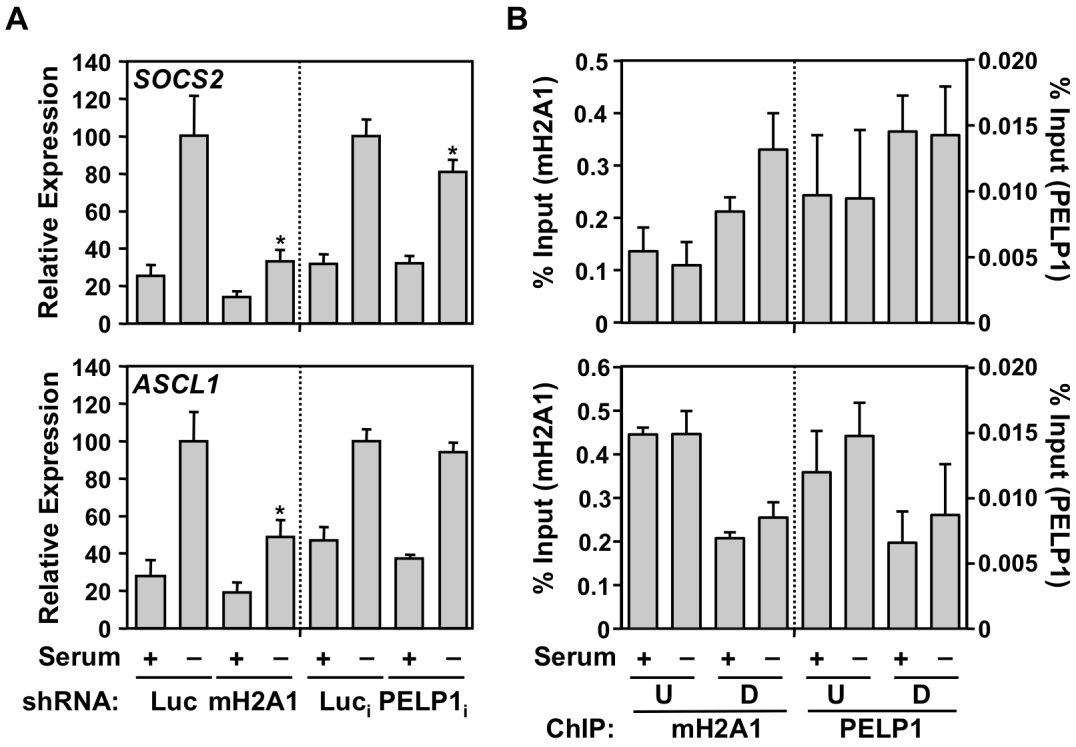
A
B
SOCS2
ASCL1
Relative Expression
% Input (mH2A1)
% Input (PELP1)
Serum
shRNA:
Luc
mH2A1
Luc$_i$
PELP1$_i$
ChIP:
mH2A1
PELP1
U
D

Figure 4.13. TPA and serum starvation does not cause loss of nucleosomes at target gene promoters. *A and B,* An H3 ChIP was performed from parental MCF-7 cells treated with vehicle (–) or 100 nM TPA (+) for 1.5 hrs (A), or with 0% serum (–) for 24 hours (B). Primers were designed to regions upstream and downstream of the TSS. Each bar represents the mean + SEM (*error bars*) from three or more independent determinations. *U, upstream of the TSS; D, downstream of the TSS.*

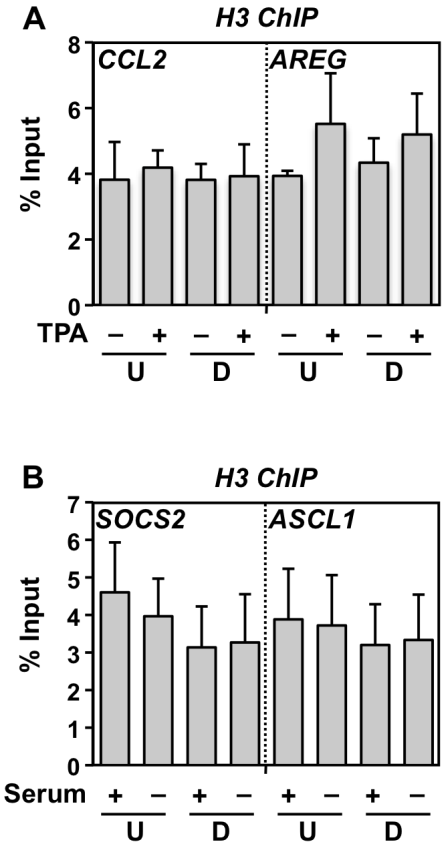
A
H3 ChIP
CCL2
AREG
% Input
8
6
4
2
0
TPA
– + – + – + – +
U D U D
B
H3 ChIP
SOCS2
ASCL1
% Input
7
6
5
4
3
2
1
0
Serum
+ – + – + – + –
U D U D

but had no effect on *AREG* expression (Figure 4.11A). In addition, like macroH2A1, PELP1 occupancy upon TPA treatment is reduced downstream of the TSS at the *CCL2* promoter (Figure 4.11B, (Gamble and Kraus, 2010)), but not at the *AREG* promoter. This result is not due to nucleosome loss, as H3 levels remain constant (Figure 4.13A). In the case of serum starvation, PELP1 acts similarly to macroH2A1 at the *SOCS2* promoter but not at the *ASCL1* promoter, although the effects were less striking (Figure 4.12 and 4.13B, (Gamble et al., 2010). Taken together, these results demonstrate that PELP1 modulates a subset of macroH2A1-regulated genes in a manner similar to macroH2A1 in both basal and signal-regulated systems.

4.4. Discussion

The histone variant macroH2A1 can both positively and negatively regulate target genes within macroH2A1-containing chromatin in a context-specific manner (Agelopoulos and Thanos, 2006; Buschbeck et al., 2009; Changolkar et al., 2007; Gamble et al., 2010; Gamble and Kraus, 2010). However, the mechanism(s) by which macroH2A1 regulates the expression of its target genes has yet to be fully elucidated. As the distinguishing feature of macroH2A1, the large C-terminal globular macro domain plays a key role in determining the specific context in which an underlying gene will be modulated through specific recruitment and physical interaction of effector proteins. Here, we identify a chromatin-associated transcriptional coregulator, PELP1, as a novel interacting protein of the macro domain of macroH2A1. Collectively, our biochemical, genomic, and gene-specific analyses suggest that macroH2A1 specifically recruits PELP1 to the genome and together, cooperatively regulates of a subset of macroH2A1 target genes.

The macro domain of macroH2A1 interacts with chromatin-associated and nucleolar components. Our GST-pull down assay identified a host of novel macro domain-interacting factors that can be classified into two categories: those that are chromatin-associated and those that are nucleolar components (Figure 4.1 and Figure 4.2 and Table 4.1). The chromatin-associated factors (PELP1, PARP-1, WDR18, and SET) are involved in cellular processes such as transcription and chromatin maintenance, while the nucleolar components (TCOF1, NCL, NPM1, MDN1, DDX46, TEX10, and Nol9) are generally involved in transcription, ribosome biogenesis/export, protein chaperoning, and RNA processing. The identification of these proteins fits well with emerging evidence that macroH2A1 is involved in regulating autosomal genes, as many of these proteins are known to function in various aspects of transcriptional control. It is interesting to note that PELP1 and PARP-1 have also been shown to interact with proteins of the same family as those we identified interacting with the macro domain of macroH2A1. For example, PELP1 can interact with WDR5 as part of the MLL1 complex (Dou et al., 2005; Kashiwaya et al., 2010) or members of the DEAD-box RNA helicase and AAA ATPase family members (Andersen et al., 2002), which are involved in RNA processing. Additionally, PARP-1 has been shown to interact with nucleolar proteins and transcriptional coregulators (nucleolin and nucleophosmin) in a number of contexts (Fu and Fenselau, 2005; Isabelle et al., 2010; Meder et al., 2005).

Macro domains have recently been identified as ligand binding domains for NAD^+ metabolites such as PAR, ADPR, and O-acetyl-ADPR (Ahel et al., 2009; Gottschalk et al., 2009; Karras et al., 2005; Kraus, 2009; Kustatscher et al., 2005; Timinszky et al., 2009). This action may change (i) the affinity of macro domain-interacting proteins or (ii) the recruitment of factors containing these domains to genomic sites of PAR accumulation (Ahel et al., 2009; Gottschalk et al., 2009;

Timinszky et al., 2009). While PARP-1 has previously been shown to associate with the macro domain of macroH2A1 in a manner dependent on macroH2A1's ability to bind NAD^+ metabolite ligands (*i.e.*, ADPR), we determined that the interaction with PELP1 is independent of ADPR binding (Figure 4.1C). This begs the question: what modulates the interaction of PELP1 with the macro domain of macroH2A1? In addition, this finding brings up an interesting question of whether or not PELP1 interacts with other macro domain-containing proteins, and whether those interactions are ligand-dependent or mediated by the non-macro domain regions of the protein. Interestingly, both PELP1 and macroH2A1 are subject to a variety of post-translational modifications (Abbott et al., 2005; Bernstein et al., 2008; Chu et al., 2006; Kashiwaya et al., 2010; Nagpal et al., 2008; Rosendorff et al., 2006), which may modulate the ability of these factors to interact. Further studies are required to determine the mechanisms that regulate these interactions.

PELP1 is a reader of the "histone code" and the "histone variant code". In a process termed the "histone code", specific combinations of covalent modifications of the histone tails of nucleosomes specify positive or negative gene expression outcomes (Jenuwein and Allis, 2001). These histone modifications exert their effects by recruiting transcriptional coregulators that can "read" these marks. PELP1 has recently been shown to be a reader of the histone code, where it specifically recognizes both H3K9me2 and H3K4me2 (Nair et al., 2010). Furthermore, PELP1 can also recruit additional chromatin modifying enzymes to the sites where it is found. For example, PELP1 has been shown to recruit KDM1 (lysine demethylase 1) and HDAC2 to nucleosomes (Choi et al., 2004; Nair et al., 2010). We show that PELP1-bound regions correlate with the linker histone H1, the histone modifications H3K27me3 and H3K9me3, and repressive transcription factors E2F6 and ZNF217

(Figure 4.5), all of which are known to generally mark heterochromatic chromatin and/or participate in the repression of gene expression (Banck et al., 2009; Reid et al., 2009; Trimarchi and Lees, 2002). Interestingly, E2F6 can act to recruit chromatin-remodeling and protein complexes that harbor histone 3 methyltransferase activity at lysine 4 and lysine 9 (Dou et al., 2005; Ogawa et al., 2002). These findings expand upon the recently identified role of PELP1 as a "reader" of histone marks. Although our correlation analysis does not indicate causality, it is also possible that these repressive transcription factors, E2F6 and ZNF217, function in recruiting PELP1 to the chromatin, much like the recruitment of histone modifying enzymes.

In a corollary to the "histone code", histone variants can also mark chromatin to specify positive or negative gene expression outcomes. As for the histone code, it follows that specific effector proteins capable of reading the "histone variant code" are necessary to facilitate gene expression outcomes. We demonstrate that PELP1 is broadly recruited to macroH2A1-containing chromatin across the genome. This data suggests that PELP1 is not only a reader of the "histone code" but is also a reader of the "histone variant code", where it specifically recognizes macroH2A1-containing nucleosomes. Furthermore, given the inclination of PELP1 to interact with histone modifying enzymes (e.g KDM1, HDAC2, p300/CBP (Choi et al., 2004; Nair et al., 2010; Vadlamudi et al., 2001)), it is possible that recruitment of PELP1 to macroH2A1-containing regions of the genome leads to further chromatin modifications. Further experiments are required to determine the role of PELP1 in further modifying macroH2A1-containing chromatin structure.

PELP1 and macroH2A1 are context-specific transcriptional coregulators. For quite a while, macroH2A1 was considered a transcriptionally repressive histone mark, exclusively. Recent work from our lab and others has determined that macroH2A1

can function as a positive or negative regulator of transcription depending on the specific context (Choi et al., 2004; Kayahara et al., 2008; Mishra et al., 2004; Nair et al., 2004; Nair et al., 2010; Singh et al., 2006; Vadlamudi et al., 2001). While originally identified as a coactivator for the estrogen receptor alpha (ERα) (Vadlamudi et al., 2001), PELP1 is now known to function as a coactivator for several transcription factors including ERα, ERβ, and RXR (Mishra et al., 2004; Singh et al., 2006; Vadlamudi et al., 2001), demonstrating that, like macroH2A1, PELP1 also modulates transcription in context-specific ways. Conversely, recent studies suggest that PELP1 can also function as a transcriptional corepressor in concert with several transcription factors, including GR, AP1, NFκB, and SRF (Choi et al., 2004; Kayahara et al., 2008). Therefore, PELP1 can either positively or negatively regulate gene expression in a context-specific fashion. The coordinated regulation of PELP1 and macroH2A1 target gene expression described above demonstrates a connection between the determinants that specify these factors as transcriptionally permissive or repressive. Specifically, at genes coregulated by macroH2A1 and PELP1, if one factor supports target gene expression so does the other and vice versa.

There is much that remains to be elucidated about the concerted roles of macroH2A1 and PELP1 in transcriptional regulation of target genes. One major question centers on identifying the determinants that allow macroH2A1 and PELP1 to function as transcriptional activators and those specific for transcriptional repression. One possibility is that further histone modifications are required to specify direction of macroH2A1/PELP1-mediated transcriptional outcomes. In addition, macroH2A1 and PELP1 are themselves targets of various covalent modifications (reviewed in (Nagpal et al., 2008; Thambirajah et al., 2009)), which may also play a role in determining the direction of regulation. Alternatively, the specific transcription factors that bind near (or are specifically recruited to) macroH2A1/PELP1 positively and negatively

regulated genes may be different. Understanding the context-specific transcriptional outcomes mediated by PELP1 and macroH2A1, will lead to a greater understanding of how particular chromatin states regulate gene expression.

4.5. Experimental Procedures

Antibodies - The rabbit polyclonal PELP1 and macroH2A1 antibodies used for Western blotting, ChIP-chip, and ChIP-qPCR were purchased from Bethyl Laboratories, Inc (A300-180A) and Millipore (07-219), respectively. The antibodies were screened for: (i) specificity by Western blotting MCF-7 cell extracts, (ii) the ability to immunoprecipitate their cognate antigens from formaldehyde crosslinked chromatin by a ChIP-Western protocol, and (iii) a reduction in Western blot signal upon knockdown of PELP1 or macroH2A1. The rabbit polyclonal H3 antibody used for Western blotting, ChIP-chip, and ChIP-qPCR was purchased from Abcam (ab1791-100). The custom rabbit polyclonal antibody against PARP-1 used for Western blotting was generated by using a purified fragment of human PARP-1 (amino-terminal, PARP-N; Pocono Rabbit Farm and Laboratory, Inc.) and previously characterized (Frizzell et al., 2009; Kim et al., 2004). The rabbit polyclonal Nucleolin (C-23) and SET antibodies used for Western blotting were purchased from Santa Cruz Biotechnology, Inc. (sc-13057 and sc-25564, respectively) and the mouse monoclonal β-Actin antibody was purchased from Sigma-Aldrich (A5316).

Oligonucleotides - The oligonucleotide sequences listed below were used for the shRNA constructs. Those sequences denoted with an asterisk (*) were chosen based on priority score according to criteria described at the website (https://rnaidesigner.invitrogen.com/rnaiexpress).

shRNA constructs -

Target	Sequence	Source
Luc	5'-gatatgggctgaatacaaa-3'	(Reynolds et al., 2004)
PELP1 #1*	5'-ggagcattcagcaggtgttac-3'	Invitrogen BLOCK-iT RNAi Designer
PELP1 #2	5'-ggaccaaggtgtatgcgatat-3'	(Dimple et al., 2008)
mH2A1 #1	5'-gcaatgcagcgagagacaaca-3'	(Gamble et al., 2010)
mH2A1 #2	5'-gcgtgtgttgtggtgctttat-3'	(Gamble et al., 2010)

GST-macro1.1 pull-down and Protein Identification - The GST-macro1.1 vector was made by cloning the non-histone region of macroH2A1.1 (e.g. amino acids 123 to 368) into pGEX-2TK. The vector was induced in BL21(DE3) and the protein was purified using glutathione-agarose. GST alone or GST-macro1.1 (2 μg) was pre-bound to 15 ul of glutathione-agarose in a 150 μl final volume of buffer containing 20 mM Tris pH 7.5, 0.1 M NaCl, 0.1 mM EDTA, 5% glycerol, 0.1% Tween-20. After 30 min of pre-binding, the beads were washed three times with the same buffer. The GST- or GST-macro1.1-bound beads were then incubated in a final volume of 150 μl with 250 μg of HeLa nuclear extract. Where indicated, 20 μM of ADPR or NAD^+ was added to the reaction. The binding reactions were nutated for 2 hrs at 4^oC. The beads were then washed 3 times using the buffer conditions noted above. For immunoblots the proteins were eluted directly with SDS and subjected to SDS-PAGE.

For mass spectrometric identification the bound proteins were eluted with reduced glutathione (Sigma) and separated by SDS-PAGE. Proteins excised from gels were digested with trypsin, and resulting peptide pools analyzed by matrix-assisted laser-desorption / ionization reflectron time-of-flight (MALDI-reTOF) MS using a BRUKER UltraFlex TOF/TOF instrument (Bruker Daltonics; Bremen, Germany)

(Erdjument-Bromage et al., 1998; Sebastiaan Winkler et al., 2002). Selected experimental masses (m/z) were taken to search the human segment of a non-redundant protein database ('NR' on April 8th 2010; ~233,131 entries; National Center for Biotechnology Information; Bethesda, MD), utilizing the Mascot Peptide Mass Fingerprint (PMF) program, version 2.3.01 for Windows (www.matrixscience.com), with a mass accuracy restriction better than 40 ppm, and maximum one missed cleavage site allowed per peptide. To confirm PMF results with scores ≤40, mass spectrometric sequencing of selected peptides was done by MALDI-TOF/TOF (MS/MS) analysis on the same prepared samples, using the UltraFlex instrument in 'LIFT' mode. Fragment ion spectra were taken to search NR using the Mascot MS/MS Ion Search program (Matrix Science, www.matrixscience.com).

Luc_i and $PELP1_i$ inducible knockdown constructs - For the "Tet-on" inducible knockdown constructs (Luc_i and $PELP1_i$), the pSUPER.retro vector (puromycin resistant) was first modified by replacing the H1 promoter with one harboring a Tet operator sequence (from the pTER+ modified vector, kindly provided by H. Th. Marc Timmers (van de Wetering et al., 2003)) using BglII and EcoRI restriction sites. The resulting vector is termed pSUPER.retro.TO (Tet operon). Double stranded oligonucleotides containing shRNA sequences targeting either luciferase (Luc control) or PELP1 were cloned into the pSUPER.retro.TO (puromycin resistant) vector using BglII and XhoI restriction sites, as described by the manufacturer.

The shRNA sequences were based on sequences reported in the literature (Dimple et al., 2008; Reynolds et al., 2004) or designed using the Invitrogen BLOCK-iT RNAi Designer (https://rnaidesigner.invitrogen.com/rnaiexpress), as noted above. All constructs were confirmed by sequencing.

Generation, culture, and treatments of MCF-7-derived cell lines - Parental MCF-7 human breast cancer cells, kindly provided by Dr. Benita Katzenellenbogen, were maintained in MEM Eagle medium containing Hanks' salts, L-glutamine, and non-essential amino acids (Sigma) supplemented with 5% bovine calf serum (CS; Sigma), 20 mM HEPES (pH 7.6), 100 units/mL penicillin, 100 μg/mL streptomycin, 25 μg/mL gentamycin, and 0.22 % sodium bicarbonate. The Luc and macroH2A1 knockdown cell lines were generated and cultured as described previously (Gamble et al., 2010).

For the "Tet-on" inducible knockdown system, parental MCF-7 cells were stably transfected with a Tet Repressor (TetR) cDNA (pcDNA6/TR; kindly provided by H. Th. Marc Timmers). Stable transfectants were clonally selected using hygromycin (200 μg/mL), expanded, and tested for TetR expression and activity by Western blotting and transient transfection/luciferase reporter gene assay, respectively (see Appendix). The resulting cell line, termed MCF-7 TetR, was maintained under similar conditions as described above, with the exception of the serum (5% Tet-approved FBS (Tet FBS); Clonetech) to reduce background shRNA expression in the absence of doxycycline. MCF-7 TetR cells were used to make the Luc_i and $PELP1_i$ knockdown cell lines by retroviral infection with the appropriate shRNA vectors.

Retroviruses were generated by transfection of the pSUPER.retro or pSUPER.retro.TO vectors described above with an expression vector for the VSV-G envelope protein into Phoenix Ampho cells using GeneJuice transfection reagent (Novagen) according to the manufacturer's protocol. The resulting viruses were collected, filtered through a 0.45 μm syringe filter to remove any remaining cells, and used to infect the MCF-7 or MCF-7 TetR cells where appropriate. Stably transduced cells were isolated under appropriate selection with puromycin (Sigma; 0.5 μg/mL) and/or G418 sulfate (Gibco/BRL; 800 μg/mL), expanded, and frozen in aliquots for

future use. The cells were grown under subconfluent conditions for routine maintenance and most experimental procedures.

Luc_i and $PELP1_i$ knockdown cell lines were maintained as noted above and treated with doxycycline (Sigma-Aldrich; 2 μg/mL) to induce the shRNA expression for a minimum of 9 days. For most experiments, only one shRNA for PELP1 was used (#2), as it gave a higher degree of PELP1 depletion. Both shRNAs were tested in gene-specific expression studies to determine off-target effects (Figure 4.9). For ChIP-qPCR and RT-qPCR experiments, only the Luc_i and $PELP1_i$ "+ dox" conditions were compared due to the apparent leakiness of the system in the "- dox" condition.

MCF-7 parental, Luc and macroH2A1 knockdown, or Luc_i and $PELP1_i$ knockdown cell were serum-starved by washing the cells in PBS and replacing the medium with MEM without serum for 24 h or treated with 12-O-Tetradecanoylphorbol-13-acetate (TPA, Enzo Life Sciences; 100 ng/mL) for 3 h (expression) or 1.5 h (ChIP), where indicated.

Chromatin immunoprecipitation assays - ChIP assays were performed essentially as described previously (Gamble et al., 2010; Krishnakumar et al., 2008). The immunoprecipitations were performed from crosslinked parental or knockdown MCF-7 cells with antibodies against macroH2A1, PELP1, or histone H3, using "no antibody" as a control. The resulting input and ChIP DNA material were used for ChIP-chip or gene-specific ChIP-qPCR analyses where indicated.

ChIP-chip - The ChIP-chip sample processing and analyses were done essentially as described previously (Gamble et al., 2010; Krishnakumar et al., 2008). Briefly, PELP1-specific immunoprecipitated genomic DNA and reference DNA was blunted, amplified by ligation-mediated PCR (LM-PCR), labeled with Cy5 and Cy3,

respectively, and used to probe a custom human oligonucleotide genomic array (Nimblegen) (Gamble et al., 2010; Krishnakumar et al., 2008). The PELP1 ChIP-chip was run in duplicate to ensure reproducibility. Detailed information about the genomic regions included on the custom array and the data from the hybridizations described in this study can be accessed from the National Institutes of Health GEO Database (http://www.ncbi.nlm.nih.gove/geo) using accession number GSE22254.

Genomic Data Analyses - The Genomic data analyses for the PELP1 ChIP-chip were performed as described previously (Gamble et al., 2010), using the statistical programming language R (R Development Core Team). All data processing scripts are available on request. Briefly, PELP1-bound regions were defined as at least three consecutive windows with (i) positive means, (ii) at least six probes, and (iii) *P*-value < 0.016. PELP1-unbound regions were defined as at least three consecutive windows with (i) negative means, (ii) at least six probes, and (iii) *P*-value < 0.016.

For PELP1-macroH2A1 genomic comparisons, the macroH2A1 data set was accessed from the National Institutes of Health GEO Database using accession number GSE9607. For expression-based classification of genes, MCF-7 expression microarray data was accessed from the National Institutes of Health GEO Database using accession number GSE9253, and expressed genes were divided into pentiles based on the degree of expression. The data were then compared to the genes represented on the ChIP-chip array, as described previously (Gamble et al., 2010).

For gene ontology analyses, specific gene lists were entered into the Generic Gene Ontology Term Finder (http://go.princeton.edu/egi-bin/GOTermFinder/GOTermFinder). A multiple testing corrected *P*-value of 0.002 was used as the cutoff for significant enrichment. Specifically, we considered genes (i) bound by PELP1 (independent of macroH2A1 status), (ii) bound by macroH2A1

(independent of PELP1 status), (iii) genes bound by both PELP1 and macroH2A1, (iv) genes bound by PELP1 and not by macroH2A1, and (v) genes bound by macroH2A1 and not by PELP1. The gene lists can be found in Table 4.3.

For the multiple ChIP-chip correlation analysis, 362 ChIP-chip data sets were accessed from the National Institutes of Health Geo Database using criteria described previously (Gamble et al., 2010). The data were processed with 1-kb windows identical to that of the macroH2A1 and PELP1 data sets and Spearman correlations were determined between PELP1 and each factor. A correlation coefficient of ±0.20 and *P*-value of $< 10^{-100}$ was used as cutoffs for significant correlation.

mRNA expression analyses by RT-qPCR - For gene-specific mRNA expression analyses, total RNA was isolated using Trizol Reagent (Invitrogen), reverse transcribed, and subjected to real-time quantitative PCR using a set of gene specific primers. All target gene transcripts were normalized to the β-actin transcript, which was unaffected by macroH2A1 or PELP1 knockdown (data not shown). All experiments were conducted a minimum of three times with independent RNA isolations to ensure reproducibility.

Quantitative PCR analyses (RT-qPCR and ChIP-qPCR) - Gene-specific mRNA expression and ChIP analyses were analyzed by quantitative PCR in a similar manner. Briefly, reactions containing DNA from either source, 1x SYBR Green PCR master mix, and forward and reverse primers (500 nM) were used in 40-45 cycles of amplification (95°C for 15 sec, 60°C for 1 min) using a Roche LightCycler® 480 System (384-well) following an initial 3 min incubation at 95°C. Melting curve analysis was performed to ensure that only the targeted amplicon was amplified.

Statistical analyses - For the ChIP-qPCR and RT-qPCR assays in Figures 4.6-4.13, a paired Student's *t*-test with a *P*-value threshold of < 0.05 was used to determine the significance of differences between the control and experimental samples. The enrichment test in Figure 4.4 was determined using a Fisher's exact test.

Primer Sequences – The primer sequences listed below were used for both RT-qPCR and ChIP-qPCR amplification reactions.

RT-qPCR -

Gene Name	**Primer Sequence**
β-ACTIN forward	5'-AGCTACGAGCTGCCTGAC-3'
β-ACTIN reverse	5'-AAGGTAGTTTCGTGGATGC-3'
AREG forward	5'-GAGAAGCTGAGGAACGAAAG-3'
AREG reverse	5'-GGCTATGACTTGGCAGTGAC-3'
ASCL1 forward	5'-ACTGGGACCTGAGTCAATGC-3'
ASCL1 reverse	5'-GCTGTGCGTGTTAGAGGTGA-3'
CCL2 forward	5'-CCCCAGTCACCTGCTGTTAT-3'
CCL2 reverse	5'-GCTTCTTTGGGACACTTGCT-3'
H2AFY forward	5'-AAGAAGGGACGGGTCACAC-3'
H2AFY reverse	5'-GGGTGGATGTTGGGTAACAC-3'
IL24 forward	5'-AGGCGGTTTCTGCTATTC-3'
IL24 reverse	5'-CTGCATCCAGGTCAGAAG-3'
MAPK12 forward	5'-ACCTGGCTGTGAACGAAG-3'
MAPK12 reverse	5'-CACCACGTACCCAGTCATC-3'
NELL2 forward	5'-TGAAGGGAACCACCTACC-3'
NELL2 reverse	5'-ATTTGCCATCCACATACG-3'

PARP1 forward	5’-GTGTGGGAAGACCAAAGGAA-3’
PARP1 reverse	5’-TTCAAGAGCTCCCATGTTCA-3’
PELP1 forward	5’- CACCAGAGACACCTGCAGAA-3’
PELP1 reverse	5’- AGCTGTGTCATCCTGCTCCT-3’
SOCS2 forward	5’-ACACGTCAGCACCATCTCTG-3’
SOCS2 reverse	5’-TGGCACCGGTACATTTGTTA-3’
TFF1 forward	5’-TGCTTCTATCCTAATACCATCG-3’
TFF1 reverse	5’-AGATCCCTGCAGAAGTGTC-3’
TMOD3 forward	5’-GGAAGTAGTAATGGTGTTGACC-3’
TMOD3 reverse	5’-GCTCATCAAATACCGGAAG-3’
TNFSF10 forward	5’-TCACATAACTGGGACCAGAG-3’
TNFSF10 reverse	5’-AGTTCACCATTCCTCAAGTG-3’
TSPAN5 forward	5’-ACACTGGACAGACCCAGCTT-3’
TSPAN5 reverse	5’-TGTCAGTGAGCAGCATTTCC-3’

ChIP-qPCR -

Gene Name	**Primer Sequence**
AREG -3.0 kb forward	5’-TTGTTCCCCTTTGTCTCTGC-3’
AREG -3.0 kb reverse	5’-GATGTGTCATGGCATTCTGG-3’
AREG +1.5 kb forward	5’-TTCCCCTGTGAGTGAAATGC-3’
AREG +1.5 kb reverse	5’-AGCCAGGTATTTGTGGTTCG-3’
ASCL1 -2.0 kb forward	5’-GACTCTGCTTTTGGGTGCTC-3’
ASCL1 -2.0 kb reverse	5’-TTCACACCTCAGGCCTTTCT-3’
ASCL1 +2.0 kb forward	5’-GAGCAACTGGGACCTGAGTC-3’
ASCL1 +2.0 kb reverse	5’-CTATAACGCGTGTGCTGCTC-3’
CCL2 -1.5 kb forward	5’-ACCTAACGAAAGCTGGGTTG-3’

CCL2 -1.5 kb reverse	5’-TTCAGGGAGTCAGGTATGGTG-3’
CCL2 +1.0 kb forward	5’-TGGCCTGAAGTTCTTCCTTG-3’
CCL2 +1.0 kb reverse	5’-GGGGTTCACTTTTTCCCTTG-3’
IL24 +2.0 kb forward	5’-AGGGCCAAGAATTCCACTTT-3’
IL24 +2.0 kb reverse	5’-GTCTTTCACAGCCCAGAAGG-3’
MAPK12 +3.0 kb forward	5’-TTCACCCCAACCAAACAGA-3’
MAPK12 +3.0 kb reverse	5’-CTCTTTCCATAGCGCTGTCC-3’
NELL2 -1.5 kb forward	5’-TCAGAATTCGGGAGCTCTTT-3’
NELL2 -1.5 kb reverse	5’-TTTCAAATTTGGGAAATTGCAT-3’
SOCS2 -2.0 kb forward	5’-AAGTTCTCTGGAAGCCACAGG-3’
SOCS2 -2.0 kb reverse	5’-CGGTGAGTTTGGATTTTTCTG-3’
SOCS2 +4.0 kb forward	5’-AGTTCTCTCGCTTGCGATTC-3’
SOCS2 +4.0 kb reverse	5’-ACCGGGATACTTGCAATCTG-3’
TFF1 -3.0 kb forward	5’-TGGGTTCCGCCCACTCT-3’
TFF1 -3.0 kb reverse	5’-CTGCCCCCGGGACTCT-3’
TMOD3 -2.5 kb forward	5’-TCTGGCCCCATATGTGGTAT-3’
TMOD3 -2.5 kb reverse	5’-TGCAGTTTGATGGTGGATTT-3’
TNFSF10 -2.0 kb forward	5’-AGGCATGAAACGAAGGAATG-3’
TNFSF10 -2.0 kb reverse	5’-CTTGACCTGACCCCGAGATA-3’
TSPAN5 -3.0 kb forward	5’-TTGACTCAGCAGTCCCTCTTC-3’
TSPAN5 -3.0 kb reverse	5’-TCCATCTGCTGGGGTATTTC-3’

REFERENCES

(2004). The ENCODE (ENCyclopedia Of DNA Elements) Project. Science *306*, 636-640.

Abbott, D. W., Chadwick, B. P., Thambirajah, A. A., and Ausio, J. (2005). Beyond the Xi: macroH2A chromatin distribution and post-translational modification in an avian system. J Biol Chem *280*, 16437-16445.

Abbott, D. W., Laszczak, M., Lewis, J. D., Su, H., Moore, S. C., Hills, M., Dimitrov, S., and Ausio, J. (2004). Structural characterization of macroH2A containing chromatin. Biochemistry *43*, 1352-1359.

Agelopoulos, M., and Thanos, D. (2006). Epigenetic determination of a cell-specific gene expression program by ATF-2 and the histone variant macroH2A. EMBO J *25*, 4843-4853.

Ahel, D., Horejsi, Z., Wiechens, N., Polo, S. E., Garcia-Wilson, E., Ahel, I., Flynn, H., Skehel, M., West, S. C., Jackson, S. P.*, et al.* (2009). Poly(ADP-ribose)-dependent regulation of DNA repair by the chromatin remodeling enzyme ALC1. Science *325*, 1240-1243.

Andersen, J. S., Lyon, C. E., Fox, A. H., Leung, A. K., Lam, Y. W., Steen, H., Mann, M., and Lamond, A. I. (2002). Directed proteomic analysis of the human nucleolus. Curr Biol *12*, 1-11.

Angelov, D., Bondarenko, V. A., Almagro, S., Menoni, H., Mongelard, F., Hans, F., Mietton, F., Studitsky, V. M., Hamiche, A., Dimitrov, S., and Bouvet, P. (2006). Nucleolin is a histone chaperone with FACT-like activity and assists remodeling of nucleosomes. EMBO J *25*, 1669-1679.

Angelov, D., Molla, A., Perche, P. Y., Hans, F., Cote, J., Khochbin, S., Bouvet, P., and Dimitrov, S. (2003). The histone variant macroH2A interferes with transcription factor binding and SWI/SNF nucleosome remodeling. Mol Cell *11*, 1033-1041.

Banck, M. S., Li, S., Nishio, H., Wang, C., Beutler, A. S., and Walsh, M. J. (2009). The ZNF217 oncogene is a candidate organizer of repressive histone modifiers. Epigenetics *4*, 100-106.

Bernstein, E., Muratore-Schroeder, T. L., Diaz, R. L., Chow, J. C., Changolkar, L. N., Shabanowitz, J., Heard, E., Pehrson, J. R., Hunt, D. F., and Allis, C. D. (2008). A phosphorylated subpopulation of the histone variant macroH2A1 is excluded from the inactive X chromosome and enriched during mitosis. Proc Natl Acad Sci U S A *105*, 1533-1538.

Brann, D. W., Zhang, Q. G., Wang, R. M., Mahesh, V. B., and Vadlamudi, R. K. (2008). PELP1--a novel estrogen receptor-interacting protein. Mol Cell Endocrinol *290*, 2-7.

Buschbeck, M., Uribesalgo, I., Wibowo, I., Rue, P., Martin, D., Gutierrez, A., Morey, L., Guigo, R., Lopez-Schier, H., and Di Croce, L. (2009). The histone variant macroH2A is an epigenetic regulator of key developmental genes. Nat Struct Mol Biol *16*, 1074-1079.

Chakravarthy, S., Gundimella, S. K., Caron, C., Perche, P. Y., Pehrson, J. R., Khochbin, S., and Luger, K. (2005). Structural characterization of the histone variant macroH2A. Mol Cell Biol *25*, 7616-7624.

Chang, C. C., Ma, Y., Jacobs, S., Tian, X. C., Yang, X., and Rasmussen, T. P. (2005). A maternal store of macroH2A is removed from pronuclei prior to onset of somatic macroH2A expression in preimplantation embryos. Dev Biol *278*, 367-380.

Chang, E. Y., Ferreira, H., Somers, J., Nusinow, D. A., Owen-Hughes, T., and Narlikar, G. J. (2008). MacroH2A allows ATP-dependent chromatin remodeling by SWI/SNF and ACF complexes but specifically reduces recruitment of SWI/SNF. Biochemistry *47*, 13726-13732.

Changolkar, L. N., Costanzi, C., Leu, N. A., Chen, D., McLaughlin, K. J., and Pehrson, J. R. (2007). Developmental changes in histone macroH2A1-mediated gene regulation. Mol Cell Biol *27*, 2758-2764.

Changolkar, L. N., and Pehrson, J. R. (2002). Reconstitution of nucleosomes with histone macroH2A1.2. Biochemistry *41*, 179-184.

Changolkar, L. N., Singh, G., and Pehrson, J. R. (2008). macroH2A1-dependent silencing of endogenous murine leukemia viruses. Mol Cell Biol *28*, 2059-2065.

Cheskis, B. J., Greger, J., Cooch, N., McNally, C., McLarney, S., Lam, H. S., Rutledge, S., Mekonnen, B., Hauze, D., Nagpal, S., and Freedman, L. P. (2008). MNAR plays an important role in ERa activation of Src/MAPK and PI3K/Akt signaling pathways. Steroids *73*, 901-905.

Choi, Y. B., Ko, J. K., and Shin, J. (2004). The transcriptional corepressor, PELP1, recruits HDAC2 and masks histones using two separate domains. J Biol Chem *279*, 50930-50941.

Chu, F., Nusinow, D. A., Chalkley, R. J., Plath, K., Panning, B., and Burlingame, A. L. (2006). Mapping post-translational modifications of the histone variant MacroH2A1 using tandem mass spectrometry. Mol Cell Proteomics *5*, 194-203.

Costanzi, C., and Pehrson, J. R. (1998). Histone macroH2A1 is concentrated in the inactive X chromosome of female mammals. Nature *393*, 599-601.

Csankovszki, G., Panning, B., Bates, B., Pehrson, J. R., and Jaenisch, R. (1999). Conditional deletion of Xist disrupts histone macroH2A localization but not maintenance of X inactivation. Nat Genet *22*, 323-324.

Dimple, C., Nair, S. S., Rajhans, R., Pitcheswara, P. R., Liu, J., Balasenthil, S., Le, X. F., Burow, M. E., Auersperg, N., Tekmal, R. R.*, et al.* (2008). Role of PELP1/MNAR signaling in ovarian tumorigenesis. Cancer Res *68*, 4902-4909.

Dou, Y., Milne, T. A., Tackett, A. J., Smith, E. R., Fukuda, A., Wysocka, J., Allis, C. D., Chait, B. T., Hess, J. L., and Roeder, R. G. (2005). Physical association and coordinate function of the H3 K4 methyltransferase MLL1 and the H4 K16 acetyltransferase MOF. Cell *121*, 873-885.

Erdjument-Bromage, H., Lui, M., Lacomis, L., Grewal, A., Annan, R. S., McNulty, D. E., Carr, S. A., and Tempst, P. (1998). Examination of micro-tip reversed-phase liquid chromatographic extraction of peptide pools for mass spectrometric analysis. J Chromatogr A *826*, 167-181.

Frizzell, K. M., Gamble, M. J., Berrocal, J. G., Zhang, T., Krishnakumar, R., Cen, Y., Sauve, A. A., and Kraus, W. L. (2009). Global analysis of transcriptional regulation by poly(ADP-ribose) polymerase-1 and poly(ADP-ribose) glycohydrolase in MCF-7 human breast cancer cells. J Biol Chem *284*, 33926-33938.

Fu, Z., and Fenselau, C. (2005). Proteomic evidence for roles for nucleolin and poly[ADP-ribosyl] transferase in drug resistance. J Proteome Res *4*, 1583-1591.

Gamble, M. J., Frizzell, K. M., Yang, C., Krishnakumar, R., and Kraus, W. L. (2010). The histone variant macroH2A1 marks repressed autosomal chromatin, but protects a subset of its target genes from silencing. Genes Dev *24*, 21-32.

Gamble, M. J., and Kraus, W. L. (2010). Multiple facets of the unique histone variant macroH2A. Cell Cycle *9*, 1-7.

Gottschalk, A. J., Timinszky, G., Kong, S. E., Jin, J., Cai, Y., Swanson, S. K., Washburn, M. P., Florens, L., Ladurner, A. G., Conaway, J. W., and Conaway, R. C. (2009). Poly(ADP-ribosyl)ation directs recruitment and activation of an ATP-dependent chromatin remodeler. Proc Natl Acad Sci U S A *106*, 13770-13774.

Hernandez-Munoz, I., Lund, A. H., van der Stoop, P., Boutsma, E., Muijrers, I., Verhoeven, E., Nusinow, D. A., Panning, B., Marahrens, Y., and van Lohuizen, M. (2005). Stable X chromosome inactivation involves the PRC1 Polycomb complex and requires histone MACROH2A1 and the CULLIN3/SPOP ubiquitin E3 ligase. Proc Natl Acad Sci U S A *102*, 7635-7640.

Isabelle, M., Moreel, X., Gagne, J. P., Rouleau, M., Ethier, C., Gagne, P., Hendzel, M. J., and Poirier, G. G. (2010). Investigation of PARP-1, PARP-2, and PARG interactomes by affinity-purification mass spectrometry. Proteome Sci *8*, 22.

Jenuwein, T., and Allis, C. D. (2001). Translating the histone code. Science *293*, 1074-1080.

Karras, G. I., Kustatscher, G., Buhecha, H. R., Allen, M. D., Pugieux, C., Sait, F., Bycroft, M., and Ladurner, A. G. (2005). The macro domain is an ADP-ribose binding module. EMBO J *24*, 1911-1920.

Kashiwaya, K., Nakagawa, H., Hosokawa, M., Mochizuki, Y., Ueda, K., Piao, L., Chung, S., Hamamoto, R., Eguchi, H., Ohigashi, H.*, et al.* (2010). Involvement of the tubulin tyrosine ligase-like family member 4 polyglutamylase in PELP1 polyglutamylation and chromatin remodeling in pancreatic cancer cells. Cancer Res *70*, 4024-4033.

Kayahara, M., Ohanian, J., Ohanian, V., Berry, A., Vadlamudi, R., and Ray, D. W. (2008). MNAR functionally interacts with both NH2- and COOH-terminal GR domains to modulate transactivation. Am J Physiol Endocrinol Metab *295*, E1047-1055.

Khan, M. M., Hadman, M., De Sevilla, L. M., Mahesh, V. B., Buccafusco, J., Hill, W. D., and Brann, D. W. (2006). Cloning, distribution, and colocalization of MNAR/PELP1 with glucocorticoid receptors in primate and nonprimate brain. Neuroendocrinology *84*, 317-329.

Kim, M. Y., Mauro, S., Gevry, N., Lis, J. T., and Kraus, W. L. (2004). NAD+-dependent modulation of chromatin structure and transcription by nucleosome binding properties of PARP-1. Cell *119*, 803-814.

Kininis, M., Chen, B. S., Diehl, A. G., Isaacs, G. D., Zhang, T., Siepel, A. C., Clark, A. G., and Kraus, W. L. (2007). Genomic analyses of transcription factor binding, histone acetylation, and gene expression reveal mechanistically distinct classes of estrogen-regulated promoters. Mol Cell Biol *27*, 5090-5104.

Kraus, W. L. (2009). New functions for an ancient domain. Nat Struct Mol Biol *16*, 904-907.

Krishnakumar, R., Gamble, M. J., Frizzell, K. M., Berrocal, J. G., Kininis, M., and Kraus, W. L. (2008). Reciprocal binding of PARP-1 and histone H1 at promoters specifies transcriptional outcomes. Science *319*, 819-821.

Kustatscher, G., Hothorn, M., Pugieux, C., Scheffzek, K., and Ladurner, A. G. (2005). Splicing regulates NAD metabolite binding to histone macroH2A. Nat Struct Mol Biol *12*, 624-625.

Ladurner, A. G. (2003). Inactivating chromosomes: a macro domain that minimizes transcription. Mol Cell *12*, 1-3.

Manavathi, B., Nair, S. S., Wang, R. A., Kumar, R., and Vadlamudi, R. K. (2005). Proline-, glutamic acid-, and leucine-rich protein-1 is essential in growth factor regulation of signal transducers and activators of transcription 3 activation. Cancer Res *65*, 5571-5577.

Meder, V. S., Boeglin, M., de Murcia, G., and Schreiber, V. (2005). PARP-1 and PARP-2 interact with nucleophosmin/B23 and accumulate in transcriptionally active nucleoli. J Cell Sci *118*, 211-222.

Mietton, F., Sengupta, A. K., Molla, A., Picchi, G., Barral, S., Heliot, L., Grange, T., Wutz, A., and Dimitrov, S. (2009). Weak but uniform enrichment of the histone variant macroH2A1 along the inactive X chromosome. Mol Cell Biol *29*, 150-156.

Mishra, S. K., Balasenthil, S., Nguyen, D., and Vadlamudi, R. K. (2004). Cloning and functional characterization of PELP1/MNAR promoter. Gene *330*, 115-122.

Nagpal, J. K., Nair, S., Chakravarty, D., Rajhans, R., Pothana, S., Brann, D. W., Tekmal, R. R., and Vadlamudi, R. K. (2008). Growth factor regulation of estrogen receptor coregulator PELP1 functions via Protein Kinase A pathway. Mol Cancer Res *6*, 851-861.

Nair, S. S., Guo, Z., Mueller, J. M., Koochekpour, S., Qiu, Y., Tekmal, R. R., Schule, R., Kung, H. J., Kumar, R., and Vadlamudi, R. K. (2007). Proline-, glutamic acid-, and leucine-rich protein-1/modulator of nongenomic activity of estrogen receptor enhances androgen receptor functions through LIM-only coactivator, four-and-a-half LIM-only protein 2. Mol Endocrinol *21*, 613-624.

Nair, S. S., Mishra, S. K., Yang, Z., Balasenthil, S., Kumar, R., and Vadlamudi, R. K. (2004). Potential role of a novel transcriptional coactivator PELP1 in histone H1 displacement in cancer cells. Cancer Res *64*, 6416-6423.

Nair, S. S., Nair, B. C., Cortez, V., Chakravarty, D., Metzger, E., Schule, R., Brann, D. W., Tekmal, R. R., and Vadlamudi, R. K. (2010). PELP1 is a reader of histone H3 methylation that facilitates oestrogen receptor-alpha target gene activation by regulating lysine demethylase 1 specificity. EMBO Rep *11*, 438-444.

Nusinow, D. A., Hernandez-Munoz, I., Fazzio, T. G., Shah, G. M., Kraus, W. L., and Panning, B. (2007). Poly(ADP-ribose) polymerase 1 is inhibited by a histone H2A variant, MacroH2A, and contributes to silencing of the inactive X chromosome. J Biol Chem *282*, 12851-12859.

Ogawa, H., Ishiguro, K., Gaubatz, S., Livingston, D. M., and Nakatani, Y. (2002). A complex with chromatin modifiers that occupies E2F- and Myc-responsive genes in G0 cells. Science *296*, 1132-1136.

Ouararhni, K., Hadj-Slimane, R., Ait-Si-Ali, S., Robin, P., Mietton, F., Harel-Bellan, A., Dimitrov, S., and Hamiche, A. (2006). The histone variant mH2A1.1 interferes with transcription by down-regulating PARP-1 enzymatic activity. Genes Dev *20*, 3324-3336.

Pehrson, J. R., and Fuji, R. N. (1998). Evolutionary conservation of histone macroH2A subtypes and domains. Nucleic Acids Res *26*, 2837-2842.

Rasmussen, T. P., Wutz, A. P., Pehrson, J. R., and Jaenisch, R. R. (2001). Expression of Xist RNA is sufficient to initiate macrochromatin body formation. Chromosoma *110*, 411-420.

Reid, G., Gallais, R., and Metivier, R. (2009). Marking time: the dynamic role of chromatin and covalent modification in transcription. Int J Biochem Cell Biol *41*, 155-163.

Reynolds, A., Leake, D., Boese, Q., Scaringe, S., Marshall, W. S., and Khvorova, A. (2004). Rational siRNA design for RNA interference. Nat Biotechnol *22*, 326-330.

Rosendorff, A., Sakakibara, S., Lu, S., Kieff, E., Xuan, Y., DiBacco, A., Shi, Y., Shi, Y., and Gill, G. (2006). NXP-2 association with SUMO-2 depends on lysines required for transcriptional repression. Proc Natl Acad Sci U S A *103*, 5308-5313.

Sebastiaan Winkler, G., Lacomis, L., Philip, J., Erdjument-Bromage, H., Svejstrup, J. Q., and Tempst, P. (2002). Isolation and mass spectrometry of transcription factor complexes. Methods *26*, 260-269.

Singh, R. R., Gururaj, A. E., Vadlamudi, R. K., and Kumar, R. (2006). 9-cis-retinoic acid up-regulates expression of transcriptional coregulator PELP1, a novel coactivator of the retinoid X receptor alpha pathway. J Biol Chem *281*, 15394-15404.

Thambirajah, A. A., Li, A., Ishibashi, T., and Ausio, J. (2009). New developments in post-translational modifications and functions of histone H2A variants. Biochem Cell Biol *87*, 7-17.

Timinszky, G., Till, S., Hassa, P. O., Hothorn, M., Kustatscher, G., Nijmeijer, B., Colombelli, J., Altmeyer, M., Stelzer, E. H., Scheffzek, K.*, et al.* (2009). A macrodomain-containing histone rearranges chromatin upon sensing PARP1 activation. Nat Struct Mol Biol *16*, 923-929.

Trimarchi, J. M., and Lees, J. A. (2002). Sibling rivalry in the E2F family. Nat Rev Mol Cell Biol *3*, 11-20.

Vadlamudi, R. K., Wang, R. A., Mazumdar, A., Kim, Y., Shin, J., Sahin, A., and Kumar, R. (2001). Molecular cloning and characterization of PELP1, a novel human coregulator of estrogen receptor alpha. J Biol Chem *276*, 38272-38279.

van de Wetering, M., Oving, I., Muncan, V., Pon Fong, M. T., Brantjes, H., van Leenen, D., Holstege, F. C., Brummelkamp, T. R., Agami, R., and Clevers, H. (2003). Specific inhibition of gene expression using a stably integrated, inducible small-interfering-RNA vector. EMBO Rep *4*, 609-615.

Wutz, A., Rasmussen, T. P., and Jaenisch, R. (2002). Chromosomal silencing and localization are mediated by different domains of Xist RNA. Nat Genet *30*, 167-174.

APPENDIX

Systems and Reagents Designed to Aid in the Study of PARP-1, PARG, and NAD^+-Synthesizing Enzymes*

* Contributors to the work described herein include: Esther Chong & Jany Chan (Appendix A.2; mutant and construct design); Dr. Mi Young Kim (Appendix A.2 and A.4; mutant design and initial construction); Dr. David A. Wacker (Appendix A.4; mutant design and initial construction); Dr. Nasun Hah and Trevor Halle (Appendix A.5; MCF-7 TetR cell line assembly and initial testing); Paul Tempst and Hediye Erdjument-Bromage (Appendix A.6, mass spectrometry analysis); Dr. Tong Zhang (Appendix A.6 & A.7; construct design and configuration); and Emily Reasor (Appendix A.7; construct development).

A.1. Summary

Poly(ADP-ribosyl)ation (PARylation) is an enzymatic reaction whereby ADP-ribose units from donor NAD^+ molecules are covalently attached onto target proteins. The regulation of this reaction is overseen by two nuclear enzymes, Poly(ADP-ribose) polymerase-1 (PARP-1) and poly(ADP-ribose) glycohydrolase (PARG), that modify target proteins in the nucleus by the addition and removal, respectively, of ADP-ribose polymers. Recent studies have revealed a role for PARP-1 in transcriptional regulation, while the role of PARG is less characterized. One of the ways in which PARP-1 (and PARG) activities might be controlled is by substrate availability (discussed in Chapter 1). For example, where does PARP-1's substrate, NAD^+, come from? How is it synthesized? How can this impact the functions of PARP-1 in the nucleus? In this Appendix, I describe systems, reagents, and initial experimental results designed to aid in the study of PARP-1, PARG, and NAD^+-synthesizing enzymes. Many of the conclusions made are preliminary and require parallel or follow-up studies to verify the results. In addition, the methodologies described can also be applied to other proteins of interest that pose similar questions.

A.2. PARG Protein Purification and Antibody Characterization

Poly(ADP-ribose) polymerase-1 (PARP-1) and poly(ADP-ribose) glycohydrolase (PARG) are enzymes that modify target proteins in the nucleus by the addition and removal, respectively, of ADP-ribose polymers (D'Amours et al., 1999; Kim et al., 2005). The molecular actions of PARP-1 are widely studied and a large number of commercially available reagents exist to aid in those studies. However, very few reagents are available in order to study the molecular actions of PARG in

vivo. I required an antibody that could be used for standard assays such as Western blotting, immunofluorescence, and immunoprecipitation. Since commercially available antibodies were not proving to be useful through initial experiments, I set out to generate an antiserum for use these types of assays. Purified, recombinant rPARG protein was used as antigen for injection into rabbits and the resulting antiserum was then tested for its ability to recognize recombinant, exogenous, and endogenous PARG protein forms in various contexts. Overall, the antiserum generated through this method proved useful in multiple assays, including chromatin immunoprecipitation.

A.2.1. Results and Discussion

Purification and characterization of wild type and catalytically inactive PARG protein. To generate an antiserum against PARG, I expressed and purified rat PARG protein from *E. coli*, which was then used as antigen for injection into rabbits. Notably, rPARG, whose domain structure is shown in Figure A.1A, is ~85% conserved in both nucleic acid and protein sequence to that of hPARG, including nearly 100% identity of the catalytic domain itself. I constructed three versions of this protein (*i.e.*, changing HIS tag location, with or without spacer) and purified them with varying success (Table A.1). Only the original construct (*i.e.*, N-terminal HIS tag with a short spacer) yielded the highest quality and quantity of rPARG full-length protein, which was subsequently used in my studies.

In addition to the wild type enzyme (Wt), a catalytically inactive mutant (Y788F/Y791A, CatMut; Figure A.1A) was also used for antiserum generation. The purified, recombinant Wt and CatMut antigens (Figure A.1B) were tested for activity in an Auto-Poly(ADP-ribosyl)ation assay. As shown in Figure A.1C, the activator-dependent auto-PARylation of PARP-1 is dramatically reduced in the presence of Wt

Figure A.1. Purification of wild type and catalytically inactive rPARG and characterization of anti-PARG antibody (generated in-house). *A,* Schematic diagram of the rat PARG structural and functional domains. The regulatory domain, catalytic domain, active site, nuclear localization signal (NLS), and nuclear export signal (NES) are shown. The open circles indicate the location of the inactivating point mutations (Tyr 788 to Phe and Tyr 791 to Ala) that inhibit PARG enzymatic activity in the catalytically inactive mutant (CatMut). *B,* Coommassie stained SDS-PAGE gel of native purified wildtype (Wt) or catalytically inactive (CatMut) rPARG from *E. coli*. The full-length rPARG protein is ~113 kDa. *C,* In vitro PARylation assay using radiolabeled ^{32}P-NAD^{+} as a substrate confirms activator-dependent auto-modification of PARP-1 is inhibited in the presence of Wt PARG, but not CatMut PARG. *D,* Primary antibody bleeds were tested for their ability to recognize PARG protein by Western blotting. Recombinant Wt or CatMut rPARG protein (*left*) or 293T cell lysates over-expressing rPARG (*right*) were analyzed. *E,* Various production bleeds were tested against recombinant protein or over-expression cell lysates, as described in panel D. A decreasing dilution series of each production bleed (1:5000, 1:15000, and 1:45000; *block arrow*) was tested and compared to the pre-immune sera (*e.g.*, isolated from the rabbit prior to antigen injection; PI) and a secondary antibody alone (*i.e.*, no primary antibody, 2°) to assess background signal. Assessment of endogenous protein detection is shown in Figure 2.1.

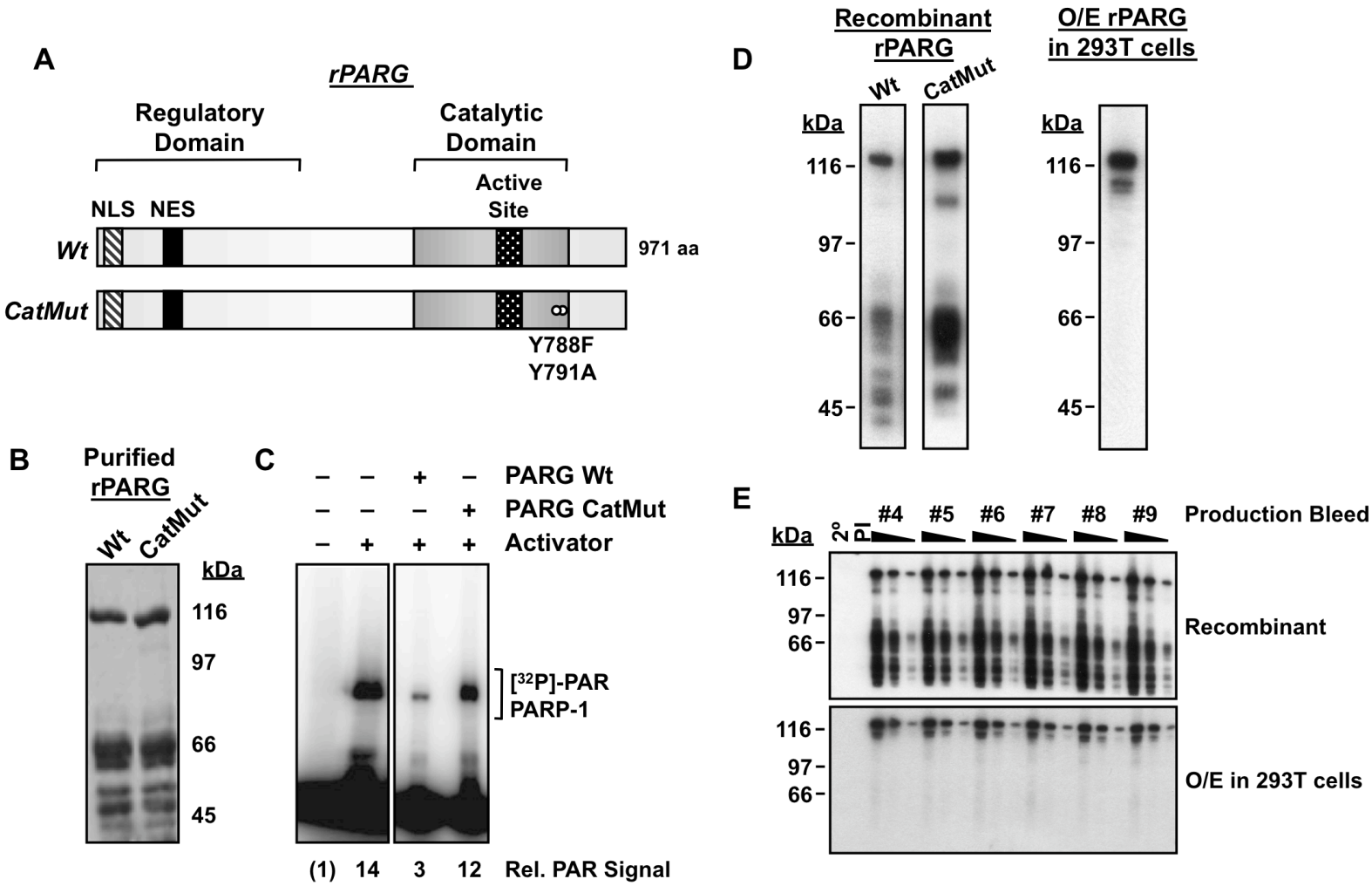
A
rPARG
Regulatory Domain
Catalytic Domain
NLS
NES
Active Site
Wt
971 aa
CatMut
Y788F
Y791A
B
Purified rPARG
Wt
CatMut
kDa
116
97
66
45
C
– – + – PARG Wt
– – – + PARG CatMut
– + + + Activator
[32P]-PAR
PARP-1
(1) 14 3 12 Rel. PAR Signal
D
Recombinant rPARG
O/E rPARG in 293T cells
Wt
CatMut
kDa
116
97
66
45
E
kDa
2°
#4 #5 #6 #7 #8 #9 Production Bleed
116
97
66
Recombinant
O/E in 293T cells

Table A.1. Summary of rPARG Wt & CatMut protein purification using various *E. coli* expression vectors and 6xHIS-tag locations.

Vector	6xHIS Location[a]	Size (kDa)	Notes
pET28a	N-term (*spacer*)	113	Original construct[b]
pET28a	N-term (*no spacer*)	113	FL/Breakdown ratio[c] ↓
pET15b	C-term (*no spacer*)	99	Smaller size; Yield ↑; Wt only

[a] Location of 6x HIS tag denoted by N- or C-terminal. *Spacer* indicates the 6x HIS tag is from the vector and a spacer is located between the tag and protein sequence. *No spacer* indicates the 6x HIS tag is placed directly before or after the cDNA by PCR.

[b] Original construct was ultimately used for purification of PARG Wt and CatMut protein for use in antisera production.

[c] FL/Breakdown ratio is the approximate ratio of the full length (FL; 113 kDa) protein product relative to the largest breakdown product (~66 kDa).

PARG, but not in the presence of CatMut PARG. These Wt and CatMut rPARG constructs were also used in gene regulatory studies described in Chapter 2.

The Wt and CatMut recombinant proteins were quantified and sent to the Pocono Rabbit Farm and Laboratory, Inc. (Canadensis, PA) for injection into a rabbit. The resulting antiserum were collected over numerous production bleeds and a final exsanguination bleed. The production bleeds were tested for PARG protein recognition against sera from the same rabbit prior to antigen injection (*i.e.*, pre-immune). The antiserum successfully detected recombinant Wt and CatMut rPARG (the antigen; Figure A.1D and A.1E), exogenously expressed rPARG in cells (Figure A.1D and A.1E), and endogenous hPARG in cells (Figure 2.1). The antiserum proved useful for Western blotting, immunoprecipitation (Figure 2.7), and chromatin immunoprecipitation (ChIP; Figure 2.7). Furthermore, the validity of the PARG antiserum was demonstrated by a reduction in signal upon expression of a sequence-specific shRNA against endogenous PARG (Figure 2.1 and 2.7). Although tested, initial immunofluorescence experiments displayed near background signals for endogenous PARG protein in cells (data not shown). This is likely due to the overall low level of PARG expressed in cells and the lack of compartmental localization.

A.2.2. Experimental Procedures

PARG expression constructs - Wild-type (Wt; kindly provided by Mitsuko Masutani) and catalytically inactive point mutants (CatMut) of rat PARG were used in the studies described herein. The catalytically inactive rat PARG contained changes at Tyr 788 and 791 to Phe and Ala, respectively (Y788F/Y791A) (Shimokawa et al., 1999). Both Wt and CatMut cDNAs were cloned into the pET28a bacterial expression vector (Novagen) using PCR-based cloning via the BamHI and XhoI restriction sites. CMV-

based mammalian expression constructs (with a carboxyl-terminal FLAG tag) were generated by PCR-based cloning of the tagged cDNAs into pCMV5.

Protein purification - hPARP-1 and Wt and CatMut rPARG were expressed in *E. coli* and purified by standard nickel-NTA affinity chromatography as described previously (Kim et al., 2004). Notably, induction of PARG proteins were done for 3hrs at 30°C.

Auto-PARylation assay – The activator-dependent auto-PARylation assay was performed essentially as described previously (Kim et al., 2004). Briefly, PARP-1 was incubated with ^{32}P-NAD^{+} (substrate) and sssp DNA (activator) in the absence and presence of purified Wt or CatMut rPARG proteins for 30 minutes at 27°C. The reactions were analyzed by SDS-PAGE, visualized by autoradiography, and quantified using ImageQuant software (Molecular Dynamics).

Exogenous expression of PARG in 293T cells - The pCMV5-PARG constructs (Wt and CatMut) were transiently transfected into 293T cells using Fugene 6 Transfection Reagent (Roche). The cells were collected 24 hrs post-transfection and whole cell lysates were subject to SDS-PAGE and Western blot analysis using PARG antiserum.

A.3. Generation and Testing of short hairpin RNAs Targeting PARP-1 and PARG in Human Cells

PARP-1 and PARG play important roles in an overlapping set of biological processes, including DNA damage detection and repair, cell death pathways, and transcriptional regulation (Kim et al., 2005). However, the mechanistic details of such processes are not fully characterized. One useful approach to further elucidate the

mechanism of action of PARP-1 and PARG is depleting the enzymes in vivo and determining the functional consequence of the targeted depletion in any of the cellular activities noted above. To this end, I designed various short hairpin (shRNA) sequences targeting either PARP-1 or PARG and used these shRNAs to generate stable depletions of PARP-1 and PARG in MCF-7 cells. Herein, I describe the design and generation of stable PARP-1 and PARG knockdown MCF-7 cell lines.

A.3.1. Results and Discussion

To explore the molecular actions of PARP-1 and PARG in vivo, I designed shRNA sequences to target the depletion of each enzyme in human cells using a retroviral delivery system. While previous groups have reported RNAi target sequences for PARP-1, none existed for PARG. Therefore, I designed shRNA sequences targeting both factors using available resources (*i.e.*, Dharmacon siDESIGN® Center software and Invitrogen BLOCK-iT™ RNAi Designer). Each target sequence (Table A.2) targeted a different nucleic acid location along the mRNA (Figure A.2A). The majority of sequences targeted exons, while two targeted 3' UTR regions. Varying the location of shRNA sequences along the mRNA may lead to varying degrees of protein depletion. Sequence accessibility, mRNA half-life, and frequency/rate of transcription and protein turnover are all factors that can alter the efficacy of shRNAs to deplete their target protein.

I cloned shRNA target sequences (six for PARP-1, four for PARG, and one for luciferase control) into the pSUPER.retro shRNA expression vectors (see Experimental Procedures), generated retrovirus, infected MCF-7 parental cells, and selected for stably transduced cells. Then, I tested the degree of shRNA-mediated knockdown of PARP-1 and PARG by Western blot analysis (Figure A.2B) and

Table A.2. Summary of shRNA sequences tested for PARP-1 and PARG stable knockdown in human cells.

	Sequence[a]	Site[b]	% KD[c]	Source[d]
hPARP-1				
#1	gggcaagcacagtgtcaaa	2829	95	{Ju, 2004 #68; Shah, 2005 #122}
#2	aagcctccgctcctgaacaat	2143	70	{Kameoka, 2005 #862}
#3	aagatagagcgtgaaggcgaa	2512	10	{Kameoka, 2005 #862}
#4	acacctctctactatataa	2942	80	Dharmacon
#5	aaaccaaagcttcgttaga	3507[e]	0	Dharmacon
#6	ggtggctgtggtatgaattca	3231[e]	0	Invitrogen
hPARG				
#1	ccagttggatggacactaa	239	10	Dharmacon
#2	caataccactcctgaaaca	1832	30	Dharmacon
#3	ttacgaaggtaccatagaa	2163	0	Dharmacon
#4	agagaccgctgaccattca	2892	50	Dharmacon

[a] The 19 or 21 bp shRNA sequence is given in the 5' to 3' orientation.
[b] Site of shRNA binding is denoted within the open reading frame relative to the start.
[c] Percent of knockdown of the target factor is relative to the Luc knockdown control in MCF-7 human breast cancer cells, as shown in Figure A.2 and Figure 2.6. Value is an average over at least two independently generated cell populations, and quantified by semi-quantitative Western blot (dilution series).
[d] shRNA sequences were based on sequences reported in the literature or designed using the Dharmacon siDESIGN® Center software or the Invitrogen BLOCK-iT™ RNAi Designer.
[e] Sequences #5 and #6 are located outside of the open reading frame, within the 3' untranslated region.

Figure A.2. Comparison of independent shRNA sequences targeting PARP-1 in MCF-7 cells. *A,* Schematic diagram of hPARP-1 mRNA (top) and hPARG mRNA (bottom) is drawn in the 5' to 3' orientation. The exons (blue bars) and 5' and 3' untranslated regions (red bars) are shown. The numbered regions represent the binding locations of the six shRNAs tested for PARP-1 knockdown and four shRNAs tested for PARG knockdown, as described in Table A.2. The shRNAs tested bind sequences within the coding region, as well as within 3' untranslated region (for PARP-1 only). *B,* Whole cell lysates were collected from Luc, PARP-1, or PARG stable shRNA-mediated knockdown cell lines. Six independent shRNA sequences (#1-6) targeting PARP-1 and four independent shRNA sequences (#1-4) targeting PARG were analyzed by Western blotting for their ability to knockdown PARP-1 relative to the Luc control (L). *C,* Stable Luc and PARP-1 knockdown cell lines were subjected to immunostaining with a PARP-1 antibody and visualized by confocal microscopy. A dotted circle denotes a single nucleus in each panel. The reduction in PARP-1 signal using a combination of shRNA #1 and #4 is consistent with panel B, which shows a high level of PARP-1 knockdown using shRNA #1 or #4, relative to the Luc control. The PARG antibody was not useful for immunostaining purposes.

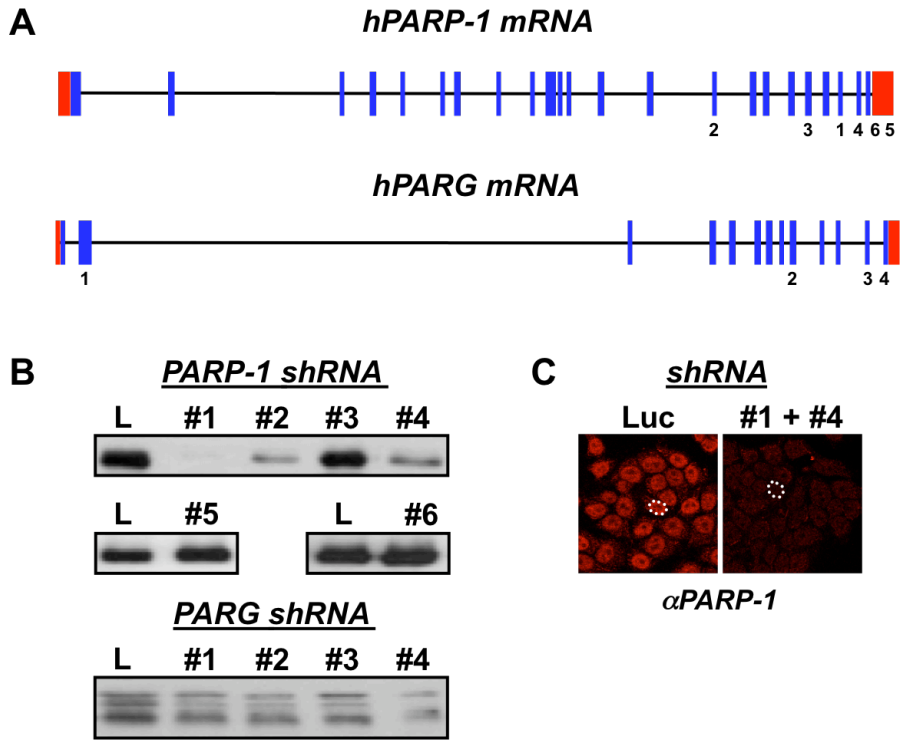
A
hPARP-1 mRNA
2
3
1 4 6 5
hPARG mRNA
1
2
3 4
B
PARP-1 shRNA
L
#1
#2
#3
#4
L
#5
L
#6
PARG shRNA
L
#1
#2
#3
#4
C
shRNA
Luc
#1 + #4
αPARP-1

immunofluorescence analysis (Figure A.2C). For PARP-1, shRNA #1, #2, and #4 showed a clear reduction of PARP-1 protein, albeit at varying levels, relative to the Luc control. This result was also apparent by immunostaining for endogenous PARP-1 protein by confocal microscopy in Luc and PARP-1 knockdown cell lines. To achieve the greatest degree of knockdown, PARP-1 shRNA #1 and #4 were combined and labeled #1 and #2, respectively, for simplicity (described in Chapter 2). For PARG, only shRNA #2 and #4 seemingly reduced endogenous PARG levels relative to the Luc control. As noted in Appendix A.2, the PARG antiserum was not useful for immunofluorescence assay due to the low abundance of PARG in MCF-7 cells. To achieve the greatest degree of knockdown, PARG shRNA #4 and #2 were combined and labeled #1 and #2, respectively, for simplicity (described in Chapter 2).

A.3.2. Experimental Procedures

Antibodies - To test the degree of knockdown by each shRNA sequence, whole cell lysates from stable knockdown cell lines were subject to SDS-PAGE and Western blot or immunostaining analysis using PARP-1 and PARG antisera. The custom rabbit polyclonal antibodies against PARP-1 and PARG were generated by using a purified fragment of human PARP-1 (amino-terminal, PARP-N (Kim et al., 2004)) and full-length rat PARG as antigens (described in Appendix A.2).

PARP-1 and PARG knockdown constructs - Short hairpin RNA (shRNA) expression constructs for retroviral-mediated knockdown of PARP-1 and PARG were made using the pSUPER.retro vector (OligoEngine). Double stranded oligonucleotides containing shRNA sequences targeting either luciferase (Luc control), PARP-1, or PARG were cloned into the vector using BglII and XhoI restriction sites as described by the

manufacturer. The shRNA sequences, listed in Table A.2, were based on sequences reported in the literature (Ju et al., 2004; Shah et al., 2005) or designed using the Dharmacon siDESIGN® Center software (www.dharmacon.com). All shRNA sequences were cloned into both pSUPER vectors (distinguished by resistance marker; puromycin or neomycin) and were confirmed by sequencing.

Generation and culture of MCF-7-derived cell lines - Parental MCF-7 human breast cancer cells, kindly provided by Dr. Benita Katzenellenbogen, were maintained in MEM Eagle medium containing Hanks' salts, L-glutamine, and non-essential amino acids (Sigma-Aldrich) supplemented with 5% bovine calf serum (CS; Sigma-Aldrich), 20 mM HEPES (pH 7.6), 100 units/mL penicillin, 100 μg/mL streptomycin, 25 μg/mL gentamycin, and 0.22 % sodium bicarbonate. Knockdown cell lines were generated by retroviral infections of parental MCF-7 cells with the shRNA expression vectors.

Retroviruses were generated by transfection of the pSUPER.retro vector described above with an expression vector for the VSV-G envelope protein into Phoenix Ampho cells using GeneJuice transfection reagent (Novagen) according to the manufacturer's protocol. The resulting viruses were collected, filtered through a 0.45 μm syringe filter to remove any remaining cells, and used to infect the parental MCF-7 cells. Stably transduced cells were isolated under appropriate selection with puromycin (Sigma-Aldrich; 0.5 μg/mL) or G418 sulfate (Gibco/BRL; 800 μg/mL) and tested for degree of knockdown by Western blotting and immunostaining analyses.

Immunofluorescence - Stable PARP-1 or PARG MCF-7 knockdown cell lines were grown on coverslips in 6-well plates for a minimum of 24 hrs. The cells were fixed in the dish with 3.7% formaldehyde solution with PBS for 20 minutes at room temperature, washed twice with PBS, and permeablized with 0.1% Triton X solution

in PBS for 20 minutes at room temperature. Cells were then washed twice with PBS and incubated with PARP-1 or PARG antibody (1:2000 – 1:5000 dilution in PBS) for 1 hour at room temperature (in the dark). After two washes with PBS, the cells were incubated with goat-α-rabbit rhodamine-conjugated secondary antibody (1:3000 dilution in PBS; Jackson) and Hoechst DNA stain (1:5000 dilution in PBS; Jackson) for 1 hour at room temperature (in the dark). Finally, the cells were washed three times with PBS and coverslips mounted onto microscope slides using Vectashield Mounting Media (Vector Laboratories). Staining was visualized using a Leica Confocal Microscope System at Cornell University's Microscope Imaging Facility.

A.4. A Complementation System for the Stable Re-expression of PARP-1 Point and Deletion Mutants in the Context of a Stable PARP-1 Knockdown

Previous studies have provided mixed results about the requirement for PARP-1's enzymatic and DNA binding activities during gene regulation. In addition, little is known about the requirement for the various functional domains of PARP-1 as it pertains to gene regulation. While the involvement of PARP-1 in transcriptional outcomes is being unveiled, the details of how PARP-1 functions at particular genes are still unknown. Questions still remain regarding the many characterized activities of PARP-1. At which genes is the catalytic activity of PARP-1 required? Does PARP-1 interact with the DNA through the DBD or protein-protein interactions through another region of the protein at particular promoters? How do post-translational modifications of PARP-1 affect its gene regulatory activities? How does the extent of PAR alter the gene expression outcome? To answer some of these questions, I devised a system to stably re-express FLAG-tagged versions of wild-type or point/deletion mutants of PARP-1 in the context of a PARP-1 knockdown cell line

using retrovirus-mediated gene transfer. By re-introducing a given PARP-1 mutant, we can further understand the mechanism of action of PARP-1 at its target genes.

A.4.1. Results and Discussion

In order to study the role of each PARP-1 domain in gene regulation, I have devised a system that allows for the exogenous expression of various PARP-1 mutants in the context of a PARP-1 stable knockdown cell line. To prevent knockdown of the re-expressed proteins in the PARP-1 MCF-7 knockdown cell lines, I generated shRNA-resistant versions of the PARP-1 wild-type and mutant cDNAs (Described in Chapter 2, Figure A.3A, and Table A.3; see Experimental Procedures). This strategy maintains a low endogenous expression of PARP-1 (shRNA is constitutively expressed), while the mutant of interest is expressed (shRNA resistant). In addition, the exogenous proteins are FLAG tagged so that their expression and localization can be monitored through the use of both protein- and FLAG-specific antibodies using various read-outs (*i.e.*, Western blotting, ChIP assay).

As shown in Figure A.3A, there are several mutants of interest that have been designed for use in this system. Each mutant obliterates an activity or domain of PARP-1, the consequences of which can be examined through various read-outs. The point mutants include: (i) a DNA binding mutant (DBDMut) that cannot bind DNA Hassa, 2001 #60; Kim, 2004 #74}; (ii) a catalytically inactive mutant (CatMut) that cannot modify target proteins Hassa, 2001 #60; Kim, 2004 #74; Marsischky, 1995 #93; Rolli, 1997 #118}; (iii) a phosphorylation mutant (PhosMut) that mimics a constitutively active PARP-1 (Kauppinen et al., 2006); and (iv) a branching mutant (BranchMut) that preferentially modifies target proteins in branched PAR formation, rather than linear (Rolli et al., 1997). All of these point mutants have been created and

Table A.3. Summary of PARP-1 point and deletion mutants designed for re-expression in PARP-1 KD cells (RNAi-resistant).

Mutant	Size (kDa)	pET19b[a]	pCMV5[b]	Express in Cells?[c]	pQCXIH[d]	Express in Cells?[e]
Wt	116	Yes	Yes	Yes	Yes	Yes
DBDMut	116	Yes	Yes	Yes	Yes	Yes
CatMut	116	Yes	Yes	Yes	Yes	Yes
PhosMut[f]	116	Yes (dbl)	Yes	Yes	Yes (sgl)	n/t[g]
BranchMut	116	Yes (RK)	Yes	Yes	Yes	n/t
ΔDBD	93	Yes	Yes	Yes	Yes	Yes
ΔBRCT	100	Yes	Yes	Yes	Yes	No[h]
ΔCAT	72	Yes	Yes	Yes	Yes	Yes
ΔNBD	85	Yes	Yes	Yes	Yes	Yes[i]
DBD-NBD	69	Yes	Yes	Yes	Yes	No[h]

[a] Most pET19b constructs were designed and cloned by D.A.W. and M.Y.K., with the exception of PhosMut and ΔDBD (K.M.F.), and BranchMut (R.K.).

[b] Mutants were cloned into the pCMV5 mammalian expression vector in both normal and RNAi-resistant forms.

[c] pCMV5 expression was tested in transient transfection/Western blot experiments using PARP-1 and FLAG antibodies in 293T cells, MCF-7 parental, Luc KD, or PARP-1 KD cells (in some cases, more than one cell type).

[d] Mutants were cloned into the pQCXIH retroviral expression vector in the RNAi-resistant form only.

[e] pQCXIH expression was tested by retroviral infection followed by hygromycin drug selection/Western blot experiments using PARP-1 and FLAG antibodies in MCF-7 Luc KD, PARP-1 cells, or both.

[f] PhosMut exists in two forms, a double mutant (dbl) or a single mutant (sgl). Only the double mutant was cloned into pET19b; both were cloned into pCMV5, and only the single mutant was cloned into pQCXIH.

[g] Mutant not tested (n/t) for expression in any cell line.

[h] ΔBRCT and DBD-NBD mutants were generally not detected as stably re-expressed in PARP-1 KD cells, although faint signals could be detected at early time points.

[i] ΔNBD mutant was detected as stably re-expressed in PARP-1 KD cells (population) but was lost over time; while stable re-expression in PARP-1 KD cells (clonal) was not detected after drug selection (Figure A.3)

Figure A.3. Stable re-expression of human PARP-1 point and deletion mutants in PARP-1 knockdown MCF-7 cells. *A,* Schematic diagram of the human PARP-1 structural and functional domains and various point and deletion mutants. The DNA binding domain (DBD), zinc fingers (Zn Fingers), nuclear localization signal (NLS), third zinc binding domain (Zn3), automodification domain (AMD), and PARP "signature" motif are also shown. Open triangles indicate the location of the 21-nucleotide shRNA recognition sequences used for knockdown. Filled circles indicate the location of the silent point mutations engineered into the cDNAs to make them resistant to the shRNAs in order to re-express them in the context of a PARP-1 knockdown. The open circle indicates the location of the various point mutations indicated. *B,* FLAG-tagged RNAi-resistant wild type and mutants described in panel A were stably re-expressed in MCF-7 PARP-1 knockdown cell lines. Re-expression was confirmed by Western blotting for PARP-1 and FLAG. An empty vector was used as a control (Empty) in both Luc and PARP-1 knockdown cell lines. Two deletion mutants, ΔBRCT and DBD-NBD, did not express in PARP-1 knockdown cells, although they were confirmed for the ability to express in another cell line. *C,* To combat differential levels of re-expression, deletion mutants were re-expressed in clonally selected PARP-1 KD cell lines. While the levels of re-expression were similar among wild type or mutant constructs, not all mutants expressed as they did in the population background (*i.e.*, ΔNBD). *Wt, wild type; DBDMut, inactive DNA binding; CatMut, catalytically inactive; PhosMut, mimics phosphorylated residues, increasing activity; BranchMut, increases branching frequency; Luc, luciferase*.

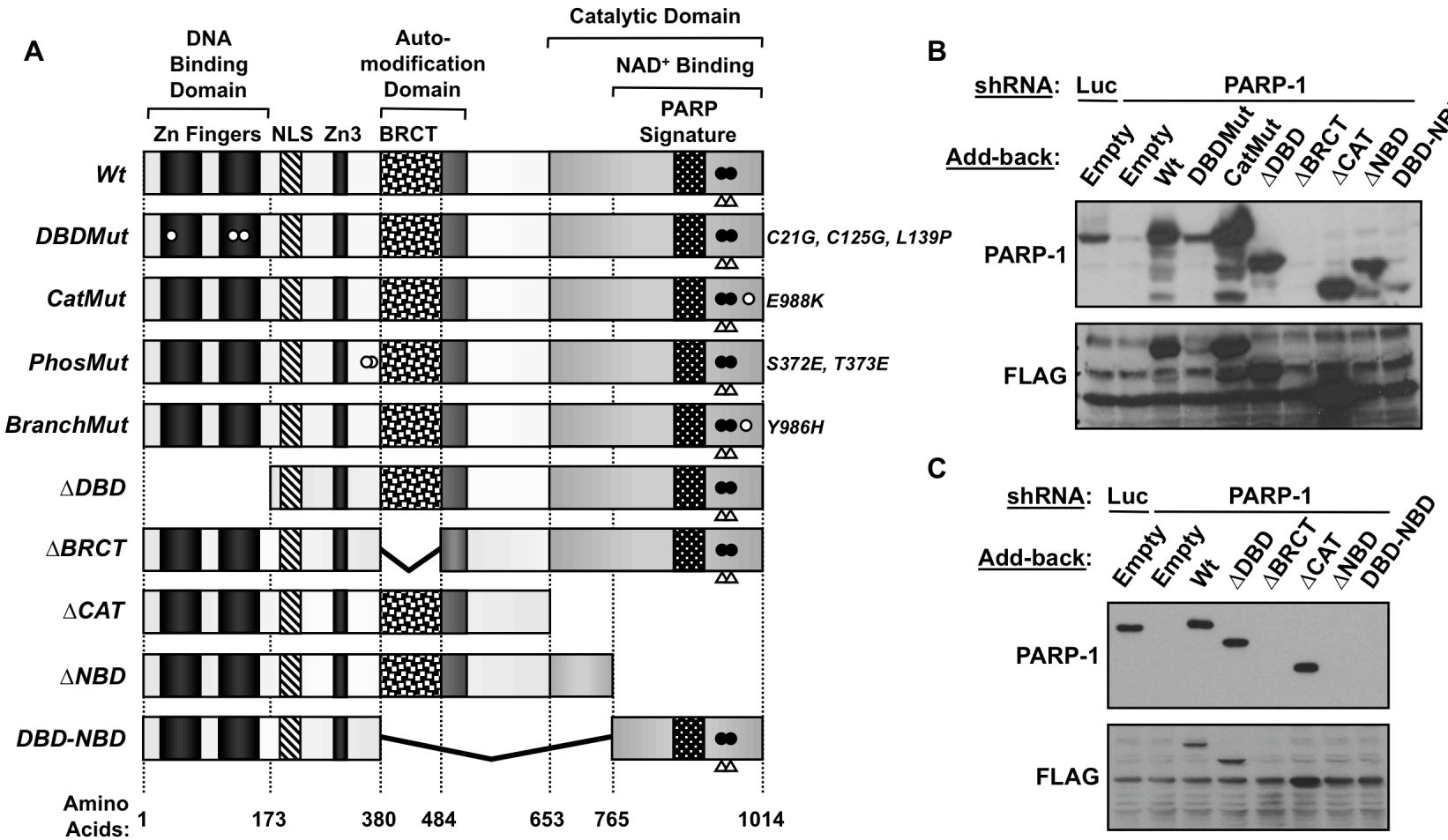
A
DNA Binding Domain
Auto-modification Domain
Catalytic Domain
NAD+ Binding
PARP Signature
Zn Fingers
NLS
Zn3
BRCT
Wt
DBDMut
C21G, C125G, L139P
CatMut
E988K
PhosMut
S372E, T373E
BranchMut
Y986H
ΔDBD
ΔBRCT
ΔCAT
ΔNBD
DBD-NBD
Amino Acids:
1
173
380
484
653
765
1014
B
shRNA:
Luc
PARP-1
Add-back:
Empty
Empty
Wt
DBDMut
CatMut
ΔDBD
ΔBRCT
ΔCAT
ΔNBD
DBD-NBD
PARP-1
FLAG
C
shRNA:
Luc
PARP-1
Add-back:
Empty
Empty
Wt
ΔDBD
ΔBRCT
ΔCAT
ΔNBD
DBD-NBD
PARP-1
FLAG

characterized in some form in previous reports. In addition to the point mutants, there are several deletion mutants, many of which also have been previously created and characterized with respect to chromatin compaction (Wacker et al., 2007). They include: (i) ΔDBD that is missing the zinc finger DNA binding region; (ii) ΔBRCT that is missing the central BRCT motif; (iii) ΔCAT that is missing the C-terminal catalytic domain; (iv) ΔNBD that is missing the NAD^+-binding region only; and (v) DBD-NBD fusion that is missing the central AMD and part of the catalytic domain.

Upon cloning the wild-type (Wt) and each mutant into the retroviral mammalian expression vector, they were introduced into the PARP-1 knockdown cell line and compared to the Luc KD control. An empty vector was used as a control for proper drug selection. Using the Luc and PARP-1 KD cell lines described in Chapter 2, some of the mutants were successfully expressed at the expected molecular weight (Figure A.3B) after retrovirus-mediated gene transfer and drug selection. However, the level of re-expression was vastly different across the panel (*i.e.*, compare Wt and DBDMut). This was likely due to a number of reasons, including differential infection rates and level of expression in each cell. In fact, initial screening of PARP-1 mutant expression via immunofluorescence suggested that only a handful of cells were expressing the mutants (data not shown). In addition, this panel of stable cell lines seemingly lost exogenous protein expression over time.

To combat some of these problems, I first clonally selected the Luc and PARP-1 KD cell lines. After screening a number of clones, I selected a single clone for each Luc and PARP-1 KD that resembled the original population for level of knockdown at the mRNA and protein level, as well as a similar profile for PARP-1-regulated genes (data not shown). Subsequently, I re-introduced the panel of mutants by retrovirus-mediated gene transfer and drug selection. This approach allowed for the same PARP-1 KD "background" for each mutant and significantly helped maintain equal

expression levels (Figure A.3C). The Wt, ΔDBD, and ΔCAT expressed well, while ΔBRCT, ΔNBD, and DBD-NBD did not, even though they were tested for ability to express in transient transfection/Western blot assay (data not shown). This could be due to several reasons, including protein mis-folding or poor integration site. Follow-up studies are necessary to determine why these particular mutants do not express. Notably, other than Wt and CatMut, no other re-expressed mutant cell line was analyzed for NAD^+ and PAR levels, as described in Chapter 2.

Initial experiments were conducted to determine the effect of ΔDBD and ΔCAT on gene expression. However, for the panel of genes tested, only a few restored gene expression levels to that of the Luc control upon Wt re-expression. In addition, there were no visible differences in gene regulatory patterns between the Wt and mutants as would be expected, given previous reports (data not shown). Furthermore, while Wt and CatMut proteins were detected at target gene promoters by ChIP assay (Krishnakumar and Kraus, 2010), these newly developed cell lines did not show detectable exogenous PARP-1 proteins (Wt or mutant) at target gene promoters (data not shown). Together, these results indicate in depth technical problems that need to be resolved in order to use this complementation system to its full potential.

A.4.2. Experimental Procedures

Antibodies - The custom rabbit polyclonal antibody against PARP-1 used for Western blotting was generated by using a purified fragment of human PARP-1 (amino-terminal, PARP-N (Kim et al., 2004)) (Pocono Rabbit Farm and Laboratory, Inc.). The mouse monoclonal FLAG antibody used for Western blotting was purchased from Sigma-Aldrich (F3165).

Oligonucleotides **-** The sequences listed below were used for site-directed mutagenesis to generate point mutants and RNAi-resistant hPARP-1 cDNAs:

PhosMut -

1. Double Mutant (Dbl; S372E, T373E)

5’ - ccacgcctccgcccgaagaagcctcggctcctgc - 3’ and

5’ - gcaggagccgaggcttcttcgggcggaggcgtgg - 3’

Specific changes relative to the first nucleotide of the first codon:

t1114g, c1115a, c1116a, a1117g, c1118a

2. Single Mutant (Sgl; T373E)

5’ - ccacgcctccgcccgaagaagcctcggctcctgc - 3’ and

5’ - gcaggagccgaggcttcttcgggcggaggcgtgg - 3’

Specific changes relative to the first nucleotide of the first codon:

a1117g, c1118a

BranchMut -

5’ - gacacgtcgctgctgcataacgagtacattgtc - 3’ and

5’ - gacaatgtactcgttatgcagcagcgacgtgtc - 3’

Specific changes relative to the first nucleotide of the first codon:

t2956c

RNAi-resistant hPARP-1 cDNAs –

1. Recognition site #1 (Wt and CatMut)

5’ - caggttacccaagggcaaacatagcgttaaaggtttgggcaaaac - 3’ and

5’ - gttttgcccaaaccttt aacgctatgtttgcccttgggtaacctg - 3’

Specific changes relative to the first nucleotide of the first codon:

g2835a, c2838t, t2841c, c2844t

2. Recognition site #2 (Wt)

5’ - ctggtgtgaatgacacgtcgctgctgtataacgagtacattgtc - 3’ and

5’ - gacaatgtactcgttatacagcagcgacgtgtcattcacaccag - 3’

Specific changes relative to the first nucleotide of the first codon:

c2946g, t2949g, a2952g, a2955g

3. Recognition site #2 (CatMut)

5’ - ctggtgtgaatgacacgtcgctgctgtataacaagtacattgtc - 3’ and

5’ - gacaatgtacttgttatacagcagcgacgtgtcattcacaccag - 3’

Specific changes relative to the first nucleotide of the first codon:

c2946g, t2949g, a2952g, a2955g

PARP-1 expression constructs - Wild-type and point/deletion mutants of human PARP-1 were used in the studies described herein. The DNA binding point mutant (DBDMut) contained changes at Cys 21 to Gly (C21G), Cys 125 to Gly (C125G), and Leu 139 to Pro (L21P) (Hassa et al., 2001; Kim et al., 2004). The catalytically inactive point mutant (CatMut) contained a change at Glu 988 to Lys (E988K) (Hassa et al., 2001; Kim et al., 2004; Marsischky et al., 1995; Rolli et al., 1997). The phosphorylation mimic point mutant (PhosMut) contained changes at Ser 372 to Glu (S372E) and Thr 373 to Glu (T373E) (Kauppinen et al., 2006). The branching point mutant (BranchMut) contained a change at Tyr 986 to His (Y986H) (Rolli et al., 1997). The CMV-based mammalian expression constructs for full length wild-type,

ΔDBD, ΔBRCT, ΔCAT, ΔNBD, and DBD-NBD deletion mutants were generated by PCR-based cloning of the tagged cDNAs (a carboxyl-terminal 6xHis/FLAG tag) into pCMV5. The pCMV5-hPARP-1-His/FLAG and pET19b-hPARP-1 wild-type vectors were used simultaneously as templates to generate the PhosMut and BranchMut point mutants by site-directed mutagenesis (QuikChange® Site-Directed Mutagenesis Kit from Stratagene) in both bacterial and mammalian expression vectors.

The pCMV5-hPARP-1-His/FLAG vectors were then used as templates to generate cDNAs resistant to the shRNAs (described in Chapter 2 and Appendix A.3) by site-directed mutagenesis (QuikChange® Site-Directed Mutagenesis Kit from Stratagene). The following nucleotides relative to the first nucleotide of the first codon were changed in the hPARP-1 cDNA: g2835a, c2838t, t2841c, c2844t (for shRNA#1) and c2946g, t2949g, a2952g, a2955g (for shRNA#2). Positive clones were identified by sequencing and then cloned into the pQCXIH retroviral expression vector (BD Biosciences; hygromycin resistant) using NotI and BamHI restriction sites.

Generation and culture of MCF-7-derived cell lines - Parental MCF-7 human breast cancer cells, kindly provided by Dr. Benita Katzenellenbogen, were maintained in MEM Eagle medium containing Hanks' salts, L-glutamine, and non-essential amino acids (Sigma-Aldrich) supplemented with 5% bovine calf serum (CS; Sigma-Aldrich), 20 mM HEPES (pH 7.6), 100 units/mL penicillin, 100 μg/mL streptomycin, 25 μg/mL gentamycin, and 0.22 % sodium bicarbonate. The shRNA knockdown + shRNA-resistant re-expression ("knockdown/add-back") cell lines used in these studies were generated by sequential retroviral infections of parental MCF-7 cells with the appropriate shRNA and cDNA expression vectors (see below). The Luc and PARP-1 knockdown cells, expressing two distinct shRNA sequences targeting the intended factor (described ini Chapter 2), were either used as a population or clonally selected.

Retroviruses were generated by transfection of the pSUPER.retro or pQCXIH vectors described above with an expression vector for the VSV-G envelope protein into Phoenix Ampho cells using GeneJuice transfection reagent (Novagen) according to the manufacturer's protocol. The resulting viruses were collected, filtered through a 0.45 μm syringe filter to remove any remaining cells, and used to infect the parental MCF-7 cells. Stably transduced cells were isolated under appropriate selection with puromycin (Sigma-Aldrich; 0.5 μg/mL), G418 sulfate (Gibco/BRL; 800 μg/mL), or hygromycin (Cellgro; 200 μg/mL), expanded, and frozen in aliquots for future use.

A.5. Tet-inducible Depletion of PARP-1 (Tet-On)

While a stable shRNA-mediated knockdown of PARP-1 has yielded interesting facets regarding the role of PARP-1 in gene regulation, there are certain drawbacks that are unavoidable with such a system. Primarily, constitutive expression of a PARP-1 shRNA over time can lead to adjustments within the cell that may not be directly attributable to the knockdown of PARP-1. In other words, there is no way to distinguish immediate early effects versus long-term compensatory effects upon PARP-1 knockdown. For this reason, and others, I developed a stable, tet-inducible knockdown system for PARP-1. This system allows for the stable integration of a PARP-1 shRNA sequence (much like described in Chapter 2 and Appendix A.2), the expression of which is controllable by doxycycline. Therefore, a time component of PARP-1 knockdown can be incorporated, yielded further information about the mechanisms of action of PARP-1 in gene regulation. This system has unveiled unique aspects of PARP-1 that were hypothesized from previous reports from our lab and others. That is, (i) chromatin-bound PARP-1 is not rapidly turned over, and (ii) the level of PARP-1 depletion at promoters is directly linked to gene regulation.

A.5.1. Results and Discussion

Previous reports from our lab used a stable, retrovirus-mediated shRNA expression cell line to deplete PARP-1 and determine the consequences as it pertains to gene regulation (Frizzell et al., 2009; Krishnakumar et al., 2008; Krishnakumar and Kraus, 2010). Unlike other knockdown systems (*i.e.*, siRNA transfection), the stable knockdown is constitutively expressed and maintained over several passages. Every effort is made to conduct experiments at the earliest time points of shRNA expression as possible using this system. However, upon several passages, the immediate early effects of PARP-1 knockdown cannot be distinguished from secondary, tertiary, or further downstream effects. How does the cell compensate for such dramatic reductions in PARP-1? Are the changes in gene regulation attributable to promoter-bound PARP-1 directly or through downstream mechanisms?

To combat this issue, I developed a stable, tet-inducible knockdown cell line for PARP-1. To generate this "Tet-on" system, two independent steps were necessary. First, parental MCF-7 cells were stably transfected with a cDNA for the Tet repressor (TetR) protein and clonally selected (Nasun Hah). Stable transfectants were expanded and tested for TetR expression by Western blotting (Figure A.4A). The resulting cell lines are terms "MCF-7 TetR". Importantly, TetR expression does not alter the endogenous levels of PARP-1, or the estrogen receptor α (ERα), an important transcription factor in the biology of MCF-7 cells. In fact, TetR expression does not alter the ability of MCF-7 TetR cells to respond to a signal, such as estrogen, as shown by profiling standard estrogen-responsive genes by RT-qPCR (Figure A.4B).

The activity of the TetR in the cells was tested by transient transfection and luciferase reporter gene assay (Figure A.4C). Here, a luciferase reporter lies downstream of a pCMV promoter harboring two Tet operon (TO) sequences. In the

absence of doxycyline (dox), the TetR would bind the TO sequences and repress the expression of the luciferase reporter, while the addition of dox would bind and sequester the TetR away from the promoter, allowing for the transcription of the luciferase reporter. Upon transfection of the reporter and subsequent dox treatment (see Experimental Procedures), the activity of luciferase was measured in the cell extracts of various MCF-7 TetR clones. Only those clones that expressed the TetR protein showed tet-responsive activity, however, to varying degrees. Therefore, the inducible knockdown cell lines were generated using MCF-7 TetR clone #3, which displayed the highest TetR expression level and activity. For the second step, a dox-responsive Luc or PARP-1 shRNA was introduced into the MCF-7 TetR cell line, resulting in inducible knockdown cell lines, Luc_i and PARP-1_i.

The cells were treated with or without dox and tested for cellular PARP-1 levels by Western blot analysis (Figure A.4D) and PARP-1 mRNA levels by RT-qPCR (Figure A.4E). Total PARP-1 protein and mRNA levels were significantly reduced after 4 days of dox treatment, as compared to the Luc_i control. Notably, PARP-1 mRNA levels are slightly reduced in the absence of dox (*i.e.*, baseline), which is likely due to the "leakiness" of the system, however protein levels remain high.

Given the level of reduction at 4 days of dox treatment, I hypothesized that PARP-1-dependent gene regulation would also be evident at that time. I examined the expression levels of previously identified PARP-1 target genes (Frizzell et al., 2009) using the Luc_i and PARP-1_i cell lines by RT-qPCR over a time course of dox treatment. My analyses showed that no target genes were regulated at early dox time points (*i.e.*, 4 days) when total PARP-1 levels are maximally reduced. However, as dox treatment time was extended out to 12 days, evidence of PARP-1-dependent gene regulation was evident (Figure A.5A). In fact, as time of dox treatment progressed, the percentage of regulated genes increased (data not shown). Concurrent with this,

Figure A.4. Generation of stable MCF-7 inducible PARP-1 knockdown cell line. *A, and B,* The Tet repressor protein (TetR) is stably expressed and active in MCF-7 cells. Parental MCF-7 cells were stably transfected with a TetR expression cDNA and clonally selected using hygromycin. Whole cell extracts were isolated from individual clones and monitored for TetR protein levels by Western blotting (A) and TetR activity using a doxycycline (dox)-inducible luciferase reporter assay (B). TetR expression has no effect on total cellular PARP-1 levels; ERα was also monitored as a loading control. Only the clones showing detectable TetR protein in panel A (*i.e.*, clones 1, 3, and 4) showed dox-inducible luciferase expression and activity, indicating an active TetR protein. MCF-7 TetR clones 3 and 4 were used in future experiments, as they displayed the highest activity. *C,* TetR expression does not disrupt signal-mediated gene expression patterns. Total RNA was isolated from vehicle (U) or estrogen-treated (E) MCF-7 TetR cells, reverse transcribed, and subjected to qPCR using gene-specific primers. Each bar represents the mean + SEM (*error bars*) from two independent determinations. *D and E,* Dox-inducible shRNA-mediated depletion of PARP-1 in MCF-7 cells. Dox-inducible shRNA constructs were stably transduced into MCF-7 TetR cells by retroviral infection. PARP-1 protein (D) and mRNA (E) levels were monitored upon treatment with dox up to 15 days, using methods previously described. Both PARP-1 protein and mRNA levels were reduced at least 90% in as early as 4 days of dox treatment, as compared to an shRNA targeting luciferase. Subsequent experiments used only shRNA #1, as it yielded faster and more effective knockdown of PARP-1. *Luc, luciferase; i, inducible; dox, doxycycline; TetR, tet repressor; TO, tet operon.*

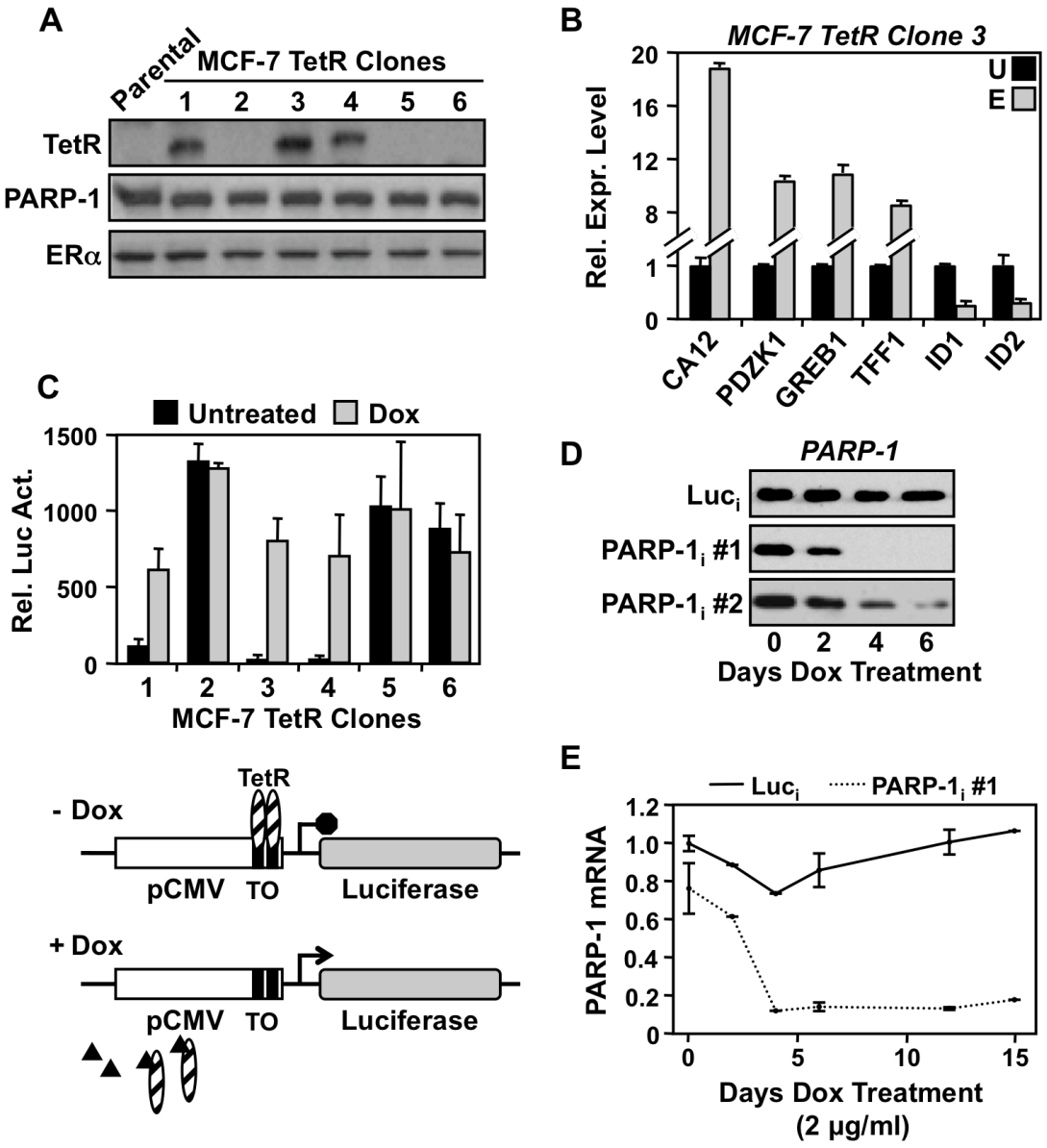
A
Parental
MCF-7 TetR Clones
1 2 3 4 5 6
TetR
PARP-1
ERα
B
MCF-7 TetR Clone 3
U
E
Rel. Expr. Level
20
16
12
8
1
0
CA12
PDZK1
GREB1
TFF1
ID1
ID2
C
Untreated
Dox
Rel. Luc Act.
1500
1000
500
0
1 2 3 4 5 6
MCF-7 TetR Clones
TetR
- Dox
pCMV
TO
Luciferase
+ Dox
pCMV
TO
Luciferase
D
PARP-1
Luc$_i$
PARP-1$_i$ #1
PARP-1$_i$ #2
0 2 4 6
Days Dox Treatment
E
Luc$_i$
PARP-1$_i$ #1
PARP-1 mRNA
1.2
1.0
0.8
0.6
0.4
0.2
0
0 5 10 15
Days Dox Treatment
(2 μg/ml)

Figure A.5. Levels of chromatin-associated PARP-1 reflect PARP-1-dependent changes in gene expression. *A*, PARP-1-dependent changes in gene expression are evident at a minimum six days shRNA induction by doxycycline (dox). Total RNA was isolated from Luc_i and PARP-1_i knockdown cells at various time point of dox treatment. The RNA was reverse transcribed and subjected to qPCR using gene-specific primers. GDF15 and PFDN1 were previously shown to be regulated by PARP-1 in MCF-7 cells by constitutive shRNA expression (Figure 2.5). *B*, Box plot of PARP-1 ChIP signals after shRNA induction by dox. The promoter occupancy of PARP-1 was examined by ChIP analyses. The box plot represents the collective data from 15 PARP-1 target gene promoters. A reduction of PARP-1 on the chromatin is significantly reduced about 50% after 12 days of dox treatment compared to the Luc_i control. Significance was determined using a Studen't t-test with a p-value threshold of < 0.01 and is denoted by an asterisk (*). However, some promoters show a slight reduction at six days, reflective of gene regulation at the same time point.

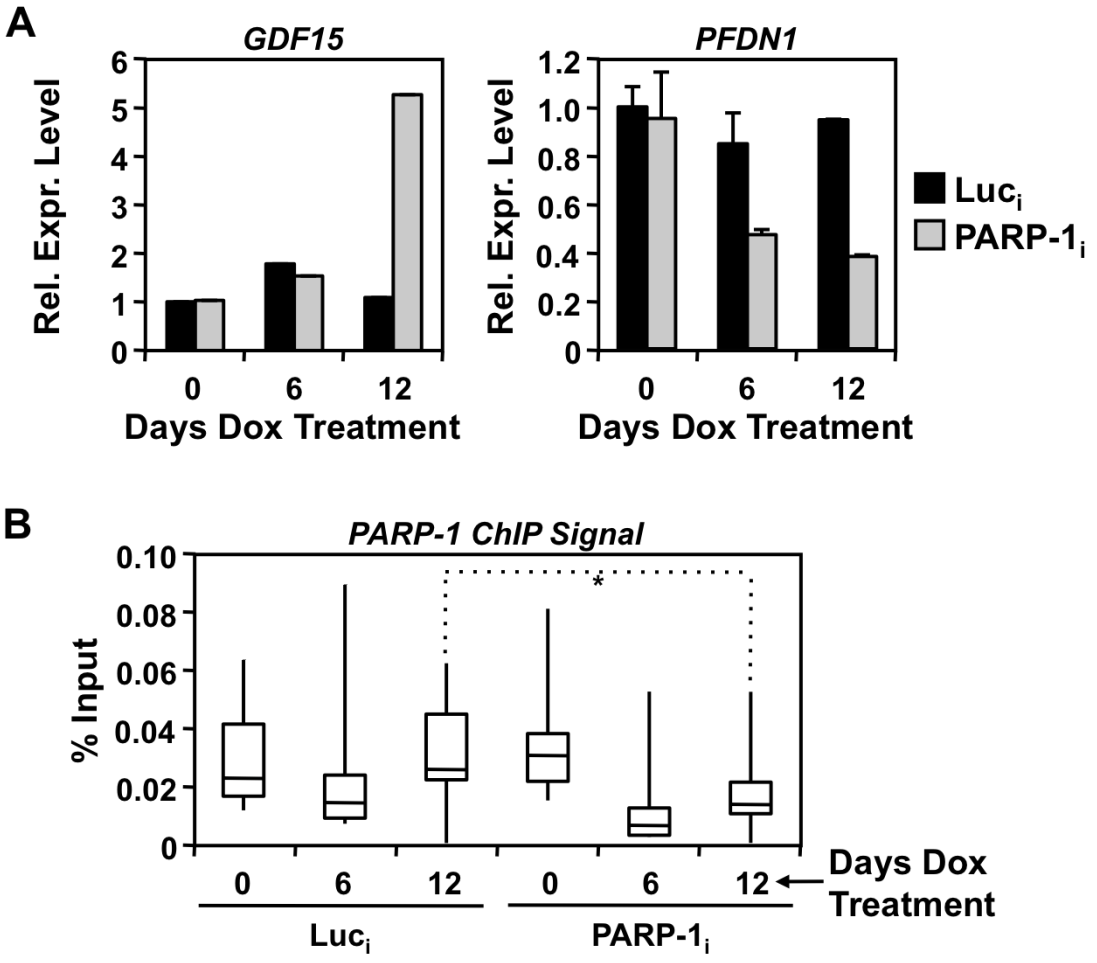
A
GDF15
PFDN1
Rel. Expr. Level
Days Dox Treatment
Luc$_i$
PARP-1$_i$
B
PARP-1 ChIP Signal
% Input
Days Dox Treatment
Luc$_i$
PARP-1$_i$

analysis of PARP-1 levels at target gene promoters by ChIP assay showed little change in PARP-1 promoter occupancy at early time points, while later time points showed reductions in PARP-1 occupancy, albeit to varying degrees (Figure A.5B). Overall, my results suggest that (i) chromatin-bound PARP-1 is not rapidly turned over, as is the case for non-chromatin-bound PARP-1, and (ii) the level of PARP-1 depletion at promoters is likely directly linked to gene regulation. However, further analysis is required to conclusively demonstrate this result in the most stringent way.

A.5.2. Experimental Procedures

Antibodies - The custom rabbit polyclonal antibody against PARP-1 used for Western blotting and ChIP assays was generated by using a purified fragment of human PARP-1 (amino-terminal, PARP-N (Kim et al., 2004)) (Pocono Rabbit Farm and Laboratory, Inc.). The custom rabbit polyclonal antibody against ERα used for Western blotting was generated using a purified fragment of human ERα (Pocono Rabbit Farm and Laboratory, Inc.) (Kim et al., 2006). The rabbit polyclonal antibody against the Tet repressor (TetR) was purchased from Abcam (ab14075).

Luciferase reporter assay – MCF-7 TetR clones were seeded at ~1.5 x 10^5 cells per well in 6-well plates and grown for 24 hrs. The cells were transfected with 800 ng pCMV-driven luciferase reporter harboring two Tet operon binding sites (pcDNA4/TO; kindly provided by H. Th. Marc Timmers) and 400 ng pCMV-β-galactosidase expression vector (used for normalization) using GeneJuice transfection reagent (Novagen) according to the manufacturer's protocol. The following day (24 hrs), cells were treated with or without doxycycliine (Sigma-Aldrich; 2 μg/mL) for an additional 24 hours. The cells were collected and lysed in ProMega 5X Lysis Buffer,

and the supernatant was collected by centrifugation. Luciferase and β-galactosidase assays were performed in parallel essentially as previously described (Kim et al., 2006). Luciferase and β-galactosidase activities were measured in extracts using a 96-well plate luminometer (LD400; Beckman Coulter). The assays were conducted twice with independent transfections to ensure reproducibility.

Oligonucleotides **-** The oligonucleotide sequences listed below were used for the shRNA constructs. Those sequences denoted with an asterisk (*) were chosen based on priority score described at the website.

Target	Sequence	Source
Luc	5' - gatatgggctgaatacaaa - 3'	(Reynolds et al., 2004)
hPARP-1 #1	5' - gggcaagcacagtgtcaaa - 3'	(Ju et al., 2004; Shah et al., 2005)
hPARP-1 #2*	5' - acacctctctactatataa - 3'	Dharmacon siDESIGN® Center

Luc_i and PARP-1_i inducible knockdown constructs **-** For the "Tet-on" inducible knockdown constructs (Luc_i and PARP-1_i), the pSUPER.retro vector (puromycin resistant) was first modified by replacing the H1 promoter with one harboring a Tet operator sequence (from the pTER+ modified vector, kindly provided by H. Th. Marc Timmers (van de Wetering et al., 2003)) using BglII and EcoRI restriction sites. The resulting vector is termed pSUPER.retro.TO (Tet operon). Double stranded oligonucleotides sequences targeting either luciferase (Luc) or PARP-1 were cloned into the pSUPER.retro.TO (puromycin resistant) vector using BglII and XhoI restriction sites, as described by the manufacturer and confirmed by sequencing.

Generation, culture, and treatments of MCF-7-derived cell lines - Parental MCF-7 human breast cancer cells, kindly provided by Dr. Benita Katzenellenbogen, were maintained in MEM Eagle medium containing Hanks' salts, L-glutamine, and non-essential amino acids (Sigma-Aldrich) supplemented with 5% bovine calf serum (CS; Sigma-Aldrich), 20 mM HEPES (pH 7.6), 100 units/mL penicillin, 100 μg/mL streptomycin, 25 μg/mL gentamycin, and 0.22 % sodium bicarbonate.

For the "Tet-on" inducible knockdown system, parental MCF-7 cells were stably transfected with a Tet Repressor (TetR) cDNA (pcDNA6/TR; kindly provided by H. Th. Marc Timmers). Stable transfectants were clonally selected using hygromycin (200 μg/mL), expanded, and tested for TetR expression and activity by Western blotting and transient transfection/luciferase reporter gene assay, respectively. The resulting cell line, termed MCF-7 TetR, was maintained under similar conditions as described above, with the exception of the serum (5% Tet-approved FBS (Tet FBS); Clonetech) to reduce background shRNA expression in the absence of doxycycline. MCF-7 TetR cells clone #3 and #4 were used to make the Luc_i and PARP-1_i knockdown cell lines by retroviral infection with the appropriate shRNA vectors. However, experiments were only conducted with MCF-7 Clone #3.

Retroviruses were generated by transfection of the pSUPER.retro.TO vectors described above with an expression vector for the VSV-G envelope protein into Phoenix Ampho cells using GeneJuice transfection reagent (Novagen) according to the manufacturer's protocol. The resulting viruses were collected, filtered through a 0.45 μm syringe filter to remove any remaining cells, and used to infect MCF-7 TetR cells. Stably transduced cells were isolated under appropriate selection with puromycin (Sigma-Aldrich; 0.5 μg/mL), expanded, and frozen in aliquots for future use. Luc_i and PARP-1_i knockdown cell lines were maintained as noted above and

treated with doxycycline (Sigma-Aldrich; 2 μg/mL) to induce the shRNA expression for a minimum of 2 days (expression analyses) and 6 days (ChIP analyses).

mRNA expression analyses by RT-qPCR - For gene-specific mRNA expression analyses, cells were treated with or without dox for the time points noted in the figure legends, or with vehicle or 17β-estradiol (E2; 100 nM) for 3 hrs. Total RNA was isolated using Trizol Reagent (Invitrogen), reverse transcribed, and subjected to real-time quantitative PCR using gene specific primers. All target gene transcripts were normalized to the β-actin transcript, which was unaffected by PARP-1 knockdown (data not shown). All experiments were conducted a minimum of two times with independent RNA isolations to ensure reproducibility.

Chromatin immunoprecipitation assays - ChIP assays were performed essentially as described previously (Krishnakumar et al., 2008). The immunoprecipitations were performed from crosslinked Luc_i and PARP-1_i knockdown MCF-7 cells with antibodies against PARP-1, using "no antibody" as a control. The resulting input and ChIP DNA material were used for gene-specific ChIP-qPCR analyses.

Quantitative PCR analyses (RT-qPCR and ChIP-qPCR) - Gene-specific mRNA expression and ChIP analyses were analyzed by quantitative PCR in a similar manner. Briefly, reactions containing DNA from either source, 1x SYBR Green PCR master mix, and forward and reverse primers (500 nM) were used in 40-45 cycles of amplification (95°C for 15 sec, 60°C for 1 min) using a Roche LightCycler® 480 System (384-well) following an initial 3 min incubation at 95°C. Melting curve analysis was performed to ensure that only the targeted amplicon was amplified.

Primer Sequences – The primer sequences listed below were used for both RT-qPCR and ChIP-qPCR amplification reactions.

RT-qPCR –

Gene Name	**Primer Sequence**
β-ACTIN forward	5'-AGCTACGAGCTGCCTGAC-3'
β-ACTIN reverse	5'-AAGGTAGTTTCGTGGATGC-3'
CA12 forward	5'-CACTGCCAGCAACAAGTC-3'
CA12 reverse	5'-ACATGTTGAAGGTGACTGAAG-3'
GDF15 forward	5'-CTACAATCCCATGGTGCTCA-3'
GDF15 reverse	5'-TATGCAGTGGCAGTCTTTGG-3'
GREB1 forward	5'-GCCGTTGACAAGAGGTTC-3'
GREB1 reverse	5'-GGGTTGAGTGGTCAGTTTC-3'
ID1 forward	5'- CCGTTCGGGCCTCAAT-3'
ID1 reverse	5'-TTTTTCCCATATTCACTTTCTCACTTC-3'
ID2 forward	5'-TATTGTCAGCCTGCATCACC-3'
ID2 reverse	5'-AATTCAGAAGCCTGCAAGGA-3'
PFDN1 forward	5'-TGCCTTCTCCCATACATTCC-3'
PFDN1 reverse	5'-CAGGATTATGGCGTCCATCT-3'
PARP1 forward	5'-GTGTGGGAAGACCAAAGGAA-3'
PARP1 reverse	5'-TTCAAGAGCTCCCATGTTCA-3'
PDZK1 forward	5'-CCTCAGTGATTGAGGATACTCCTGTA-3'
PDZK1 reverse	5'-CAACCCCCAATCCTGTTAGGAT-3'
TFF1 forward	5'-TGCTTCTATCCTAATACCATCG-3'
TFF1 reverse	5'-AGATCCCTGCAGAAGTGTC-3'

ChIP-qPCR –

Gene Name	**Primer Sequence**
ABHD2 forward	5’-GCCTCCACTCTGAGGAACAG-3’
ABHD2 reverse	5’-TTGTTCATTGGGCAGTTCAG-3’
ASCL1 forward	5’-CAAGAGAGCGCAGCCTTAGT-3’
ASCL1 reverse	5’-GCAAAAGTCAGTGCTGAACG-3’
GDF15 forward	5’-CTCAGATGCTCCTGGTGTTG-3’
GDF15 reverse	5’-CTCGGAATCTGGAGTCTTCG-3’
GREB1 forward	5’-TGGGATTTTACCTCAAAGTGC-3’
GREB1 reverse	5’-AGGTCCTCAAGAGCTGCAAG-3’
ID1 forward	5’-TCCGTTCGGGCCTCAAT-3’
ID1 reverse	5’-TTTTTCCCATATTCACTTTCTCACTTC-3’
ITPR1 forward	5’-ACTGAGGTCGCGGTTTGTAT-3’
ITPR1 reverse	5’-AAGGAGCCGTGTTGTGACTT-3’
LGALS3BP forward	5’-GGGCACCCCTCTCTCTACAC-3’
LGALS3BP reverse	5’-TGATTGTTGCTGGACTCAGG-3’
NAT1 forward	5’-CCGGCTGAAATAACCTGGTA-3’
NAT1 reverse	5’-TATGTGCCAGCCACACTTTC-3’
NELL2 forward	5’-TCCCCGGAGGAGCAGTCT-3’
NELL2 reverse	5’-CGCCCGAACCTGTTGTAAAG-3’
NVL forward	5’-TGCAACCAAACGGATCAATA-3’
NVL reverse	5’-TGAATTAAGTATTAGATTTCCCACTCA-3’
PVALB forward	5’-GCTCCCCTATCTGCACACTC-3’
PVALB reverse	5’-CAAAGGCTGTTTGGAAGCTC-3’
RAPGEF4 forward	5’-GTAACTCCCGACGACAGCTC-3’
RAPGEF4 reverse	5’-CTGTCACAGCCTGGAAACAA-3’

SCN1A forward	5'-ACCCTCCTCTCTCTCCTTGC-3'
SCN1A reverse	5'-GGGAGGAGGAGAAATTCGTT-3'
SOCS2 forward	5'-TTCAAGCTTTCGAGCAGTGA-3'
SOCS2 reverse	5'-CCCTTAACAATCACGGGAAA-3'
TMOD3 forward	5'-TGCCTCTCTTGGGCTTTAGA-3'
TMOD3 reverse	5'-TTGTAAAGAAGCGCACATGG-3'

A.6. Tet-inducible Over-expression of PARP-1 (Tet-Off)

PARP-1 binds to a variety of nuclear proteins and is likely a member of multiple complexes within cells. Most of the complexes were discovered under various conditions of signal-mediated transcriptional activation (*i.e.*, NF-κB; (Hassa et al., 2001; Hassa and Hottiger, 1999; Hassa and Hottiger, 2002; Kameoka et al., 2000)). The list of factors with which PARP-1 has been shown to interact includes transcription factors (*i.e.*, NF-κB, RAR), transcriptional coregulators (*i.e.*, Mediator, histone deacetylases 1,2,3), DNA repair proteins (*i.e.*, DNA Ligase III), and centromeric or telomeric proteins (*i.e.*, CENP-A). However, complexes in which PARP-1 has been identified have been isolated based on other factors, not PARP-1. To identify the composition of complexes in which PARP-1 is central, I have developed an inducible expression system in MCF-7 cells to isolate PARP-1 and identify and characterize PARP-1-interacting proteins.

A.6.1. Results and Discussion

Previous reports have identified numerous PARP-1 binding partners ranging from transcription factors to DNA repair proteins. However, the composition of

complexes in which PARP-1 is central has yet to be determined. To isolate native PARP-1 complexes from human cells, initial experiments constitutively expressed FLAG-tagged PARP-1. However, due to the toxic levels of PARP-1, stable integration and expression of PARP-1-FLAG proved unsuccessful. To get beyond this technical hurdle, I developed a stable, tet-inducible expression cell line for PARP-1. Using MCF-7 Tet-Off cell line constitutively expressing the Tet activator (commercially available), I introduced a dox-responsive expression construct for FLAG-tagged PARP-1 (Wt and CatMut) and GFP (control) by retrovirus-mediated gene transfer. In this system, the absence of dox represses transcription of the target gene, while the addition of dox induces the binding of the Tet activator to the Tet operon sequences, leading to active expression of the gene. FLAG-tagged PARP-1 was efficiently expressed after 4 days of dox treatment (Figure A.6A).

PARP-1 was immunoprecipitated from the cells after 4 days of dox treatment using FLAG affinity resin. After a series of washes, the bound proteins were eluted from the resin using the FLAG peptide as a competitor. The resulting fractions from each step of the immunoprecipitation were analyzed by Western blot using both PARP-1- and FLAG-specific antibodies (Figure A.6B). PARP-1 was only captured in the FLAG-PARP-1 expressing cell line as compared to the GFP control. In addition, endogenous PARP-1 does not bind the resin, as it is only found in the unbound fraction. The eluates were separated by SDS-PAGE and visualized by silver staining (Figure A.6C). PARP-1-specific bands were excised from the gel, trypsinized, and protein fragments were identified by mass spectrometry.

While many of the excised bands were unable to be identified due to low quantity, three proteins were successfully identified by mass spectrometry analysis (Figure A.6C). Importantly, the bait protein, PARP-1, was identified. The other two proteins were identified as NCL (nucleolin) and PRTF (polymerase I and transcript

Figure A.6. A Tet-off PARP-1 over-expression cell line reveals PARP-1 interactors. *A*, FLAG-tagged PARP-1 is only expressed in the absence of doxycycline (dox). GFP and PARP-1-FLAG cell lines, wild type (Wt) or catalytically inactive mutant (CatMut), were grown in the absence and presence of dox (2 μg/mL) for four days. Whole cell extracts were then subjected to Western blotting analysis for FLAG-tagged PARP-1. *B*, PARP-1 was immunoprecipitated (IP) from GFP and PARP-1-FLAG cell lines treated with dox (as in panel A) using FLAG-conjugated resin and eluted using FLAG peptide. Fractions at each stage of the IP were subjected to SDS-PAGE and Western blotting analysis using PARP-1- and FLAG-specific antibodies. Endogenous PARP-1 that is not FLAG-tagged is seen in the unbound (Un) fraction, relative to the input (In) or elutions (E), while FLAG-tagged PARP-1 is captured. *C*, The resulting eluates from (B) were subjected to SDS-PAGE and visualized by silver stain. PARP-1-specific protein bands were excised from the gel, trypsinized, and identified by mass spectrometry. PARP-1 (the bait) and two identified interacting proteins are shown (Nucleolin and PTRF). *D*, Description of PARP-1-interacting proteins identified in (C). For each identified protein, the gene symbol, protein name, and known cellular functions are listed.

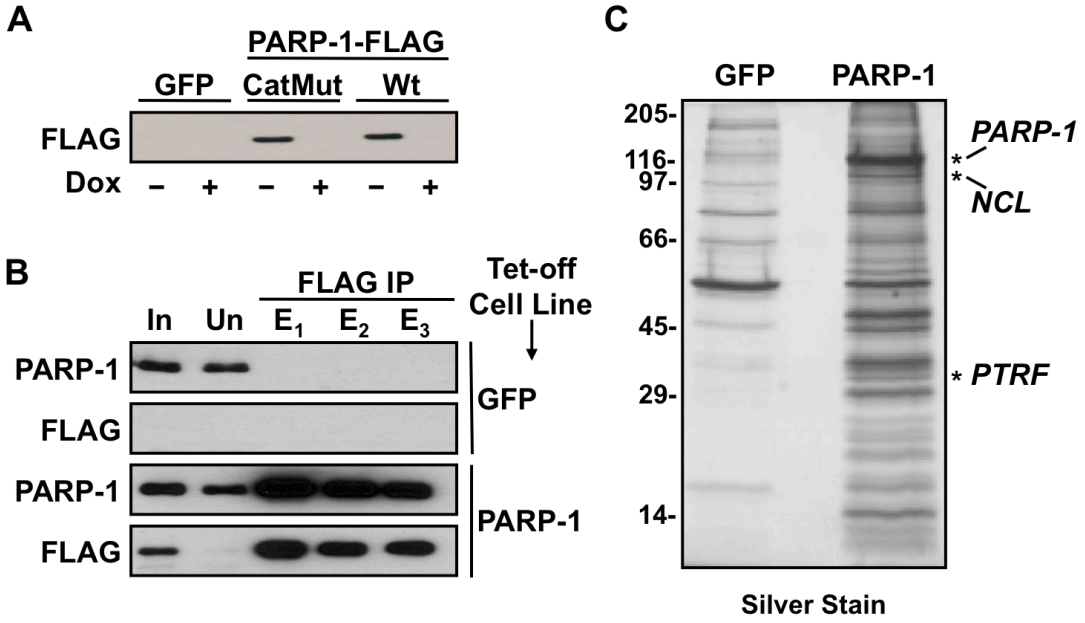

D

Gene Symbol	Protein Name	GeneCards® Accession No.[a]	Protein Function[b]
NCL	Nucleolin	GC02M232027	Involved in rDNA transcription, maturation, and ribosomal nuclear export
PTRF	Polymerase I and transcript release factor	GC17M040555	Involved in the rDNA transcription (dissociation of transcription complexes and reinitiation of polymerase I on nascent rRNA transcripts), formation of caveolae, and insulin-regulated gene expression

[a] From GeneCards®, a searchable, integrated database of human genes that
[b] Based on GeneCards® description.

release factor), both of which are involved in rDNA transcriptional processes (Figure A.6D). Notably, NCL was identified previously as a PARP-1 complex-containing protein (Ju et al., 2004). Together, these results provide a feasible system to isolate and identify PARP-1-interacting or complex components. However, additional chromatography steps are likely required in order to fully elucidate PARP-1-containing complex components. For example, glycerol gradient fractionation was applied to an attempt to separate various complexes. Although this particular method was not successful, other chromatography or gradient techniques can be applied to enhance the complex purification. In addition, verification of all identified proteins is also required to draw strong and conclusive results about interacting proteins. Furthermore, this system is applicable to all PARP-1 deletion mutants described in Appendix A.2, which can provide domain-specific and activity-dependent interactions.

A.6.2. Experimental Procedures

Antibodies - The custom rabbit polyclonal antibody against PARP-1 used for Western blotting was generated by using a purified fragment of human PARP-1 (amino-terminal, PARP-N (Kim et al., 2004)) (Pocono Rabbit Farm and Laboratory, Inc.). The mouse monoclonal antibody against FLAG used for Western blotting was purchased from Sigma-Aldrich (F3165).

PARP-1 expression constructs - Wild-type (Wt) and catalytically inactive (E988K; CatMut) human PARP-1 were used in the studies described herein. The Tet-inducible retroviral mammalian expression constructs were generated by sub-cloning the tagged cDNAs (a carboxyl-terminal 6xHis/FLAG tag) from the pCMV5 vector to the pREV-TRE vector (Clonetech) using BamHI and XbaI restriction sites. The control vector

expressed GFP (untagged) and was generated in the same way by T.Z. Although not shown, wild-type and catalytically inactive (Y788F/Y791A) rat PARG Tet-inducible retroviral mammalian expression constructs were also generated by PCR-based cloning of the tagged cDNAs (a carboxyl-terminal FLAG tag) into pREV-TRE. [In addition, both PARP-1 (Wt and CatMut) and PARG (Wt and CatMut) tagged cDNAs were inserted into the pTRE-TIGHT (Clonetech) retroviral mammalian expression vector for use with the Tet-On MCF-7 cell line in a similar manner.]

Generation, culture, and treatments of MCF-7-derived cell lines - Tet-Off MCF-7 human breast cancer cells (Clonetech) were maintained in MEM Eagle medium containing Hanks' salts, L-glutamine, and non-essential amino acids (Sigma-Aldrich) supplemented with 5% Tet-approved FBS (Tet FBS; Clonetech), 20 mM HEPES (pH 7.6), 100 units/mL penicillin, 100 μg/mL streptomycin, 25 μg/mL gentamycin, and 0.22 % sodium bicarbonate. The Tet-inducible exogenous expression cell lines used in these studies were generated by retroviral infections of Tet-Off MCF-7 cells with the pREV-TRE expression vectors. [In a similar manner, Tet-On MCF-7 (Clonetech) cell lines were generated with the pTRE-TIGHT expression vectors. However, these cell lines not used after initial testing displayed considerable basal expression of the tagged protein (*i.e.*, the system was quite leaky).]

Retroviruses were generated by transfection of the pREV-TRE vectors described above with an expression vector for the VSV-G envelope protein into Phoenix Ampho cells using GeneJuice transfection reagent (Novagen) according to the manuf/acturer's protocol. The resulting viruses were collected, filtered through a 0.45 μm syringe filter to remove any remaining cells, and used to infect the Tet-Off MCF-7 cells. Stably transduced cells were isolated under appropriate selection with hygromycin (Cellgro; 200 μg/mL), expanded, and frozen in aliquots for future use.

GFP and PARP-1 Wt or CatMut Tet-Off cell lines were maintained as noted above in the presence of doxycycline (Sigma-Aldrich; 2 μg/mL) to maintain expression of the exogenous protein in the "off" state. To induce expression, doxycycline was removed for a minimum of 4 days.

FLAG immunoprecipitation and protein identification - GFP and PARP-1 Wt Tet-Off cell lines were seeded in 4 15-cm dishes each and grown in the absence of doxycycline for at least 4 days. Cells were washed with PBS, scraped, and collected by centrifugation. Cells were lysed in 2.5 mL of lysis buffer [20 mM Tris•HCl (pH 7.5), 420 mM NaCl, 10% glycerol, 0.5 mM EDTA, 0.1% NP-40, 1 mM DTT, 1mM PMSF, 40 μg/mL aprotinin, 40 μg/mL leupeptin, and a protease inhibitor cocktail (Roche Molecular Biochemicals)], and dounced on ice twice every 10 minutes for a period of 30 minutes, following an initial 8-10 dounces. Lysates were then mixed in a 1:1 ratio with dilution buffer [20 mM Tris•HCl (pH 7.5), 10% glycerol, 0.5 mM EDTA, 0.1% NP-40, 1 mM DTT, 1mM PMSF, 40 μg/mL aprotinin, 40 μg/mL leupeptin, and a protease inhibitor cocktail (Roche Molecular Biochemicals)], incubated at 4°C for 30 minutes, and centrifuged for 4°C for 20 minutes at a speed of 17,000 rpm (Sorvall SS-34 rotor). The supernatent was then transferred to a 15-mL conical vial and incubated with 50 μl of FLAG affinity resin (Sigma-Aldrich; A1080) at 4°C for 3 hrs, following equilibration of the resin with dilution buffer. FLAG resin was collected using a clinical centrifuge, washed four times with wash buffer [20 mM Tris•HCl (pH 7.5), 200 mM NaCl, 0.5 mM EDTA, 0.1% NP-40, 1 mM DTT, 1mM PMSF, and a protease inhibitor cocktail (Roche Molecular Biochemicals)], and bound proteins were eluted by competition with FLAG peptide (Sigma-Aldrich; F3290) in elution buffer [20 mM Tris•HCl (pH 7.5), 200 mM NaCl, 10% glycerol, 0.2 mM

EDTA, 0.1% NP-40, 1 mM DTT, 1mM PMSF, 500 μg/mL insulin, 200 μg/mL FLAG peptide, and a protease inhibitor cocktail (Roche Molecular Biochemicals)].

For mass spectrometric identification, the bound proteins were separated by SDS-PAGE and visualized by silver staining. Proteins excised from the gel were digested with trypsin and resulting peptide pools were analyzed by matrix-assisted laser-desorption / ionization reflectron time-of-flight (MALDI-reTOF) MS using a BRUKER UltraFlex TOF/TOF instrument (Bruker Daltonics; Bremen, Germany) (Erdjument-Bromage et al., 1998; Sebastiaan Winkler et al., 2002). Selected experimental masses (m/z) were taken to search the human segment of a non-redundant protein database ('NR' on April 8th 2010; ~233,131 entries; National Center for Biotechnology Information; Bethesda, MD), utilizing the Mascot Peptide Mass Fingerprint (PMF) program, version 2.3.01 for Windows (www.matrixscience.com), with a mass accuracy restriction better than 40 ppm, and maximum one missed cleavage site allowed per peptide. To confirm PMF results with scores $\leq$40, mass spectrometric sequencing of selected peptides was done by MALDI-TOF/TOF (MS/MS) analysis on the same prepared samples, using the UltraFlex instrument in 'LIFT' mode. Fragment ion spectra were taken to search NR using the Mascot MS/MS Ion Search program (Matrix Science, www.matrixscience.com).

A.7. Reagents to Study NAD^+-Synthesizing Enzymes

PARPs and Sirtuins (SIRTs) are two families of enzymes that utilize NAD^+ to carry out ADP-ribosyalation and deacetylation reactions, respectively, which occur in all cellular compartments. Therefore, it is conceivable that NAD^+ is synthesized in the nucleus, cytoplasm, and mitochondria to supply these types of enzymes with a substrate. In fact, not only is NAD^+ synthesized in these compartments from dietary

products (the De Novo Pathway), the product of PARP and SIRT enzymatic reactions, nicotinamide (NAm), is also recycled to re-synthesize NAD^+ (the Salvage Pathway) (Kim et al., 2005). Within these pathways, there are a series of enzymes that participate in the synthesis of intermediate products, all in an effort to generate NAD^+ (Figure A.7A). Some are solely active in the De Novo Pathway (*i.e.*, NADS), while others are involved solely in the Salvage Pathway (*i.e.*, NRK1). Still others are active in both pathways, such as NMNATs, which are crucial for the final conversion step to NAD^+. Part of understanding how PARPs and SIRTs gene regulatory functions in vivo is being able to understand how substrate availability can affect their actions. Therefore, in an effort to study the NAD^+-metabolic pathway enzymes and their potential effects on PARP-1's gene regulatory functions in particular, I obtained all cDNAs, expressed them in mammalian cells, and determined their cellular localization patterns by immunofluorescence assays. My results suggest that NMNAT-1 is not the only nuclear NAD^+-synthesizing enzyme, as previously thought.

A.7.1. Results and Discussion

Regarding the enzymes involved in the NAD^+-synthesis pathway (Figure A.7A), there is little information known about their involvement with transcriptional regulation. To determine if there are such potential functions for any of these enzymes to affect gene regulation on their own or in combination with NAD^+-utilizing enzymes (*i.e.*, PARPs, SIRTs), one would expect those enzymes to be localized completely or partially in the nucleus. To answer this question, I obtained cDNAs for the enzymes highlighted in Figure A.7A and exogenously expressed FLAG-tagged versions in 293T cells by transient transfection assay. They include: nicotinate phosphoribosyl transferase (NPT), NAD^+ synthetase (NADS), nicotinamide mononucleotide

Figure A.7. Schematic of the NAD^+ synthesis pathway. *A*, NAD^+ is synthesized via the de novo pathway and the salvage pathway. The enzymes responsible for the ultimate synthesis of NAD^+ are highlighted in blue (modified from Kim et al., 2005). *B*, cDNAs for the enzymes from panel (A) were FLAG-tagged, cloned into the pCMV5 mammalian expression vector, and tested for expression by transient transfection in 293T cells. Whole cell extracts were isolated 24 hrs post transfection and subjected to Western blotting using a FLAG-specific antibody. The enzymes within each pathway are indicated. Three constructs, NPT, NMNAT-3, and NRK1 did not display a visible FLAG signal, indicating the exogenous protein did not express, the protein is mis-folded and degraded, or the FLAG peptide was cleaved.

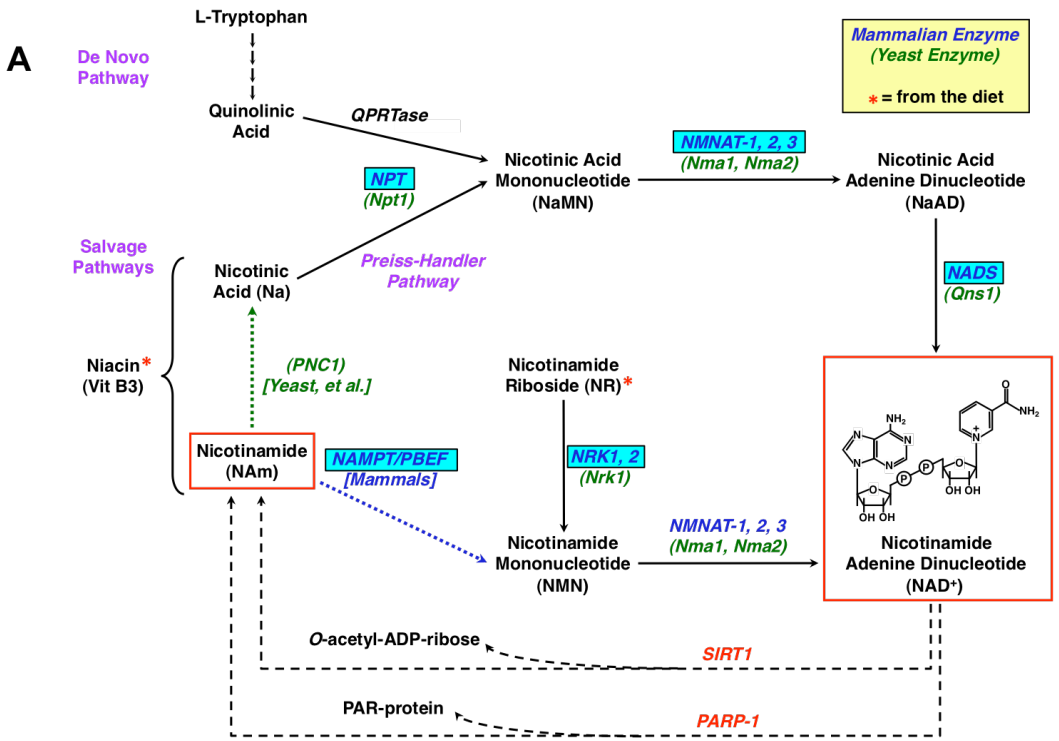

Modified from Kim et al.., *Genes & Development*, 2005

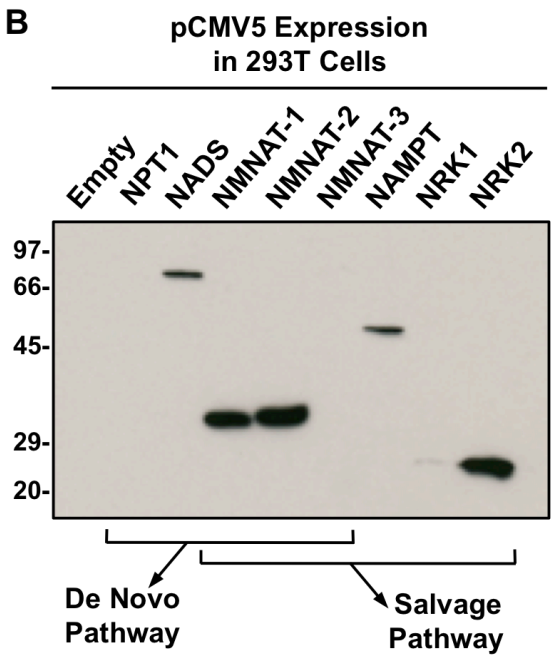

adenylyltransferase -1, -2, -3 (NMNAT), nicotinamide phosphoribosyltransferase (NAMPT), and nicotinamide riboside kinase -1, -2 (NRK).

Western blot analysis using a FLAG-specific antibody showed that one some of the enzymes were expressed (at the correct molecular weight), while others were not (Figure A.7B). For those that did not express (*i.e.*, NPT, NMNAT-3, and NRK1), there are several explanations including: (i) the protein is toxic to the cells and was thus degraded; (ii) the protein was expressed, but the FLAG-tag was cleaved from the protein; or (iii) the localization of these particular enzymes are within membranous organelles that could not be lysed with the protocol used. Since protein-specific antibodies do not exist for nearly all of these proteins, the second explanation could not be eliminated. The third explanation makes sense considering previous reports suggesting NMNAT-3 localizes to the mitochondria (Berger et al., 2004). A cellular fractionation of the lysates is required in order to determine if this is true.

To determine the cellular localization of those enzymes that expressed (*i.e.*, NADS, NMNAT-1, NMNAT-2, NAMPT, and NRK2), I performed the same transient transfection experiment followed by immunofluorescence analysis. In this assay, the cells were co-stained with an antibody against FLAG (green) to detect the exogenous protein and PARP-1 (red) to detect a nuclear protein (Figure A.8A). NMNAT-1 clearly localized to the nucleus, overlaying nearly perfectly with PARP-1. NMNAT-2 anti-localized with PARP-1, and seemingly concentrated near the nuclear membrane, perhaps indicative of localization to the endoplasmic reticulum or golgi apparatus. Antibodies against proteins specific to the endoplasmic reticulum and the golgi apparatus would be necessary to compare with the localization patterns of NMNAT-2 to confirm this result. NADS localized to the entire cytoplasm in a uniform manner. Interestingly, NRK2 and NAMPT seemingly localized to the nucleus and cytoplasm, a result that was seen throughout cross sections of the entire cell (data not shown). This

Figure A.8. NAD^+-synthesizing enzymes localize to various cellular compartments. *A*, 293T cells transfected with each enzyme from Figure A.7 were subjected to immunostaining with a FLAG-specific antibody (green) and visualized by confocal microscopy. The cells were co-stained with a PARP-1-specific antibody (red), as a control for nuclear localization. *B*, The same experiment was conducted in the presence of leptomycin B (LepB), which blocks nuclear export, to determine if NMNAT-1 is the only nuclear NAD^+ synthesizing enzyme. LepB caused NAMPT to be sequestered in the nucleus, indicating that NAMPT actively shuttles between the cytoplasm and nucleus compartments in vivo.

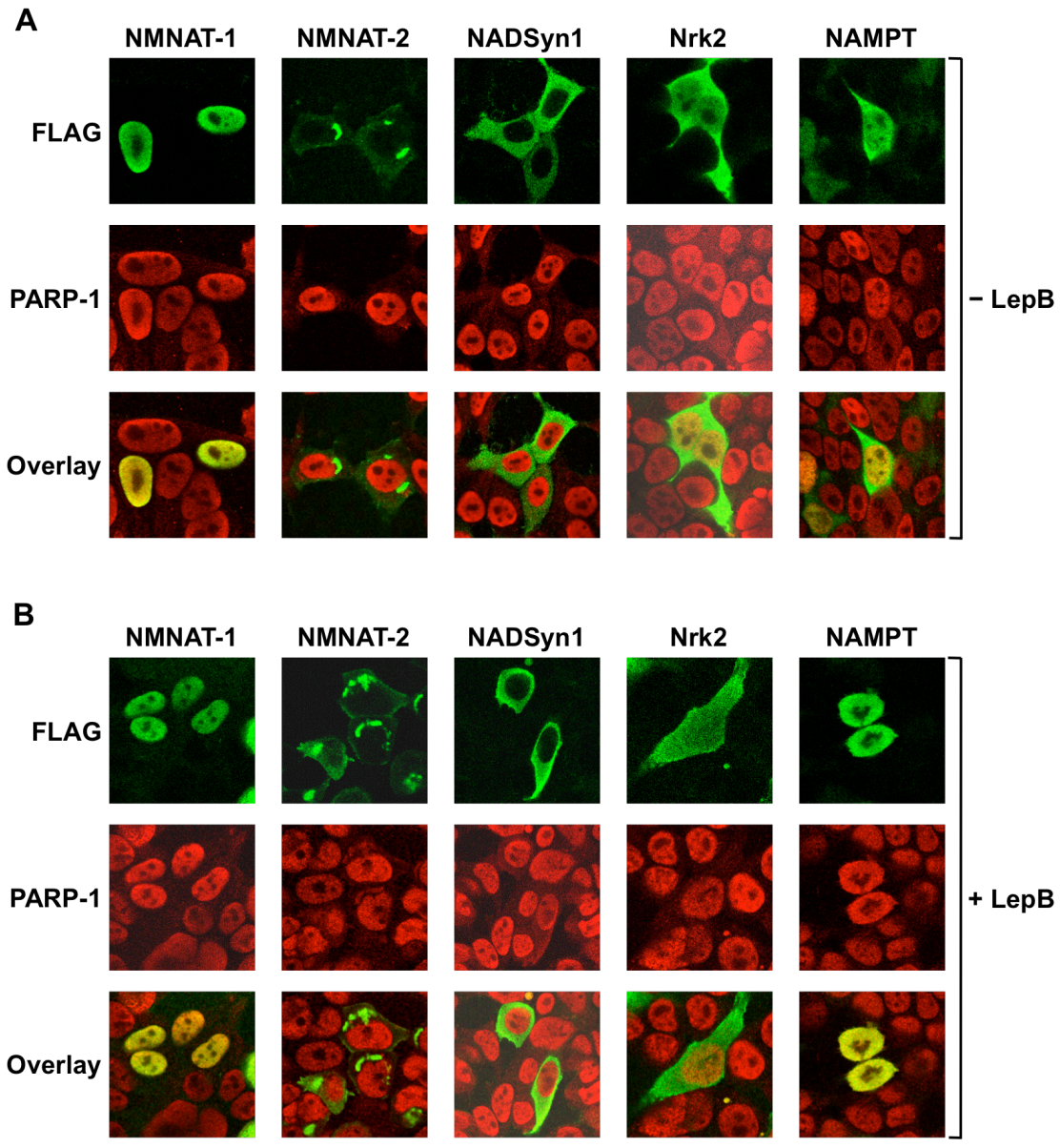
A
NMNAT-1
NMNAT-2
NADSyn1
Nrk2
NAMPT
FLAG
PARP-1
Overlay
− LepB
B
NMNAT-1
NMNAT-2
NADSyn1
Nrk2
NAMPT
FLAG
PARP-1
Overlay
+ LepB

suggests that perhaps these particular enzymes are shuttled between compartments. To answer this question, the cells were treated with leptomycin B (LepB), an inhibitor of nuclear export. Treatment with LepB had no effect on NRK2 localization, suggesting that NRK2 is ubiquitously expressed throughout the cell. However, treatment with LepB caused a large percentage of NAMPT to be sequestered in the nucleus, indicating that NAMPT actively shuttles between the cytoplasm and nucleus.

Taken together, these results suggest that while it is possible that any of these enzymes can affect total cellular NAD^+ concentrations, it is likely that NMNAT-1 and NAMPT can affect local, nuclear NAD^+ concentrations that can ultimately change the activities of NAD^+-utilizing enzymes, such as PARPs and SIRTs. In addition, nuclear localization of NMNAT-1 and NAMPT also leaves the possibility for gene regulatory functions independent of their enzymatic activity. In fact, a recent report suggests that both NMNAT-1 and NAMPT can not only localize to the nucleus, but also can localize to chromatin, and can alter the gene regulatory activities of SIRT1 through physical interactions (Zhang et al., 2009). It is highly likely that PARP-1 gene regulatory functions are also altered by NMNAT-1 and NAMPT. While the total NAD^+ levels created by NMNAT-1 and NAMPT are important, it still remains elusive how direct and promoter-localized NAD^+ concentrations contribute.

A.7.2. Experimental Procedures

Antibodies - The mouse monoclonal antibody against FLAG used for Western blotting and immunostaining was purchased from Sigma-Aldrich (F3165). The custom rabbit polyclonal antibody against PARP-1 used for immunostaining was generated by using a purified fragment of human PARP-1 (amino-terminal, PARP-N (Kim et al., 2004)) (Pocono Rabbit Farm and Laboratory, Inc.).

NAD^+-synthesizing enzymes expression constructs - The cDNAs for NPT and NAMPT were purchased from ATCC. The cDNAs for NADS, NMNAT-1, NMNAT-2, NMNAT-3, NRK1, and NRK2 were kindly provided by Dr. Nobumasa Hara, Dr. Mathias Ziegler, Dr. Hiremagalur Jayaram, Dr. Hong Zhang, Dr. Charles Brenner (both NRK1 and 2), respectively. The pCMV mammalian expression constructs were generated by PCR-based cloning of the tagged cDNAs (an amino- or carboxy-terminal FLAG/6xHis tag) into pCMV5. All constructs were confirmed by sequencing. The ability to express was tested by transient transfection in 293T cells followed by Western blotting with a FLAG-specific antibody.

Immunofluorescence – 293T cells transiently transfected with FLAG-tagged cDNAs were grown on coverslips in 6-well plates for a minimum of 24 hrs. The cells were treated with or without 10 ng/mL leptomycin B (LepB, LC Laboratories) for 2 hrs prior to fixation. The cells were fixed in the dish with 3.7% formaldehyde solution with PBS for 20 minutes at room temperature, washed twice with PBS and subsequently permeablized with 0.1% Triton X solution in PBS for 20 minutes at room temperature. Cells were then washed twice with PBS and incubated with FLAG or PARP-1 antibody (1:2000 – 1:5000 dilution in PBS) for 1 hour at room temperature (in the dark). After two washes with PBS, the cells were incubated with goat-α-rabbit rhodamine-conjugated or goat-α-mouse FITC-conjugated secondary antibody (1:3000 dilution in PBS; Jackson) and Hoechst DNA stain (1:5000 dilution in PBS; Jackson) for 1 hour at room temperature (in the dark). Finally, the cells were washed three times with PBS and coverslips mounted onto microscope slides using Vectashield Mounting Media (Vector Laboratories). Staining was visualized using a Leica Confocal Microscope System at Cornell University's Microscope Imaging Facility.

REFERENCES

Berger, F., Ramirez-Hernandez, M. H., and Ziegler, M. (2004). The new life of a centenarian: signalling functions of NAD(P). Trends Biochem Sci *29*, 111-118.

D'Amours, D., Desnoyers, S., D'Silva, I., and Poirier, G. (1999). Poly(ADP-ribosyl)ation reactions in the regulation of nuclear functions. Biochem J *342*, 249-268.

Erdjument-Bromage, H., Lui, M., Lacomis, L., Grewal, A., Annan, R. S., McNulty, D. E., Carr, S. A., and Tempst, P. (1998). Examination of micro-tip reversed-phase liquid chromatographic extraction of peptide pools for mass spectrometric analysis. J Chromatogr A *826*, 167-181.

Frizzell, K. M., Gamble, M. J., Berrocal, J. G., Zhang, T., Krishnakumar, R., Cen, Y., Sauve, A. A., and Kraus, W. L. (2009). Global analysis of transcriptional regulation by poly(ADP-ribose) polymerase-1 and poly(ADP-ribose) glycohydrolase in MCF-7 human breast cancer cells. J Biol Chem *284*, 33926-33938.

Gamble, M. J., Frizzell, K. M., Yang, C., Krishnakumar, R., and Kraus, W. L. (2010). The histone variant macroH2A1 marks repressed autosomal chromatin, but protects a subset of its target genes from silencing. Genes Dev *24*, 21-32.

Hassa, P. O., Covic, M., Hasan, S., Imhof, R., and Hottiger, M. O. (2001). The enzymatic and DNA binding activity of PARP-1 are not required for NF-kappa B coactivator function. J Biol Chem *276*, 45588-45597.

Hassa, P. O., and Hottiger, M. O. (1999). A role of poly (ADP-ribose) polymerase in NF-kappaB transcriptional activation. Biol Chem *380*, 953-959.

Hassa, P. O., and Hottiger, M. O. (2002). The functional role of poly(ADP-ribose)polymerase 1 as novel coactivator of NF-kappaB in inflammatory disorders. Cell Mol Life Sci *59*, 1534-1553.

Ju, B. G., Solum, D., Song, E. J., Lee, K. J., Rose, D. W., Glass, C. K., and Rosenfeld, M. G. (2004). Activating the PARP-1 sensor component of the groucho/ TLE1 corepressor complex mediates a CaMKinase IIdelta-dependent neurogenic gene activation pathway. Cell *119*, 815-829.

Kameoka, M., Ota, K., Tetsuka, T., Tanaka, Y., Itaya, A., Okamoto, T., and Yoshihara, K. (2000). Evidence for regulation of NF-kappaB by poly(ADP-ribose) polymerase. Biochem J *346 Pt 3*, 641-649.

Kauppinen, T. M., Chan, W. Y., Suh, S. W., Wiggins, A. K., Huang, E. J., and Swanson, R. A. (2006). Direct phosphorylation and regulation of poly(ADP-ribose) polymerase-1 by extracellular signal-regulated kinases 1/2. Proc Natl Acad Sci U S A *103*, 7136-7141.

Kim, M. Y., Mauro, S., Gevry, N., Lis, J. T., and Kraus, W. L. (2004). NAD+-dependent modulation of chromatin structure and transcription by nucleosome binding properties of PARP-1. Cell *119*, 803-814.

Kim, M. Y., Woo, E. M., Chong, Y. T., Homenko, D. R., and Kraus, W. L. (2006). Acetylation of estrogen receptor alpha by p300 at lysines 266 and 268 enhances the DNA binding and transactivation activities of the receptor. Mol Endocrinol.

Kim, M. Y., Zhang, T., and Kraus, W. L. (2005). Poly(ADP-ribosyl)ation by PARP-1: 'PAR-laying' NAD+ into a nuclear signal. Genes Dev *19*, 1951-1967.

Krishnakumar, R., Gamble, M. J., Frizzell, K. M., Berrocal, J. G., Kininis, M., and Kraus, W. L. (2008). Reciprocal binding of PARP-1 and histone H1 at promoters specifies transcriptional outcomes. Science *319*, 819-821.

Krishnakumar, R., and Kraus, W. L. (2010). PARP-1 regulates chromatin structure and transcription through a KDM5B-dependent pathway. Mol Cell *39*, 736-749.

Marsischky, G. T., Wilson, B. A., and Collier, R. J. (1995). Role of glutamic acid 988 of human poly-ADP-ribose polymerase in polymer formation. Evidence for active site similarities to the ADP-ribosylating toxins. J Biol Chem *270*, 3247-3254.

Reynolds, A., Leake, D., Boese, Q., Scaringe, S., Marshall, W. S., and Khvorova, A. (2004). Rational siRNA design for RNA interference. Nat Biotechnol *22*, 326-330.

Rolli, V., O'Farrell, M., Menissier-de Murcia, J., and de Murcia, G. (1997). Random mutagenesis of the poly(ADP-ribose) polymerase catalytic domain reveals amino acids involved in polymer branching. Biochemistry *36*, 12147-12154.

Sebastiaan Winkler, G., Lacomis, L., Philip, J., Erdjument-Bromage, H., Svejstrup, J. Q., and Tempst, P. (2002). Isolation and mass spectrometry of transcription factor complexes. Methods *26*, 260-269.

Shah, R. G., Ghodgaonkar, M. M., Affar el, B., and Shah, G. M. (2005). DNA vector-based RNAi approach for stable depletion of poly(ADP-ribose) polymerase-1. Biochem Biophys Res Commun *331*, 167-174.

Shimokawa, T., Masutani, M., Nagasawa, S., Nozaki, T., Ikota, N., Aoki, Y., Nakagama, H., and Sugimura, T. (1999). Isolation and cloning of rat poly(ADP-ribose) glycohydrolase: presence of a potential nuclear export signal conserved in mammalian orthologs. J Biochem *126*, 748-755.

van de Wetering, M., Oving, I., Muncan, V., Pon Fong, M. T., Brantjes, H., van Leenen, D., Holstege, F. C., Brummelkamp, T. R., Agami, R., and Clevers, H. (2003). Specific inhibition of gene expression using a stably integrated, inducible small-interfering-RNA vector. EMBO Rep *4*, 609-615.

Wacker, D. A., Ruhl, D. D., Balagamwala, E. H., Hope, K. M., Zhang, T., and Kraus, W. L. (2007). The DNA binding and catalytic domains of poly(ADP-ribose) polymerase 1 cooperate in the regulation of chromatin structure and transcription. Mol Cell Biol *27*, 7475-7485.

Zhang, T., Berrocal, J. G., Frizzell, K. M., Gamble, M. J., Dumond, M. E., Krishnakumar, R., Yang, T., Sauve, A. A., and Kraus, W. L. (2009). Enzymes in the NAD+ Salvage Pathway Regulate SIRT1 Activity at Target Gene Promoters. J Biol Chem *284*, 20408-20417.